



The
University
Of
Sheffield.

Behavioural and microglial responses to lingual nerve injury and the potential role of resolvin receptors and microRNA

By:

Diana Tavares Ferreira

A thesis submitted in partial fulfilment of the requirements for the degree of Doctor of
Philosophy

The University of Sheffield
Faculty of Medicine, Dentistry and Health
School of Clinical Dentistry

September 2017

ACKNOWLEDGMENTS

I would like to thank my supervisors, Professor Fiona Boissonade and Dr Dan Lambert, for the trust they placed in me to work on this project and for their help and supervision during the last four years. I would also like to express my gratitude for their valuable input into this thesis. I am also grateful to Dr Emma Bird for her knowledge and laboratory assistance. My thanks are also extended to the lab technicians, Dr Matt Worsley and Brenka McCabe, for all the technical help provided.

A special thanks to Dr Milena De Felice for all the advice and motivation, for always being ready to help and for making working in the lab even more enjoyable. Further thanks to my friends in the Dental School and in Sheffield for making the PhD less 'painful' and for the vital support and encouragement, in particular during the last months of writing up.

I would also like to acknowledge Pfizer Neusentis for the financial contribution to this project, and a special thanks to the Genetics group at Eli Lilly for welcoming me into their team during my six months HEFCE scheme placement.

Last but not least, I would like to thank all my family and friends in Portugal for, even in the distance, supporting and believing in me.

It has been a great experience, where I grew both professionally and personally, and I am ever grateful for being able to pursue my career in research.

ABSTRACT

Injury to the lingual nerve can occur during routine oral surgery and may leave the affected patients with permanent sensory disturbances, including pain. The medical treatments are only partially effective and the mechanisms behind the development of persistent neuropathic pain following lingual nerve injury (LNI) are not fully understood.

An emerging line of investigation has suggested that resolvins (endogenous lipid mediators derived from *omega-3* fatty acids) may have a crucial role in inflammation- and pain-associated diseases. Resolvins mediate their actions through G protein-coupled receptors (GPCR): GPR32, BLT1, FPR2/ALX and ChemR23. Recent findings have also suggested that microRNAs (miRNA) can contribute to the altered gene expression that occur following nerve injury.

The work reproduced in this thesis used an animal model of neuropathic pain to better characterise the effect of LNI in terms of behavioural and microglial response and to investigate the expression of resolvin receptors and miRNAs following such injury. In addition, human lingual nerve neuroma tissues were analysed to investigate the expression of resolvin receptors and miRNAs and relate with clinical pain symptoms.

The behavioural study showed a reduction in the time and volume of reward consumed at specific time-points after LNI. In addition, this injury led to the activation of microglial cells in the trigeminal nucleus caudalis (Vc) in early time-points post-injury, which decreased overtime, being only mildly activated on day 28 post-injury. Resolvin receptors were expressed in specific cells across the nervous system. ChemR23, in particular, was up-regulated at specific levels of the Vc up to 28 days following LNI. Specific miRNAs were identified after LNI. miR-138 was differentially expressed between rat CCI and Sham groups and miR-29a was differentially expressed between painful and non-painful human lingual nerve neuromas. Further target prediction studies suggested that these miRNAs may regulate genes involved in the inflammatory events following LNI, axon re-growth and pain transmission mechanisms.

In conclusion, the work conducted in this thesis identified a novel behavioural model for investigating the potential mechanisms behind the development of chronic pain after LNI in the rat. The up-regulation of ChemR23 in the ipsilateral side of the Vc and the dysregulation of specific miRNAs at the site of injury following LNI suggest that they may be potential targets for improved therapeutics for neuropathic pain, in particular that arising from LNI.

LIST OF CONTENTS

<u>ACKNOWLEDGMENTS</u>	ii
<u>ABSTRACT</u>	iii
<u>LIST OF CONTENTS</u>	iv
<u>LIST OF FIGURES</u>	ix
<u>LIST OF TABLES</u>	xiii
<u>LIST OF ABBREVIATIONS</u>	xiv
<u>1. GENERAL INTRODUCTION</u>	1
1.1. Pain	2
1.1.1. Nociceptive pain pathways	3
1.1.2. Neuropathic pain	6
1.1.3. Mechanisms of chronic neuropathic pain following peripheral nerve injury	7
1.1.3.1. <i>Peripheral nerve injury and neuroma formation</i>	7
1.1.3.2. <i>Peripheral sensitisation</i>	10
1.1.3.3. <i>Central sensitisation and neuronal plasticity</i>	13
1.1.3.4. <i>Glial cells activation</i>	14
1.2. Resolvin receptors	17
1.2.1. Resolvins	17
1.2.1.1. <i>Biosynthesis and identification of different resolvins</i>	18
1.2.1.2. <i>Actions of resolvins in disease models</i>	20
1.2.1.3. <i>Resolvins mechanisms of action</i>	22
1.2.2. Receptors	25
1.3. MicroRNA	30
1.3.1. miRNA biogenesis and regulation	30
1.3.2. miRNA-mRNA binding and target prediction	33
1.3.3. miRNAs in pain	35
1.3.4. Resolvins and miRNAs	37
1.4. Lingual nerve injury and clinical implications	38
1.5. Animal models of neuropathic pain and behavioural assessment of orofacial pain	41
1.6. Overview, aims and hypothesis	42

<u>2. GENERAL MATERIAL AND METHODS</u>	44
2.1. Introduction	45
2.2. Animal experiments	45
2.2.1. Surgical procedures	45
2.2.2. Behavioural testing.....	46
2.2.3. Terminal procedures.....	48
2.2.4. Collection and preparation of rat tissue	48
2.3. Human studies	48
2.3.1. Human lingual nerve neuromas	49
2.3.2. Human tissue preparation.....	49
2.4. Immunohistochemical methods	50
2.4.1. Rat tissue	50
2.4.2. Human tissue	51
2.4.3. Immunohistochemical protocol.....	51
2.4.4. Specificity controls	52
2.5. Image acquisition and analysis	55
2.5.1. Fluorescence microscopy	55
2.5.2. Confocal microscopy	56
2.6. miRNA extraction	57
2.6.1. miRNA extraction from rat tissue	57
2.6.2. miRNA extraction from human tissue	58
2.7. TaqMan® Low Density Array (TLDA)	59
2.7.1. Reverse Transcription to cDNA.....	59
2.7.2. Preamplification reaction	60
2.7.3. TaqMan® real-time PCR reactions.....	60
2.8. miRNA validation	62
2.9. Statistical analysis	63
2.9.1. Behavioural analysis	63
2.9.2. Quantification from image analysis	63
2.9.3. miRNA analysis	64
2.9.4. Target prediction and enrichment analysis	65
2.10. Reproducibility of image analysis	65

<u>3. EFFECT OF LINGUAL NERVE INJURY ON FEEDING BEHAVIOUR.....</u>	71
3.1. Introduction	72
3.2. Methodological approach	72
3.2.1. Preliminary studies	75
3.2.1.1. <i>Testing conditions</i>	75
3.2.1.2. <i>Choice of reward</i>	76
3.3. Results	76
3.3.1. Training period and baseline	76
3.3.2. Observational notes	80
3.3.3. Time drinking post-surgery	83
3.3.4. Number of attempts post-surgery	90
3.3.5. Volume ingested post-surgery	92
3.4. Discussion.....	95
<u>4. CHARACTERISATION OF MICROGLIAL RESPONSE TO LINGUAL NERVE INJURY.....</u>	102
4.1. Introduction	103
4.2. Methodological approach	104
4.3. Results	105
4.3.1. Morphological changes and qualitative analysis.....	105
4.3.2. Microglia response on day 3 following lingual nerve injury	115
4.3.3. Microglia response on day 7 following lingual nerve injury	117
4.3.4. Microglia response on day 28 following lingual nerve injury	119
4.3.5. Comparison of microglia response over time	121
4.4. Discussion.....	123
<u>5. RESOLVIN RECEPTORS EXPRESSION.....</u>	128
5.1. Introduction	129
5.2. Methodological approach	129
5.3. Results	131
5.3.1. Expression of resolvin receptors	131
5.3.1.1. <i>Human tissue</i>	131
5.3.1.1. <i>Rat tissue</i>	136
5.3.2. ChemR23 expression following lingual nerve injury	146

5.3.2.1. <i>ChemR23</i> expression in the trigeminal nucleus caudalis on day 3 following lingual nerve injury.....	155
5.3.2.2. <i>ChemR23</i> expression in the trigeminal nucleus caudalis on day 7 following lingual nerve injury.....	157
5.3.2.3. <i>ChemR23</i> expression in the trigeminal nucleus caudalis on day 28 following lingual nerve injury.....	159
5.3.2.4. Comparison of <i>ChemR23</i> expression over time.....	161
5.4. Discussion.....	163
<u>6. MICRORNA EXPRESSION FOLLOWING LINGUAL NERVE INJURY</u>	<u>169</u>
6.1. Introduction.....	170
6.2. Methodological approach.....	170
6.3. Results.....	172
6.3.1. miRNAs in rat tissues.....	172
6.3.1.1. miRNA target prediction and gene enrichment analysis.....	173
6.3.1.2. Novel rat miRNAs.....	180
6.3.2. miRNAs in human lingual nerve neuroma.....	182
6.3.2.1. Clinical data analysis.....	182
6.3.2.2. miRNA expression analysis.....	183
6.3.2.3. miRNA target prediction and gene enrichment analysis.....	184
6.4. Discussion.....	190
<u>7. GENERAL DISCUSSION.....</u>	<u>198</u>
7.1. Summary of findings.....	199
7.2. Animal model of neuropathic pain: effect of LNI in feeding behaviour and microglia response.....	200
7.3. Resolvin receptors and miRNA expression.....	203
7.3.1. Resolvin receptors expression.....	203
7.3.2. miRNA expression.....	205
7.4. General approach and study limitations.....	205
7.5. Future studies.....	207
7.6. Conclusion.....	208

<u>APPENDIX</u>	209
Appendix 1: Target genes and pathways predicted to be under control of the miRNAs identified	209
Appendix 2: Details of the rat diet used in this thesis	218
<u>REFERENCES</u>	219

LIST OF FIGURES

Figure 1.1. The main classes of primary afferent neurones and their organisation in the dorsal horn.....	4
Figure 1.2. Schematic representation of peripheral nerve injury and subsequent cellular events.....	9
Figure 1.3. The sequence of events that lead to peripheral sensitisation.	11
Figure 1.4. The sequence of events that contribute to central sensitisation.....	16
Figure 1.5. Biosynthesis of resolvins.	19
Figure 1.6. Secondary structure common to GPCR.....	25
Figure 1.7. Summary of miRNA biogenesis and regulation of gene expression.....	32
Figure 1.8. Types of miRNA-mRNA binding.	34
Figure 1.9. Lingual nerve, trigeminal ganglion and brainstem.	40
Figure 2.1. Chronic constriction injury of the rat lingual nerve.....	46
Figure 2.2. The Ugo Basile Orofacial Stimulation Test equipment.....	47
Figure 2.3. Representation of the serial collection of brainstem sections.....	50
Figure 2.4. Representation of the serial collection of neuroma sections.	51
Figure 2.5. Image analysis using Image Pro-Plus.	56
Figure 2.6. TLDA microfluidic card.	61
Figure 2.7. Scatter plots showing linear relationship between Iba1 initial and repeated measurements in sections from control naïve and sham animals.	67
Figure 2.8. Scatter plots showing linear relationship between Iba1 initial and repeated measurements in sections from injured (CCI) animals.	68
Figure 2.9. Scatter plots showing linear relationship between ChemR23 initial and repeated measurements in sections from control naïve and sham animals.....	69
Figure 2.10. Scatter plots showing linear relationship between ChemR23 initial and repeated measurements in sections from injured (CCI) animals.	70
Figure 3.1. Diagram representing the methodological approach with training, surgery, testing and data analysis.....	74
Figure 3.2. Example of drinking behaviour recording by the Ugo Basile software.	76
Figure 3.3. Time drinking during training period and day 0.....	78
Figure 3.4. Number of attempts during training period and day 0.....	79
Figure 3.5. Volume ingested (mL) during the training period and day 0.	80

Figure 3.6. Percentage of body weight gain in average by group at the end of experiment.	81
Figure 3.7. Data recorded by ORO software.....	82
Figure 3.8. Time drinking decreased following lingual nerve injury.	84
Figure 3.9. Box plot with total time drinking values within each group.	86
Figure 3.10. Maximum contact time.	87
Figure 3.11. Box plot with maximum time drinking per testing within each group.....	89
Figure 3.12. Number of attempts.	90
Figure 3.13. Box plot of number of attempts within each group.	91
Figure 3.14. Volume of reward ingested during the period testing.	92
Figure 3.15. Box plot with volume ingested.	94
Figure 4.1. Lingual nerve and the brainstem.....	104
Figure 4.2. Microglia response in the trigeminal nucleus.....	106
Figure 4.3. Activated microglial cells on day 3.	106
Figure 4.4. Microglia response in the Vc at 3, 7 and 28 days following LNI (CCI group).	110
Figure 4.5. Microglia response in the Vc at 3, 7 and 28 days following sham operation of the lingual nerve (Sham group).....	112
Figure 4.6. Microglia in the control naïve group.	113
Figure 4.7. Representative images of microglia response (Iba1 expression) to lingual nerve injury at 720 μ m caudal to obex.....	114
Figure 4.8. Analysis of microglial response on day 3 by quantification of positive area of Iba1 staining.	116
Figure 4.9. Analysis of microglial response on day 7 by quantification of Iba1 staining.	118
Figure 4.10. Analysis of microglial response on day 28 by quantification of Iba1 staining.	120
Figure 4.11. Comparative analysis of microglia response between time points.....	122
Figure 5.1. GPR32 is co-localised with S-100.....	132
Figure 5.2. GPR32 and PGP9.5 dual labelling in human lingual nerve neuroma.	133
Figure 5.3. BLT1 and PGP9.5 dual labelling.....	134
Figure 5.4. BLT1 seems to be expressed in Schwann cells.	135
Figure 5.5. FPR2/ALX is expressed in spinal cord dorsal horn neurones.	137
Figure 5.6. FPR2/ALX is not expressed in spinal cord astrocytes.	138

Figure 5.7. FPR2/ALX is expressed neurones within brainstem trigeminal nucleus ...	139
Figure 5.8. ChemR23 is expressed in spinal cord dorsal horn neurones.	141
Figure 5.9. Confocal microscopy shows co-localisation of ChemR23 and NeuN.....	142
Figure 5.10. ChemR23 is not expressed in spinal cord astrocytes.	143
Figure 5.11. ChemR23 is expressed in neurones within the brainstem trigeminal nucleus.	144
Figure 5.12. ChemR23 is not expressed in microglial cells within the brainstem trigeminal nucleus.....	145
Figure 5.13. ChemR23 expression in the trigeminal nucleus in relation to microglial activation.....	147
Figure 5.14. ChemR23 and microglia following lingual nerve injury.	148
Figure 5.15. ChemR23 and microglia expression three days following lingual nerve injury in the Vc at 960 um caudal to obex.....	149
Figure 5.16. ChemR23 in CCI group.	151
Figure 5.17. ChemR23 in Sham group.	153
Figure 5.18. ChemR23 in the control naïve group.....	154
Figure 5.19. ChemR23 expression on day 3 following lingual nerve injury.	156
Figure 5.20. ChemR23 expression on day 7 following lingual nerve injury.	158
Figure 5.21. ChemR23 expression on day 28 following lingual nerve injury.	160
Figure 5.22. Comparison of ChemR23 expression at different time points.	162
Figure 6.1. Diagram of the methodological approach.....	171
Figure 6.2. miRNA validation and correlation scatter plots.	173
Figure 6.3. CyTargetLinker analysis and network visualisation of differentially expressed rat miRNAs and their predicted target genes.	175
Figure 6.4. Circos v0.67 plot of rno-miR-138-1 and its target genes.	176
Figure 6.5. Circos v0.67 plot of rno-miR-667 and its target genes.....	177
Figure 6.6. Circos v0.67 plot of rno-miR-138 (blue) and rno-miR-667 (green) and regulatory target genes.	178
Figure 6.7. Example of genes and pathways targeted by miR-667 and miR-138.....	180
Figure 6.8. Results of the BLAST search	181
Figure 6.9. Pearson correlation scatter plot.....	183
Figure 6.10. miRNA validation and correlation scatter plots.	184
Figure 6.11. CyTargetLinker analysis and network visualisation of differentially expressed human neuromas miRNAs and their predicted target genes.	185

Figure 6.12. Circos v0.67 plot of hsa-miR-29a and regulatory target genes.	186
Figure 6.13. Circos v0.67 plot of hsa-miR-500a and regulatory target genes.	187
Figure 6.14. Circos v0.67 plot of hsa-miR-29a (blue) and hsa-miR-500a (green) and regulatory target genes.	188
Figure 6.15. Example of genes and pathways targeted by miR-500a and miR-29a.	190
Figure 7.1. Feeding behaviour and Iba1 and ChemR23 expression following lingual nerve injury	201
Figure 7.2. Analysis of Iba1 (microglial marker) and ChemR23 expression correlation following lingual nerve injury.....	204
Figure A1. Details of the rat diet.....	218

LIST OF TABLES

Table 1.1. The main classes of primary afferent neurones.	4
Table 1.2. Bio-actions of resolvins.	24
Table 1.3. Resolvins and their receptors.	26
Table 1.4. Summary of miRNAs altered in different pain models.	35
Table 2.1. Details of antibodies and dilutions used in the animal studies.	53
Table 2.2. Details of antibodies and dilutions used in the human studies.	54
Table 2.3. Reaction mix for miRNA reverse transcription (RT).	59
Table 2.4. Parameters used in the thermal cycler for Reverse Transcription	59
Table 2.5. Pre-amplification reaction mix.	60
Table 2.6. Pre-amplification parameters	60
Table 2.7. TaqMan [®] array components.	61
Table 2.8. Parameters used in the TaqMan [®] array RT-qPCR amplification.	62
Table 2.9. Components in miRNA reverse transcription (RT) reaction	62
Table 2.10. Parameters used in thermal cycler for miRNA reverse transcription	62
Table 2.11. Reaction mix for RT-qPCR miRNA validation.	63
Table 2.12. Pearson correlations between initial and repeated measurements.	66
Table 3.1. Measurements.	73
Table 3.2. Characteristics of animals subjects used for the behavioural testing.	75
Table 4.1. Criteria for qualitative microglia characterisation.	105
Table 4.2. Qualitative analysis of microglial response.	108
Table 4.3. Statistical differences between time points.	122
Table 5.1. Statistical differences between time-points.	162
Table 6.1. MiRNAs differentially expressed in the rat lingual nerve.	172
Table 6.2. Clinical information of the patients included in this study	182
Table 6.3. miRNA differentially expressed in human lingual nerve neuromas.	183
Table 7.1. Fatty acid composition in the rat diet used.	207

LIST OF ABBREVIATIONS

5-HT	Serotonin (5-hydroxytryptamine)
AA	Arachnoid Acid
AMPA	Amino-Hydroxy-Methyl-Isoxazolepropionic Acid
ASIC	Acid-sensing ion channel
AT-Rv	Aspirin triggered- resolvin
ATP	Adenosine 5'-triphosphate
BDNF	Brain derived neurotrophic factor
BL	Baseline
BLT1	Leukotriene B ₄ receptor
CaMKII	Ca ²⁺ /calmodulin-dependent kinase II
cAMP	Cyclic adenosine monophosphate
CCI	Chronic constriction injury
ChemR23	Chemerin receptor 23
CL	Contralateral
CFA	Complete Freund's adjuvant
CGRP	Calcitonin gene-related peptide
CNS	Central Nervous System
COX	Cyclooxygenase
Cy3	Indocarbocyanine
CRG	Carrageenan
DGCR8	DiGeorge syndrome critical region 8
DHA	Docosahexaenoic acid
DRG	Dorsal root ganglion
ENK	Enkephalin
EP	E prostanoid receptor
EPA	Eicosapentaenoic acid
FITC	Fluorescein isothiocyanate
FPR	N-formyl peptide receptor
FPR2/ALX	Lipoxin A ₄ receptor
GABA	Gamma-Aminobutyric Acid
GAL	Galanin
GDNF	Glial-derived neurotrophic factor

GFAP	Glial fibrillary acidic protein
GPCR	G protein-coupled receptor
GPR32	G protein-coupled 32
H	Hour
HSP	Heat shock proteins
HRP	Horseradish peroxidase
IASP	International Association for the Study of Pain
Iba1	Ionized calcium-binding adapter molecule 1
IL	Interleukin
IL	Ipsilateral
ION	Infraorbital nerve
LNI	Lingual nerve injury
LTB₄	Leukotriene B ₄
LPS	Lipopolysaccharide
MAPK	Mitogen-activated protein kinases
mGluR	Metabotropic glutamate receptor
MHC	Major histocompatibility complex
Min	Minute
MiRNA	MicroRNA
mL	Mililiter
mRNA	Messenger RNA
NEN	Nerve-end-neuroma
NeuN	Neuronal Nuclei, neuronal marker
NF-κB	Nuclear factor-κB
NGF	Nerve growth factor
NIC	Neuroma-in-continuity
NK1	Neurokinin-1
NMDA	N-methyl-D-aspartate
NO	Nitric oxide
NPY	Neuropeptide Y
OCT	Optimal cutting temperature compound
OX-42	Anti-Integrin αM CD11b antibody
PAS	Positive area of staining
PBS	Phosphate buffered saline

PCR	Polymerase chain reaction
PDCD4	Programmed cell death 4
PDL	Poly-D-lysine
PG	Prostaglandin
PGP9.5	Protein Gene Product 9.5
PKA/C	Protein Kinase A/C
PNI	Peripheral nerve injury
PTX	Pertussis toxin
PUFA	Polyunsaturated fatty acids
RISC	RNA-induced silencing complex
Rv	Resolvin
RT	Reverse Transcription
SAA	Serum Amyloid A
S	Second
S-100	S-100 proteins
SEM	Standard error of mean
snRNA	Small nuclear RNA
SP	Substance P
TG	Trigeminal ganglion
TLDA	TaqMan [®] low density array cards
TLR	Toll-like receptors
TM	Transmembrane
TNF-α	Tumor necrosis factor alpha
TRBP	TAR RNA-binding protein 2
TrkA	Tyrosine kinase A
TRP	Transient receptor potential
TTX-R	Tetrodotoxin-resistant
TTX-S	Tetrodotoxin-sensitive
UTR	Untranslated region
VAS	Visual analogue scale
Vc	Trigeminal nucleus caudalis
VIP	Vasoactive intestinal polypeptide
VGSC	Voltage-gated sodium channels
WDR	Wide dynamic range

CHAPTER 1
GENERAL INTRODUCTION

1.1. Pain

Pain is defined by the International Association for the Study of Pain (IASP) as “an unpleasant sensory and emotional experience associated with actual or potential tissue damage, or described in terms of such damage”. Pain includes an emotional component that inevitably results in a subjective experience generated within the brain (Basbaum et al., 2009). The sensory component involves peripheral and central neurones that play an active role in pain processing along with glial cells (the cells that surround and interact with the neurones in the nervous system) and also components of the immune system (Grace et al., 2014). Pain is perceived as a protective mechanism, serving as a threat alarm to the body (Guillot et al., 2012). However, when it evolves to a chronic state, pain no longer serves any biological function, and it becomes a very complex disease (Pasero, 2004). Neuropathic pain results from damage directly to the peripheral or central nervous system and it is one type of chronic pain. It is estimated that neuropathic pain affects 7-10% of the world population (Colloca et al., 2017) having a great impact on the quality of the patient’s life. In addition, poorly managed pain has socio-economic consequences manifested in lost productivity and high healthcare costs. The work described in this thesis sought to investigate the expression of resolvins receptors (an emerging class of molecules with potential to treat pain-associated diseases) and microRNAs (miRNA) following lingual nerve injury (LNI). Both pre-clinical models and human tissues were used to study these molecules in an *in vivo* context and to correlate with clinical pain history, respectively. The pre-clinical method, in particular, was characterised in terms of feeding behaviour and microglial response.

In this chapter, first, nociceptive pain pathways and the main mechanisms involved in peripheral nerve injury and the development of chronic pain are described. Second, the literature on resolvins receptors and miRNAs will be reviewed and, finally, the rationale for this work with aims and objectives will be explained.

1.1.1. Nociceptive pain pathways

Nociceptive (or physiological) pain occurs in the presence of an actual or potential damaging stimulus (noxious stimulus) (Woolf and Ma, 2007). Pain sensations are transmitted from the periphery to central areas via nociceptors (high-threshold sensory afferents) that are capable of detecting noxious stimuli. Nociceptive afferents are free nerve endings (containing unencapsulated dendrites with unspecialised receptors), and they are pseudo-unipolar, meaning that both peripheral and central terminals arise from a common cell body (Basbaum et al., 2009). There are three main classes of primary afferent neurones: A β -nerve fibres, A δ -nerve fibres and C-fibres (table 1.1). Myelinated, and large diameter A β -fibres are responsible for low-threshold stimuli such as a light touch. A δ - are lightly myelinated fibres that together with unmyelinated and small diameter C-fibres respond to high-threshold stimuli (nociception). A δ -fibres can be further divided into type I and type II. Type I A δ -fibres respond to mechanical and chemical stimuli, and have a high-threshold for heat stimuli (>52°C). Type II A δ -fibres respond to thermal and chemical stimuli, and are mostly mechanically insensitive (Woolf and Ma, 2007). In general, C-fibres respond to mechanical, thermal and chemical stimuli and thus, are polymodal (Basbaum et al., 2009). Peptidergic C-fibres are capable of releasing neuropeptides (such as substance P (SP) and calcitonin-gene related peptide (CGRP)), and express the tyrosine kinase A (TrkA) receptor (targeted by nerve growth factor, NGF). In contrast, non-peptidergic C-fibres express G protein-coupled receptors (GPCR) of the Mas-related genes family and the purinergic receptor P2X3 (Basbaum et al., 2009). C-fibres convey pain sensation slower than A δ -fibres. Thus, two categories of pain can be identified: a first pain described as a distinct and localised sensation, transmitted mainly via A δ -fibres; and a second pain, more diffuse and usually longer lasting that is propagated via C-fibres (Moulin, 2013, Bhave and Gereau, 2004). Fibres from the body project to the dorsal horn of the spinal cord that is organised in different laminae (cytoarchitectonic division first proposed by Bror Rexed (Rexed, 1952)) (figure 1.1). Fibres from the orofacial region (e.g. trigeminal nerve) terminate in the brainstem, which consists of a principal nucleus (discriminative and tactile information) and a spinal trigeminal nucleus, which can be divided in three subnuclei: oralis, interpolaris and caudalis. Evidence has shown that nociceptive fibres of the trigeminal nerve terminate mainly in the trigeminal nucleus caudalis (Vc), which, similarly to the spinal cord dorsal horn, is organised in laminae (Sessle, 2005), and therefore has also been designated “medullary dorsal horn” (Sessle, 2000). Specific detail of lingual nerve projections to the

Vc are described in section 1.4 in this chapter. C-fibres and some of A δ -fibres project mainly to lamina I and II. In contrast, A β -fibres that respond to non-noxious stimuli project to laminae III, IV and V (Basbaum and Woolf, 1999, Sessle, 2005). Within the dorsal horn and Vc, post-synaptic neurones (that will carry the signal to the brain) can be specific to each type of fibres input or receive input from all three (wide dynamic range neurones, WDR neurones) (Basbaum et al., 2009, Sessle, 2005).

Table 1.1. The main classes of primary afferent neurones.

Type of fibre	Stimulus modality	Diameter	Myelination	Conduction velocity
Aβ-fibres	Light touch (non-noxious stimuli)	large	highly	> 40 ms ⁻¹
Aδ-fibres Type I	Mechanical, thermal, chemical stimuli	medium	lightly	> 2 ms ⁻¹
Aδ-fibres Type II	Thermal and chemical stimuli			
Peptidergic C-fibres	Mechanical, thermal, chemical stimuli	small	unmyelinated	< 2 ms ⁻¹
Non-peptidergic C-fibres				

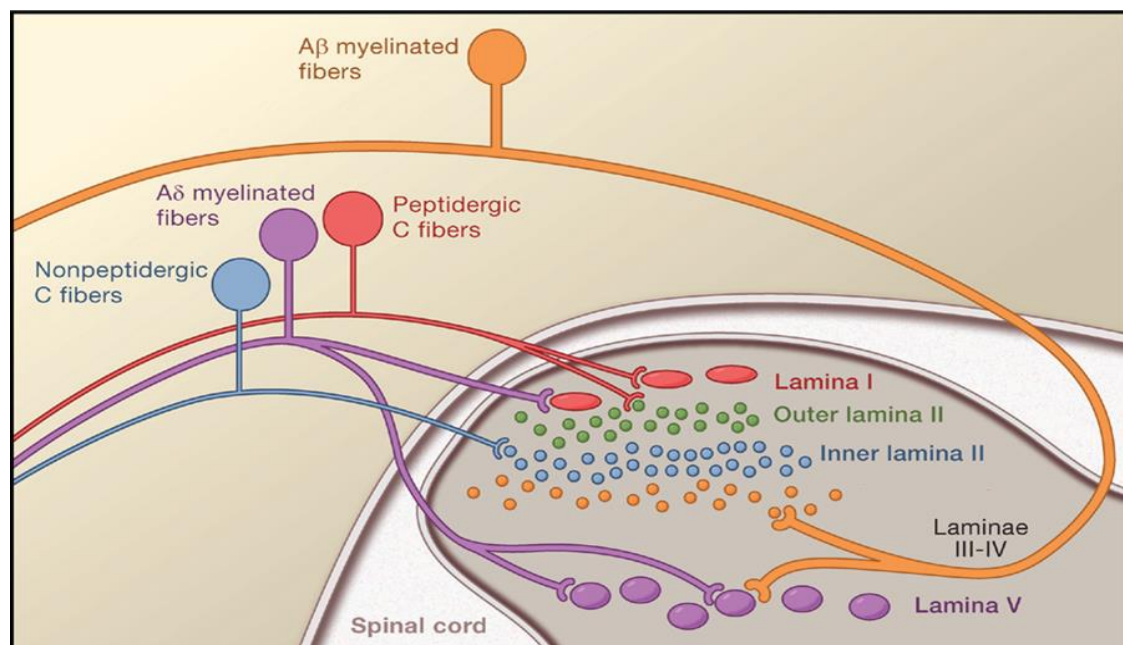


Figure 1.1. The main classes of primary afferent neurones and their organisation in the dorsal horn. The unmyelinated, peptidergic C (red) and non-peptidergic C-fibres (blue) terminate in lamina I and lamina II. The myelinated A δ -fibres (purple) project mainly to laminae I and V. Innocuous input carried by myelinated A β -fibres (orange) terminates in laminae III, IV and V. Image taken with permission from: Basbaum et al. (2009).

When nociceptors detect an intense thermal, mechanical or chemical stimulus, the information is converted into electrical signals (transduction) and transmitted along to the dorsal root ganglion (or trigeminal ganglion in the orofacial region), where the cell bodies are located, and then to central terminals (Woolf and Ma, 2007). The different noxious stimuli are transduced by specific receptors present in the nerve end terminals. Ionotropic receptors act via the influx of ions (Na^+ , K^+ or Ca^{2+} , Cl^-) (Voets et al., 2004). Other receptors such as GPCR are metabotropic, acting mainly via activation of the coupled G-protein. Consequently, different second messengers such as cyclic adenosine monophosphate (cAMP) and protein kinases A and C (PKA and PKC, respectively) or mitogen-activated protein kinases (MAPK) are activated. These second messengers can modulate the activity of ion channels (e.g. phosphorylation) and/or other cell functions (Woolf and Ma, 2007).

Transient receptor potential (TRP) ion channels are key sensory transducers, especially for thermal and chemical inputs (Julius, 2013, Patapoutian et al., 2009, Wang and Woolf, 2005). Multiple TRP ion channels have been identified, such as TRPV1-4, TRPM8 and TRPA1, each responding to specific stimuli. TRPV1-4 are heat-sensitive and permeable to Ca^{2+} , but with different threshold for temperature detection ($>43^\circ\text{C}$, 52°C , 31°C and 25°C , respectively). In addition, these receptors can also respond to chemical stimuli. For instance, TRPV1 detects capsaicin (the pungent ingredient of chilli peppers) and H^+ . This receptor is mainly expressed in $\text{A}\delta$ - and C-fibres and produces burning pain (Julius, 2013). TRPM8 is cold-sensitive (threshold of $<25^\circ\text{C}$) and also responds to menthol (Frederick et al., 2007). TRPA1 detects noxious cold ($<17^\circ\text{C}$) and is a non-selective cation channel permeable to Ca^{2+} , Na^+ , and K^+ , that also responds to mustard oil (Zygmunt and Högestätt, 2014). It is present in a subpopulation of $\text{A}\delta$ - and C-fibres (Julius, 2013, Wang and Woolf, 2005). In addition, some TRP receptors such as TRPV4 and TRPA1 have also been suggested to detect mechanical stimuli and produce mechanical hyperalgesia (Wei et al., 2009, Alessandri-Haber et al., 2006).

Voltage-gated ion channels are ionotropic receptors that upon activation and influx of ions can directly generate an action potential, transmitting the pain sensation to central terminals (conduction). In this regard, voltage-gated sodium channels (VGSC) have an important role (Lai et al., 2004, Wood et al., 2004). VGSC can be divided in tetrodotoxin (TTX)-sensitive ($\text{Na}_v1.1$, 1.2, 1.3, 1.4 1.6, 1.7) and TTX-resistant ($\text{Na}_v1.5$, 1.8 and 1.9) (Novakovic et al., 1998, Waxman et al., 1999). $\text{Na}_v1.7$, 1.8 and 1.9 are expressed mostly in nociceptive neurones and it is believed that they play a pivotal role in pain transmission

(Akopian et al., 1996, Wood et al., 2004). Potassium channels are expressed across the nervous system and are also capable of modulating action potentials (Busserolles et al., 2016). Other receptors (e.g. P2X3, ASIC) are also present in peripheral nerve endings. They respond to the different mediators that may be produced endogenously in response to tissue damage or nerve injury (Basbaum et al., 2009). These mediators can sensitise the nociceptors by lowering the noxious threshold and enhancing the pain sensation (this topic will be discussed in greater detail in section 1.1.3.2).

In central synapses, various neurotransmitters and receptors are involved (Pasero, 2004). Ionotropic receptors such as N-methyl-D-aspartate (NMDA) and α -amino-3-hydroxy-5-methyl-4-isoxazolepropionic acid (AMPA) are Ca^{2+} -permeable channels that can encode the signal in seconds. In contrast, multiple GPCR (such as the metabotropic glutamate receptor, mGluR) modulate the signal via ligand binding and activation of second messengers (thus, slower transmission) (Basbaum et al., 2009). Glutamate is a key player in the central transmission (Basbaum et al., 2009). Under normal conditions, glutamate induces temporary activation of AMPA (Milligan and Watkins, 2009). The information is, then, transmitted to higher parts in the brain where pain sensations are perceived. The synaptic connections between pre- and post-synaptic neurones can be influenced by inhibitory GABAergic and glycinergic interneurons. GABA (gamma-aminobutyric acid) and glycine are the major inhibitory neurotransmitters and have receptors (permeable to Cl^-) present in both pre- and post-synaptic neurones (Lau and Vaughan, 2014). Particularly under conditions of injury, glial cells can also be activated and influence the pain transmission (further discussed in section 1.1.3.4).

1.1.2. Neuropathic pain

Neuropathic pain is the result of a “lesion or disease of the somatosensory nervous system” as defined by the IASP. It is estimated to affect 7-10 % of the world population (Moulin, 2013). It can result from injury, drug treatment (e.g. chemotherapy), metabolic disease, infection and/or inflammation and it is described as burning, shooting, stabbing or like an electric shock (Pasero, 2004). Unlike nociceptive pain, neuropathic pain is usually sustained and chronic, undergoing multiple changes that cause abnormal processing of the sensory input (Dworkin et al., 2003). Neuropathic pain can be characterised by hyperalgesia and/or allodynia. Hyperalgesia consists of an increased response to a noxious stimulus, and allodynia corresponds to a noxious response to a normally innocuous stimulus (Ji et al., 2011). Moreover, a distinct characteristic of

neuropathic pain is the generation of pain in the absence of a detectable stimulus (Woolf and Mannion, 1999). Spontaneous pain can arise as a result of abnormal discharges from nociceptors or low-threshold A β -fibres (Costigan et al., 2009).

1.1.3. Mechanisms of chronic neuropathic pain following peripheral nerve injury

In the case of nociceptive pain, the nociceptors are activated only in the presence of a noxious stimulus and the pain sensation should cease when the initial stimulus is removed, and tissues reach homeostasis (Woolf and Ma, 2007). However, in the case of chronic pain the mechanisms involved are much more complex. Following peripheral nerve injury (PNI), afferent fibres have the ability to change their structure and function, eliciting a change in neuronal excitability that can generate action potentials to sub-threshold stimuli or even in the absence of any detectable stimulus (Vaso et al., 2014). This change in excitability is a trigger for chronic pain because it allows the transmission of a continuous pain signal to the central nervous system (CNS) that might be further amplified, creating a positive feedback loop (Gold and Gebhart, 2010). Chronic pain involves not only neurones but also glial cells such as astrocytes and microglia (at least, in male subjects). Additionally, A β -fibres that typically do not respond to noxious stimuli can be sensitised by inflammatory mediators and contribute to the development of persistent pain (Costigan et al., 2009, Linley et al., 2010). Following PNI, altered gene expression of cytokines, cytokine receptors and voltage-gated channels, increased glutamate release and receptor functions also contribute to the changes that enhance the pain signal transmission (Xu and Yaksh, 2011).

1.1.3.1. Peripheral nerve injury and neuroma formation

PNI leads to the release of pro-inflammatory mediators in order to start the regeneration process and recruit immune cells. The main cellular events that occur following PNI are represented in figure 1.2. At the cellular level, nerve sprouting starts within hours following peripheral nerve injury. It is considered that the endogenous cellular and molecular signalling response to PNI is critical and correlates with the outcome of nerve regeneration (Robinson et al., 2000). When an axon is damaged, the associated Schwann cells proliferate and alter their gene expression resulting in up-regulation of neurotrophic factors (such as NGF) and down-regulation of myelin proteins (Steed, 2011). If the axon starts to regenerate, the Schwann cells uncouple, differentiate

and re-start synthesis of myelin again; if not, they undergo apoptosis and, therefore, it is considered that they may become less suitable to support axon regeneration over time (Steed, 2011). If the axon can reach the distal end, the nerve is regenerated; however, nerve regeneration can face many obstacles. If the healing process is not controlled, the accumulation of immune cells, Schwann cells, fibroblasts and collagen fibres will surround the injured nerve and lead to the formation of a swollen and disordered mass, termed a neuroma (Vora et al., 2007). Depending on the extent of initial damage, two types of neuroma may emerge. In neuroma-in-continuity (NIC) there is still a connection between distal and proximal ends (but it may contain few number of axons); in nerve-end-neuroma (NEN) there is a complete separation between distal and proximal ends. PNI leads to intensified transcription of proteins necessary for axonal regeneration and the dysregulation of receptors that transmit sensory information together with changes in number, diameter and excitability may contribute to the sensory disturbances reported by the patients (Rosén et al., 2016). The persistent inflammatory process also contributes to the continuous activation of receptors at nerve end terminals (peripheral sensitisation). In addition, the transmission of a continuous pain signal may create an amplified signal in central neuronal circuits (central sensitisation).

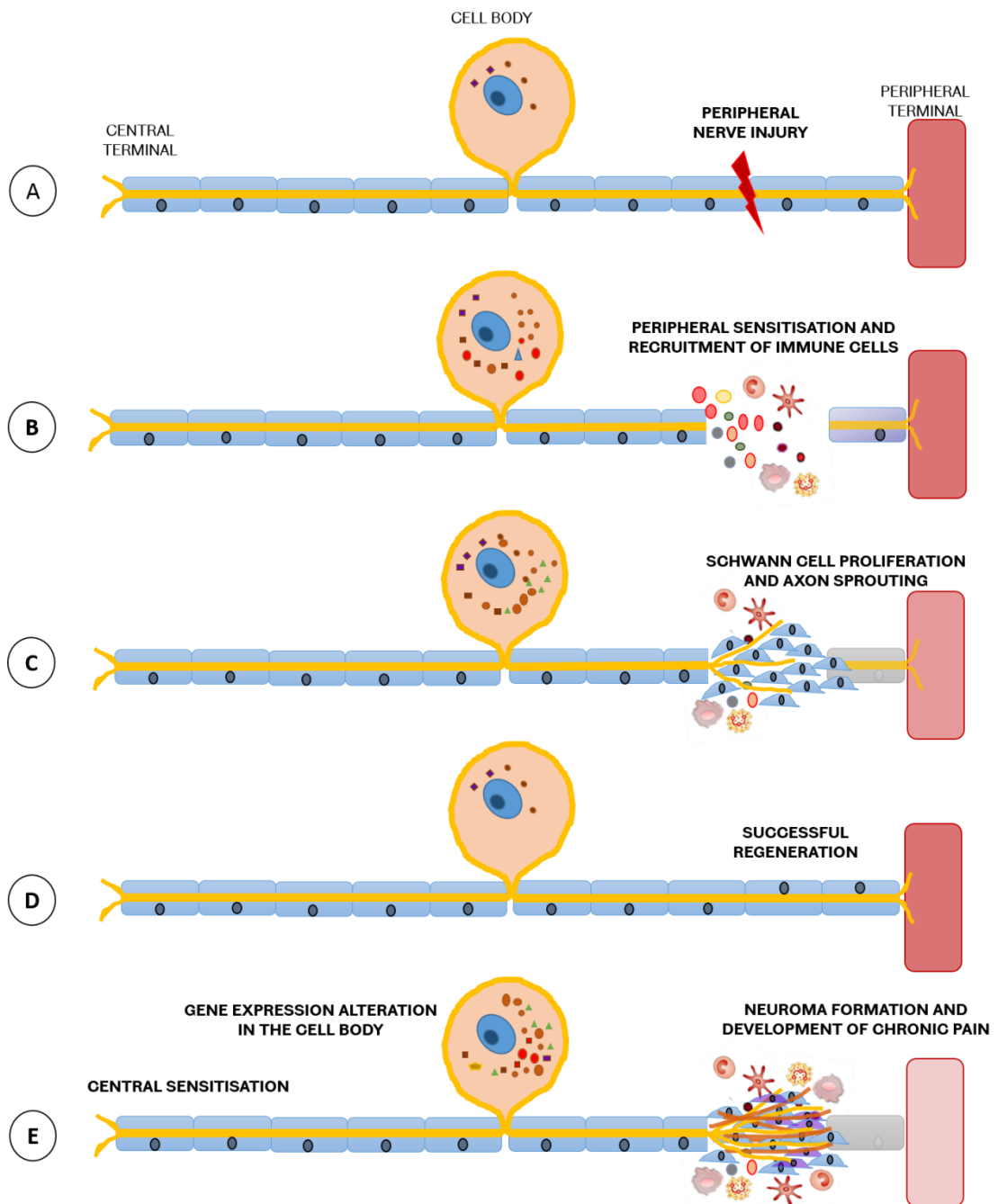


Figure 1.2. Schematic representation of peripheral nerve injury and subsequent cellular events. Injury to a peripheral nerve (A) leads to the release of pro-inflammatory mediators that will not only activate receptors present at nerve end terminals (peripheral sensitisation) but also recruit immune cells to start the healing process (B). (C) Schwann cells start to proliferate to support the starting of the axon sprouting. If the axon can re-grow and reach the distal end, the nerve is regenerated successfully (D). The uncontrolled accumulation of immune cells and fibrotic connective tissue can obstruct the axon from reaching the distal end, forming instead a disordered mass termed neuroma (E). This process is complemented with altered gene expression and the transmission of a continuous pain signal may be further amplified in central terminals (central sensitisation).

1.1.3.2. Peripheral sensitisation

PNI induces an inflammatory process that is coordinated by multiple inflammatory mediators released at the site of injury by recruited immune cells and also nerve end terminals (Cheng and Ji, 2008). The main events that lead to peripheral sensitisation are described in figure 1.3.

Bradykinin (that is produced by proteolytic enzymes within the fluid exudate) activates mast cells. Upon activation (degranulation), mast cells release pro-inflammatory mediators such as histamine and tumour necrosis factor alpha (TNF- α) that will, subsequently, recruit neutrophils and macrophages. In addition, histamine will act on H1 receptors and increase the permeability to Ca²⁺. TNF- α is also known to induce pain behaviours such as hyperalgesia and allodynia (Sorkin et al., 1997, Wagner and Myers, 1996). Platelets (and also mast cells in rats) release serotonin that directly sensitise nociceptors by binding to 5-hydroxytryptamine (5-HT) receptor. Neutrophils contribute to the recruitment of macrophages by releasing cytokines such as interleukin (IL)-1 β . Macrophages are important in the process of phagocytosis of dead tissue and apoptotic neutrophils. However, they can also release prostaglandins (PG) such as PGE2 that sensitise the receptor E prostanoid (EP), causing hyperalgesia. As a result of exocytosis or cell lysis there is an outflow of adenosine 5'-triphosphate (ATP) (Fabbretti, 2013). ATP activates P2X3 receptors, inducing transmission of pain signals (Barclay et al., 2002). In fact, different studies have shown that ATP applied to the skin or injected intradermally induces pain (Bleehen and Keele, 1977, Burnstock and Wood, 1996, Dunn et al., 2001).

Schwann cells release neurotrophic factors (such as NGF) which are important for nerve regrowth after injury (Gaudet et al., 2011). However, highly increased NGF levels in inflamed or damaged tissue (Frade and Barde, 1998) can activate the TrkA receptor, promoting the release of SP and CGRP (Weidner et al., 2000). Consequently, these factors will further cause vasodilation and plasma extravasation, amplifying the inflammatory process. A common characteristic in many inflammatory exudates is low pH (high H⁺), which activates directly acid-sensing ion channels (ASIC) (Sutherland et al., 2001). H⁺ also activates TRPV1 (Smith et al., 2002).

This 'soup' of inflammatory mediators contributes to the sensitisation of nociceptors (defined by the IASP as an increased responsiveness to a noxious stimulus, and/or recruitment of a response to a normally innocuous stimulus (IASP, 2014)).

The role of TRPV1 in heat-evoked pain and inflammatory pain has been particularly studied. For instance, a study carried out in TRPV1 knock-out mice showed that TRPV1 is important in inflammation-induced heat hyperalgesia (Caterina et al., 2000). In addition, this receptor can be sensitised by different mediators released during an inflammatory process (see figure 1.3). The role of TRPV1 in neuropathic pain is not fully understood. Hudson et al. (2001) and Walker et al. (2003) have shown the accumulation of TRPV1 at the injury site (partial sciatic nerve ligation). A study performed by Biggs et al., (2007a) in adult ferrets demonstrated that TRPV1 was increased in the early stages after a LNI but decreased to a basal level by 3 months. In addition, studies carried out in human tissues, specifically in lingual nerve neuroma, showed that TRPV1 levels were not correlated with the symptoms of pain reported (Biggs et al., 2007b). Taken together, these studies suggest that TRPV1 may be involved in the initiation but does not necessarily play a role in the maintenance of neuropathic pain. Evidence suggests that TRPA1 is activated by bradykinin and ATP and contributes to the generation of pain (Bandell et al., 2004, Jordt et al., 2004). TRPA1 is also increased after a nerve injury and has been associated with the generation of hyperalgesia (Frederick et al., 2007). However, studies conducted in human lingual nerve neuromas did not show a correlation between TRPA1 expression levels and the symptoms of pain (Morgan et al., 2009). Sodium channels such as Na_v1.7, 1.8 and 1.9 can be altered as to their level of expression and location after an injury (Ji et al., 2011, Kuner, 2010, Linley et al., 2010, Bhave and Gereau, 2004). Under normal conditions, they are distributed throughout the neuron, but studies conducted in both human and animal tissues have shown that after PNI they accumulate in abnormally high concentrations at sites of injury (Coward et al., 2000, Devor et al., 1993, Devor et al., 1989, Kretschmer et al., 2002, Bird et al., 2013, Bird et al., 2007, Davies et al., 2006). In fact, two studies conducted in human tissues by Bird et al., (2007) and (2013) demonstrated that, particularly, Na_v1.7, 1.8 and 1.9 were expressed in human lingual nerve neuroma, and Na_v1.8 levels of expression were correlated with symptoms of pain following LNI. Sodium channel, voltage-gated, type III, alpha subunit (Na_v1.3) levels of expression in the peripheral nervous system decrease following birth (Suzuki et al., 1988), but it has been demonstrated that after a peripheral injury the expression of Na_v1.3 increases in dorsal root ganglion (DRG) neurones (Waxman et al., 1994, Dib-Hajj et al., 1999, Black et al., 1999). In contrast, the expression of Na_v1.3 in trigeminal system does not seem to be correlated with injury (ferret trigeminal nerve injury) (Davies et al., 2006). Sodium Channel, Voltage-Gated, Type VII, Alpha subunit (Na_v1.7), in turn, has been

suggested to play a role in inflammatory but not in neuropathic pain (Nassar et al., 2005, Nassar et al., 2004), as Na_v1.7 knockout mice still develop mechanical allodynia after spinal nerve injury.

1.1.3.3. Central sensitisation and neuronal plasticity

In central terminals, as a result of the hyperactivity of nociceptors, there is an increased release of neurotransmitters and neuromodulators such as glutamate, SP, CGRP and ATP (figure 1.4). This leads to the hyperactivity of second-order neurones and facilitates the transmission of pain information to the brain (central sensitisation) (Guillot et al., 2012, Kuner, 2010). The NMDA receptor is blocked by Mg²⁺ under normal conditions (Milligan and Watkins, 2009). A co-release of glutamate and neuromodulators such as SP and CGRP mediates NMDA activation (loss of Mg²⁺ block) leading to cell depolarisation and influx of Ca²⁺. The AMPA receptor is also sensitised by glutamate, and the accumulation of intracellular Ca²⁺ activates multiple Ca²⁺-dependent signalling pathways and second messengers such as Ca²⁺/calmodulin-dependent kinase-II (caMKII) (Basbaum et al., 2009). These events can further sensitise AMPA and NMDA receptors and induce the release of neurotransmitters and neuromodulators (Woolf and Salter, 2000). Activation of other receptors such as purinergic receptors by ATP, mGluR by glutamate, neurokinin 1 receptor by SP, calcitonin receptor-like receptor (CRLR) by CGRP and the release of brain-derived neurotrophic factor (BDNF) contribute to increased pain transmission. In addition, neural plasticity (i.e. the capacity of neurones to alter their function, chemical profile, or structure) is necessary for the maintenance of persistent pain (Woolf and Salter, 2000). Long-term changes include modifications in gene expression at the transcriptional level (Costigan et al., 2009, Woolf and Ma, 2007). This will result in an increase in the production of receptors and ion channels (e.g. TRP channels and VGSC) and central mediators (BDNF, SP) leading to phenotypic changes within the nociceptive system that contribute for an established phase of chronic pain (Woolf and Salter, 2000). Another important component for central sensitisation is disinhibition. Under normal conditions, the release of GABA and glycine from inhibitory interneurons decreases the excitability of nociceptors. However, under conditions of injury, this inhibition can be lost, contributing to hyperalgesia (see figure 1.4) (Lau and Vaughan, 2014). For instance, the release of PG such as PGE₂ and BDNF in central terminals seems to block inhibitory neurotransmission (Basbaum et al., 2009, Ahmadi et al., 2002).

1.1.3.4. Glial cells activation

Glial cells (oligodendrocytes, astrocytes and microglia) are part of the CNS corresponding to around 70% of the total cell population. These cells surround neurones, and besides providing protection/nutrition, they also play an important role in the generation and maintenance of persistent pain (Guillot et al., 2012). Oligodendrocytes are responsible for the production of the myelin sheath in the CNS and a direct role in chronic pain has not been reported to date. Microglial cells correspond to 5-10% of the glia (Moulin, 2013). Microglia express the major histocompatibility complex (MHC), which has a role in presenting antigens to T lymphocytes, and they also release several mediators under conditions of inflammation and injury (Piehl and Lidman, 2001). Astrocytes correspond to the largest population of glial cells in the CNS. They regulate extracellular pH, ion and neurotransmitter concentration (such as glutamate), thus are essential for the maintenance of homeostasis (Milligan and Watkins, 2009).

Under normal conditions, microglia and astrocytes are quiescent but upon activation they undergo hypertrophy, proliferate and increase expression of different proteins and mediators. For instance, astrocytes increase the production of glial fibrillary acidic protein (GFAP; it is used as an astrocyte marker).

Evidence has suggested that the proliferation of astrocytes starts relatively late and progresses slowly, but is sustained for a longer period when comparing with the microglial response (Raghavendra et al., 2003, Hashizume et al., 2000). Both astrocytes and microglia express receptors capable of detecting multiple mediators (figure 1.4). For instance, following peripheral nerve injury, nociceptor terminals release fractalkine (a membrane-bound chemokine) that activates the chemokine receptor CX3CR1 (Verge et al., 2004) and heat shock proteins (HSP) that can bind to toll-like receptors (TLR) (Tanga et al., 2005), leading to mobilisation of internal Ca^{2+} . As a consequence, pro-inflammatory cytokines such as TNF- α , IL-1 β and IL-6 are released from microglial cells (Winkelstein et al., 2001), creating an excitatory positive-feedback loop that contributes to central sensitisation (Ji et al., 2013). In addition, ATP binds to P2X4 in microglia causing the release of BDNF that will interfere in the inhibitory actions of GABA (Coull et al., 2005). In astrocytes, there is also a reduction in the uptake of glutamate, leading to hyperexcitability of post-synaptic neurones (Ji et al., 2013).

Of note, the role of microglial cells in pain has been particularly studied over the past few years and evidence suggests that they may be implied in pain sex differences. Work conducted by Sorge et al. (2011) has demonstrated that Toll-like receptor 4

(expressed in microglial cells) contributed to the development of neuropathic pain sensitivity only in male mice, in a mechanism dependent on testosterone. Further studies also concluded that P2X4R-induced release of BDNF by microglia was only present in male mice (Sorge et al., 2015). It has been suggested that female mice use a different mechanism, as equal levels of pain behaviour were observed in both male and female mice. Female mice seem to use preferentially adaptive immune system, with infiltrating T cells being present following injury. Interestingly, T cell-deficient female mice respond to a glial inhibitor and reverse the pain behaviour (Sorge et al., 2015). Microglia activation will be further discussed in more detail in chapter 4, in particular, in response to the LNI in the male rat.

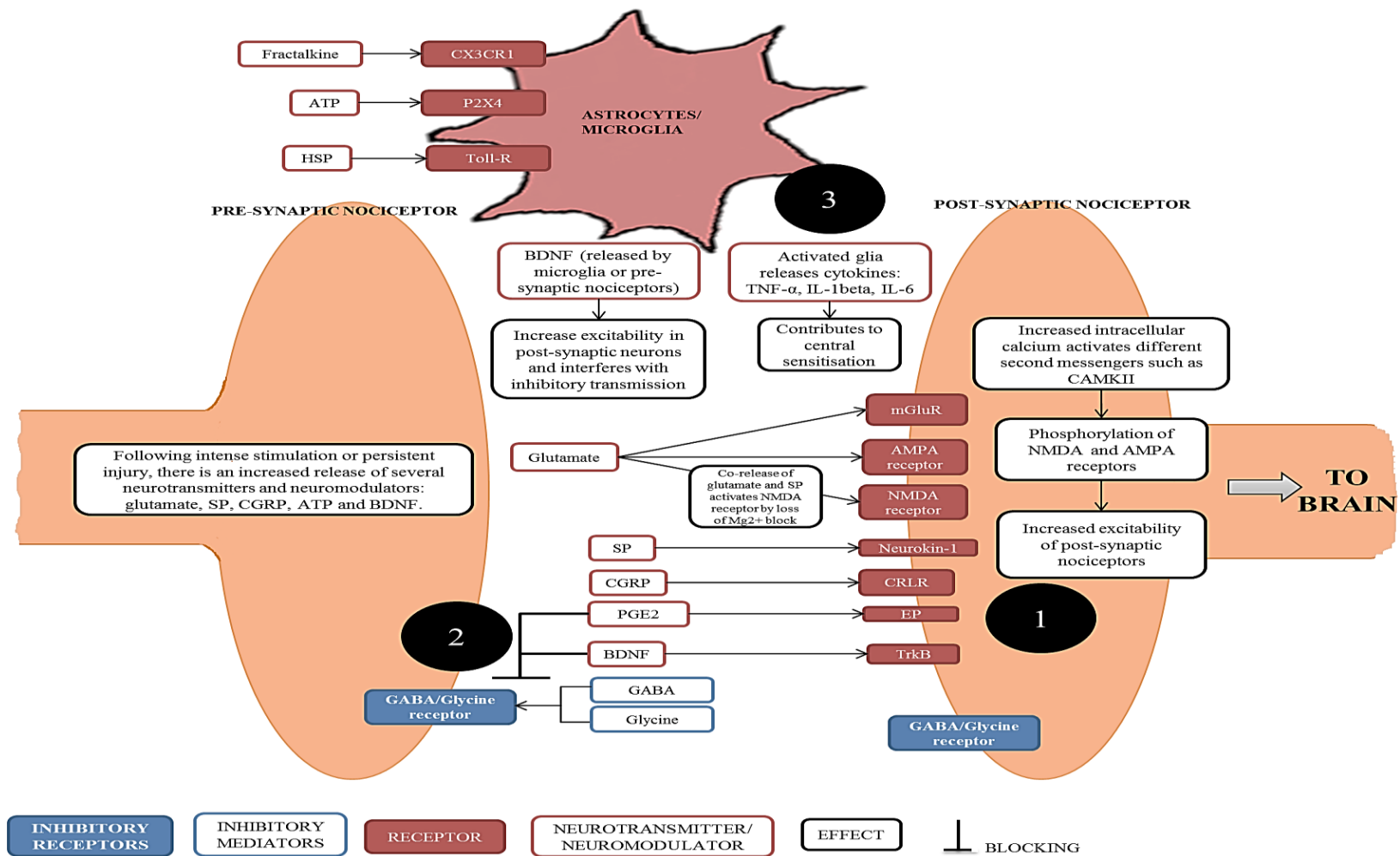


Figure 1.4. The sequence of events that contribute to central sensitisation. 1) Increased release of neurotransmitters and neuromodulators and increased activity of post-synaptic receptors. 2) Loss of GABA and glycine inhibition (disinhibition). 3) Glial cells activation (microglia only in male subjects).

1.2. Resolvin receptors

1.2.1. Resolvins

Resolvins were originally isolated from inflammatory exudates in the murine air pouch model of acute inflammation (after injection of TNF- α) (Serhan et al., 2000, Serhan et al., 2002) and later they were also found in human blood (Arita et al., 2005b, Hong et al., 2003, Mas et al., 2012). Resolvins are endogenous lipid mediators derived from the *omega*-3 polyunsaturated fatty acids (PUFA) present in dietary essential fat (Serhan et al., 2002). The benefits of omega-3 PUFA on human health have been known since the beginning of the twentieth century. It was demonstrated that the exclusion of lipids from the diet resulted in several pathologies and premature death (Burr, 1929). More recently, the ‘Gruppo Italiano per lo Studio della Streptochinasi nell'Infarto Miocardico’ (GISSI; Italian group for the study of the survival of Myocardial Infarction) recruited over 11,000 patients who had survived a myocardial infarction. In a randomized trial, they were supplemented with 1 g daily of *omega*-3 PUFA (in addition to aspirin treatment). The results revealed that the risk of death in the group treated with *omega*-3 PUFA was significantly decreased (GISSI, 1999). Several explanations were presented for such benefits: *omega*-3 PUFA function as direct antagonists of arachidonic acid (AA), thus, inhibiting the formation of PG or leukotrienes, or serve as alternative substrate generating less potent products, among others (Connor, 2000). However, the lack of molecular evidence together with the high doses required, led scientists, particularly in the Serhan laboratory in Harvard Medical School, to question whether the omega-3 PUFA intake would be metabolised into bioactive compounds. By means of an unbiased system approach with liquid chromatography tandem-mass spectrometry (LC-MS/MS) based lipidomics it was possible to identify different bioactive products during the resolution phase of acute inflammation (after injection of TNF- α). These molecules activated mechanisms of resolution and therefore were named specialised pro-resolving mediators (Arita et al., 2005a, Hong et al., 2003, Serhan et al., 2002, Serhan et al., 2000). Among these mediators are resolvins and so called because they are produced during the resolution phase of inflammation via cell-cell interactions (Serhan et al., 2000).

1.2.1.1. Biosynthesis and identification of different resolvins

The *omega*-3 fatty acids eicosapentaenoic acid (EPA) and docosahexaenoic acid (DHA) are enzymatically metabolised to E-resolvins and D-resolvins, respectively, in a multi-step reaction during endothelial cell-neutrophil interactions that occur in the resolution of inflammation (figure 1.5). Resolvins derived from the *omega*-3 EPA (E-series) are metabolized via acetylated cyclooxygenase 2 (COX-2) or cytochrome P450 and 5-lipoxygenase (LOX). Resolvins derived from the *omega*-3 DHA (D-series) are metabolised via 15-LOX and 5-LOX. D-series resolvins can also use the biosynthetic pathway of the acetylated COX-2 and 5-LOX to obtain aspirin triggered (AT)-resolvins (for a complete review, please, see Bannenberg and Serhan, 2010). It is believed that the treatment, in particular, with aspirin enhances the production of these molecules (Serhan et al., 2002). The acetylation of COX-2 by aspirin stops the production of prostaglandins but the acetylated enzyme is still able to generate other bioactive compounds, such as resolvins (Arita et al., 2005b, Bannenberg and Serhan, 2010, Serhan et al., 2002). Several resolvins have been identified, each with a unique structure and a stereospecific activity. Within the D-series, resolvin (Rv) D1 was the first resolvin identified (Serhan et al., 2002). It was primarily isolated from inflammatory exudates in vivo (murine air pouch model of inflammation) and later in human blood (Mas et al., 2012). It was also found in trout brain (Hong et al., 2005), suggesting the evolutionary conservation of this resolvin. AT- RvD1 differs from RvD1 in the stereochemistry of the 17-OH group. Even though, evidence suggests that both RvD1 and AT-RvD1 do not show significant differences in potency, AT-RvD1 seems to be more resistant to catalyse than RvD1 (Sun et al., 2007). Additional members of this family - RvD2, D3 and D5 - were identified, arising from similar routes, but with a distinct chemical structure and other potential roles (Dalli et al., 2013, Chiang et al., 2012, Spite et al., 2009, Mas et al., 2012).

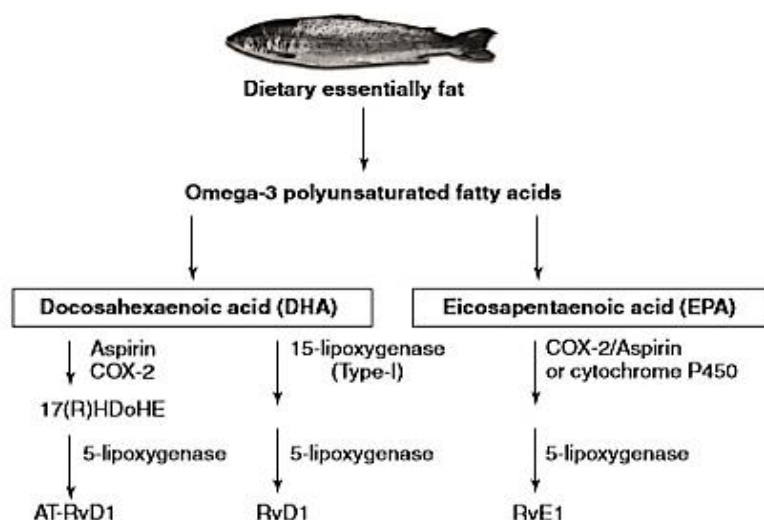


Figure 1.5. Biosynthesis of resolvins. Resolvins are derived from omega-3 PUFA prevenient from dietary essential fat (especially enriched in fish). Multiple synthetic enzymes, including COX-2, cytochrome P450, and 5- and 15-LOX are involved. RvD1 and AT-RvD1 are derived from DHA, whereas Rv1 is derived from EPA. For a detailed review of the biosynthesis of resolvins please see Bannenberg and Serhan, 2010. Image taken with permission from Ji et al. (2011).

For instance, RvD3 and AT-RvD3 appear in the late phase of resolution of inflammation (Dalli et al., 2013). In the E-series, RvE1 was the first resolvin identified in exudates from murine dorsal pouches after treatment with aspirin and EPA (Serhan et al., 2000). In humans, RvE1 was also identified in individuals taking aspirin (Arita et al., 2005a). RvE1 is also produced by *Candida albicans* (Haas-Stapleton et al., 2007). More recently, RvE2 and RvE3 have also been identified (Isobe et al., 2012, Tjonahen et al., 2006). Further studies in healthy volunteers have characterised the presence of resolvins in human blood and breast milk. Psychogios et al. (2011) reported that RvE1 and RvD1 were present in plasma collected from healthy volunteers taking *omega-3* PUFA. Mas et al. (2012) identified RvD1 and RvD2 in human plasma and serum following supplementation. More recently, Weiss et al. (2013) demonstrated the presence of resolvins in human milk during the first month of lactation. The levels of resolvins seem to reflect *omega-3* dietary intake (Arita et al., 2005a), and during an inflammatory response the biosynthesis of resolvins increases with time (Mas et al., 2012). However, due to an increase in the sensitivity of the LC-MS-MS technique, a recent publication has reported the presence of some resolvins (such as RvD1 and RvE1) in human blood of healthy volunteers in picogram to nanogram range (bioactive range) without known

supplementation with *omega*-3 PUFA (Colas et al., 2014). In addition, resolvins were also identified in lymphoid tissues in the bioactive range of action (Colas et al., 2014). Because resolvins were originally isolated from inflammatory exudates during the resolution phase, their role in the regulation of inflammation and associated diseases has been particularly studied (discussed in section 1.2.1.2). However, further investigation is required, for instance, to evaluate whether diseases characterised by persistent inflammation result from failure in the resolution because of the absence of specific mediators (e.g. resolvins) or because of changes in their receptors and pathways (Fredman et al., 2012). In addition, resolvins are endogenous lipid mediators and, thus are rapidly metabolised (Hong et al., 2008). Therefore, some studies have focused in the synthesis of more stable analogues (Ji et al., 2011). For instance, adding substitutes to the C18 makes RvE1 analogues resistant to oxidation but keeps similar activity to RvE1 *in vivo* (Arita et al., 2006). In fact, an RvE1 analogue is in clinical trials for ophthalmic indications (Serhan, 2014).

1.2.1.2. Actions of resolvins in disease models

Resolvins have both anti-inflammatory and pro-resolution actions: they block the production of pro-inflammatory mediators, regulate leukocyte trafficking to inflammatory sites and, at the same time, promote the clearance of neutrophils (Serhan et al., 2008). In addition, recent studies have shown that resolvins can attenuate chronic pain without affecting basal pain sensitivity (Xu et al., 2013, Ji et al., 2011). A summary of the main actions of resolvins is described in table 1.2.

Anti-inflammatory and pro-resolving actions of resolvins

Inflammation is characterised by the release of several pro-inflammatory mediators derived from AA, such as PG and leukotrienes that regulate oedema and neutrophil recruitment (Serhan and Savill, 2005). With time, leukocyte recruitment increases and monocytes and macrophages appear. After the initial pro-inflammatory events, there is a class switch and mobilisation of *omega*-3 PUFA from circulation and formation of pro-resolving mediators (Mittal et al., 2010). The acute inflammatory response has a protective role that will culminate in the restoration of tissue homeostasis (Freire and Van Dyke, 2013). However, if left uncontrolled, this response fails to exert the protective function, and results in several chronic conditions (Bannenberg et al., 2007, Freire and Van Dyke, 2013). The resolution of inflammation is now understood as an active process

rather than the traditional view that consisted in the simple termination of pro-inflammatory events (Fredman et al., 2012, Freire and Van Dyke, 2013). Resolution involves the biosynthesis of specialised molecules such as resolvins (Serhan and Chiang, 2013). Inflammation is a common component in many diseases and, in fact, a growing body of evidence is suggesting that the failure in the resolution process of inflammation may result in several chronic pathologies such as atherosclerosis (Tabas, 2010) and Alzheimer's (Wang et al., 2015). The role of resolvins in treating inflammatory conditions has been demonstrated through several studies using well-characterised animal models of inflammation. In a mouse air pouch model (inflammatory model that allows the isolation of contained inflammatory exudates and their direct lipidomic analysis), RvD1 and RvE1 (100 ng/mouse) were able to stop neutrophil recruitment after TNF- α injection (Serhan et al., 2002, Serhan et al., 2000). In a zymosan-induced peritonitis model, RvE1 regulated cytokine and chemokine expression; RvE1 was also responsible for stopping neutrophil infiltration, induced macrophages phagocytosis, and regulated dendritic cell migration (Arita et al., 2005a). Krishnamoorthy et al. (2010) showed that RvD1 promotes macrophages phagocytosis and reduces actin polymerization (an important event for neutrophil recruitment). Inflammation is highly associated with adipose tissue (Bannenberg et al., 2005). In obese-diabetic mice, RvD1 reduced the accumulation of macrophages in the adipose tissue and improved insulin sensitivity (Hellmann et al., 2011). RvD2 regulated leukocytes and controlled microbial sepsis (Spite et al., 2009). RvD3 application resulted in decreased neutrophil infiltration and stimulation of IL-10, in both murine peritonitis and dorsal skin pouches (Dalli et al., 2013). In a murine peritoneal *E. coli* infection, RvD5 promoted phagocytosis of *E. coli* and led to the inhibition of TNF- α (Chiang et al., 2012). In the same study, RvD5 reduced the antibiotic requirements for bacterial clearance.

Analgesic actions of resolvins

The presence of multiple mediators that characterises an inflammatory process, can lead to the sensitisation of nociceptors, and in the particular case of inflammatory pain, inflammation is a crucial component (Sommer and Birklein, 2011). In 2010, Xu and colleagues tested, for the first time, the role of RvE1 and RvD1 in inflammatory pain. Three different models of inflammatory pain were used: Carrageenan (CRG), that produces heat hyperalgesia, paw oedema and neutrophil infiltration; Intraplantar injection of formalin, that creates two phases of spontaneous pain behaviour; and complete

Freund's adjuvant (CFA) that produces inflammatory pain for weeks, with mechanical allodynia and heat hyperalgesia. The results showed that resolvins can reduce inflammatory pain symptoms, without changing basal pain sensitivity, at nanogram dose ranges (Xu et al., 2010). Intraplantar pre-treatment with resolvins reduced CRG-elicited paw oedema, neutrophil infiltration and heat hyperalgesia. Pre-administration of RvE1 in the spinal cord (intrathecal) reduced the second phase of formalin-induced inflammatory pain. Intrathecal injection of RvE1, three days after CFA injection, also temporarily reduced CFA-induced heat hyperalgesia in a dose-dependent manner. Of note, Xu et al. (2010) have also showed that DHA and EPA alleviate inflammatory pain but the doses required were 1000 times higher to that of resolvins. In a mouse model of postoperative pain (hindpaw incision), spinal administration (intrathecal) of RvD1 attenuated mechanical allodynia (Xu et al., 2010). Pre-treatment with resolvins also alleviated pain behaviour induced by TRPV1/A1 agonists (Park et al., 2011). RvD2 and RvE1 inhibited capsaicin actions on TRPV1 and RvD2 and RvD1 blocked mustard oil actions on TRPA1. In adjuvant-induced arthritis, AT-RvD1 also reduced hyperalgesia (Lima-Garcia et al., 2011). Xu et al. (2013) reported that the intrathecal pre-treatment with RvE1 prevented chronic constriction injury (CCI)-induced mechanical allodynia (neuropathic pain model). RvE1 (intrathecal post-administration) also reduced mechanical allodynia and heat hyperalgesia for 2 h, three weeks after spinal nerve ligation (SNL). Thus, RvE1 may also be used to treat established neuropathic pain in the late phase. All together, these studies suggest that the analgesic effect is time-dependent: the best results were observed when the resolvins were administered in advance or in the first hour after injury.

1.2.1.3. Resolvins mechanisms of action

One of the mechanisms that has been identified for resolvin action is their blocking of TRP receptors, particularly TRPV1 and TRPA1 (Park et al., 2011). However, the inhibitory actions of resolvins are not generated by direct antagonism, instead they seem to be mediated via specific GPCRs (discussed in further detail in section 1.2.2) (Ji et al., 2011, Park et al., 2011). This permits a clear separation of resolvins from classic TRP antagonists that show strong side effects, such as hyperthermia (Gavva et al., 2008). A further mode of action of resolvins seems to be the regulation of microglia activation (Xu et al., 2013). RvE1 prevented the up-regulation of the microglia marker Iba1, but the expression of astrocyte marker GFAP was not altered. Resolvins seem to function without disrupting normal physiological mechanisms, thus it has been reported that they are not

immunosuppressive (Serhan, 2010). However, because they act on immune cells it is necessary to investigate potential side effects (Ji et al., 2011). Resolvins through GPCR act in diseases associated with pain and inflammation due to the mentioned properties: anti-inflammatory, pro-resolving and analgesic (see table 1.2) (Serhan et al., 2008, Ji et al., 2011).

Table 1.2. Bio-actions of resolvins.

Resolvin	Model	Action/Effect	References
RvD1	Mouse dorsal air pouch	Stops neutrophil recruitment	(Serhan et al., 2002)
	After LTB ₄ administration	RvD1 blocks actin polymerisation and CD11b up regulation	(Krishnamoorthy et al., 2010)
	Zymosan-stimulated peritonitis	Attenuates leukocyte infiltration and neutrophil recruitment Limits LTB ₄ synthesis	(Norling et al., 2012) (Fredman et al., 2014)
AT-RvD1	Murine peritonitis	Stops neutrophil infiltration and trans endothelial migration, suppress cytokine production	(Sun et al., 2007)
	Mouse TMJ inflammation	Protects inflammation in the TMJ	(Norling et al., 2011)
	Adjuvant-induced arthritis	Decreases joint stiffness and hyperalgesia	(Lima-Garcia et al., 2011)
RvD2	mouse burn injury	Prevents thrombosis and subsequent dermal necrosis; Inhibits TNF- α and IL-1 β	(Bohr et al., 2013)
	Inflammatory pain	Inhibits TRPV1 and TRPA1 activation; Inhibits spontaneous pain	(Park et al., 2011)
	Caecal ligation and puncture	Decreases cytokine production and neutrophil recruitment; increases peritoneal mononuclear cells and macrophage phagocytosis.	(Spite et al., 2009)
RvD3 AT-RvD3	Peritonitis	Blocks neutrophil transmigration and enhances macrophage phagocytosis and efferocytosis	(Dalli et al., 2013)
RvD5	Murine peritoneal E.coli	Enhances phagocytosis of E.coli and reduces TNF- α	(Chiang et al., 2012)
RvE1	Mouse dorsal air pouch	Stops neutrophil migration	(Serhan et al., 2000)
	Zymosan-induced peritonitis	Blocks IL-12 production and stops neutrophil recruitment	(Arita et al., 2005a)
	Spinal nerve injury	Temporarily reduces mechanical allodynia and heat hyperalgesia	(Xu et al., 2013)
	CCI	Prevents mechanical allodynia	
	Formalin	Reduces second phase of formalin-induced inflammatory pain	(Xu et al., 2010)
	CRG	Reduces neutrophil infiltration, reduces heat hyperalgesia, reduces IL-1 β , IL-6, TNF- α	
	CFA	Reduces heat hyperalgesia	
	Hindpaw incision	Attenuates mechanical allodynia	
	Capsaicin	Inhibits capsaicin-induced heat hyperalgesia	(Park et al., 2011)
RvE2	Zymosan-induced peritonitis	Induces macrophage non-phlogistic phagocytosis of apoptotic neutrophils	(Oh et al., 2012)
RvE3	Zymosan-induced peritonitis	Limits neutrophil infiltration	(Isobe et al., 2012)

LTB₄: Leukotriene B₄ (pro-inflammatory mediator); TMJ: Temporomandibular joint; CCI: Chronic constriction injury; CRG: Carrageenan; CFA: Complete Freund's adjuvant.

1.2.2. Receptors

The actions of resolvins are mediated by GPCRs (Im, 2012). As represented in figure 1.6, GPCRs are seven transmembrane (TM) proteins (also called 7TM receptors) that convey a variety of physiological signals via GTP-binding proteins. When activated, the GPCR initiates a cascade reaction that results in the dissociation of the G protein into subunits $G\alpha$, $G\beta$ and $G\gamma$. To further transmit the signal each subunit stimulates different second messengers (Kobilka, 2007).

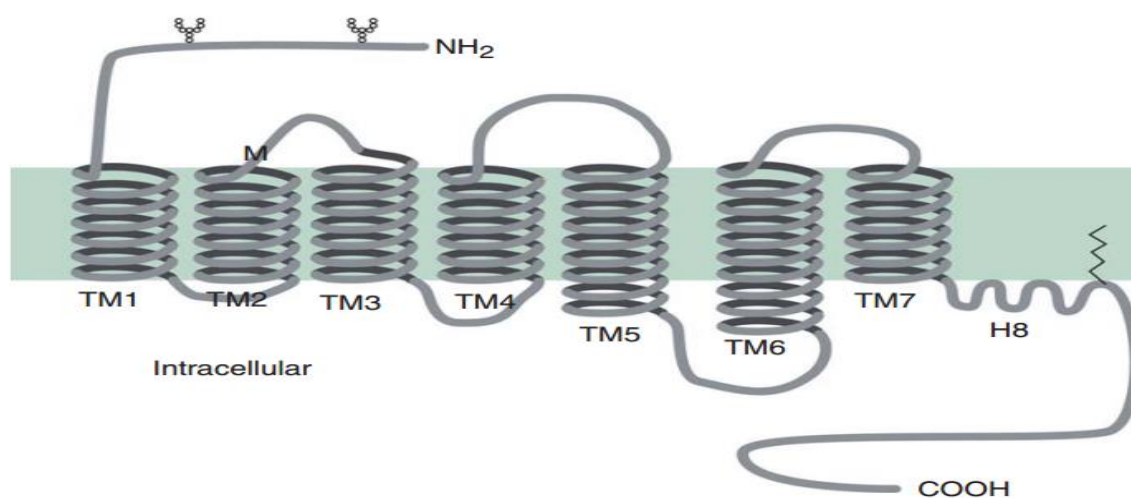


Figure 1.6. Secondary structure common to GPCR. GPCR are seven transmembrane proteins with an extracellular N-terminal domain and an intracellular C-terminal. It is connected to different sub-units of G proteins (not shown) that will activate different second messengers; TM: transmembrane. Taken with permission from: Kobilka (2007).

Initial receptor screening studies used pertussis toxin (PTX, a specific inhibitor for $G\alpha_i$ -coupled GPCR) to verify whether GPCR were involved in resolvins signal transduction. The PTX treatment reduced resolvins actions, suggesting that resolvins act via PTX-sensitive GPCR (Arita et al., 2005a, Krishnamoorthy et al., 2010). To date, four GPCR have been identified as resolvins receptors: FPR2/ALX (lipoxin A4 receptor), GPR32 (G protein-coupled receptor 32), ChemR23 (chemerin receptor 23) and BLT1 (leukotriene B₄ receptor 1) (see table 1.3).

Table 1.3. Resolvins and their receptors.

RECEPTOR	RESOLVIN	METHOD	REFERENCE
GPR32	RvD1, AT-RvD1	GPCR β -arrestin reporter system ^b ; Radioligand specific binding; ShRNA knockdown; Ligand selectivity using ECIS ^c .	(Krishnamoorthy et al., 2010)
	RvD3, AT-RvD3	GPCR β -arrestin reporter system ^b ; Ligand selectivity using ECIS ^c .	(Dalli et al., 2013)
	RvD5	GPCR β -arrestin reporter system ^b .	(Chiang et al., 2012)
BLT1	RvE1	Luciferase-reporter system ^a ; Radioligand specific binding; PTX sensitivity	(Arita et al., 2007)
FPR2/ALX	RvD1, AT-RvD1	GPCR β -arrestin reporter system ^b ; Radioligand specific binding; ShRNA knockdown; Ligand selectivity using ECIS ^c .	(Krishnamoorthy et al., 2010)
ChemR23	RvE1	Luciferase-reporter system ^a ; Radioligand specific binding; PTX sensitivity.	(Arita et al., 2005a, Arita et al., 2007, Xu et al., 2010)

a- Screening system for identifying receptor candidates, which tests the ability of receptor-ligand coupling to counteract TNF- α NF- κ B activation (see Arita et al. (2005a)).

b- Investigates, in a ligand-dependent way, the coupling of intracellular β -arrestin with the cytoplasmatic domain of GPCR. This system allows monitoring of ligand-receptor interactions without classic second messengers involved (see Krishnamoorthy et al. (2010)).

c- Studies impedance changes upon ligand binding to receptors (see Krishnamoorthy et al. (2012)).
ECIS: electrical cell substrate impedance sensing; PTX: Pertussis toxin.

The actions of RvD1 are mediated by FPR2/ALX and GPR32 (Krishnamoorthy et al., 2010). It seems that, at low concentrations of this resolvins, the GPR32 is activated and an increase in concentration activates FPR2/ALX (Norling et al., 2012). This suggests that at least in neutrophils, GPR32 has a homeostatic/physiological role, whereas FPR2/ALX seems to be activated in pathological situations. GPR32 is also activated by RvD3, AT-RvD3 (Dalli et al., 2013) and RvD5 (Chiang et al., 2012). FPR2/ALX and GPR32 do not seem to be linked to the classic second messengers of GPCR signal transduction, as they do not activate Ca²⁺ or cAMP signalling in isolated human neutrophils (Krishnamoorthy et al., 2010).

The actions of RvE1 are mediated by ChemR23 and BLT1 (Arita et al., 2005a, Arita et al., 2007). RvE1 functions as an agonist for ChemR23. RvE1 also binds to BLT1 in neutrophils, being a partial agonist. Of note, some authors questioned the binding of RvE1 to ChemR23 (Bondue et al., 2011, Davenport et al., 2013). However, these reviews were

based on unpublished data, and no information was available regarding the confirmation of synthesis and structure of the resolvins used for that claim. Arita et al. (2005a) using a screening system that tested the ability of RvE1 to inhibit TNF α -induced NF- κ B activation in HEK293 cells, after transfection with candidate GPCR, demonstrated the high-affinity for ChemR23 (see table 1.3). Further studies with tritium-labelled RvE1 (synthetic integrity confirmed by HPLC) have demonstrated that RvE1 binds to ChemR23-transfected Chinese hamster ovary (CHO) cells (Arita et al., 2005a). Thus, with the data available, ChemR23 must be accepted as RvE1 receptor. ChemR23 and other GPCR such as FPR2/ALX have the capacity to form heterodimers (de Poorter et al., 2013) and Krishnamoorthy et al. (2010) suggested that it is possible that resolvins could signal through heterodimeric GPCR.

Of note, the GPCR implicated in resolvins actions belong to the same GPCR family rhodopsin (based on sequence similarity and phylogenetic inference) and present highly conserved regions (Krishnamoorthy et al., 2010).

GPR32

GPR32 (also known as probable G-protein coupled receptor 32) is an orphan GPCR. GPR32 is a member of the rhodopsin family and consists of 356 deduced amino acids (Bäck et al., 2014). The gene that encodes GPR32 maps to the human chromosome 19. It shares a sequence identity of 35-39% homology with members of the chemoattractant receptor sub-family, especially with FPR2/ALX (Marchese et al., 1998). It was identified in 2010 as a RvD1 receptor (Krishnamoorthy et al., 2010). As mentioned above also RvD3 and RvD5 mediate, at least, part of their actions by binding to GPR32 (Chiang et al., 2012, Dalli et al., 2013). To date, very little is known about this receptor. However, evidence suggests that the role of RvD1 in reducing neutrophil recruitment and in stimulating macrophage phagocytosis is in part mediated via the GPR32 receptor (Krishnamoorthy et al., 2010). Expression levels of GPR32 were increased following monocyte exposure to zymosan for 24 to 48 h (Krishnamoorthy et al., 2010). Norling et al. (2012) suggested that GPR32 is involved in the regulation of homeostasis, at least, in neutrophils. The mRNA levels of this receptor have also been identified in macrophages, arterial and venous tissue and also in monocytes and neutrophils (Krishnamoorthy et al., 2010). Of note, the murine orthologue of human GPR32 has not been identified to date.

However, an orthologue has been identified in the chimpanzee, which is a pseudogene (similar but non-functional gene) in mouse and rat (Krishnamoorthy et al., 2010) .

BLT1

BLT1 is a GPCR that belongs to the rhodopsin family and it is also known as a leukotriene B₄ (LTB₄) receptor (Lundeen et al., 2006)). It consists of 352 deduced amino acids. Two receptors for LTB₄ have been recognised: high-affinity BLT1 and low-affinity BLT2 (Lundeen et al., 2006). Both genes are located near to each other in the human genome (chromosome 14). BLT1 is highly expressed in vascular smooth cells, endothelial cells and leukocytes, especially granulocytes (Bäck et al., 2014, Qiu et al., 2006), in contrast with BLT2 that is ubiquitously expressed (Bäck et al., 2014). BLT1 and BLT2 share 45% amino acid sequence homology (Lundeen et al., 2006). BLT1 plays an important role in many chronic diseases such as arthritis, atherosclerosis, asthma and cardiovascular diseases (Arita et al., 2007) and mediates pro-inflammatory actions of LTB₄. LTB₄ is produced by activated leukocytes (Goldman and Goetzl, 1984). This chemotactic molecule promotes the recruitment of neutrophils, eosinophils and macrophages to inflamed sites (Zhai et al., 2010). Initial studies demonstrated that RvE1 attenuates neutrophil recruitment (Arita et al., 2005a). However, the known receptor for RvE1 at that time, ChemR23, is not significantly expressed in neutrophils. Further studies have shown that BLT1 is also a receptor for RvE1 (Arita et al., 2007). RvE1 acts as a partial agonist of BLT1, blocking LTB₄ binding to BLT1 on neutrophils. In BLT1 knockout mice, the blockade of neutrophil recruitment by RvE1 is reduced in a model of zymosan-induced peritonitis (Arita et al., 2007). RvE1 does not bind to BLT2, despite the structure similarity to BLT1 (Arita et al., 2007).

FPR2/ALX

FPR2/ALX is a chemoattractant receptor belonging to the GPCR class A (rhodopsin) with an extracellular N-terminal and an intracellular C-terminal and consists of 351 deduced amino acids (Bäck et al., 2014). The gene that encodes this receptor maps to the human chromosome 19. The murine orthologue is *fpr2* (Dufton and Perretti, 2010). There is 65% overall homology in deduced amino acid sequences between human and murine receptor (Takano et al., 1997, Fiore et al., 1994, Chiang et al., 2003). This receptor was initially named formyl-peptide receptor-like 1 (FPRL1) given the sequence homology

(69%) with the N-formyl peptide receptor (FPR) family but had low affinity for formyl peptides (Ye et al., 1992). Further studies demonstrated the high affinity for the endogenous ligand lipoxin A₄ (Fiore et al., 1994) and thus, the recommended nomenclature is FPR2/ALX (Bäck et al., 2014). In addition to lipoxin A₄, FPR2/ALX can bind other lipid mediators, such as RvD1, and peptides and proteins such as annexin and serum amyloid A (SAA) (Cooray et al., 2013). Hence, FPR2/ALX has the particular capacity to bind distinct ligands and is classified as a multi-recognition receptor, showing cell and ligand specific activity (Norling et al., 2012). For instance, lipoxin A₄ binding inhibits neutrophil recruitment and promotes the activation of monocytes (Chiang et al., 2006). The internalisation of FPR2/ALX seems to be important for phagocytic action of lipoxin A₄ and annexin-derived peptides (Maderna et al., 2010). FPR2/ALX is known to be expressed by neutrophils, monocytes, macrophages, immature dendritic cells and in T cells (Maddox et al., 1997). A recent study also reported the expression of this receptor in astrocytes in the spinal cord (Abdelmoaty et al., 2013). The stimulation of neutrophils with TNF- α and IL-8 produced significant increment in FPR2/ALX expression (Norling et al., 2012). Notably, Maderna et al. (2010) and Spurr et al. (2011) reported that FPR2/ALX expression rapidly increases with the increase concentration of its agonists and it has been demonstrated that FPR2/ALX responds only to high concentrations of RvD1 (Norling et al., 2012). FPR2/ALX is up-regulated in patients with Crohn's disease and enhances macrophage clearance and inhibits cytokine release (Prescott and McKay, 2011).

ChemR23

ChemR23 is a GPCR of the rhodopsin family, previously known as chemokine-like receptor 1 (CMKLR1). It consists of 371 amino acids with seven hydrophobic domains (Bäck et al., 2014). The gene that encodes this receptor maps to the human chromosome 12 and it is conserved in several species, including mouse and rat (Methner et al., 1997). ChemR23 is expressed in dorsal horn neurones, and also in DRG neurones that co-express TRPV1 (Xu et al., 2010). It is also expressed in macrophages, monocytes and dendritic cells (Arita et al., 2005a), but not significantly in neutrophils (Wittamer et al., 2003). It has also been suggested to be expressed in microglia (Xu et al., 2013). ChemR23 is activated by the chemotactic protein chemerin (Cash et al., 2008), and was also known previously as a co-receptor for some primary HIV-1 strains (Samson et al., 1998). In 2005,

Arita et al. identified ChemR23 as a high affinity receptor for RvE1. It has been demonstrated that RvE1 binding to ChemR23 regulates dendritic cell migration, the production of IL-12 and blocks TNF- α signalling, in animal models of acute inflammation. Human ChemR23 shares an overall similarity of 86% in the deduced amino acids sequence with the rat orthologue, with the largest sequence differences detected in the N-terminal and in the second extracellular loop (Mårtensson et al., 2006). ChemR23 and FPR2/ALX share an overall 36.4% similarity in their deduced amino acid sequences, especially the second intracellular loop and the seventh TM (Arita et al., 2005a).

1.3. MicroRNA

MicroRNAs (miRNAs) are a class of post-transcriptional regulators that are, frequently, evolutionarily conserved (Sayed and Abdellatif, 2011). They are short non-coding RNA sequences of approximately 22 nucleotides capable of repressing the expression of a variety of genes by interacting with the 3' untranslated region (UTR) of messenger RNA (mRNA). miRNAs are produced by RNA polymerase II and are processed by Drosha and Dicer enzymes (Gregory et al., 2006). They were first identified by Lee et al. (1993) in *C. elegans* and, since then, their roles in many cellular processes, such as immune and inflammatory responses, have been demonstrated.

1.3.1. miRNA biogenesis and regulation

Initially (in the nucleus) the transcription of miRNAs is conducted by RNA polymerase II, producing primary miRNA (pri-miRNA) hairpins (figure 1.7). This process is influenced by RNA Polymerase II-associated transcription factors and epigenetic control (Ha and Kim, 2014). miRNA genes can be located within the intron region of protein coding genes and be transcribed by their own promoter or within regions of coding genes (in exons) and transcribed by the host promoter (Hausser and Zavolan, 2014). In addition, miRNAs can be found in clusters and be transcribed together as polycistronic units. Next, the pri-miRNA can be processed through canonical or non-canonical pathways to generate mature miRNAs (Li and Rana, 2014). In the canonical pathway, Drosha (a nuclear protein that belongs to the RNase III-type endonucleases family) recruits DiGeorge syndrome critical region 8 (DGCR8) to form the microprocessor complex that digests the pri-miRNA and releases the precursor miRNA (pre-miRNA), a hairpin-shaped RNA of approximately 65 nucleotides in length. Drosha-

DGCR8 processing is crucial for the determination of miRNA specificity as it defines the end (miRNA seed) of a miRNA. DGCR8 is important for Drosha-miRNA binding stability. miRNA can also be produced through non-canonical pathways such as spliceosome-dependent mechanisms (Ha and Kim, 2014). The pre-miRNA is then transported to the cytoplasm by exportin 5 where further processing is conducted by Dicer (RNase III-type endonuclease) together with TRBP (TAR RNA-binding protein 2). The pre-miRNA is cleaved by Dicer near the terminal loop, releasing a small RNA duplex. Subsequently, the miRNA duplexes are preferentially loaded into particular types of AGO proteins forming the RNA-induced silencing complex (RISC), that regulates all miRNA silencing processes. The guide strand is determined during the AGO loading step mainly based on the relative thermodynamic stability of the two ends of the small RNA duplex. The strand with relatively unstable 5' end is typically selected as the guide strand (Bartel, 2004), and the other strand, denominated 'passenger strand' or 'miRNA*' is usually degraded; however, this is not a strict process and there is evidence that the passenger strand can also be loaded into the RISC complex and regulate mRNA expression (even though less biologically active) (Bartel, 2004). The entire process of miRNA biogenesis and function of miRNAs is highly regulated (Ha and Kim, 2014). For instance Drosha is dependent on phosphorylation by glycogen synthase kinase 3 β (GSK3 β) for proper nuclear localization (Tang et al., 2011) and DGCR8 is crucial for the stabilisation of Drosha through protein-protein interactions (Han et al., 2009); this cross-regulatory loop controls initial pre-miRNA abundance and is a deeply conserved mechanism (Han et al., 2009). In the cytoplasm, Dicer-TRBP is also regulated. Extracellular signal-regulated kinase 1 (ERK1) or ERK2 phosphorylation contributes to TRBP stabilization (Paroo et al., 2009). Within the RISC complex, AGO2 protein can be phosphorylated by MAPK-activated protein kinase 2 (MAPKAPK2) (Zeng et al., 2008), contributing to the stabilization of the protein. miRNAs themselves may undergo several modifications, such as uridylation (Heo et al., 2008).

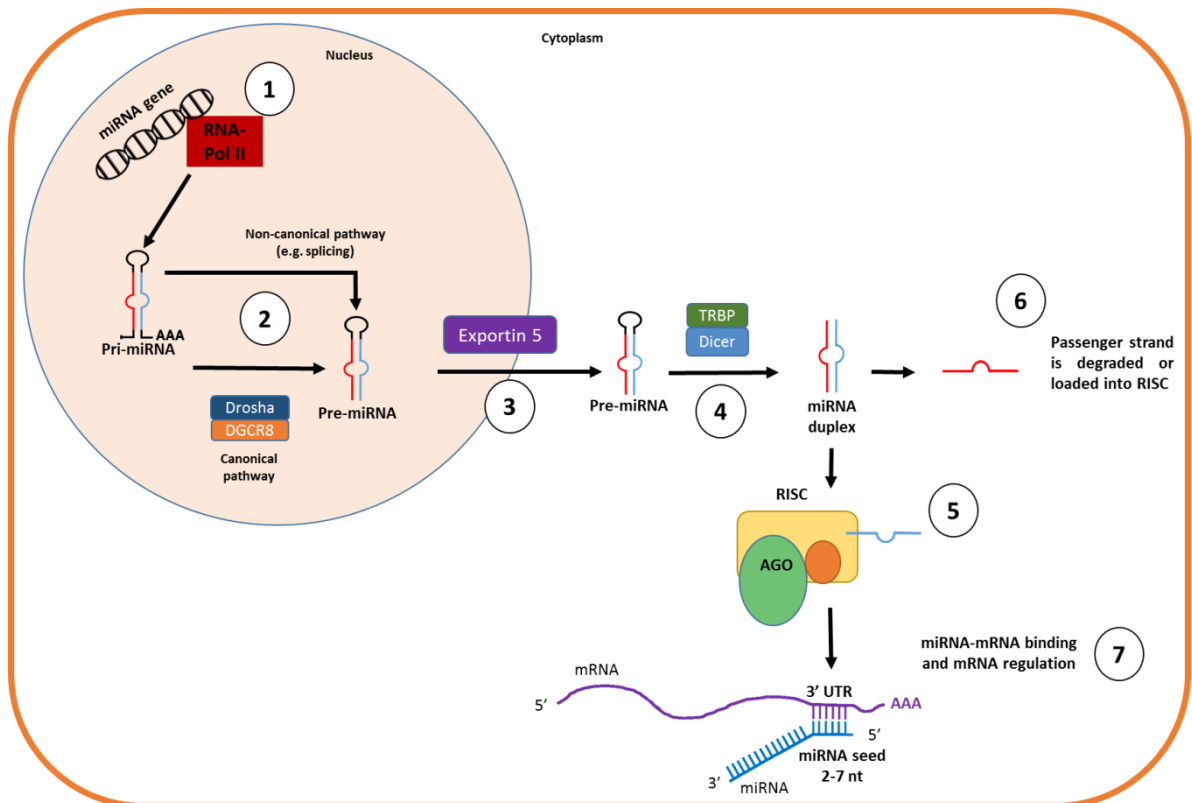


Figure 1.7. Summary of miRNA biogenesis and regulation of gene expression. miRNA biogenesis is tightly controlled and regulation can occur at any step. 1) miRNA are transcribed by RNA-polymerase II to produce pri-miRNA. 2) The pri-miRNA is processed by the Drosha-Dicer microprocessor (canonical pathway) or through non-canonical pathways, such as spliceosome-dependent mechanisms and pre-miRNA is formed. 3) The pre-miRNA is, then, transported to the cytoplasm by exportin 5 where further processing takes place to complete miRNA maturation. 4) Dicer, together with its co-factor TRBP, cleaves the pre-miRNA near the terminal loop and a small RNA duplex is released. 5) The miRNA (guide strand) is loaded into AGO proteins forming the RNA-induced-silencing-complex (RISC). 6) The passenger strand (also denominated miRNA*) is, usually, degraded but can also be loaded into the RISC complex. 7) miRNA within the RISC complex binds the target mRNA and the mRNA is either degraded or repressed, preventing its expression. The miRNA seed (2-7 nucleotides on the 5' end is highly conserved and an exact match to the 3' UTR of the mRNA results in a strong regulation of the mRNA expression. However, alternative binding is possible (see figure 1.8).

1.3.2. miRNA-mRNA binding and target prediction

Most protein-coding genes may be under control of miRNA and many miRNA are highly conserved (Christodoulou et al., 2010). In fact, more than 60% of human protein-coding genes contain at least one conserved miRNA-binding site (Ha and Kim, 2014). For instance, Wheeler et al. (2009) demonstrated that, at least, 34 miRNA families have been conserved from *C. elegans* to humans, and Chiang et al. (2010) showed that 196 miRNA families are conserved among mammals. Conservation is important for miRNA-mRNA binding, but other non-conserved sites also exist. The binding sites for the miRNA are typically located in the 3' untranslated region (UTR) of the mRNA (see figure 1.8). The nucleotides spanning from position 2 to 7 at the 5' end of miRNAs, denominated 'miRNA seed', are crucial for target binding (Lewis et al., 2003). Some miRNAs have a common evolutionary origin but differ in the miRNA seed and Kim et al. (2013) demonstrated the importance of the miRNA seed by deleting separately the miRNA genes of miR-141 and miR-200c (these miRNAs belong to the highly conserved family miR-200 and diverge by only one nucleotide in their miRNA seeds) and found that their targets barely overlap. A perfect Watson-Crick pairing between the miRNA seed and the mRNA (termed 8mer) usually represents a very strong prediction for miRNA-mRNA binding in particular when conservation of the target site is also present (Friedman et al., 2009). Additional improvement to miRNA-mRNA binding prediction includes the presence of adenine at position 1 (7mer-A1) or an extra nucleotide matching at position 8 (7mer-m8) of the miRNA (Lewis et al., 2005). Although an exact match in the seed region is a good indication for miRNA targeting, it is not an absolute requisite, and alternative binding arrangements are possible (see figure 1.8), including 3' compensatory sites and centred pairing within the 13-16 nucleotides (Grimson et al., 2007, Shin et al., 2010).

For miRNA target prediction purposes, an 8mer site is classified as the most efficient, followed by 7mer-m8 and 7mer-A1; the least efficient is a 6mer site (Grimson et al., 2007). However, it was found that the efficacy is highly dependent on the context of each individual site. For instance, an 8mer in the path of the ribosome (within 15 nucleotides from the stop codon) seems to be less efficient than a 7mer in the UTR (Bartel, 2009). Some publicly available algorithms for miRNA target prediction, such as TargetScan, take the context into account and report the context scores to rank the miRNA target predictions (Agarwal et al., 2015).

1.3.3. miRNAs in pain

Although there are some studies reporting the role of miRNA in the nervous system, they have been focused mainly in the development of the nervous system and only recently started to be studied in conditions of chronic pain (Sayed and Abdellatif, 2011). The alterations in expression and function of a variety of receptors and mediators that characterise persistent pain suggested that miRNA may be implied in these pathological changes. A summary of the main miRNAs altered in pain models are described in table 1.4.

Table 1.4. Summary of miRNAs altered in different pain models.

miRNA	Model	Cell/tissue	Regulation	Target	References
miR-1a-3p	CFA	DRG	Down	NI	(Kusuda et al., 2011) ^a
	Capsaicin	DRG	Up	NI	
		SCDH	NC	NI	
	SCI	SCDH	NC	NI	(Strickland et al., 2011) ^{b, c}
miR-7a	SNL/CCI	DRG	Down (7, 14 d)	Sodium channel sub-unit $\beta 2$	(Sakai et al., 2013) ^{a, c}
	CFA	DRG	NC		
miR-21	SNL	SCDH	Up	NI	(Sakai and Suzuki, 2013) ^{a, c}
	CFA	SCDH	NC		
	SCI	Astrocyte	Up		
miR-96	CCI	DRG	Down	Nav1.3	(Chen et al., 2014) ^a
miR-103	SCI	SCDH	Up	Subunits of Cav1.2 L-type calcium channels	(Favereaux et al., 2011) ^{c, d}
miR-124a	Formalin	SCDH	Down (8, 24h)	MeCP2	(Kynast et al., 2013) ^{a, c}
	CFA	TG	Down (24h) Up (12d)	NI	(Bai et al., 2007) ^{a, c}
miR-183	SNL	DRG	Down	BDNF, Nav1.3	(Lin et al., 2014) ^{a, c}
miR-219	CFA	SCDH	Down	CaMKII γ	(Pan et al., 2014) ^a

a- TaqMan based quantitative polymerase chain reaction (PCR); b- Locked nucleic-acid-based quantitative PCR; c- Locked nucleic acid based *in situ* hybridisation; d- Sybr green-based quantitative PCR. NI: Not identified; NC: Not changed; CCI: Chronic constriction injury; CFA: Complete Freund's adjuvant; DRG: Dorsal root ganglion; SCDH: Spinal cord dorsal horn; SCI: Spinal cord injury; SNL: Spinal nerve ligation; TG: Trigeminal ganglion.

Expression of miRNA in peripheral nervous system was first reported in a model of inflammatory muscle pain (Bai et al., 2007). The changes in expression were quantified in the trigeminal ganglion after injection of CFA into the rat masseter muscle (that is innervated by the mandibular division of the trigeminal ganglion). This initial study demonstrated the down-regulation of different miRNAs (miR-10a, -29a, -98, -99a, -124a, -134, and -183) in the trigeminal ganglion ipsilateral to the injury site but no specific targets were predicted.

Findings suggest that different miRNA change their expression dependently on the specific pain condition. For instance in the case of neuropathic pain and inflammatory pain different miRNAs are regulated. Kusuda et al. (2011) showed that miR-16 expression was decreased in the DRG in inflammatory pain (after CFA injection) but not in neuropathic pain (partial sciatic nerve injury). Tam Tam et al. (2011) showed that miR-143 was decreased in DRG in inflammatory pain caused by CFA injection but not after nerve transection of sciatic nerve. The expression of miR-21 is up-regulated while miR-7a is down regulated in neuropathic pain (spinal nerve ligation) but not in inflammatory pain (hindpaw injection of CFA) (Sakai et al., 2013, Sakai and Suzuki, 2013).

Importantly, evidence has suggested that miRNA can regulate ion channels expression and, thus, modulate pain threshold. In fact, the specific deletion of Dicer resulted in expression changes of sodium channels $Na_v1.7$, 1.8 , 1.9 in mice DRG nociceptors and reduced inflammatory pain thresholds (Zhao et al., 2010). Chen et al. (2014) suggested that miR-96 inhibits sodium channel $Na_v1.3$ mRNA in DRG. In neuropathic pain model (CCI of rat sciatic nerve) miR-96 was decreased while $Na_v1.3$ expression was increased. In addition, intrathecal administration of miR-96 alleviated neuropathic pain behaviours and decreased $Na_v1.3$ expression. In the late phase of neuropathic pain, miR-7a is significantly decreased in the DRG after spinal nerve injury (Sakai et al., 2013). Intrathecal administration of MiR-7a alleviates neuropathic pain behaviours by targeting the β_2 subunit of the VGSC and normalising hyperexcitability of nociceptors (Lopez-Santiago et al., 2006, Sakai et al., 2013).

Expression of miR-124a is down regulated in spinal cord dorsal horn neurones after peripheral injection of formalin (Kynast et al., 2013). MeCP2 is recognised as a target for miR-124. MeCP2 is a transcriptional regulator involved in inflammatory pain that targets BDNF. Intrathecal administration of miR-124a decreased BDNF levels and, thus, it may play an important role in inflammatory pain (Kynast et al., 2013).

MiR-103 was the first well characterised miRNA in neuropathic pain (Favereaux et al., 2011). This miRNA was down-regulated in the spinal cord dorsal horn neurones after spinal cord injury and the intrathecal injection of miR-103 alleviated neuropathic pain behaviours. miR-103 targets the three subunits of the voltage-dependent calcium channel Cav1.2 L-type (which underlie long-term changes in neuropathic pain (Fossat et al., 2010).

In a model of CFA-induced inflammatory pain, miR-219 was down regulated in dorsal horn neurones, 1 to 10 days after CFA injection (Pan et al., 2014). The NMDA receptor and CaMKII γ (a element of the NMDA receptor signalling cascade) are validated targets for miR-219 (Kocerha et al., 2009) and the levels of CaMKII γ were increased in mice treated with CFA (subcutaneous injection in the hindpaw). Thus, miR-219 shows a promising role in the regulation of chronic inflammatory pain by targeting crucial components involved in chronic pain.

Recent evidence has also suggested that miRNAs may play a role in the pain differences observed between genders. Linnstaedt et al. (2015) has found that the genes of the miRNAs differentially expressed in patients with post-traumatic musculoskeletal pain (blood samples) were enriched on the X chromosome.

1.3.4. Resolvins and miRNAs

A recent line of investigation links the actions of resolvins to miRNA regulation. Recchiuti et al. (2011) reported that RvD1 up-regulated miR-21, miR-146b and miR-219 and down-regulated miR-208a in a murine model of peritonitis. These same miRNAs were significantly regulated by RvD1 in human macrophages overexpressing recombinant RvD1 receptors FPR2/ALX or GPR32. The miRNAs regulated by RvD1 target cytokines and proteins involved in the immune system. For instance, miR-219 targets the enzyme 5-LOX and reduces leukotriene production (Recchiuti et al., 2011). Krishnamoorthy et al. (2012) demonstrated that RvD1 through FPR2/ALX and GPR32 regulated specific miRNAs in the resolution of inflammation. For instance, it was reported that the administration of RvD1 up-regulated miR-208a and IL-10, in exudates from transgenic mice overexpressing FPR2/ALX. miR-208a down-regulated mRNA levels of the pro-inflammatory PDCD4 (Programmed Cell death 4), a suppressor of IL-10 in macrophages (IL-10 is a potent anti-inflammatory mediator). In contrast, in FPR2/ALX knockout mice, RvD1 did not reduce leukocyte infiltration and the levels of miR-208a and IL-10 were not altered (Krishnamoorthy et al., 2012).

To date, miRNA regulated by resolvins of the E-series have not been identified. However, Wang et al. (2014) reported a mechanism by which BLT1 regulates several miRNA in macrophages, but this process was initiated by LTB₄ and not RvE1.

Additionally, there is no data at this point regarding resolvins regulating miRNA in pain-associated conditions.

1.4. Lingual nerve injury and clinical implications

The lingual nerve innervates the anterior two-thirds of the tongue (the posterior one-third is innervated by the glossopharyngeal), the bottom of the mouth and the lingual gingivae. It is a part of the mandibular branch of the trigeminal nerve (the fifth cranial nerve) and it crosses between the medial pterygoid muscle and the mandible, passing anteriorly underneath the oral mucosa, just below the third molar tooth (figure 1.9-A). Trigeminal nerve fibres that contain the lingual nerve enter the brainstem at the level of the pons and descend to the medulla forming the trigeminal nucleus (figure 1.9-B). Second order neurones in the trigeminal nucleus cross the midline and ascend to the contralateral thalamus via the trigeminothalamic tract reaching the ventral posterior medial (VPM) of the thalamus. These nuclei send their axons to the somatosensory cortex in the brain where information from the lingual nerve is processed in terms of discriminative component (identification of location, intensity and quality of the stimulus). The lingual nerve is responsible for general somatic afferent innervation transmitting mechanical, thermal and noxious stimuli. In addition, it also contains fibres from the facial nerve carrying taste information and parasympathetic and sympathetic afferents within the chorda tympani.

Because of its proximity to the teeth and alveolar bone, the lingual nerve is vulnerable to injury during routine oral surgery, such as removal of the third molar or local anaesthetic injection (Meyer, 2013). The majority of patients recover after some time but others are left with permanent sensory disturbances (0.3%) (Atkins, 2017). The most common symptoms described by the patients on the ipsilateral site of the tongue affected by the injury are numbness (hypoesthesia), tingling, itching or tickling (paraesthesia) and burning, pricking or tenderness (dysaesthesia) (Meyer, 2013). It is, therefore, a debilitating complication with a negative impact on the patient's life as it affects their basic daily routine and social interactions such as eating, speaking, drinking, teeth brushing, kissing (Renton, 2013).

Patients with persistent sensory disturbances may be referred for repair, consisting of surgical removal of the injury site (the neuroma), followed by apposition of the proximal and distal ends via epineurial sutures (Robinson et al., 2004, Ziccardi, 2013). The majority of patients have significant improvement in their symptoms post-repair, and reduced problems with speech and eating. Despite this improvement some patients still mention unpleasant abnormal sensations following surgical repair (Robinson et al., 2000). For instance, a study conducted in the UK with 53 patients that underwent lingual nerve repair, found that 26% of patients after surgery repair still reported pain (compared to 30% before), 45% reported spontaneous tingling (compared to 47% pre-repair). Only numbness, tongue biting and taste disturbance were significantly improved following repair (64% to 11%, 74% to 49% and 64% to 57% respectively) (Robinson, 2013). Several explanations have been suggested and the extent of the initial injury seems to be the main determinant of the outcome of repair (Cheung et al., 2010); in contrast, the time of repair after injury does not seem to have an effect on the recovery (Robinson and Smith, 1996).

Patients that do not meet the criteria for surgical repair or that report ongoing sensory disturbances following repair are recommended to follow pharmacological therapy that includes anti-epileptics (e.g. gabapentin or pregabalin), anti-depressives (e.g. amitriptyline) or opioids (e.g. tramadol); however, they have variable degrees of success (Ruggiero, 2013). The clinical management of dysaesthesia after LNI is very difficult (Pippi et al., 2017) and there is a clear need to better understand the mechanisms behind the development of persistent pain following this type of injury and develop pharmacological alternatives that better address the cellular and molecular events that arise after injury. It is important that any novel medical treatment complements and enhances the progression of nerve regeneration.

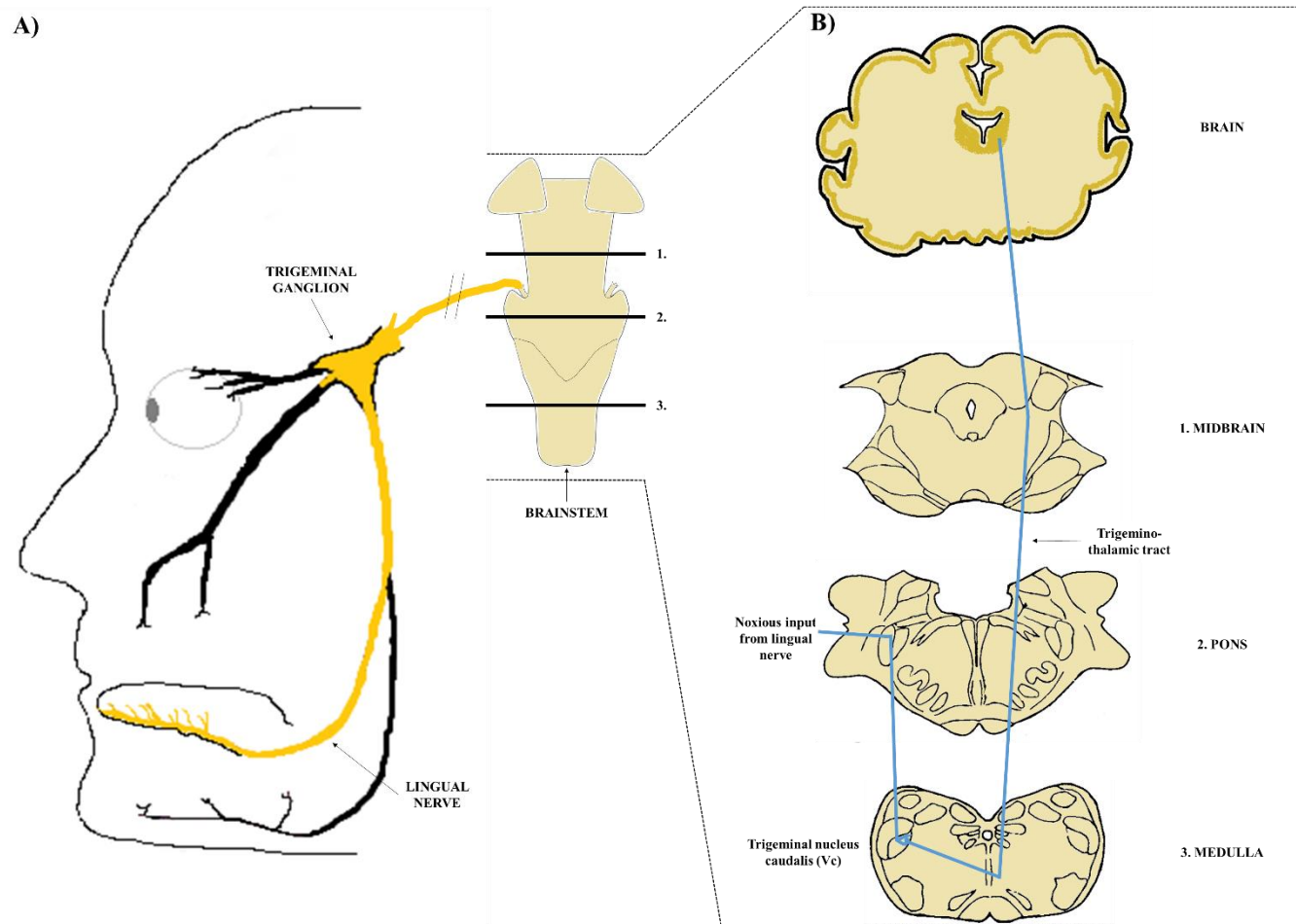


Figure 1.9. Lingual nerve, trigeminal ganglion and brainstem. A) Lingual nerve is part of the trigeminal nerve and is responsible for innervating the tongue. B) Lingual nerve terminals transmitting noxious information (e.g. pain) are projected mainly to the trigeminal nucleus caudalis (Vc) in the medullar part of the brainstem. Brainstem drawing taken from Henssen et al. (2016) and brainstem cross-sections adapted from Tohyama et al. (1979) under Creative Commons Attribution License (CC BY).

1.5. Animal models of neuropathic pain and behavioural assessment of orofacial pain

One way to study the complex mechanisms of pain-associated diseases across the neuraxis is using pre-clinical models (such as the rat) to mimic, for instance, peripheral nerve injuries. One of the first models of neuropathic pain was developed in 1979 and involved the whole nerve transection in an intact limb leading to autotomy behaviour (self-mutilation) (Wall et al., 1979). Later, Bennett and Xie (1988) described a model of partial injury to the sciatic nerve: chronic constriction injury (CCI), in which four chromic gut sutures are loosely ligated around nerve; this method constricts the nerve, but not all fibres and produces oedema surrounding the injured part of the nerve. Later, Vos et al. (1994) adapted and characterised the model in the orofacial system, more specifically in the infraorbital nerve (ION), reporting altered behaviour post-injury such as face-grooming activity. The work described in this thesis adapted the CCI model to the lingual nerve injury.

One of the main disadvantages associated with the use of animals in particular in pain studies is the fact that they cannot self-report, unlike human subjects. Even though animal behaviours in response to noxious stimuli can be objectively measured, the most commonly used behavioural methods assess mainly reflexes (such as withdrawal from applied stimuli and jumping, etc.) or innate responses (such as biting, licking and guarding) that can be even accomplished by decerebrated animals (Mogil, 2009). Because pain is an emotional and sensorial experience that requires extensive cognitive cerebrospinal processing (Price, 2000), these type of responses have been questioned whether they are actually measuring the overall pain experience or just the sensory alterations that are normally present. In addition, there have been several reports of investigator bias induced in these types of experimental assessments (Mogil, 2017). Consequently, over the past years, there has been a considerable shift in the use of more clinically relevant methods of assessing pain in animals in order to improve pre-clinical translation into the clinic. Examples are the development of grimace scale to investigate spontaneous pain symptoms by evaluating natural body and face expressions (Sotocinal et al., 2011) or operant tests (such as conflict paradigm or reward-conflict assays) in which non-reflexive measures require training and learning and, thus, involve cerebrospinal integration (that could not be performed after decerebration) (Murphy et al., 2014, Mogil, 2009).

In terms of orofacial pain assessment, several operant behavioural tests are now available. The Orofacial Stimulation test (Ugo Basile, developed by Fehrenbacher, Henry, Hargreaves) (Cha et al., 2012) and the Orofacial Pain Assessment Device (OPAD) allow the animal to get a reward or avoid a noxious stimuli applied in the orofacial region (Neubert et al., 2005). Another example is the dolognawmeter, in which the animals “gnaw through polyethylene foam and ethylene vinyl acetate resin dowels” to get a food reward (Dolan et al., 2010); this method in particular may be useful to study muscle and joint pain (for instance, derived from cancer), but it may not be easy to distinguish motor from sensory impairment. The escape test gives the animals a choice between a non-noxious aversive stimulus (e.g., light) against an alternative noxious aversive stimulus (e.g. temperature) (Ding et al., 2005, Mauderli et al., 2000). The escape test is considered relatively easy to apply as little training is required (Vierck et al., 2008). A similar test in concept is the conditioning place preference paradigm, in which animals avoid locations in which they experience pain, or move to locations in which they had relief from pain (Cahill et al., 2013). There has also been developed a method so that the animals could self-administrate analgesics by pressing a lever, but this test in particular requires extensive training to obtain reproducible results (Martin et al., 2006). When performing and analysing behavioural data from animal models of pain it is also necessary to take into account the evolutionary role of rodents and acknowledge the difficulty that is measuring pain in animals that are preys in their natural habitat and should not demonstrate too much pain to potential predators (Murphy et al., 2014). The lingual nerve in particular is difficult to assess with traditional reflexive measures due to its anatomical location and in chapter 3 a novel behavioural method to investigate LNI is reported.

1.6. Overview, aims and hypothesis

As described in the above literature review, chronic pain is a complex disease and involves multiple mechanisms. Neuropathic pain in the orofacial region, and in particular that arising as a consequence of LNI, can have a negative effect on the patient’s life. Even though it is an important clinical problem, its underlying cause is not fully understood and the available medical treatments are only partially effective. Therefore, there is a clear need to better understand the mechanisms underlying this type of pain so that better therapeutics can be developed.

Resolvins act via GPCRs (ChemR23, BLT1, GPR32 and FPR2/ALX) and recent studies have shown that resolvins can attenuate inflammatory and neuropathic pain through those receptors. Resolvin receptors are known to be expressed in a variety of immune cells that participate in the inflammatory process. However, very little is known about the expression of those receptors in the nervous system, in pain processing tissues. miRNAs are known to control many cellular processes including immune responses and a growing body of evidence shows their role in chronic pain. In addition, it is suggested that resolvins can regulate miRNA through the mentioned receptors.

Therefore, it was hypothesised that resolvin receptors are expressed within nervous system tissues responsible for pain processing and can contribute to the molecular and physiological changes that occur following peripheral nerve injury. It was also hypothesised that aberrant miRNA expression also contributes to these processes.

To test these hypotheses, the CCI model of neuropathic pain was adapted to the rat lingual nerve. In addition, human tissues were included in order to establish correlations with clinical pain when applicable.

The overall aim of this study was to characterise changes in feeding behaviour following LNI and correlate these changes with altered expression of potential modulators of neuronal excitability; namely microglial activation, resolvin receptors and miRNA. The specific objectives are listed below.

1. Investigate and characterise feeding behaviour following LNI, using the Ugo Basile Orofacial Test.
2. Characterise the microglial response to LNI in a rat model, over a specific time period using the microglial marker, Iba1.
3. Identify the specific cells expressing resolvin receptors within the nervous system and characterise their expression following LNI.
4. Investigate the expression of miRNAs following LNI and identify potential targets and pathways relevant in the context of nerve injury and chronic neuropathic pain..
5. Correlate any changes in microglial response, resolvin receptor and miRNA expression with changes in feeding behaviour.

CHAPTER 2
GENERAL MATERIAL AND METHODS

2.1. Introduction

This chapter describes the general materials and methods used to carry out the studies reported in this thesis.

2.2. Animal experiments

A total of 30 adult male Sprague-Dawley rats (200-250 g) were used in the studies reported in this thesis. They were supplied by Charles River UK and kept in a 12 h light-dark cycle (lights on at 7 am and off at 7 pm each day) with free access to food and water. Animals were allowed to acclimatise in the Biological Services Unit at the University of Sheffield for at least 1 week following arrival and were housed in groups of 3 or 4 rats per cage (each cage had bedding, wood shavings and one cardboard tube) in a room controlled for temperature (19-23°C) and relative humidity (40-70%). All efforts were made to minimise animal suffering beyond the necessary and to reduce the number of animals used in the studies herein reported. All animal experiments were carried out in accordance with the UK Home Office Animals (Scientific Procedures) Act 1986 and the ARRIVE guidelines (Kilkenny et al., 2010) were followed to report the animal experiments in this thesis. The model of neuropathic pain used was chronic constriction injury (CCI) of the lingual nerve, adapted from Bennett and Xie (1988).

2.2.1. Surgical procedures

All surgical instruments were sterilised in an autoclave (Prestige Medical Classic Autoclave) before conducting any surgical procedure in order to reduce the risk of infection and contamination. In addition, the surgical table and surrounding area were disinfected with hibitane (5% concentrate in 75% alcohol, SSL International plc UK) prior to the surgical procedure. At first, anaesthesia was induced in the animals with 4% isoflurane (IsoFlo® 100% w/w) and 4% oxygen in an anaesthetic machine. The area of incision, below the left side of the mandible, was shaved and cleaned with hibitane. Animals were, then, transferred to the surgical table and placed on a heating pad covered with surgical drape to keep the animal's body temperature at $37\pm 2^\circ\text{C}$; each animal was maintained under anaesthesia for the duration of the procedure by inhalation of 2-2.5% isoflurane and 2% oxygen. Prior to initiating the surgical procedure, it was determined that the reflex withdrawal of the paw was absent, by pinching the paw and the heart beat was continuously monitored for the entire duration of the surgery. Using an operating

microscope, an incision was made beneath the left side of the mandible and the left lingual nerve was exposed by separating the surrounding muscular and connective tissue with the appropriate surgical instruments (blunt dissecting scissors, blade and surgical tweezers). In the experimental group, two chromic gut sutures were tied loosely around the lingual nerve 2 mm apart (figure 2.1). In the sham control group, the left lingual nerve was exposed but no sutures were tied around the nerve (no nerve injury). The surgical site was irrigated with sterile saline and the subcutaneous tissue and the skin were closed in layers with 4-0 Vicryl sutures.

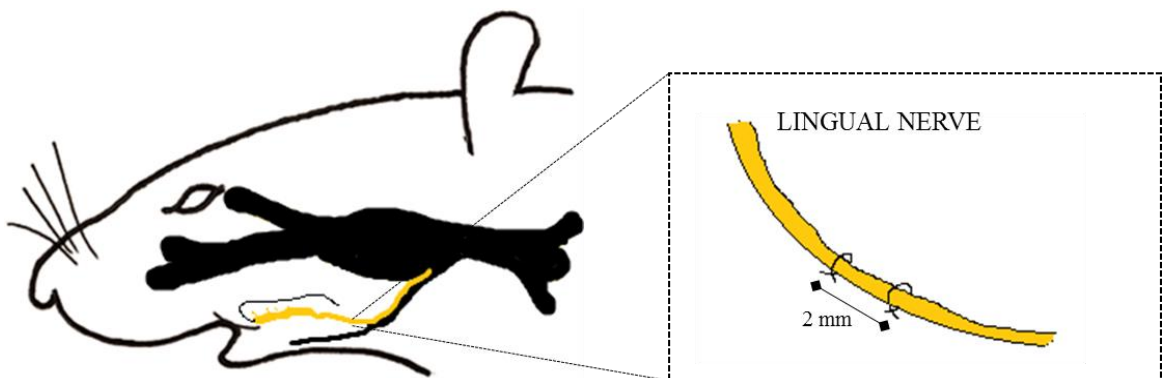


Figure 2.1. Chronic constriction injury of the rat lingual nerve. Rat drawing adapted from Csáti et al. (2015). Images not to scale.

Animals were randomly allocated to experimental (CCI) or control (sham) groups on the day of surgery. Animals were left to recover for a period of 3, 7 or 28 days. The specific number of animals used in each group are described in more detail in each results chapter (chapters 3-6).

2.2.2. Behavioural testing

The lingual nerve innervates the tongue and, therefore, its receptive field is very difficult to access using standard behavioural methods (for instance, testing for withdrawal threshold to von Frey hair). In addition, as discussed in the literature review (section 1.5 in chapter 1), in recent years there has been a shift away from the use of behavioural methods that rely largely on reflex responses to assess pain behaviour in animals. To overcome these issues, a method was developed using the Orofacial

Stimulation Test (code 31300, Ugo Basile, Comerio, VA, Italy) to evaluate the effect of lingual nerve injury on feeding behaviour. In this test the rat voluntarily inserts the snout through an opening and uses the tongue to access a reward (chocolate milk) from a bottle (figure 2.2-A). Animals were trained to use the equipment for five days prior to surgery. The test was, then, performed on day 0 (day of the surgery) and, subsequently, on days 1, 3, 5, 7, 14, 18, 21, and 28 after surgery. Time points were chosen based on the literature (Cha et al., 2012, Zuo et al., 2013) and previous work conducted in Professor Boissonade's laboratory (Biggs et al., 2007a, Bird et al., 2003, Bird et al., 2002, Bowler et al., 2011, Davies et al., 2006, Evans et al., 2014, Loescher et al., 2001, Smith et al., 2005). The test consisted of 10 min acclimatisation (with no access to the reward as the opening was covered) and 10 min recording with access to the reward bottle (opening cover removed). The equipment was connected to a computer where ORO software (Ugo Basile, Comerio, VA, Italy) was installed and automatically recorded the number of feeding attempts and duration of feeding every time the infrared barrier crossing the opening to the reward was interrupted (figure 2.2-B). In addition, volume consumed was quantified by subtracting the initial and final volume in the bottle. Animals were not deprived from food or water prior to testing, as the main goal of this test was to investigate the willingness of the animal to access the reward even though they had LNI. The behavioural testing results and further discussion are reported in detail in chapter 3.

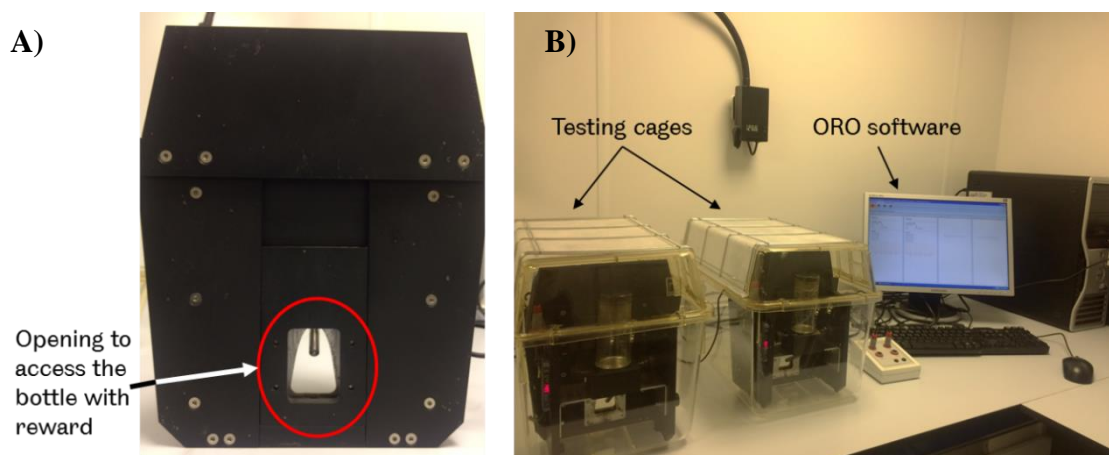


Figure 2.2. The Ugo Basile Orofacial Stimulation Test equipment. A) Opening that allows the rat to insert the snout and access the reward bottle. B) Representation of behavioural testing settings with testing cages connected to the ORO software that automatically records the testing parameters.

2.2.3. Terminal procedures

At the end of the recovery period the animals were anaesthetised with an overdose of pentobarbitone (Pentobarbital Sodium 20% w/v, JML) and transcardially perfused with phosphate buffered saline (PBS) prewash followed by 4% paraformaldehyde (for immunohistochemistry) or perfused with only cold PBS (for miRNA extraction, to remove any possible blood derived cross-contamination). The brainstem, trigeminal ganglia and left and right lingual nerves were removed and prepared for either immunohistochemistry or miRNA extraction. In preliminary studies, the spinal cord was also removed and prepared for immunohistochemistry.

2.2.4. Collection and preparation of rat tissue

Tissues collected for immunohistochemical processing (brainstem and spinal cord) were immediately placed in 4% paraformaldehyde (Fisher Scientific, UK) for 4 h at 4°C, followed by 30% sucrose solution overnight in order to cryoprotect the tissue. Before freezing and storage, brainstem and spinal cord tissues were prepared by removing the meninges and a subtle mark was made across the right ventral side of each tissue for identification of ipsilateral/contralateral side. Next, tissues were placed vertically in a mould (brainstem was placed so that the rostral part was at the bottom and the most caudal part at the top; spinal cord was placed so that lumbar part was at the bottom and the most cervical part at the top), embedded in optimal cutting temperature (OCT) compound (Sakura Finetek, Europe BV, The Netherlands) and frozen in a cryostat in fast-freezing mode. Once completely frozen, the block was removed from the mould, trimmed and stored at -80°C until required for cutting and immunostaining.

Tissue collected for miRNA extraction was immediately snap frozen in liquid nitrogen and subsequently stored at -80°C. Time between animal culling and tissue snap-freezing was kept to the minimum possible. Lingual nerves were the first to be collected (~5 min), then brainstem (not used in the miRNA study) and last, trigeminal ganglia (~15 min).

2.3. Human studies

Human tissues were obtained from the archive of human lingual nerve neuromas from Charles Clifford Dental Hospital, Sheffield, UK. All neuromas were collected with the informed consent from the patients. The study received approval and was conducted in

accordance to the South Sheffield Research Ethics Committee (06/Q2305/151) STH13926 (Mechanisms of oro-facial pain, histological, genomic and proteomic investigations) and East of England - Cambridge Central Research Ethics Committee (17/EE/0238) STH 19847 (The use of lingual nerve and tooth pulp tissue to identify molecules linked with chronic pro-facial pain).

2.3.1. Human lingual nerve neuromas

LNI can occur after routine oral surgery (such as the removal of the lower third molar) or facial trauma and the current treatment involves surgically removing the abnormal part of the nerve (the neuroma) prior to carrying out a nerve repair procedure, as mentioned in section 1.4 in chapter 1. The pain history and symptoms (pain, tingling or discomfort on the side of the tongue innervated by the injured nerve) were obtained by the clinician pre-operatively as described in Robinson et al. (2000). In addition, patients were also asked to score the discomfort, tingling and pain using visual analogue scales. For a detailed description of the surgical removal of the neuroma, repair of the nerve and collection of clinical history see Robinson et al. (2000). The neuroma samples were also characterised by their macroscopical characteristics at the time of surgical removal. Neuromas with parts of the nerve connecting the gap between the central and distal ends were classified as neuromas-in-continuity (NIC); the samples with nerve-end swelling on the central part and no visible link between the central and distal ends were classified as nerve-end-neuromas (NEN).

2.3.2. Human tissue preparation

Lingual nerve neuroma processing has been described previously by Bird et al. (2013) and the preparation of the neuroma tissues was conducted by Dr Emma Bird. Briefly, following surgical removal of the neuroma, the specimen was fixed in 2% Zamboni's fixative (0.1 M phosphate buffer, pH 7.4, containing 4% paraformaldehyde and 0.2% picric acid) for 24 h at 4°C. Next, it was cryoprotected in 30% sucrose for 12 h at 4°C. The tissue was placed horizontally and orientated so that the distal part of the neuroma was on the left and the central part on the right (marked by the presence of surgical suture) and embedded in OCT compound (Sakura Finetek, Europe BV, The Netherlands) on a cryostat in fast-freezing mode. Once it was completely frozen, the OCT

block containing the tissue was removed from the cryostat and stored at -80°C until necessary for further processing.

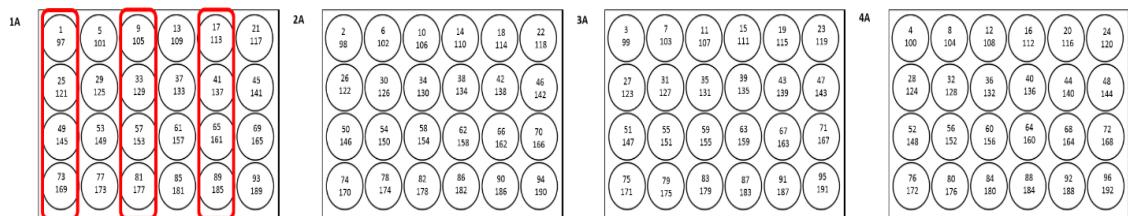
2.4. Immunohistochemical methods

Immunohistochemical methods were used to determine the microglia response to (described in detail in chapter 4) and the expression of resolvins receptors (described in detail in chapter 5).

2.4.1. Rat tissue

Prior to staining, the rat brainstem sections were cut ($30\ \mu\text{m}$) on a cryostat, and placed free floating in 24-well plates with phosphate-buffered saline (PBS) in a serial way described in figure 2.3. At the end of the immunohistochemical protocol, the sections were subsequently mounted on slides in a way such that each section analysed would be $240\ \mu\text{m}$ apart. The obex (most caudal part of the fourth ventricle) was used as reference point and a total of $3360\ \mu\text{m}$ of the caudal medulla of the brainstem was analysed.

A) Serial collection of brainstem sections onto 24-well plates (free floating in PBS).



B) Sections mounted onto gelatine-coated slides at the end of immunostaining and prior to image analysis.

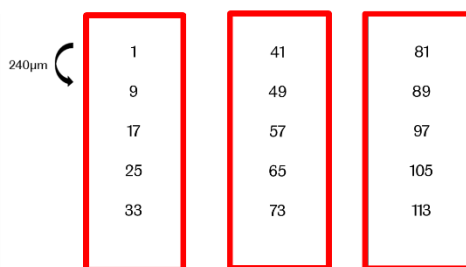


Figure 2.3. Representation of the serial collection of brainstem sections. A) Brainstem sections were cut from caudal to rostral until reference point (obex) in order represented. B) In red the sections used for immunostaining and analysis. The numbers represent section number (not distance or position).

2.4.2. Human tissue

Serial 14 μm sections were cut on a cryostat and collected onto poly-D-lysine (PDL, Sigma-Aldrich Company Ltd, Gillingham, UK) coated microscope slides in two sets of 15 slides (1A-1O and 2A-2O) with three sections per slide (figure 2.4). In total 90 sections were collected from each neuroma sample and in each microscope slide each section was 210 μm apart from each other. Sections were left to air dry for 1 h at room temperature, prior to staining. Alternatively, sections were stored at -80°C until required for further processing. The remaining neuroma tissue was processed for miRNA extraction (see sub-section 2.6.2 in this chapter).

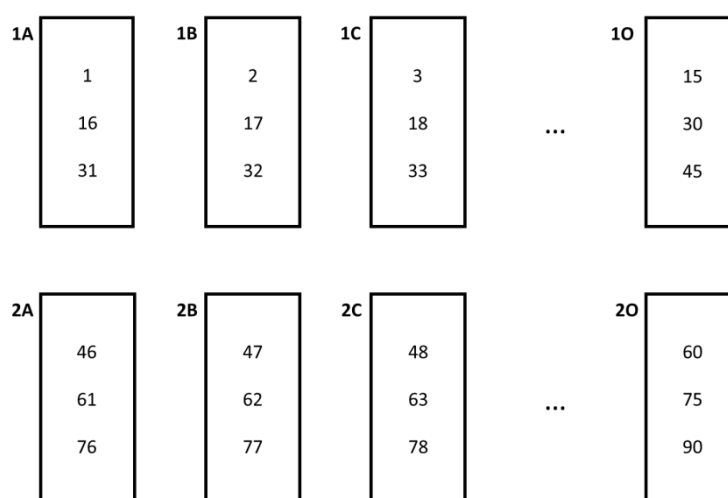


Figure 2.4. Representation of the serial collection of neuroma sections. A total of 90 sections were cut from a human lingual nerve neuroma in 2 sets of 15 slides (3 sections per slide).

2.4.3. Immunohistochemical protocol

The general protocol used was as follows: after washing in PBS containing 0.5% Triton X-100 (PBST) (2×10 min), sections were incubated in 10% normal donkey serum (NDS) for 1 h at room temperature, with the purpose of decreasing non-specific background staining. Next, sections were incubated with primary antibodies (tables 2.1 and 2.2) overnight at 4°C . Sections were then washed in PBS (2×10 min) and incubated with the respective secondary antibody (tables 2.1 and 2.2) for 90 min at room temperature and in the absence of light. Finally, the sections were washed in PBS (2×10 min) and mounted in Vectashield medium (Vector Laboratories, UK) and the slide coverslipped. In the case of brainstem sections, they were first mounted onto gelatine-

coated microscope slides (as represented in figure 2.3-B above) and, subsequently, mounted in Vectashield medium and coverslipped.

2.4.4. Specificity controls

Specificity controls for ChemR23 and FPR2/ALX in the spinal cord and brainstem were performed by pre-absorbing the primary antibody with a blocking peptide. The primary antibody was pre-incubated with its respective blocking peptide (10 $\mu\text{g}/\text{mL}$) for 24 h at 4°C before proceeding with the normal immunohistochemical protocol. For all the other primary antibodies, no blocking peptides were available and immunohistochemical controls were performed by incubating the tissue sections with the secondary antibody alone.

Table 2.1. Details of antibodies and dilutions used in the animal studies.

Primary antibody	Immunogen	Range of dilutions	Optimal dilution	Supplier (catalog number)	Secondary antibody	Range of dilutions	Optimal dilution	Supplier (catalog number)
Goat anti-ChemR23	N-terminal extracellular domain of ChemR23 reactive with mouse and rat	1:50-1:500	1:400	Santa Cruz, Biot (sc-32652)	Donkey anti goat Cy3	1:500-1:1000	1:500	Jackson Immunoresearch (705-15-147)
Rabbit anti FPR2/ALX	Synthetic peptide to the second extracellular loop (between 300-350 amino acids) reactive with human, mouse and rat	1:500-1:2000	1:1000	Novus Biologicals (NLS1878)	Donkey anti rabbit Cy3	1:500-1:1000	1:500	Jackson Immunoresearch (711-165-151)
Rabbit anti-IBA	Synthetic peptide corresponding to the C-terminus of Iba1, reactive with rat, mouse and human	1:500-1:2000	1:1000	WAKO (019-19741)	Donkey anti rabbit-FITC	1:500-1:1000	1:500	AnaSpec (60659-FITC)
Mouse anti-NeuN, clone A60 (reactive with rat)		NA	1:500	Millipore (MAB377)	Donkey anti mouse FITC	NA	1:500	Jackson Immunoresearch (711-095-150)
Mouse anti-GFAP, clone GA5 (reactive with rat)		NA	1:300	Vector laboratories (VP-G805)	Donkey anti mouse FITC	NA	1:500	Jackson Immunoresearch (711-095-150)

NA: Not applicable

Table 2.2. Details of antibodies and dilutions used in the human studies.

Primary antibody	Immunogen	Range of Dilution	Optimal Dilution	Supplier (catalog number)	Secondary antibody	Range of dilutions	Optimal Dilution	Supplier (catalog number)
Rabbit anti-human GPR32	Synthetic peptide mapping to 281-300 amino acids	1:50- 1:500	1:100	Genetex (GTX71225)	Donkey anti rabbit Cy3	NA	1:500	Jackson Immunoresearch (711-165-151)
Rabbit anti human BLT1	Synthetic peptide to the c-terminal region of human receptor	1:100- 1:300	1:200	Abcam (ab101801)	Donkey anti rabbit Cy3	NA	1:500	Jackson Immunoresearch (711-165-151)
Mouse anti S-100, clone 15E2E2 (reactive with human)		NA	1:200	Millipore (MAB079-1)	Donkey anti mouse FITC	NA	1:500	Jackson Immunoresearch (711-095-150)
Mouse anti human PGP9.5, clone 31A3		NA	1:1000	Ultraclone (31A3)	Donkey anti mouse FITC	NA	1:50	Jackson Immunoresearch (711-095-150)

NA: Not applicable

2.5. Image acquisition and analysis

2.5.1. Fluorescence microscopy

Images of the rat brainstem tissue sections were captured using a Zeiss Axioplan fluorescence microscope, and excitation/emission filter sets for FITC (Fluorescein isothiocyanate), Cy3 (Indocarbocyanine) or DAPI (4',6-diamidino-2-phenylindole) detection. The images were analysed using Image-Pro Plus (Media Cybernetics, USA) to determine the positive area of staining (PAS, %) for Iba1 and ChemR23 expression. When acquiring the images, the same software settings were applied and images were code-blinded to reduce potential acquisition variability and investigator induced bias. An area of interest was pre-determined, first within the whole brainstem section and, then, the camera window and magnification (details of the area of interest are described in the respective chapters 4 and 5). A threshold was then applied to the image to define the range of intensities to be included in the measurements. The upper level of the threshold was always set to the maximum (255) while the lower limit was subjectively set so that the highlighted area matched as closely as possible the positive labelling viewed down the microscope. Every effort was made to ensure that the counts were not biased to include more or less positive cells (please see reproducibility tests in section 2.10.1 of this chapter). Figure 2.5 exemplifies the image analysis processing, showing a region of the brainstem and the usual procedure to establish the threshold and calculate the PAS (%).

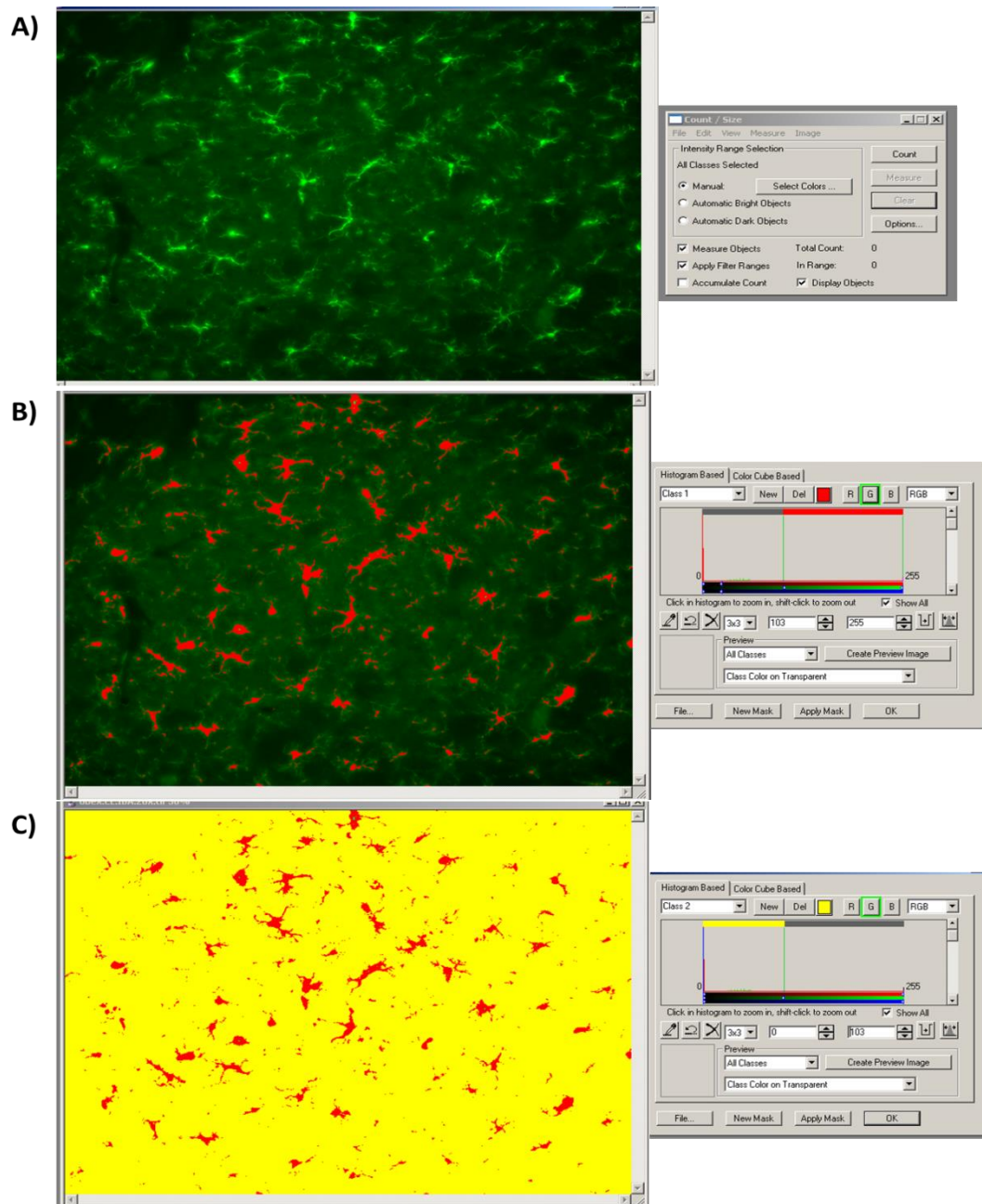


Figure 2.5. Image analysis using Image Pro-Plus. A) The immunohistochemistry labelling. B) Processed image indicating area of positive labelling. C) Positive labelling (red) and background (yellow), used to calculate the percentage area of positive staining (% PAS).

2.5.2. Confocal microscopy

Images of tissue with ChemR23 antibody staining were also acquired with Nikon A1 confocal microscope. The system has a violet diode 405 nm laser, an argon ion 457-

514 nm laser, a sapphire 561nm laser and a red diode 642 nm laser. The images were then processed using Image J software.

2.6. miRNA extraction

To increase the yield and quality of miRNA extracted different protocols and optimisation methods were applied depending on the source of tissue (please see following sub-sections for more details). RNase-free or nuclease-free water, filter tips for pipettes, gloves and cleaned bench were always used to avoid contamination sources.

2.6.1. miRNA extraction from rat tissue

The mirVana™ miRNA Isolation Kit (Applied Biosystems) was used to isolate miRNA from rat tissues. The manufacturer's protocol was followed; briefly, the tissue removed from the -80°C freezer and, without thawing, was disrupted using a sonicator. Tissue was placed on lysis/binding buffer (1/10 volumes per tissue mass) and mixed. 1/10 volume of miRNA homogenate additive was added to the tissue lysate and mixed by vortexing. The mixture was left on ice for 10 min. Acid-Phenol:Chloroform was added to the previous mixture (volume equivalent to solution before addition of homogenate additive) and mixed by vortexing for 30-60 s. To separate the aqueous and organic phases, the mixture was centrifuged for 5 min at 10,000 x g at room temperature. The aqueous phase was transferred to a fresh tube and the organic phase discarded. 100 % ethanol (Sigma, UK) was added to the aqueous phase and pipetted onto a clean Filter Cartridge. Using a collection tube provided the mixture was centrifuged for 15 s. The flow-through was discarded and 700 µL of miRNA Wash Solution 1 were applied to the Filter Cartridge. After centrifuging and discarding the flow-through, a second wash with 500 µL of Wash Solution 2/3 was conducted twice as in the previous wash. The tube was centrifuged for a further 1 min to assure residual fluid has been removed. Finally, the Filter Cartridge was transferred to a fresh collection tube and 100 µL Elution Solution (pre-heated at 95°C) was applied to the centre of the filter. The tube was centrifuged for 30 s and the eluate (that contains the RNA) was collected. Before further analysis or storage at -80°C, the final RNA sample was analysed using a NanoDrop Spectrophotometer (NanoDrop 2000, Thermo Scientific).

2.6.2. miRNA extraction from human tissue

The RecoverAll™ total Nucleic Acid Isolation Kit (Applied Biosystems) was used to extract total RNA from human neuroma tissues. As the samples used in this thesis were frozen and not embedded in paraffin, the deparaffinisation step in the manufacturer's protocol was omitted. Next, the tissues were cut in smaller pieces and added to a digestion buffer. If necessary, the sample was also sonicated to disrupt as much as possible the tissue architecture. 4 μ L of protease (included in the kit) was added to each neuroma sample. The sample was incubated in a heat block for 15 min at 50°C and subsequently for another 15 min at 80°C. A mixture of Isolation additive and ethanol was added to the previous sample. A Filter Cartridge in a collection tube was used to pass the previous mixture by centrifuging for 30 s. The flow-through was discarded and the same collection tube was used for the following washing steps: first, Wash 1 solution and, second, Wash 2/3 Solution. Each time the sample was centrifuged and the flow-through discarded with an additional spin for 30 s to assure the residual fluid was removed. Next, DNase mix was prepared (6 μ L of 10X DNase Buffer, 4 μ L of DNase, 50 μ l of Nuclease-free water per sample) and added to the centre of the Filter Cartridge and incubated for 30 min period at room temperature. At the end of incubation period, 700 μ L of Wash 1 Solution was added to the Filter Cartridge and let to incubate for 60 s at room temperature. After centrifuging for 30 s, the flow-through was discarded and 500 μ L of Wash 2/3 Solution was applied to the Filter and centrifuged. An additional wash with Wash 2/3 Solution was performed. To remove residual fluid an extra spin was conducted for 1 min. The Filter Cartridge was transferred to a fresh collection tube and 60 μ L of the Elution Solution (at room temperature) was applied to the centre of the filter and incubated for 1 min at room temperature. Finally, the previous mixture was centrifuged at 10,000 x g and the eluate (containing RNA) was collected and stored at -80°C. Bioanalyser, which measures the RNA integrity number (RIN) using electrophoretic separation and laser-induced fluorescence detection of the RNA, and a NanoDrop Spectrophotometer (NanoDrop 2000, Thermo Scientific) were used to assess the quality and yield of the RNA collected before using in further analysis.

2.7. TaqMan[®] Low Density Array (TLDA)

TaqMan[®] Low Density Array (TLDA) Rodent MicroRNA Cards v.3 A and B or TaqMan[®] Human MicroRNA Cards v.3 A and B were used to investigate the presence and expression of miRNAs in rat and human tissues, respectively.

2.7.1. Reverse Transcription to cDNA

All miRNA samples were initially reverse transcribed using Taqman[®] MicroRNA Reverse Transcription (RT) Kit (Applied Biosystems) and the respective RT primers. The RT reaction mix was prepared as described in table 2.3. The components were allowed to thaw slowly on ice and, then, added together in a microcentrifuge tube.

Table 2.3. Reaction mix for miRNA reverse transcription (RT).

RT reaction mix components	Volume per reaction (μL)
RNase inhibitor (20 U/ μl)	0.10
dNTPs with dTTP (100 mM)	0.20
RT buffer (10 X)	0.80
MultiScribe [™] reverse transcriptase (50 U/ μL)	1.50
Megaplex [™] RT primers (human or rat pools A and B)	0.80
MgCl ₂ (25 mM)	0.90
Nuclease-free water	0.20
RNA sample	5.5
<i>Total</i>	10.0

In order to keep the starting RNA concentration (50 ng) constant across all samples, the volume of RNA sample and nuclease-free water were adjusted accordingly. The tube was mixed and briefly spun before incubating on ice for 5 min. Subsequently the tube was loaded on the thermal cycler using the cycling conditions described in table 2.4.

Table 2.4. Parameters used in the thermal cycler for Reverse Transcription

Step	Temperature ($^{\circ}\text{C}$)	Time
Cycle (40)	16	2 min
	42	1 min
	50	1 sec
Hold	85	5 min
Hold	4	∞

2.7.2. Preamplification reaction

The Preamplification reaction was performed to increase specific cDNA in downstream miRNA analysis. The reaction was prepared as described in table 2.5.

Table 2.5. Preamplification reaction mix.

Reaction mix components	Volume per reaction (mL)
TaqMan PreAmp Master Mix (2X)	12.5
Megaplex PreAmp primers (10X)	2.5
Nuclease-free water	7.5
RT cDNA	2.5
<i>Total</i>	25.0

The components were thawed on ice and added together in a microcentrifuge tube. The tube was mixed and incubated on ice for 5 min before loading to the thermal cycler using the parameters described on table 2.6.

Table 2.6. Preamplification parameters

Step	Temperature	Time
Hold	95	10 min
Hold	55	2 min
Hold	72	2 min
Cycle (12)	95	15 sec
	60	4 min
Hold	99.9	10 min
Hold	4	∞

At the end of the run, the preamplified product was diluted (1:4) in 75 μ L of 0.1X Tris-EDTA buffer (pH 8.0).

2.7.3. TaqMan[®] real-time PCR reactions

The TaqMan[®] microRNA array (TLDA) cards were stored at 4°C and allowed to reach room temperature before being loaded with the PCR reaction mix. Each card contained up to 380 preloaded miRNA probes and endogenous control (RNU48 and small nuclear RNA (snRNA) U6). The components described in table 2.7 (contains a 12.5%

excess) were added together and 100 μ L of the PCR reaction mix was loaded into each port of the TLDA card (figure 2.6).



Figure 2.6. TLDA microfluidic card. Each card contains 8 ports that will supply the 384 wells with the PCR reaction mix.

Table 2.7. TaqMan[®] array components.

Component	Volume per card (mL)
TaqMan[®] Universal PCR master mix, No AmpErase[®] UNG, 2X	450
Diluted PreAmp product	9
Nuclease-free water	441
<i>Total</i>	900

The card was centrifuged for 2 min at 300 x g (Sorvall Legend XT/XF), sealed using appropriate carriage sealer (Applied Biosystems) and, subsequently, the reservoir ports were removed. The sealed card was loaded on a 7900HT Real-Time PCR System with 384-Well Block and the manufacturer's recommended settings were used (table 2.8).

Table 2.8. Parameters used in the TaqMan® array RT-qPCR amplification.

Step	Temperature (°C)	Time
Cycle (40)	50	2 min
	94.5	10 min
	97.0	30 sec
Hold	59.7	1 min

2.8. miRNA validation

The expression of specific miRNAs identified with TLDA arrays were validated with TaqMan® MicroRNA Assays (triplicate per sample) and performed in a Rotor Gene real time PCR machine (Qiagen).

First each RNA sample was reverse transcribed with specific TaqMan® probes for the miRNA of interest and endogenous control. The components used are described in table 2.9.

Table 2.9. Components in miRNA reverse transcription (RT) reaction

Component	Volume per reaction (µl)
RNase inhibitor (20U)	0.19
100 mM dNTP (25X)	0.15
10x RT buffer	1.5
Multiscribe RT enzyme (50U/ µl)	1.0
5X miRNA RT probe	3.0
Nuclease-free water	4.16
10 ng RNA	5.0
<i>total</i>	<i>15.0</i>

The RT mix was loaded onto the thermal cycler using the parameters specified in table 2.10.

Table 2.10. Parameters used in thermal cycler for miRNA reverse transcription

Step	Temperature (°C)	Time
Annealing	16	30 min
Extension	42	30 min
Denaturation	85	5 min
Hold	4	∞

The reverse transcribed product was preamplified as described in section 2.6 and the RT-qPCR reaction mix (table 2.9) was loaded onto specific tubes that were loaded onto the Rotor-Disc 72.

Table 2.11. Reaction mix for RT-qPCR miRNA validation

Component	Volume per well (μl)
2\times TaqMan[®] Universal PCR Master Mix, No AmpErase[®] UNG	5
Diluted PreAmp product	0.8
TaqMan[®] Probe 20X	0.5
Nuclease-free water	3.7
<i>Total</i>	10

Rotor-Gene 2.1.0.9 software was used to set the real time qPCR reaction (initial enzyme activation at 95°C for 10 min, and cycling conditions set at 95°C for 15 sec followed by 60°C for 60 sec, for 40 cycles). A no template control (NTC, no PreAmp product) sample was added to test for cDNAcontamination.

2.9. Statistical analysis

2.9.1. Behavioural analysis

Comparisons between groups were statistically evaluated using a two-way repeated measures-ANOVA in GraphPad Prism (version 7.02 for Windows, GraphPad software, San Diego, CA, USA). When differences were found to be statistically significant ($p \leq 0.05$), a Sidak *post hoc* correction was applied. To test for differences between time-points compared to the baseline within each group, a one-way ANOVA was performed followed by Dunnet's *post hoc* correction. Assumptions of heterogeneity of variance and sphericity (Mauchly's sphericity test) were tested automatically by the GraphPad software and when violated, Greenhouse Geisser corrected values were reported.

2.9.2. Quantification from image analysis

Statistical comparisons between groups were made using GraphPad Prism (version 7.02 for Windows, GraphPad software, San Diego, CA, USA). For quantification of ChemR23 and Iba1 staining, a two-way ANOVA repeated measures followed by Tukey's *post hoc* test (if previous test statistically significant) was performed to determine differences between groups and Vc rostral caudal level. Differences were considered

statistically significant when $p \leq 0.05$. The reproducibility of the method was tested by repeating quantification in some of the sections as reported in section 2.10.1 in this chapter.

2.9.3. miRNA analysis

Delta C_t (ΔC_t) normalisation method was applied to the rat and human miRNA results and the snRNAU6 endogenous control used. Two additional normalisation methods were applied to the results obtained from human samples due to higher variability in miRNA expression. They were: geometric mean normalised (the average C_t value for each sample was calculated, then all C_t values were scaled according to the ratio of those average C_t values across samples) and normdelta C_t ranked (delta C_t were normalised between 0 and 1 based on max/min values across samples). However, no significant differences were found between methods and delta C_t normalisation methods were applied to the results reported in chapter 6 (for both human and rat miRNA). Prior to normalisation, any miRNA probes with undetected values in two of either the experimental or control samples were removed from further analysis. The non-parametric RankProd (R package version 3.0.0 (Hong, F. et al., 2011) statistical test or independent t-test were performed to calculate statistical differences between groups. Results were considered statistically significant with a $p \leq 0.05$. No C_t cut-off value was applied.

For miRNA validation of miRNA screening, it was used the comparative delta delta C_t ($2^{(-\Delta\Delta C_t)}$) method. First, delta C_t (ΔC_t) values for each miRNA were obtained after normalising to snRNAU6, a common reference gene used in miRNA studies (it is highly expressed and relatively stable across tissues) and to keep the same normalisation method as used in the TLDA card analysis. The relative expression for each miRNA in the experimental lingual nerve (CCI in the rat tissue and painful group in the human tissues) was compared with the control lingual nerves (sham in the rat tissues and non-painful in the human tissues) and calculated using the equation $2^{-\Delta\Delta CT}$, where $\Delta\Delta CT = \Delta C_T$ (experimental) $- \Delta C_T$ (control).

Correlation studies with behavioural or clinical data were conducted. Differences between samples were evaluated using independent samples t-test with equal variance assumed. Pearson correlation was used to examine the association between pain VAS score with discomfort VAS score, and between miRNA expression and pain, tingling and discomfort VAS score (human samples) or feeding behaviour (rat samples).

2.9.4. Target prediction and enrichment analysis

Target genes potentially regulated by significantly differentially expressed miRNAs were predicted using the consensus of three publicly available miRNA target databases: Targetscan (<http://www.targetscan.org>), MicroCosm (<http://www.ebi.ac.uk/enright-srv/microcosm>) and miRTarBase (<http://mirtarbase.mbc.nctu.edu.tw>). The predicted target false positive rate was significantly reduced by applying a cut-off of -0.4 in the context++ scores for TargetScan results (Agarwal et al., 2015) and each miRNA target was cross referenced against this gene set. Enrichment and pathway analysis of predicted miRNA gene targets was undertaken using Metacore™ process networks, pathway maps and GO molecular functions/processes. Top pathways were ranked based on z-score and the additional enriched gene count per pathway. Interactions between miRNAs and their target gene networks for each tissue were visualised using CytarGetlinker v3.0.1 an open source software package for Cytoscape v.4.0 (Kutmon M. et al., 2013). Circos v0.67 (Krzywinski, M. et al., 2009) was used to display interaction between miRNAs and target genes in a circular layout, facilitating the visualisation of the position of the miRNAs and target genes in the respective genome.

2.10. Reproducibility of image analysis

In order to determine the reproducibility of image quantification of ChemR23 and Iba1 staining, repeated measurements (PAS%) on a set of 10 sections per group were conducted on a different day in the same area of interest (AOI), both ipsilateral and contralateral of the trigeminal nucleus caudalis (Vc). Pearson correlation coefficients were calculated between initial and the repeated measurements (table 2.12) and plotted in a graph (figures 2.7-2.10).

The scatter plots showed a strong linear Pearson correlation between initial and repeated measurements.

Table 2.12. Pearson correlations between initial and repeated measurements.

	Group		AOI	Pearson r
ChemR23	Naïve		IL	0.97
			CL	0.98
	Sham	DAY 3	IL	0.97
			CL	0.97
		DAY 7	IL	0.96
			CL	0.97
		DAY 28	IL	0.97
			CL	0.98
	CCI	DAY 3	IL	0.95
			CL	0.95
		DAY 7	IL	0.95
			CL	0.96
		DAY 28	IL	0.94
			CL	0.94
Iba1	Naïve		IL	0.98
			CL	0.96
	Sham	DAY 3	IL	0.95
			CL	0.95
		DAY 7	IL	0.99
			CL	0.96
		DAY 28	IL	0.94
			CL	0.99
	CCI	DAY 3	IL	0.99
			CL	0.94
		DAY 7	IL	0.99
			CL	0.95
		DAY 28	IL	0.98
			CL	0.98

AOI: Area of interest; CL: contralateral; IL: Ipsilateral

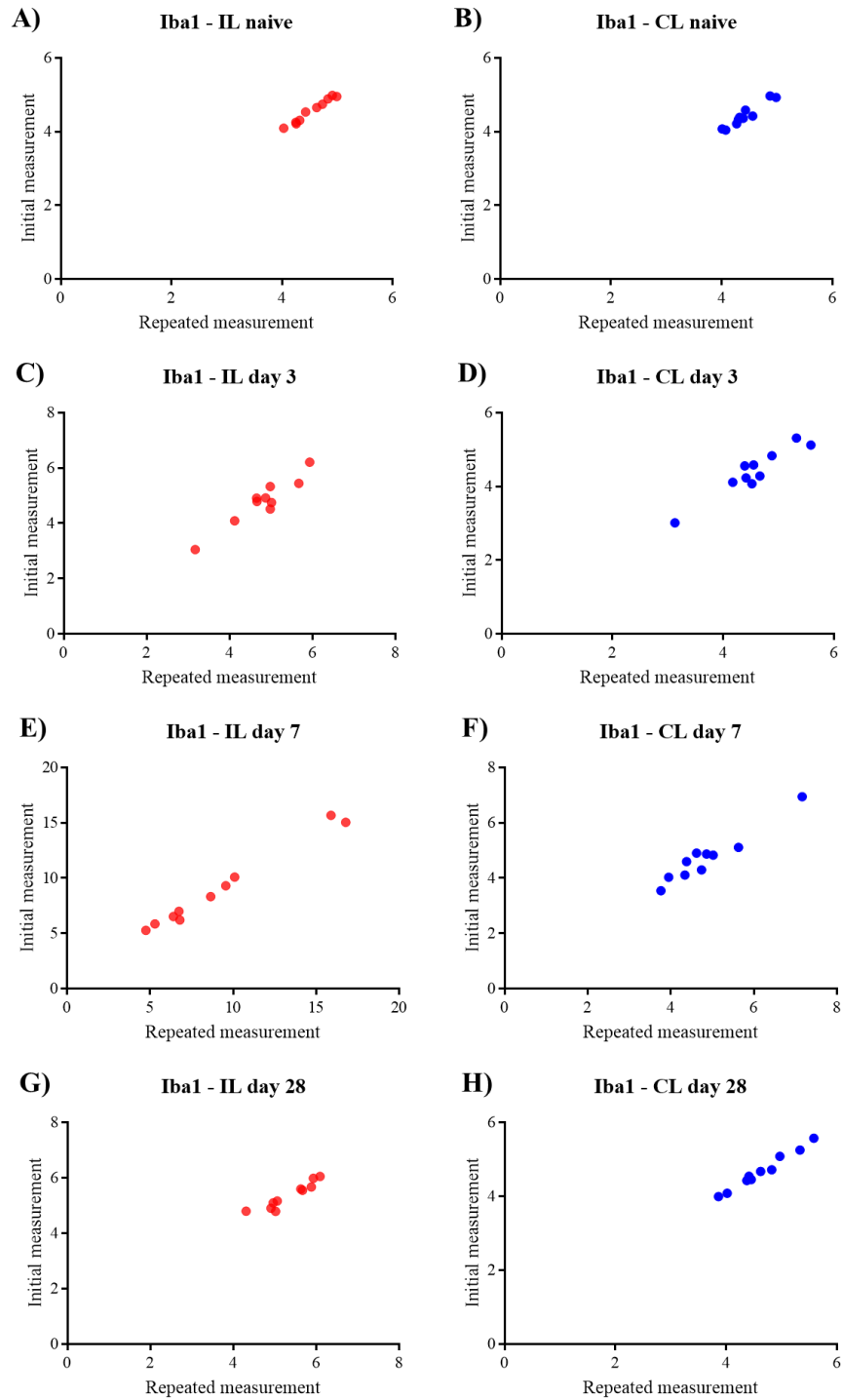
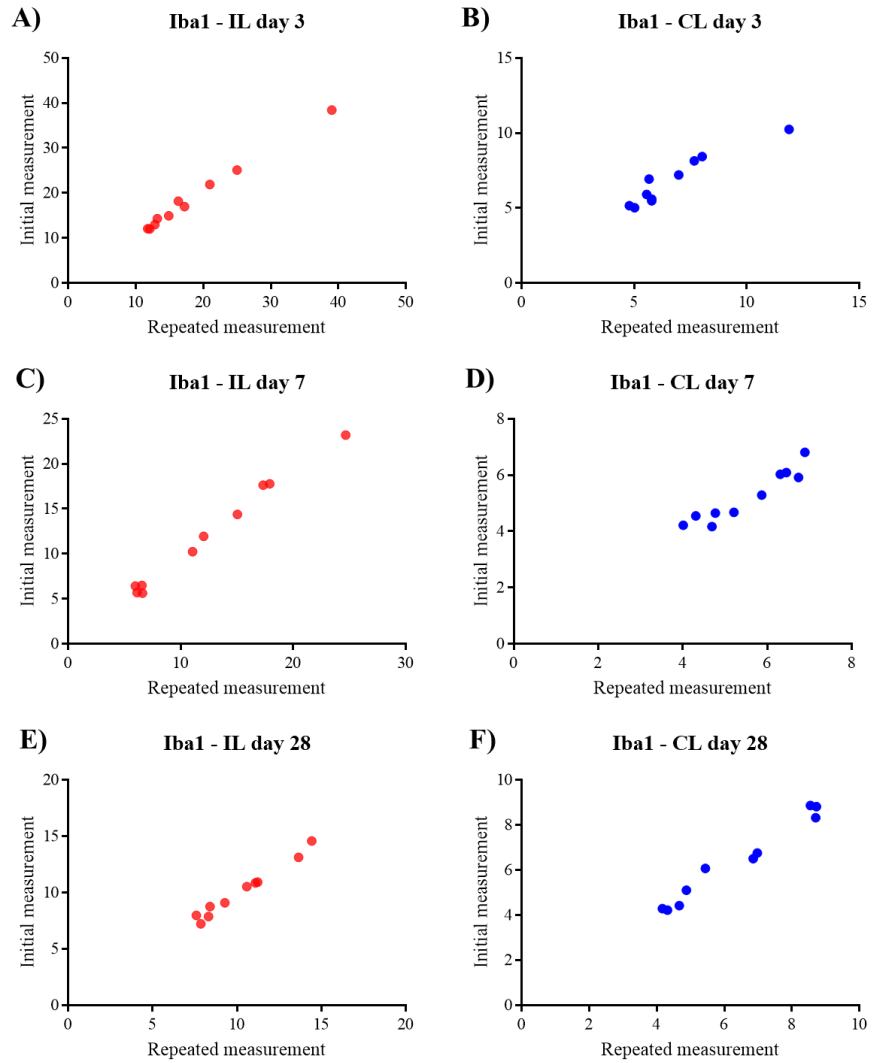


Figure 2.7. Scatter plots showing linear relationship between Iba1 initial and repeated measurements in sections from control naïve and sham animals. A-B) Iba1 expression in naïve control. C-D) Iba1 expression in sham day 3. E-F) Iba1 expression in sham day 7. G-F) Iba1 expression in sham day 28.



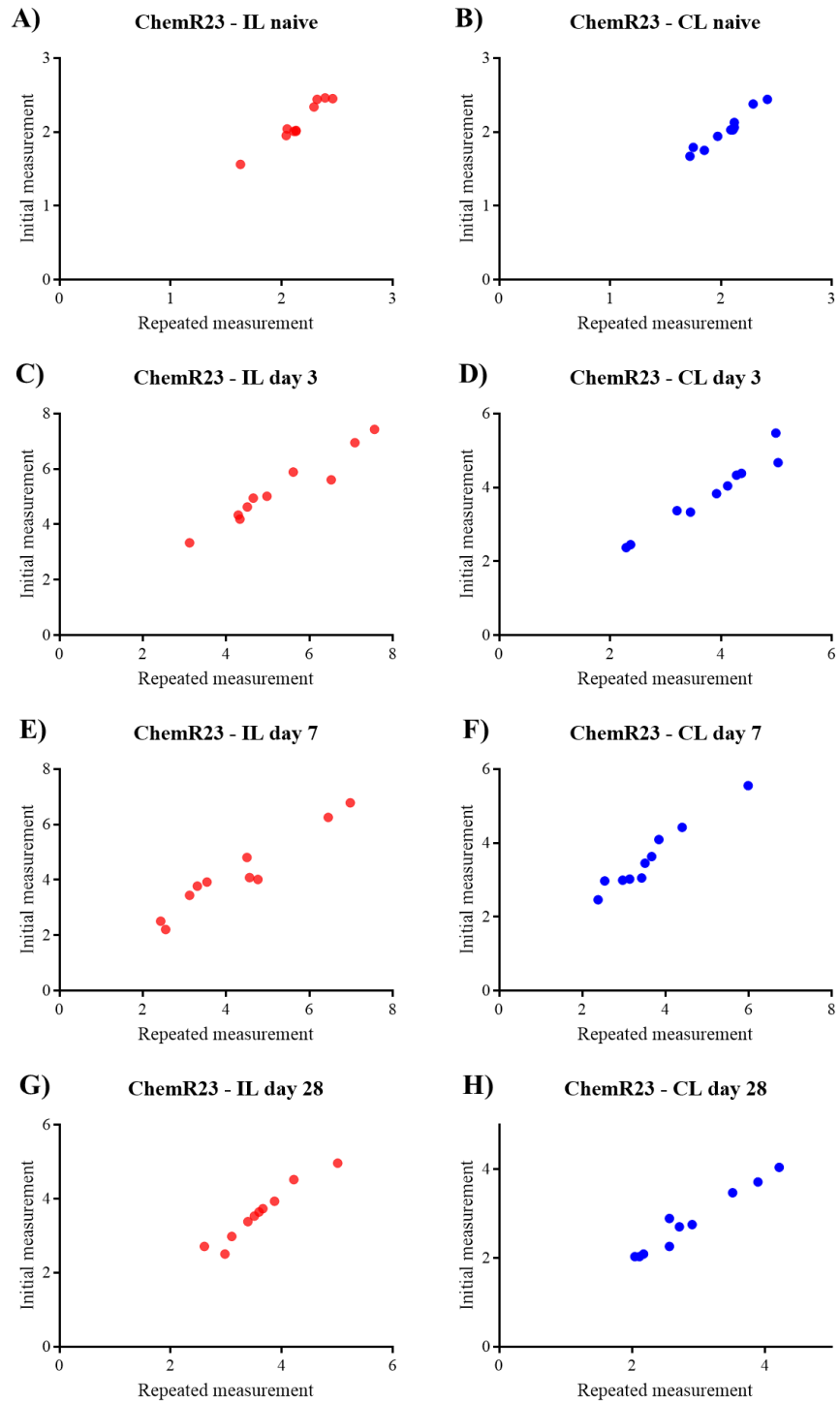


Figure 2.9. Scatter plots showing linear relationship between ChemR23 initial and repeated measurements in sections from control naïve and sham animals. A-B) ChemR23 expression in naïve control. C-D) ChemR23 expression in sham day 3. E-F) ChemR23 expression in sham day 7. G-F) ChemR23 expression in sham day 28.

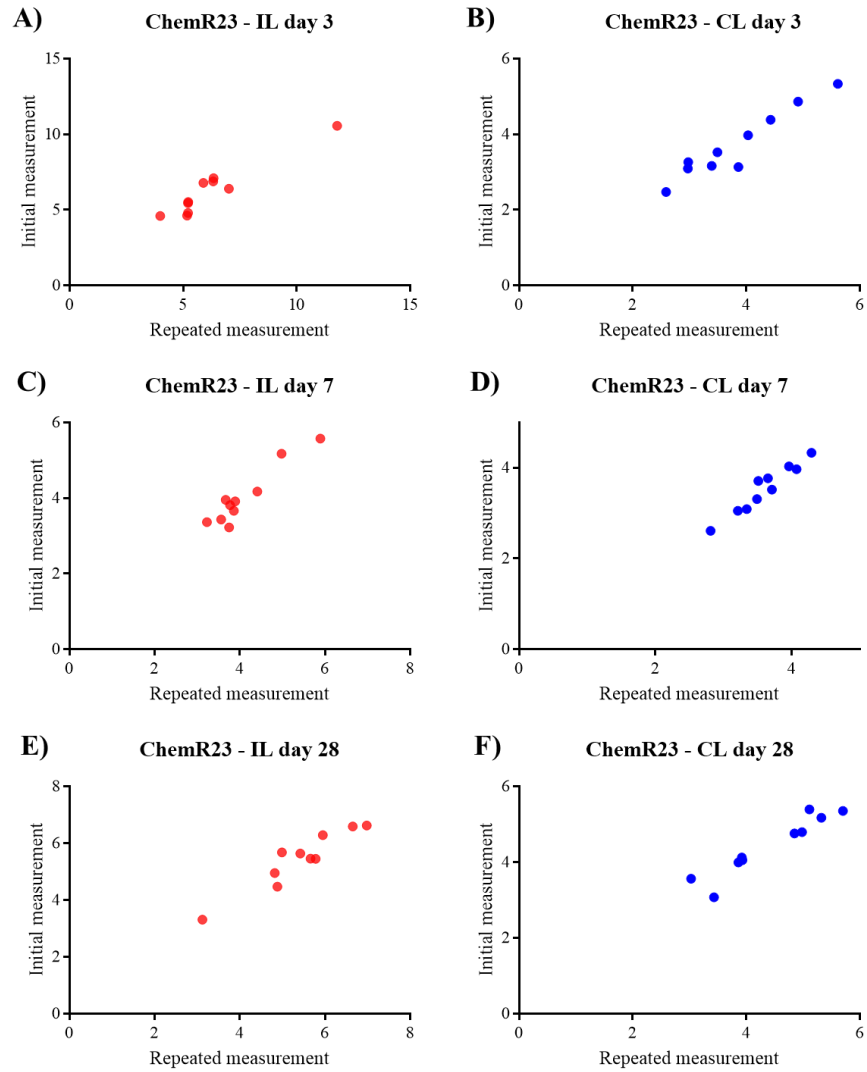


Figure 2.10. Scatter plots showing linear relationship between ChemR23 initial and repeated measurements in sections from injured (CCI) animals. A-B) ChemR23 expression in CCI day 3. C-D) ChemR23 expression in CCI day 7. E-F) ChemR23 expression in CCI day 28.

CHAPTER 3
EFFECT OF LINGUAL NERVE INJURY ON
FEEDING BEHAVIOUR

3.1. Introduction

Behavioural analysis is a key component of any experiment using animal models and in particular in the study of pain, as discussed previously in the literature review (section 1.5 in chapter 1). Animal behaviour studies can be used to investigate the external manifestations of molecular and cellular changes that occur as a consequence of disease or nerve injury, and behavioural data is crucial to enable correlation of animal findings with clinical data. In this chapter, the Orofacial Stimulation Test (code 31300, Ugo Basile, Comerio, VA, Italy), developed by Fehrenbacher, Henry and Hargreaves was adapted for the study of feeding behaviour following lingual nerve injury (LNI). It was hypothesised, based on human clinical observations, that LNI in the rat would affect the feeding behaviour observed using this test, because the lingual nerve innervates the tongue and, in this behavioural test, the tongue is required to access the reward. In this model animals could choose between drinking or avoiding painful/non-comfortable movement of the tongue.

The overall aim was investigate and characterise feeding behaviour following LNI, using the Ugo Basile Orofacial Test. The specific objectives were:

1. Investigate whether LNI affects time spent drinking (total and longest uninterrupted time drinking);
2. Investigate whether LNI affects the number of attempts made to drink;
3. Investigate whether LNI affects total volume of reward ingested.

3.2. Methodological approach

As mentioned in section 2.2.2 in chapter 2, the behavioural assessment consisted of measurement of the duration of feeding, number of feeding attempts and volume ingested over a given period of time, as well as maximum and minimum ingestion volumes (table 3.1). With the exception of volume measurement (conducted by investigator), all other measurements were automated via an infra-red barrier present between the opening to the reward (access window) and the reward bottle.

Table 3.1. Measurements.

Measurement	Description	Automatic
Total time drinking	Overall duration (in seconds) of drinking within the testing period.	YES
Maximum and minimum	Longest and shortest, respectively, uninterrupted time drinking within the testing period.	YES
Number of attempts	Number of attempts made to access the reward.	YES
Volume	Total volume in mL consumed during testing period	NO

One week prior to surgery animals were trained to use the behavioural equipment. Sessions consisted of a 10 min acclimatisation period in the behavioural cage without access to the reward as opening was covered and a further 10 min recording with access to the reward bottle (the cover of opening to the reward was removed). Behavioural assessment took place immediately before the surgery (day 0) and subsequently between days 1 and 28 after surgery (figure 3.1). On day 0 animals were randomly divided in two groups: CCI (n=6) and sham-control (n=6). In the CCI (experimental) group the left lingual nerve was constricted and in the sham-operated (control) group, the nerve was just exposed, not injured. A total of 12 animals were used, 6 animals per group (table 3.2). However, the animals were trained and tested in sets of 4, so that each set would include 2 experimental (CCI) and 2 control (Sham) animals (figure 3.1). On the first training day the animals were randomly given a sequential code and a tail mark for identification. On the surgery day (day 0 of testing) the animals were randomly allocated to the experimental group (CCI) or the control group (sham group) and given a different code for the type of surgery (associated with the tail mark). This was conducted blind to the investigator and only at the time of data analysis both codes were matched and the behavioural data associated to the groups (CCI or sham) analysed.

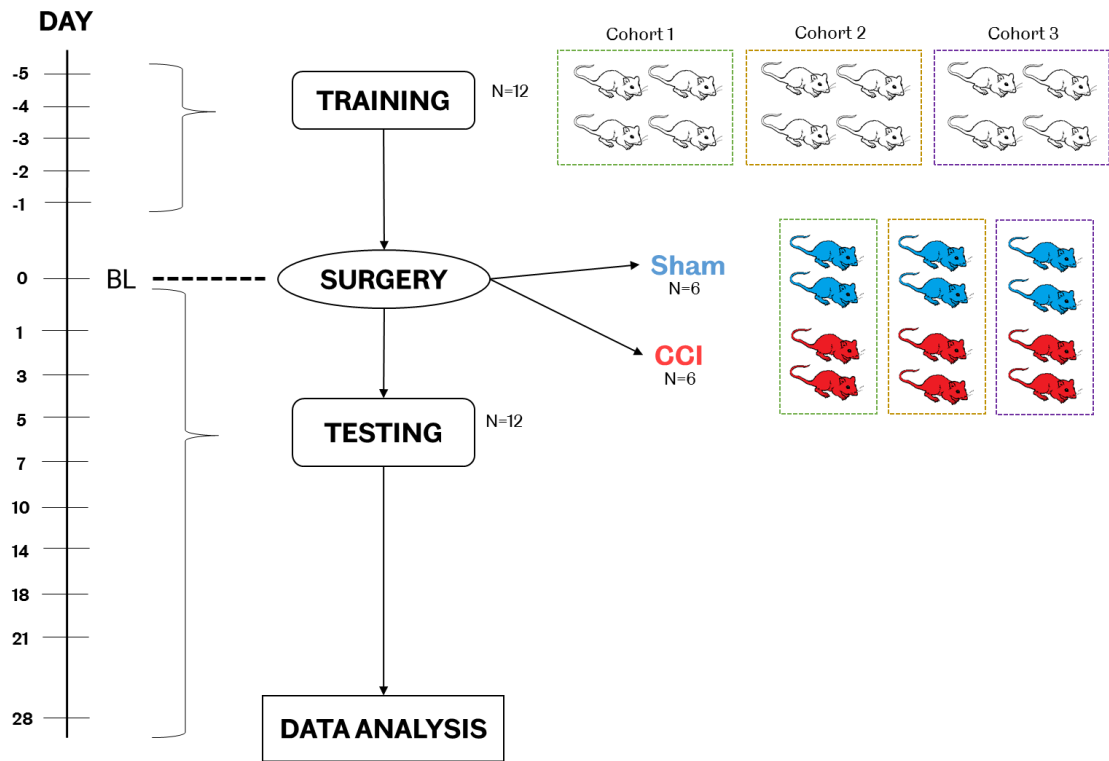


Figure 3.1. Diagram representing the methodological approach with training, surgery, testing and data analysis. The colours represent the type of surgery: in red animals that underwent CCI (chronic constriction injury) and in blue animals that underwent sham operation.

Table 3.2. Characteristics of animals subjects used for the behavioural testing.

ANIMAL	Weight (g)			Date		
	Arrival	Day 0	Day 28	Training	Day 0	Day 28
<u>CCI group</u>						
1	200-225	275	370	01-05/02/16	08/02/16	07/03/16
2	200-225	341	481	01-05/02/16	08/02/16	07/03/16
3	200-225	325	390	08-12/02/16	15/02/16	14/03/16
4	200-225	293	370	08-12/02/16	15/02/16	14/03/16
5	200-225	384	480	15-19/02/16	22/02/16	21/03/16
6	200-225	431	549	15-19/02/16	22/02/16	21/03/16
<u>Sham group</u>						
7	200-225	301	437	01-05/02/16	08/02/16	07/03/16
8	200-225	310	450	01-05/02/16	08/02/16	07/03/16
9	200-225	343	474	08-12/02/16	15/02/16	14/03/16
10	200-225	353	475	08-12/02/16	15/02/16	14/03/16
11	200-225	395	501	15-19/02/16	22/02/16	21/03/16
12	200-225	409	518	15-19/02/16	22/02/16	21/03/16

Statistical tests (discussed in more detail in chapter 2, section 2.8.1) were used to evaluate differences between injured animals (CCI group) and controls (sham-group) over a period of 28 days (two-way ANOVA repeated measures) and to explore potential differences at each time-point compared to the baseline within each group (one-way ANOVA repeated measures). Wherever applicable, two-way ANOVA was followed by Sidak's *post hoc* test and one-way ANOVA was followed by Dunnet's *post hoc* test.

3.2.1. Preliminary studies

3.2.1.1. Testing conditions

Animals were kept in a 12h dark/light cycle and were tested at approximately the same time on the testing day (between 7:30 – 10:30 am). The animals were not deprived of food or water, and no mechanical or thermal stimuli were applied. The animals were trained in pairs (2 animals simultaneously but in a separate testing cage). The optimal position of the bottle containing the reward to be accessed by the animal was established in preliminary studies with animals not included in the results reported in the subsequent results sections. The testing cage was cleaned in between tests with water; however, the use of detergent was avoided due to the strong odour. To record all information no beam cut-off was pre-specified. All the conditions were then maintained for the entirety of the experiments.

3.2.1.2. Choice of reward

Based on the literature, sweetened milk was initially used as a reward in preliminary studies. However, the animals did not demonstrate interest in the sweetened milk. Therefore, a chocolate drink (Sainsbury's own brand) was subsequently tested and this reward was used in the results reported in this chapter. Each training/testing period, the animal had 20 mL total of reward available.

3.3. Results

3.3.1. Training period and baseline

All 12 animals were trained for 5 days consecutively before the surgery. The images in figure 3.2 demonstrate the progressive training undertaken and the automatic recording by the Ugo Basile software, suggesting the animals increased interest in the reward during the training period.

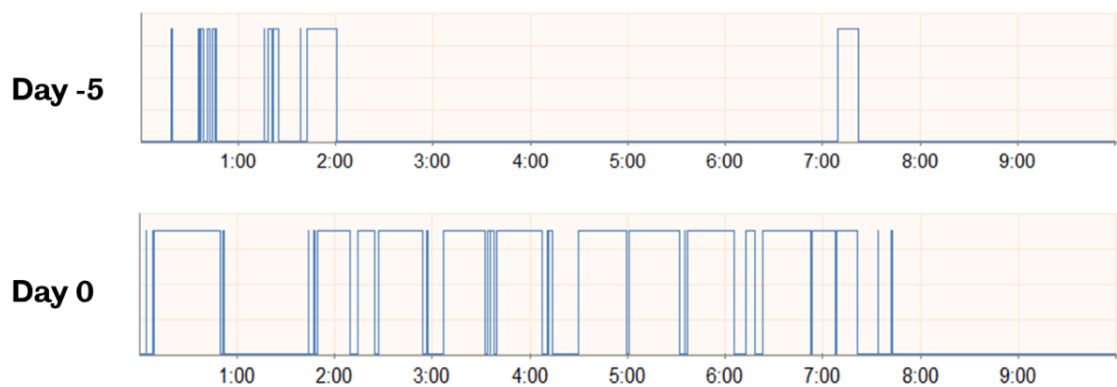


Figure 3.2. Example of drinking behaviour recording by the Ugo Basile software. The blue lines correspond to the time and duration of the infrared beam break. The longer the blue line, the longer is the continuous time drinking. In this example it is possible to observe the increase in number of times and duration of feeding attempts during the training period.

There was an increase in the time drinking as well as in the longest time uninterrupted (maximum) with the progression of training (figure 3.3). On the first day of training the animals were accessing the reward bottle on average for 49.31 s in the sham group and for 57.21 s in the CCI group. By day 0 this had increased to 375.74 s for the sham group and 389.37 s for the CCI group. However, no statistical differences were found between groups in the time drinking ($F(1, 10)=0.888, p=0.368$, two-way ANOVA repeated measures) or in the maximum time ($F(1, 10)=1.523, p=0.245$, two-way ANOVA repeated measures). The minimum time drinking recorded within the 10 min was 0.04 s (not shown).

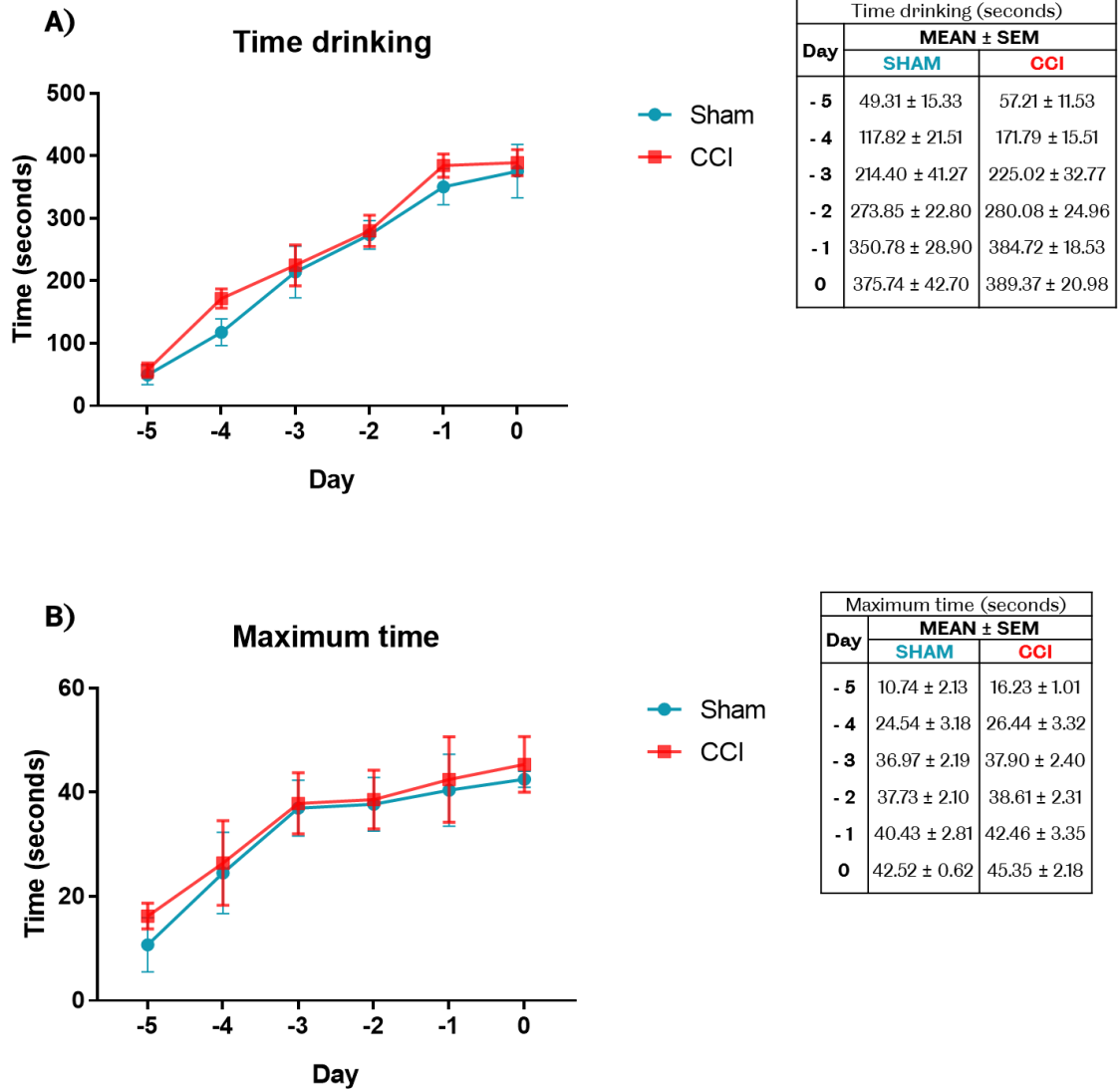


Figure 3.3. Time drinking during training period and day 0. A) Total time drinking, in seconds, at each training day up to day 0 (pre-surgery), demonstrating the progressive training. B) Within each training the longest time drinking (maximum) was also recorded and it also increase over the 5 days of training period. No statistical differences were found between groups prior to surgery in both measurements.

The number of attempts also increased overall from the first day of training (average of 13.33 attempts in the sham group and 16.67 attempts in the CCI group) to the day 0 before the surgery (average of 43.83 attempts in the sham group and 39.17 attempts in the CCI group) (figure 3.4). No statistical differences were found between groups ($F(1, 10)=0.002, p=0.964$).

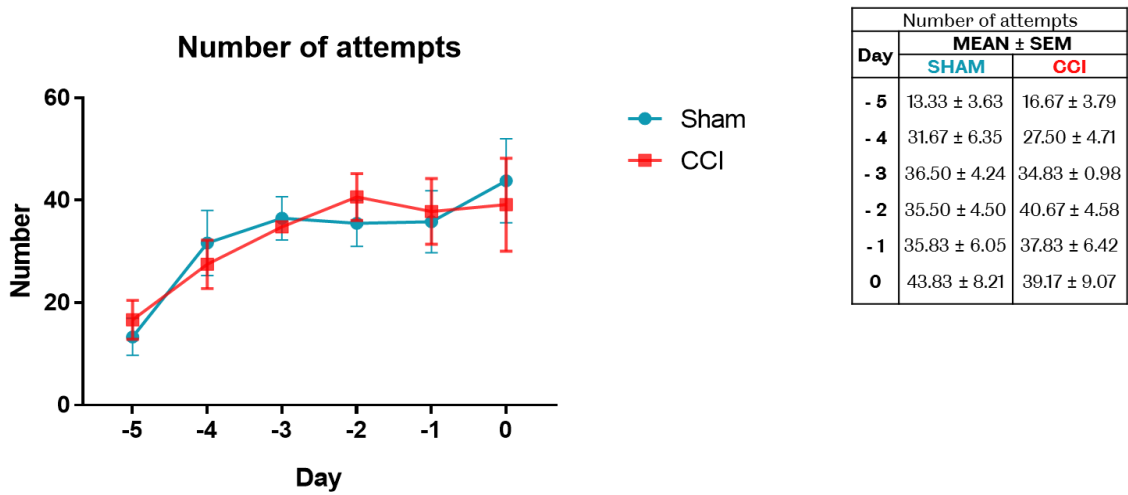


Figure 3.4. Number of attempts during training period and day 0. The number of attempts to reach the reward increased from first day of training (day -5) up to day 0 (pre-surgery). No statistical differences were found between groups prior to surgery.

In the same way as the other measurements, the volume ingested increased during the training period (figure 3.5). On the first training day the animals were drinking an average of 1.67 mL in the sham group and 3.83 mL in the CCI group; on day 0 before the surgery the animals were drinking in average 14 mL in the sham group and 12.67 mL in the CCI group. No statistical differences were found between groups ($F(1, 10)=0.512$, $p=0.491$).

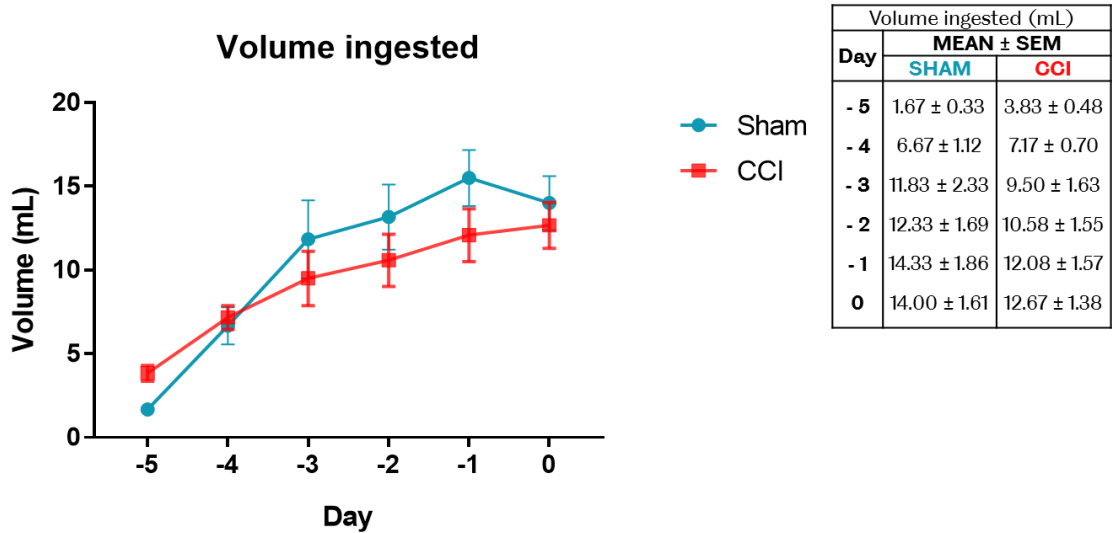


Figure 3.5. Volume ingested (mL) during the training period and day 0. The volume ingested increased during the training period and on day 0 (pre-surgery) in both groups. No statistical significant differences were found between groups.

Based on the training data, day 0 was chosen as the baseline (BL) for the analysis of the testing data. In addition to the raw values, all data was also adjusted to the percentage of BL (considering BL as 100% and values for each time point post-injury calculated accordingly). For the subsequent results in this chapter analyses on both raw data and percentage adjusted values are reported.

3.3.2. Observational notes

Animals in both groups increased weight over time (table 3.2), however, the CCI group on day 28 had, on average, a 7% lower body weight gain compared to the sham group (figure 3.6), but this was not statistically significant. On day 1 of testing it was possible to observe local swelling around the area of surgery in all animals; the swelling generally disappeared by day 3 or 5. Overall, animals in the CCI group demonstrated

more signs of nerve injury. For instance, one of the animals in the CCI group had marks of blood around the snout on day 7; this was probably from tongue biting, an expected symptom of injury.

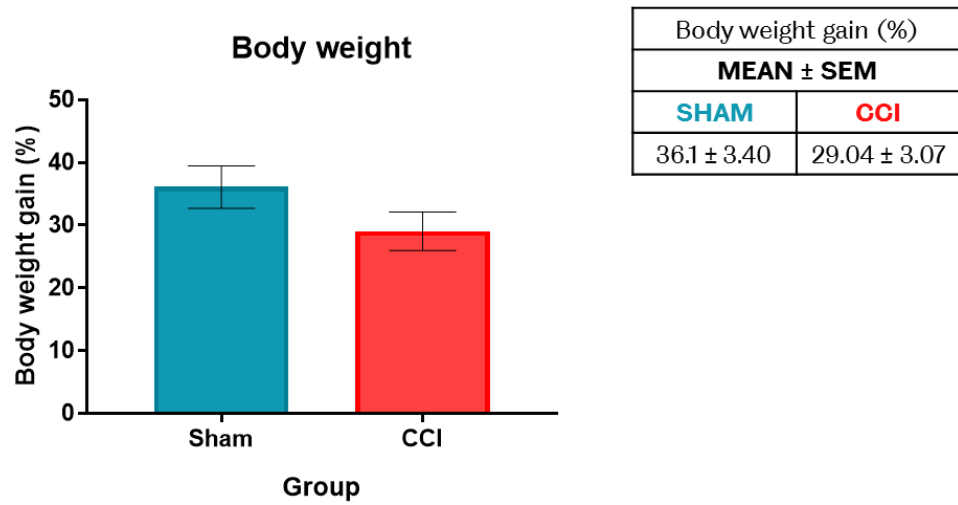


Figure 3.6. Percentage of body weight gain in average by group at the end of experiment. The CCI group had a lower body weight gain at 28 days post-injury but no statistically significant differences were found between groups.

Representative graphs derived from ORO software at selected time points are shown in figure 3.7. The blue lines correspond to the duration of interruption of infrared barrier and, thus, the duration and number of attempts to access the reward. In the next sections, data derived from ORO software (plus volume ingested) of all animals at all time points was analysed and it will be discussed in further detail.

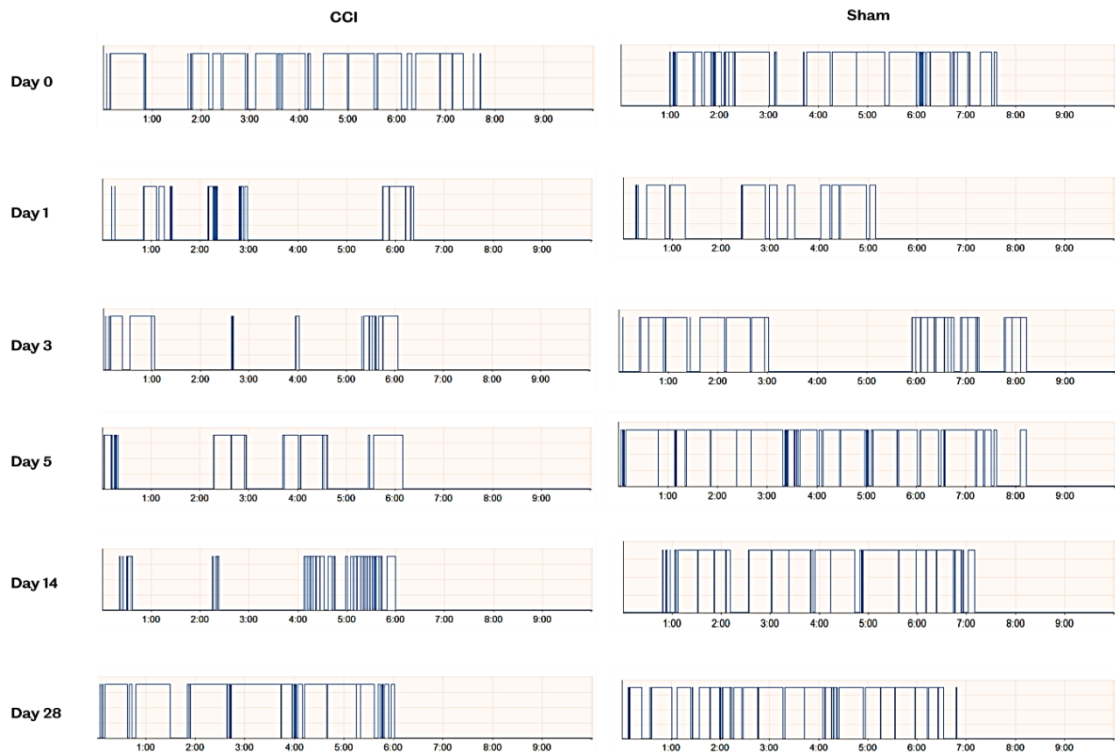
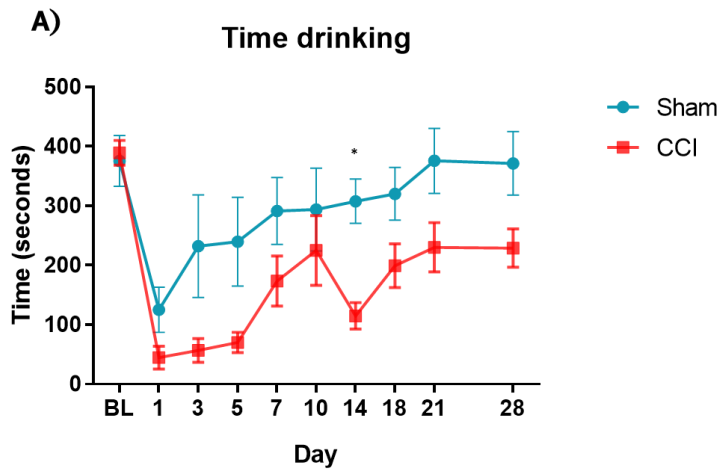


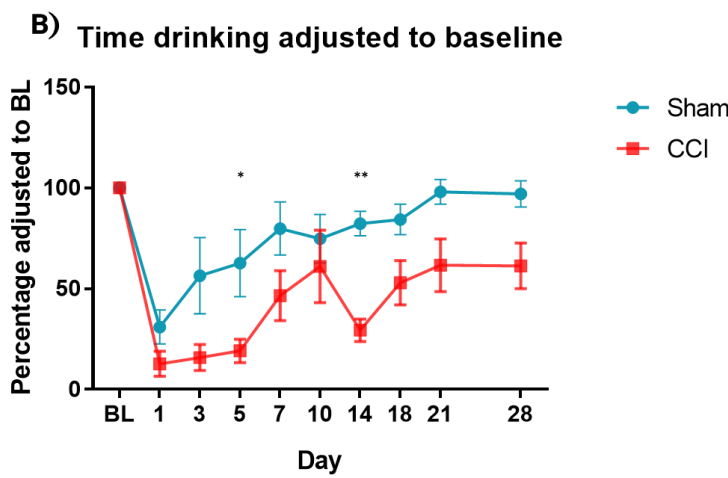
Figure 3.7. Data recorded by ORO software. Representative graphs (on days 0, 1, 3, 5, 14 and 28 post-surgery) automatically produced by the ORO software showed the duration and number of attempts to get the reward per testing. The higher the number of blue lines the higher the number of attempts and the longer the blue line, the longer was the duration of accessing the reward. On the left, graphs obtained from one animal of the CCI group and on the right graphs obtained from one animal of the Sham group.

3.3.3. Time drinking post-surgery

Total time drinking within the 10 min (600 s) of testing was decreased following surgery, with stronger effect in the CCI group. On day 1 it was substantially decreased in both groups: the sham group was drinking on average for 125.14 s and the CCI group for 44.79 s corresponding to a decrease of approximately 70% (sham) and 88% (CCI) when comparing to BL (percentage of values adjusted) (figure 3.8). However, while the animals on the sham group showed a rapid increase on day 3 (average of 232.30 s), the CCI group continued drinking for less time (average of 56.76 s) and in this group, the biggest increase in time drinking was observed from day 5 to day 7 (70.12 s to 173.43 s, respectively). On day 14 it was possible to observe that the CCI group had a decrease in the time spent drinking (average of 114.89 s on day 14 from 225.02 s on day 7) and also when compared to the sham group (average of 307.84 s on day 14). Overall, there was a statistical significant difference on the time drinking when comparing to the CCI and sham groups ($F(1, 10)=5.317, p=0.044$, two-way ANOVA repeated measures). When adjusting the values to percentage of baseline similar statistically significant results were obtained ($F(1, 10)=8.815, p=0.014$, two-way ANOVA repeated measures). On day 14 there was a significant difference between CCI and sham group ($p=0.047$, Sidak's *post hoc* test); when adjusting to BL days 5 (adjusted $p=0.043$, Sidak's *post hoc* test) and 14 (adjusted $p=0.006$, Sidak's *post hoc* test) post-surgery were significantly different between groups.



Day	Time drinking (seconds)	
	SHAM	CCI
BL	375.74 ± 42.70	389.37 ± 20.98
1	125.14 ± 37.85	44.79 ± 19.32
3	232.30 ± 86.42	56.76 ± 19.95
5	239.77 ± 74.43	70.12 ± 17.20
7	291.47 ± 56.10	173.43 ± 42.06
10	293.98 ± 69.56	225.02 ± 58.62
14	307.84 ± 37.20	114.89 ± 22.20
18	320.39 ± 44.35	199.42 ± 36.71
21	375.84 ± 54.72	230.31 ± 41.54
28	371.63 ± 53.60	229.14 ± 32.41



Day	Time drinking adjusted to BL (%)	
	SHAM	CCI
BL	100.00 ± 0.00	100.00 ± 0.00
1	30.98 ± 8.40	12.70 ± 6.18
3	56.42 ± 18.91	15.86 ± 6.41
5	62.72 ± 16.61	19.13 ± 5.79
7	79.84 ± 13.21	46.53 ± 12.38
10	74.81 ± 11.97	61.04 ± 17.99
14	82.32 ± 6.06	29.40 ± 5.55
18	84.36 ± 7.54	52.96 ± 11.03
21	98.02 ± 6.13	61.64 ± 13.08
28	97.09 ± 6.47	61.34 ± 11.32

Figure 3.8. Time drinking decreased following lingual nerve injury. A) Total time drinking within each testing period was decreased following LNI. On day 14 there was a statistical significant difference between groups B) Total time drinking adjusted to percentage of baseline (BL) found a statistical difference between groups on days 5 and 14. Two-way ANOVA repeated measures followed by Tukey's *post hoc* test. Asterisks (*) represent statistical significant differences (* $p < 0.05$, ** $p < 0.01$).

When evaluating the effect of surgery just within each group, it was possible to observe a clear decrease following injury in the experimental CCI group, ($F(1.676, 8.382)=15.77, p=0.002$, one-way ANOVA repeated measures) and when adjusting to the baseline ($F(1.539, 7.696)=14.87, p=0.003$, one-way ANOVA repeated measures) (figure 3.9-A, -C). When analysing each day against the BL it was possible to verify that there was a statistically significant difference between BL and days 1, 3, 5 and 14 post-surgery (BL vs day 1 $p=0.001$, BL vs day 3 $p=0.001$, BL vs day 5 $p=0.001$, BL vs day 14 $p=0.0005$, Dunnett's *post hoc* test). When adjusting to the percentage of BL, days 1, 3, 5, 7, 14 and 18 following surgery were found to be statistically different (BL vs day 1 $p=0.0002$, BL vs day 3 $p=0.0002$, BL vs day 5 $p=0.0002$, BL vs day 7 $p=0.036$, BL vs day 14 $p=0.0003$, BL vs day 18 $p=0.039$, Dunnett's *post hoc* test). In the sham group, there was also a statistical difference when compared to the BL ($F(1.958, 9.788)=4.918, p=0.034$, one-way ANOVA repeated measures) with day 1 being the only day with a statistically significant difference (BL vs day 1 $p=0.004$) compared to BL (figure 3.9-B). Similarly, when adjusting to percentage of BL there was also a statistical difference ($F(2.399, 12)=5.817, p=0.014$, one-way ANOVA repeated measures) (figure 3.9-D); and similarly only day 1 after surgery is significant (BL vs day 1 $p=0.002$, Dunnett's *post hoc* test).

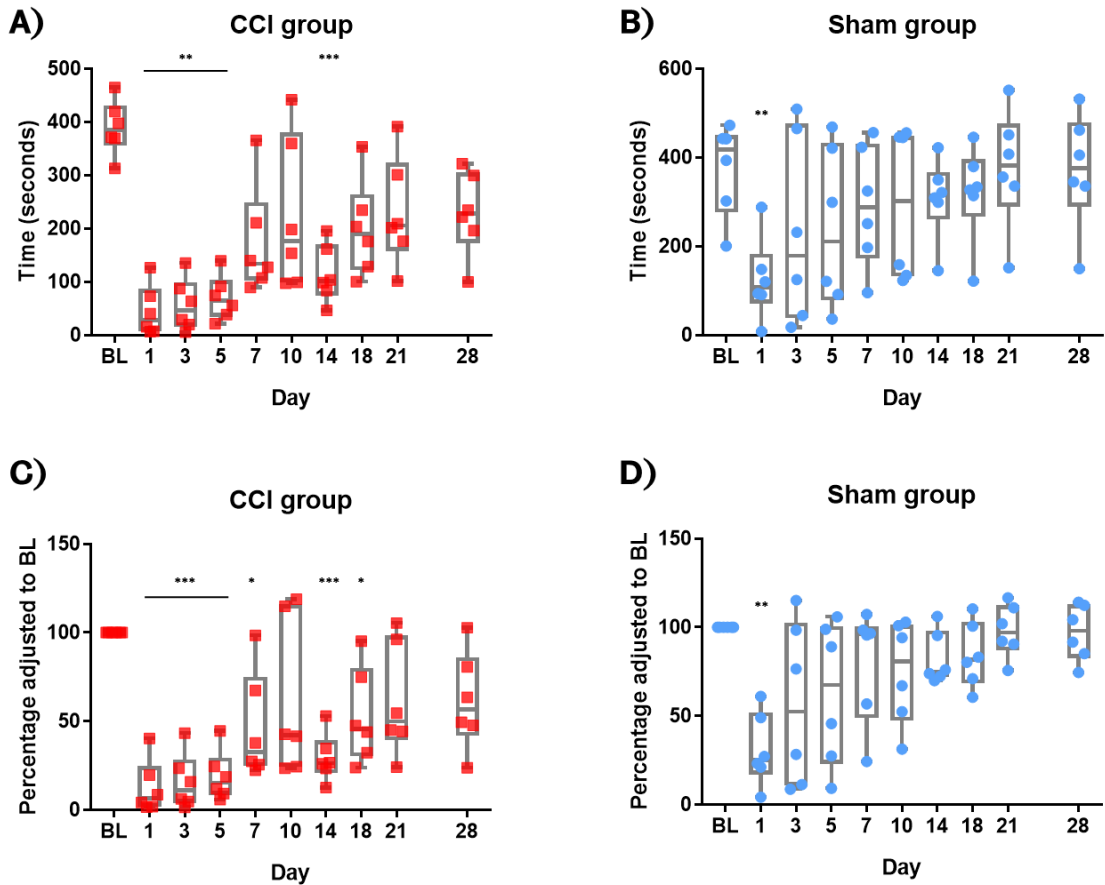


Figure 3.9. Box plot with total time drinking values within each group. Within the CCI group, days 1, 3, 5 and 14 after injury were found to be statistically different compared to BL (A). Data adjusted to percentage of BL showed that days 1 to 7 and 14 to 18 post-injury were statistically significant when compared to BL percentage values (C). Within the Sham group, only day 1 post-surgery was found to be statistically significantly decreased compared to BL, either raw values (B) or percentage adjusted to BL values (D). One-way ANOVA repeated measures followed by Dunnet's *post hoc* test. Asterisks (*) represent statistical significant differences (* $p < 0.05$, ** $p < 0.01$, *** $p < 0.005$).

The maximum contact observed (longest time uninterrupted) within each testing period was not statistically different between groups ($F(1, 10)=3.615, p=0.086$, two-way ANOVA repeated measures); when adjusting to percentage of BL no statistically significant differences were found ($F(1, 10)=3.333, p=0.098$, two-way ANOVA repeated measures) (figure 3.10). The minimum contact time uninterrupted was 0.04 s for all animals at all time-points, probably because no cut-off was included.

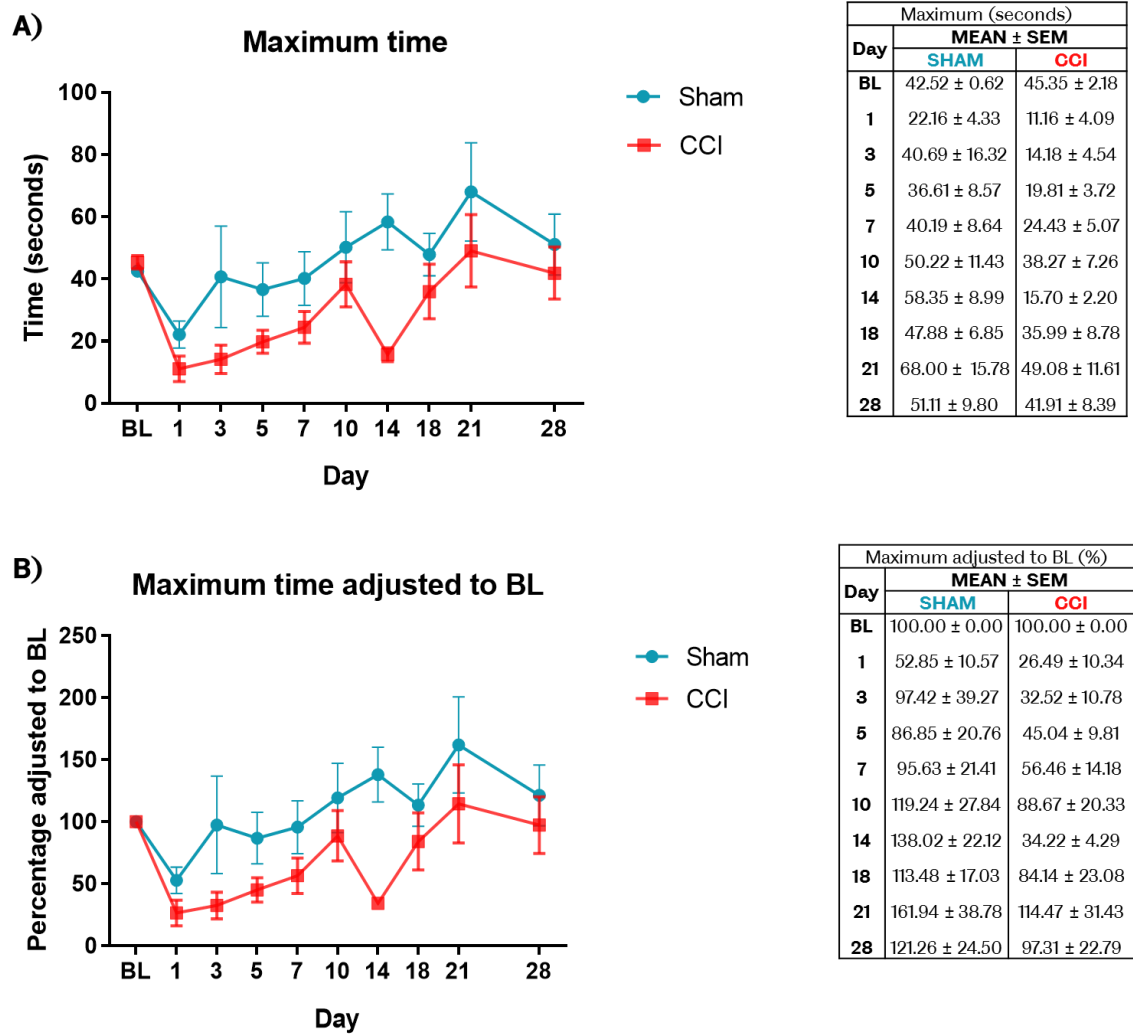


Figure 3.10. Maximum contact time. A) The longest uninterrupted time accessing the reward during each testing period was not found to be statistically significantly different between groups when using raw values (A) or when adjusting to percentage BL values (B). Two-way ANOVA repeated measures.

When analysing the maximum time accessing the reward data within each group, it was possible to observe a decrease following injury in the experimental CCI group ($F(1.708, 8.539)=7.727, p=0.014$, one-way ANOVA repeated measures) and when adjusting to percentage of the BL ($F(1.61, 8.049)=6.981, p=0.020$, one-way ANOVA repeated measures) (Figure 3.11-A, -C). Similar to the total time drinking analysis, when analysing each day against the BL it was possible to verify that there was a statistically significant difference between BL and days 1, 3, 5 and 14 post-surgery (BL vs 1 $p=0.011$, BL vs 3 $p=0.014$, BL vs 5 $p=0.020$, BL vs 14 $p=0.0001$, Dunnet's *post hoc* test); when adjusting to percentage of BL comparable results were obtained (BL vs 1 $p=0.004$, BL vs 3 $p=0.008$, BL vs 5 $p=0.012$, BL vs 14 $p=0.0001$, Dunnet's *post hoc* test). Within the Sham group no statistically significant differences were found (figure 3.11-B, -D) with raw data values ($F(2.828, 14.14)=2.814, p=0.080$) or when adjusting to percentage of BL ($F(2.77, 13.85)=2.788, p=0.08$).

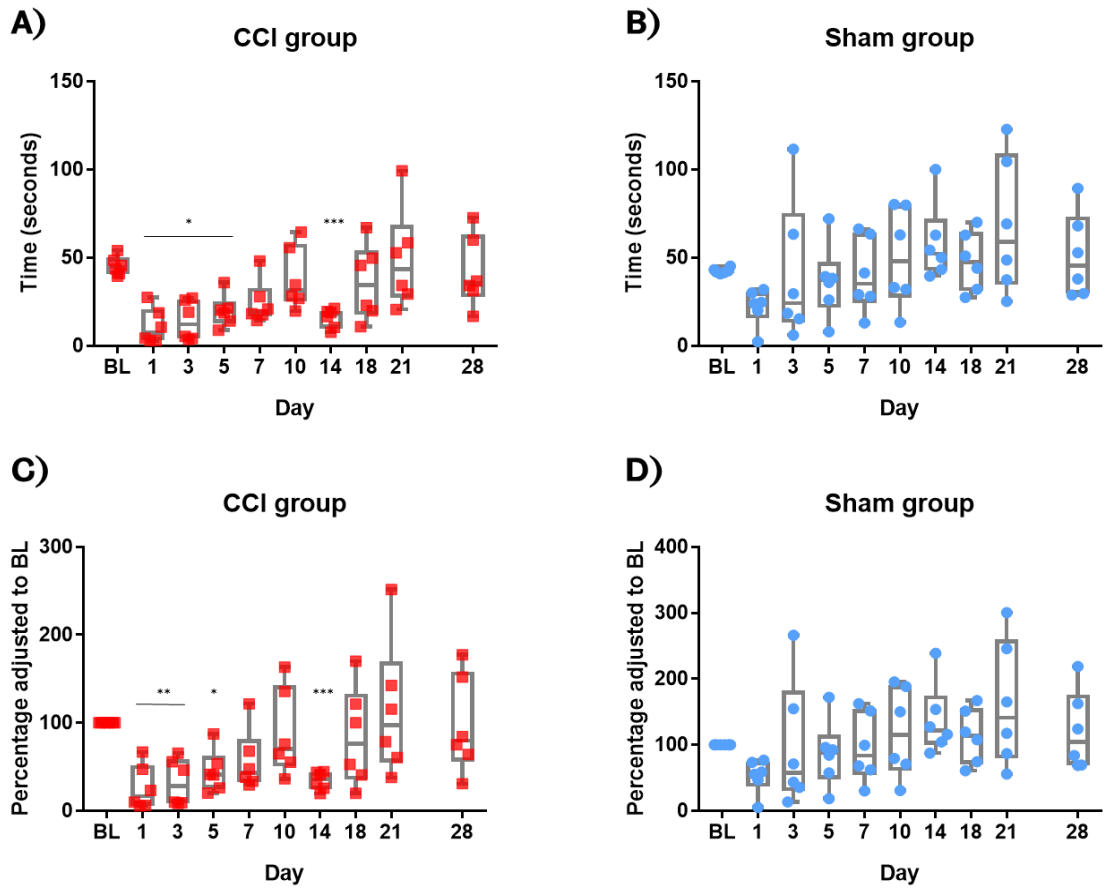


Figure 3.11. Box plot with maximum time drinking per testing within each group. Within the CCI group it was found a statistically significant decrease in the longest uninterrupted time accessing the reward on days 1 to 5 and 14 compared to BL, using raw values (A) and percentage adjusted to BL (C). No statistically significant differences were found within the Sham group (B and D). One-way ANOVA repeated measures followed by Dunnet's *post hoc* test. Asterisks (*) represent statistical significant differences (* $p < 0.05$, ** $p < 0.01$, *** $p < 0.005$).

3.3.4. Number of attempts post-surgery

The number of attempts correspond to the exact sum of infrared counts and when comparing both groups, the difference in the number of attempts was not statistically significant following surgery ($F(1, 10)=0.471, p=0.508$, two-way ANOVA repeated measures); comparably, when adjusting the results to percentage of BL no statistically significant differences were found ($F(1, 10)=0.143, p=0.713$, two-way ANOVA repeated measures). On day 1 there was a decrease in both groups maintained until day 3 (figure 3.12). From day 3 to day 5 both groups showed an increase in the number of attempts. On day 28 the sham group reaches an average of 45.67 attempts and the CCI group 38.67 attempts.

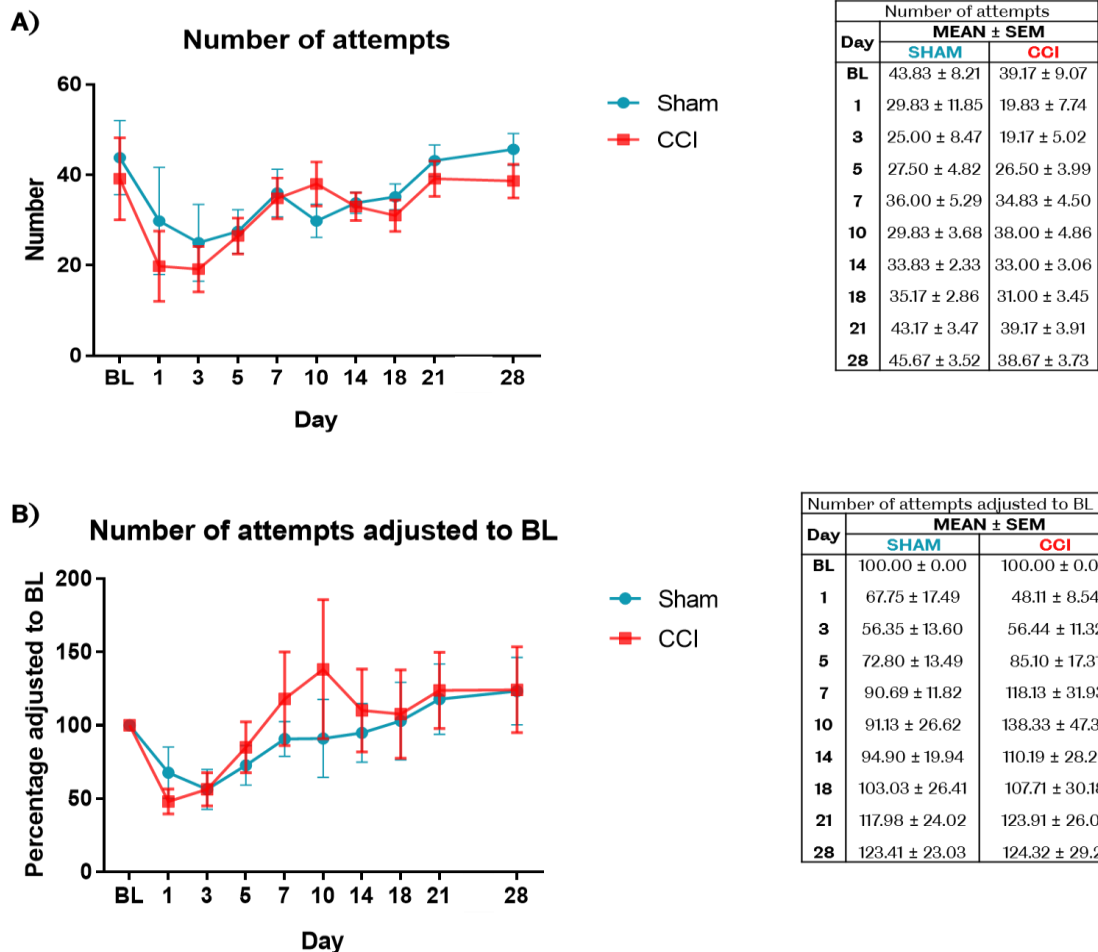


Figure 3.12. Number of attempts. No statistically significant differences were found between groups in the number of attempts to access the reward during the testing period when analysing raw values (A) or when analysing percentage adjusted to BL values (B). Two-way ANOVA repeated measures.

When analysing the number of attempts data within each group no statistical differences were observed within either group (figure 3.13). Within the CCI group no statistical differences were observed following LNI ($F(2.569, 12.85)=2.554, p=0.107$, one-way ANOVA repeated measures); in the number of attempts adjusted to percentage of BL also no statistical differences were found ($F(1.573, 7.866)=2.794, p=0.127$, one-way ANOVA repeated measures). In the Sham group no statistical differences were found in the number of attempts following sham-operation ($F(2.28, 11.4)=1.862, p=0.198$, one-way ANOVA repeated measures); similarly, when adjusting to percentage of BL no statistically significant differences were found ($F(2.052, 10.26)=2.433, p=0.136$, one-way ANOVA repeated measures).

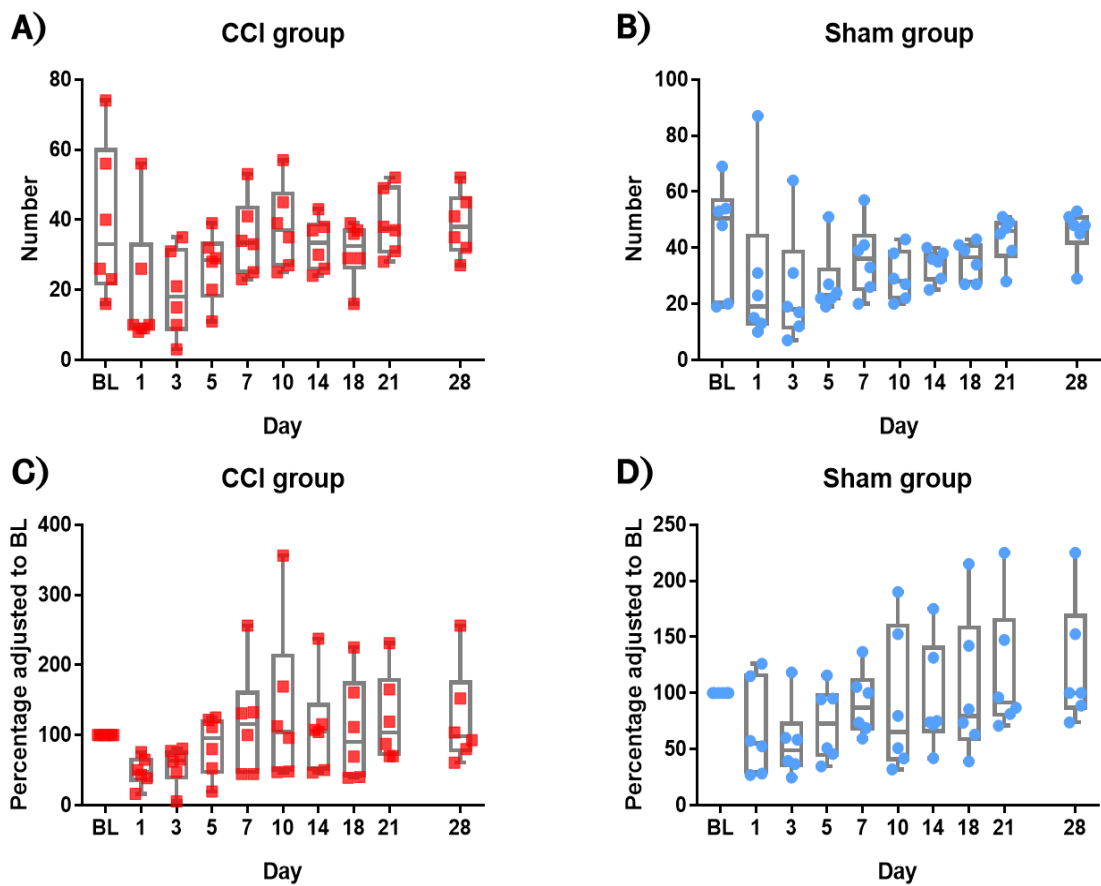


Figure 3.13. Box plot of number of attempts within each group. No statistical significant differences were found when analysing number of attempts within CCI group (A and B) or Sham group (B and D). One-way ANOVA repeated measures.

3.3.5. Volume ingested post-surgery

Total volume of reward ingested (from a total of 20 mL available at the beginning of testing) was decreased following surgery, with slightly bigger effect on the CCI group (figure 3.14); however no statistical differences were found between groups ($F(1, 10)=3.508, p=0.091$) even when adjusting to percentage of BL ($F(1, 10)=4.881, p=0.052$).

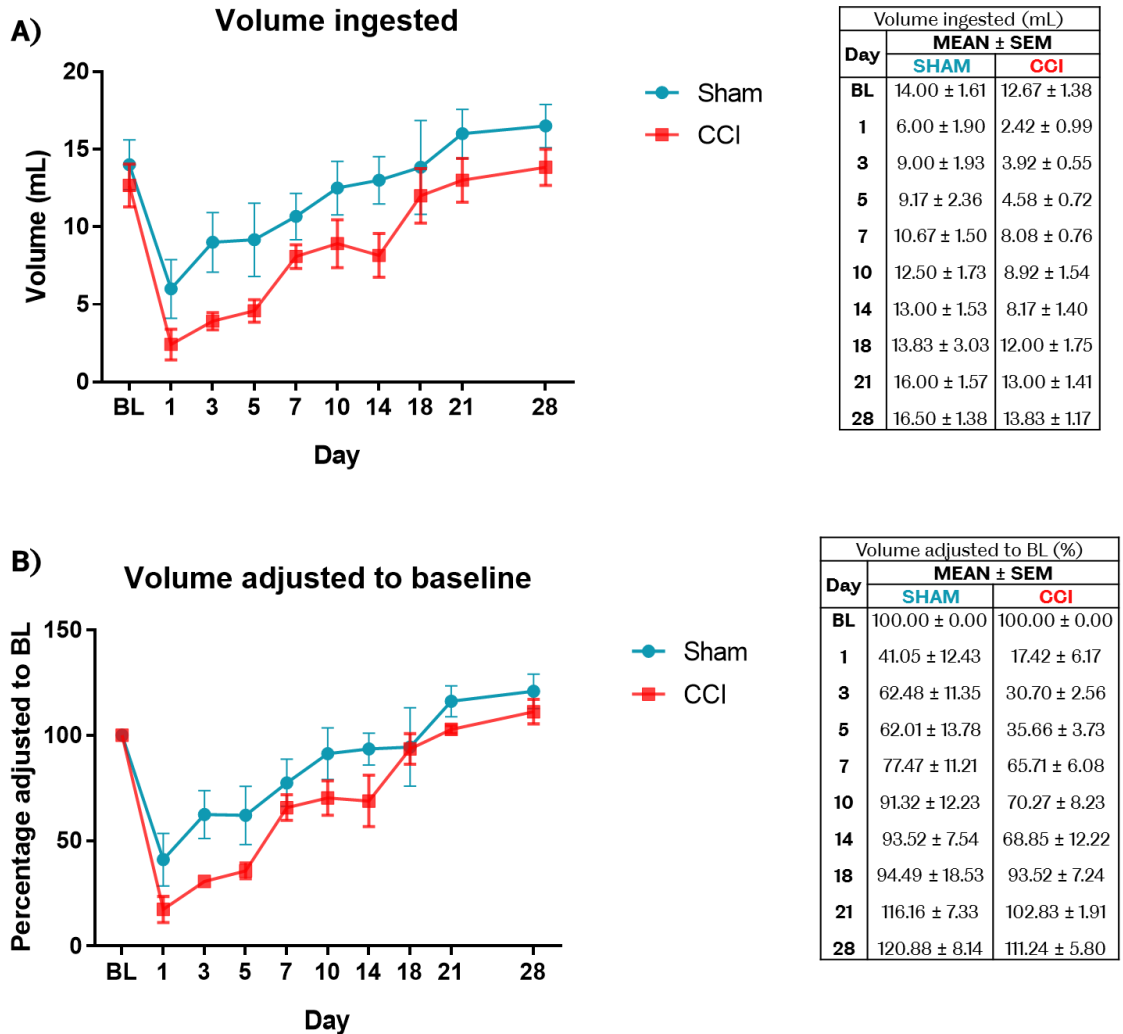


Figure 3.14. Volume of reward ingested during the period testing. Data analysis of the volume of reward ingested found no statistically significant differences between groups in either raw values (A) and percentage adjusted to BL values (B). Two-way ANOVA repeated measures.

When evaluating the effect of surgery on volume ingested within each group (figure 3.15), statistical differences were observed following surgery in the CCI group ($F(2.433, 12.16)=21.16, p<0.0001$, one-way ANOVA repeated measures); when analysing against the BL, statistical differences were found on days 1, 3, 5 and 7 (BL vs day 1 $p=0.001$, BL vs day 3 $p=0.001$, BL vs day 5 $p=0.001$, BL vs day 7 $p=0.044$, Dunnet's *post hoc* test). Statistically significant differences were also found when adjusting the values to percentage of BL ($F(2.708, 13.54)=27.63, p<0.0001$, one-way ANOVA repeated measures). When analysing against the BL, differences were also present on days 1, 3, 5 and 7 (BL vs day 1 $p=0.001$, BL vs day 3 $p=0.001$, BL vs day 5 $p=0.001$, BL vs day 7 $p=0.012$, Dunnet's *post hoc* test). In the sham group statistical differences were found ($F(2.983, 14.92)=9.349, p=0.001$, one-way ANOVA repeated measures) with specific differences found on day 1 post-injury when comparing against BL (BL vs day 1 $p=0.034$, Dunnet's *post hoc* test); a similar pattern was observed when adjusting values from the Sham group to percentage of BL ($F(2.401, 12)=7.378, p=0.006$), with differences on day 1 when compared against BL (BL vs day 1 $p=0.025$, Dunnet's *post hoc* test).

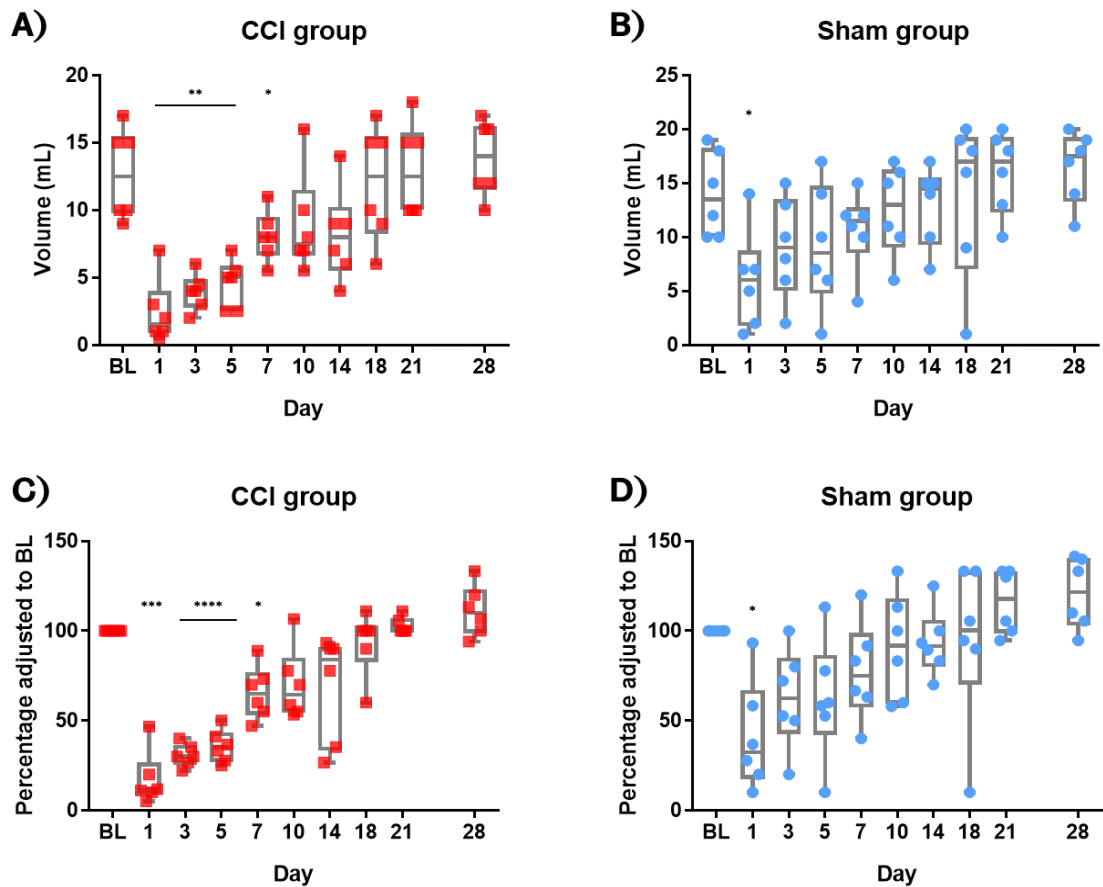


Figure 3.15. Box plot with volume ingested. Within the CCI group, days 1 to 7 after injury were found to be statistically different when comparing against BL (A). Data adjusted to percentage of BL showed identical results (C). Within the Sham group, only day 1 post-injury was found to be statistically significantly decreased when compared against BL with both raw values (B) or percentage adjusted to BL values (D). One-way ANOVA repeated measures followed by Dunnet's *post hoc* test. Asterisks (*) represent statistical significant differences (* $p < 0.05$, ** $p < 0.01$, *** $p < 0.005$).

3.4. Discussion

Experimental settings and considerations

In this chapter, the Ugo Basile Orofacial Stimulation equipment was adapted and used to develop a behavioural test in a LNI model of neuropathic pain in the rat. As mentioned in the literature review (section 1.5 in chapter 1), the use of animal models for the study of pain has its own challenges and limitations. One of them relies on how to assess the effect of injury and level of pain as non-human animals such as rodents cannot self-report (a disadvantage compared to humans). In addition, the majority of the tests used to date have been based on reflex behaviours or innate responses (Mogil and Crager, 2004) which excludes the important component of pain processing in higher parts of the brain (for instance, voluntary actions) and the validity of the reflex responses as reliable measures of pain have been questioned (Vierck et al., 2008). The use of reflex behavioural tests has also been reported in studies conducted in the orofacial region, with most of them using the infraorbital nerve (ION) injury model over the years (Vos et al., 1994, Kernisant et al., 2008, Xu et al., 2008). The CCI pain model used in the present study was based on studies reported by Bennett and Xie (1988) who first described this model in the sciatic nerve, and later, Vos et al. (1994) adapted and characterised the model in the orofacial system, reporting altered behaviour post-injury such as face-grooming activity. In the particular case of the LNI as a model for studying nerve injury and pain, very few studies to date have reported behavioural testing (discussed below). This may be due to the specific characteristics of the nerve that need to be taken into account. For instance, the intra-oral location of the nerve's receptive field makes it difficult to assess the direct responses to stimulation using traditional methods (e.g. Von Frey hair). To try to overcome the particular limitations of this animal model in view of its receptive field and also in an attempt to move away from behaviour based on reflex responses, the Ugo Basile Orofacial Stimulation was adapted to investigate the effect of lingual nerve CCI on feeding behaviour. This test used operant measures of pain (non-reflexive measures that involve cerebrospinal integration and that cannot be performed after decerebration) (Mogil, 2009), in which the animals were trained to access a bottle that contained a reward. In order to obtain the reward, they needed to use the tongue; this allowed the animals to make a choice between receiving the positive reward (chocolate drink) or avoiding potential pain caused by movement of the tongue and/or contact of the tongue with the feeding bottle. The first report describing the use of this equipment in an animal model

of chronic pain was applied to the study of CCI of the infraorbital nerve (Cha et al., 2012). In the study reported in this chapter several adaptations were made in order to better suit the nerve and model. For instance, no noxious (thermal or mechanical) stimuli were applied to the face as the lingual nerve does not innervate the facial area. In addition, the animals were not deprived of food or water before the test as the main goal was to evaluate the willingness of the animals to get the reward regardless of the fasting/starving state, as this was considered to potentially dilute the injury effect and force the animals to get the reward even in a painful condition. Animals were tested for 10 min based on previous reports in the literature (Cha et al., 2012, Zuo et al., 2013) and preliminary studies. Also based on preliminary studies, animals were tested in pairs and chocolate drink was used for the reward. Other studies have used sweetened milk (Cha et al., 2012, Zuo et al., 2013), however no consistent results were obtained when using sweetened milk in preliminary studies. This difference may be explained by the fact that the animals in this study were not fasted prior to testing.

Feeding behaviour following lingual nerve injury

To evaluate the feeding behaviour in this study three measurements were tested: number of attempts to reach the reward, the total time, maximum and minimum uninterrupted time drinking, and the volume of reward ingested (of a total of 20 mL available) over the period of testing. When analysing the raw data regarding time drinking, a statistical difference was observed between groups (CCI experimental and sham control) in the total time drinking, and specifically on day 14 following injury (both raw values and when adjusting to percentage of baseline). When adjusting the values to baseline, it was possible to observe that also day 5 was statistically significantly different. No statistical significant differences were found between groups in either the number of attempts or the volume ingested. Even though the time and volume graphs follows the same pattern, the units of measure are not directly comparable and that can explain the fact that in the time drinking there was a statistical difference but not on the volume ingested. It is interesting to note that the control group used in this study (sham operated animals) also had, to some extent, a decrease in the time and volume ingested following surgery in particular on day 1. This suggests the potential existence of post-surgical pain. The inclusion of another control group (naïve animals) in a future study or the application of local anaesthetic/analgesic in the surgical area may help clarify this result.

When analysing the results within each group (CCI or Sham) at each time point against baseline, it was possible to observe a clear effect of the type of surgery. In the CCI group, time drinking, maximum and volume ingested were significantly decreased compared to baseline for up to 5 or 7 days, and on day 14 for time drinking only. This analysis demonstrated the different effect of sham operation compared to CCI, as in the Sham group only on day 1 post-surgery was found a statistical significant difference against baseline in time drinking and volume ingested. This again suggests a post-surgical effect and not the development of neuropathic pain.

To the best of my knowledge, this is the first time this operant behavioural test has been used to assess behavioural change following LNI. However, Boucher et al. (2013) have conducted a two-bottle conflict paradigm test (one with capsaicin and the other with vehicle) to study LNI in the rat and reported that, similar to the injured animals, the sham-operated animals also had enhanced avoidance of capsaicin (which is indicative of chemical hyperalgesia) over time. It was suggested that the lingual nerve exposure is invasive by itself, thus, even the sham animals were affected; this may explain the variability found within the sham group in the results of this chapter.

The results reported in this chapter are in accordance with previous electrophysiological and neuropeptide studies conducted in Professor Boissonade's laboratory as the greatest changes were found in early days following injury. Studies on the effect of injury to trigeminal nerve fibres found that spontaneous activity was the highest 3 days after LNI in the ferret (Yates et al., 2000) with decrease, then, at 3 weeks and increase at 3 months. Mechanical sensitivity (tested by direct pressure on the neuroma with a glass probe) was also present at 3 days following LNI in the same study. Studies on the inferior alveolar nerve in the ferret also detected spontaneous activity 3 days after injury (Bongenhielm and Robinson, 1996, Bongenhielm and Robinson, 1998). Davies et al. (2006) has also shown that specific sodium channels ($Na_v1.9$ and 1.8) were increased following injury to the inferior alveolar nerve and that was suggested to be associated with the development of ectopic activity detected at day 3 in the previous study mentioned. In the same line, several neuropeptides (SP, CGRP, vasoactive intestinal polypeptide (VIP), enkephalin (ENK), galanin (GAL), and neuropeptide Y (NPY)) were found to be accumulated at the site of injury at 3 days after inferior alveolar nerve injury (Bird et al., 2002) and LNI (Bird et al., 2003) and decreased by week 3. Even though different species were used between this study and the ones mentioned above (rat and ferret, respectively)

and statistically significant differences between CCI and sham were found only on day 5 and 14 in this study, the previous data is in line with the findings reported in this chapter as the highest effects on feeding behaviour were found in early time points following LNI, within the CCI group; in addition, no statistical differences were found between groups or when comparing against baseline within each group on day 21 (3 weeks after injury). Previous studies in the lingual nerve reported the presence of spontaneous activity and increase of SP, CGRP and VIP levels at 3 months following LNI so in a future study it may be necessary to evaluate whether the feeding behaviour is affected beyond day 28 post-injury and up to 3 months. Similarly, electrophysiological studies on day 14 following LNI may help clarify whether there is spontaneous activity at this specific time point that could contribute to the decrease on the total time drinking on day 14 in the CCI group. A study conducted in the rat mental nerve (also part of the mandibular division of the trigeminal nerve) found that on day 14, nerve growth factor (NGF) was increased in the ipsilateral site of the skin (Evans et al., 2014). NGF is an important growth factor in nerve regeneration, but increased release of NGF can activate TrkA receptor and lead to the release of SP and CGRP, that will extend the inflammatory event and further sensitise nociceptors. Evidence has also shown that administration of SP (Smith et al., 2005) and CGRP (Loescher et al., 2001) can contribute to the development of spontaneous activity in the inferior alveolar nerve. Therefore, further characterisation of neuropeptides expression specifically on day 14 after LNI in the rat is required to identify the potential cause of the behavioural findings here reported.

Because the lingual nerve contains taste fibres (from the chorda tympani), possible effect of surgery on taste should also be acknowledged. It would be possible, if taste fibres would have been damaged, that the animals had lost the learning of the reward acquired during the training period (as the potential positive effect of getting the reward would have been lost). However, it is also necessary to acknowledge that this study conducted a unilateral injury to the lingual nerve, thus, the contralateral side of the tongue was still innervated by intact lingual nerve fibres. This together with the fact that no differences were observed between groups in the number of attempts to get the reward, suggests that taste was possibly not affected and results are due to sensory disturbances (that may include pain) only. In addition, there are also studies done in the reward effect, showing that the animals learn that the reward is safe to ingest and increase the consumptions after subsequent exposure over time (Yamamoto, 2008). In a study conducted to characterise

the emotional effects (anxiety and depression) of lingual nerve and chorda tympani injury, it was observed a reduction in the intake and preference for sweet solutions compared to sham operated animals (Choi et al., 2013). However, this study applied bilateral transection to the lingual nerve and chorda tympani, thus affecting the taste transmission and thus the effect of injury affected both sides of the tongue. Comparing those to the results reported in this chapter, it was also observable a decrease in the time and volume of reward; however, because only the left lingual nerve was injured, only one side of the tongue was affected; thus the animals could possibly still taste the chocolate on the other side of the tongue. A study conducted by Bartoshuk et al. (2005) reported that damage in taste nerves could lead to disinhibition of trigeminal nociceptive pathways; however, Boucher et al. (2014) did not find any correlation between chorda tympani damage and central disinhibition. Further studies analysing taste buds on the tongue, brain imaging or even the use of preference conditioning behavioural tests (in which the animal can choose between a positive reward and a vehicle) can help clarify the effect of CCI in the lingual nerve and its fibres.

Animals in the CCI group had lower percentage of body weight gain over the 28 period when compared to the Sham group. Vos et al. (1994) have found that animals with injury to the infraorbital nerve had a slower daily increase in weight comparing to the control group using a normal diet (not reward testing). Additionally, another study on the functional role of the lingual nerve in breastfeeding has found that unilateral LNI had no effect on the survival of rat pups in contrast with bilateral injury (Yokouchi et al., 2007), suggesting that sensory input and not only motor function can affect the feeding behaviour.

Lab environmental factors

Previous studies have evaluated the influence of the laboratory environment factors on animal behaviours and found that several factors external from the experiment can influence the behavioural results (Mogil, 2017, Sorge et al., 2014). For instance a study conducted by Chesler et al. (2002) ranked genetic and laboratory factors from an archive of thermal nociception behavioural studies and found that the experimenter was the main cause of differences (even more than the animal strain); it was suggested that possibly the animal handling technique caused stress in the animals. Other factors such as sex and order of testing also seemed to have an effect. Therefore, the development of investigator-independent tests becomes especially relevant when evaluating pain behaviours (Neubert

et al., 2005). In the study reported in this chapter, the equipment automatically recorded the duration of drinking and number of attempts and animals could choose whether they wanted to access the reward. This, possibly, reduced experimenter-induced bias and stress (as the only contact was when transferring cages). In addition, the order of testing was done randomly and always with two animals at the same time (in separate cages).

Statistical analysis considerations

A two-way ANOVA repeated measures was used to find statistical differences between groups because the animals were tested for feeding behaviour at multiple time-points. To evaluate differences within each group, one-way ANOVA repeated measures was used and in this case the results reported are corrected for sphericity (one of the assumptions of ANOVA). To correct for multiple comparisons and avoid false positives a *post hoc* test was conducted when the ANOVA was significant. In the case of one-way ANOVA repeated measures, Dunnett's *post hoc* test was chosen because it was decided to compare only to the baseline value (pre-surgery). In the case of two-way ANOVA repeated measures, it was used Sidak's *post hoc* test as it was more powerful (taking into account the sample size). It was decided not to use Bonferroni test because it is the most conservative test and because of the sample size in this case it could lead to false negatives. The percentage values adjusted to BL were used to correct for the individual differences of each animal.

Limitations of the study

One of the limitations of this study was the use of adult male rats only. There is evidence that the majority of chronic pain patients are middle-aged females and in addition, there is some evidence that female rats are more sensitive than male rats in acute assays (Mogil, 2017), thus the inclusion of female and older rats can help studies to be more clinically translatable. This study did not include a naïve control group, thus, statistical analyses were performed within each group against baseline data (pre-surgery data); however this does not include potential variation that may occur during the progressive testing in naïve animals and therefore, future studies should include naïve animals. Because the animals were not fasting it is difficult to control whether the animals ate just before the test been conducted; however, the increasing interest in the reward demonstrated in the training period did not suggest that was interfering with the animals

reward interest. In addition, the behaviour testing was conducted at the beginning of the light cycle (when the animals were potentially less active); however, all tests were conducted approximately at the same time of the day and thus comparable within this study.

Conclusion and future studies

In conclusion, the behavioural test conducted showed that LNI had an effect on feeding behaviour, particularly decreasing time drinking in early days post-injury. This results are in line with previous studies that have shown the development of spontaneous activity and mechanical sensitivity and the increase in the expression of several neuropeptides associated with increase in nociceptive transmission, such as SP and CGRP, in early days after LNI; this suggests that the use of the Ugo Basile orofacial test can help characterise pre-clinical studies of LNI. Future studies derived from this work need to apply a multidimensional approach (with additional brain imaging and analysis of gustatory fibres) to better translate to clinical studies (Navratilova et al., 2015, King and Porreca, 2014). An interesting follow up would be to investigate whether the application of anti-epileptic drugs, such as gabapentin or pregabalin (that have shown to reduce neuropathic pain (Bennett and Simpson, 2004, Serpell and Group, 2002)) would reverse the effect of CCI on feeding behaviour.

CHAPTER 4
**CHARACTERISATION OF MICROGLIAL
RESPONSE TO LINGUAL NERVE INJURY**

4.1. Introduction

Evidence over the past years has suggested that not only neurones, but also glial cells may play a role in the development and maintenance of chronic sustained pain as discussed in the literature review (section 1.1.3.4 in chapter 1). Microglia, in particular, are known as the resident immune cells of the central nervous system (CNS). Therefore, it is considered that they respond to any threat such as injury, infection, inflammation and any derived diseases (Lull and Block, 2010). Microglia are constantly checking the surrounding environment in order to maintain homeostasis and identify any signal that requires a response; under these normal circumstances, microglial cells are quiescent, presenting a ramified morphology with long and thin extensions from the cell body and are spaced throughout the tissue. It is considered that during this state they have low expression of proteins from the major histocompatibility complex (MHC) (Lawson et al., 1990). However, in the presence of specific extracellular signals such as pathogens, antigens or the presence of dead cells, microglia proliferate and respond by shifting morphology to an amoeboid form with shorter ramifications that will facilitate mobility and phagocytosis (Lull and Block, 2010). In addition, microglia also change in gene expression that may lead to alterations in surface receptors and the release of several inflammatory mediators (Zhang et al., 2003). If not controlled, the release of pro-inflammatory mediators can further contribute to central sensitisation and maintenance of chronic pain (Tsuda et al., 2003).

Lingual nerve injury (LNI) can lead to painful sensory alterations in some patients (Robinson et al., 2004) and it is considered that changes in central mechanisms may be responsible for the persistent sensory alterations as the majority of patients that undergo surgical repair continue to report symptoms of pain (Robinson, 2013). Therefore, it was hypothesised that LNI can lead to central changes and activate microglial cells; this activation can, subsequently, create a positive feedback loop.

The overall aim of this study was to characterise the microglial response to LNI in a rat model, over a specific time period and using the microglial marker, Iba1. The specific objectives were:

1. Investigate microglial morphological changes in the trigeminal nucleus (Vc) of naïve-control, sham and injured animals (qualitative analysis).
2. Investigate microglial response by quantifying Iba1 area of staining at day 3, 7 and 28 following LNI (quantitative analysis).

4.2. Methodological approach

As described in chapter 1, the central terminals of the lingual nerve fibres (as part of the trigeminal nerve) are located in the trigeminal nucleus caudalis (Vc) in the medullar part of the brainstem (figure 4.1 in red).

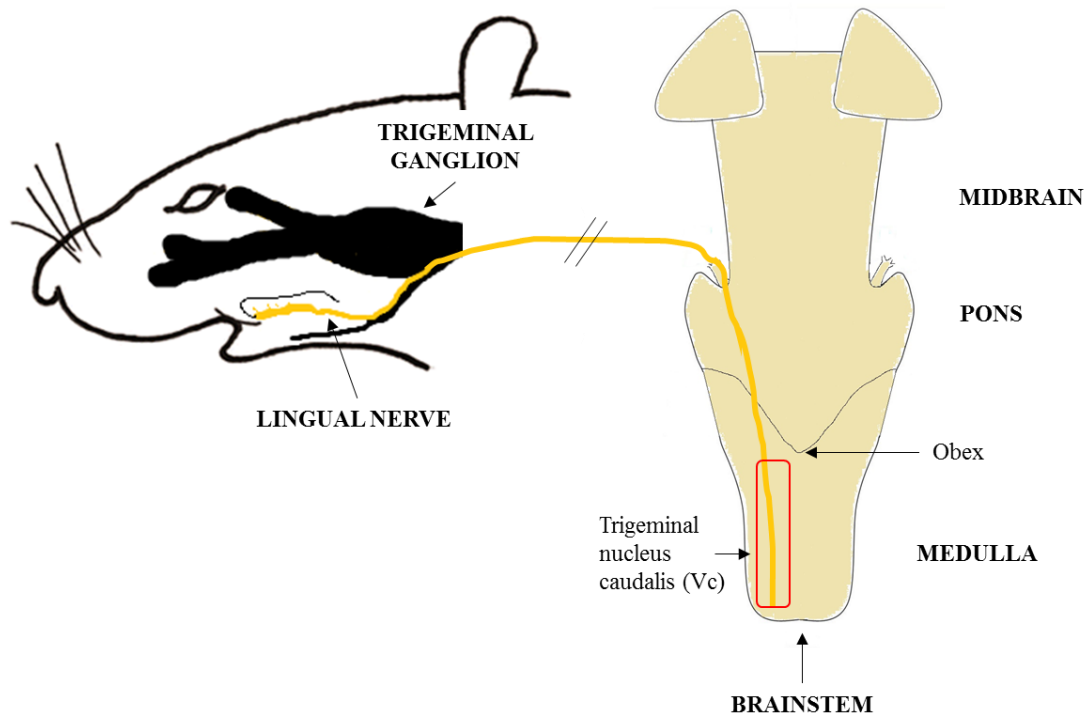


Figure 4.1. Lingual nerve and the brainstem. Lingual nerve fibres transmitting nociceptive information are considered to enter the brainstem at the level of the pons and descend to the trigeminal nucleus caudalis (represented in red). Rat drawing adapted from Csáti et al. (2015) and brainstem drawing adapted from Henssen et al. (2016).

The detailed methods used to collect, prepare and stain brainstem sections were described in sections 2.2.4 and 2.4.1 in chapter 2. In order to have an overall representation, 15 brainstem sections per animal were analysed starting at the level of the obex (considered 0 μm) and then at 240 μm apart from each section until 3360 μm caudal to obex (please see figure 2.3 in section 2.4.1 of chapter 2). Brainstem sections analysed were collected from animals that had chronic constriction injury of the lingual nerve (CCI group) and were left to recover for 3 (n=5), 7 (n=3) or 28 (n=5) days, and from animals that were sham-operated (Sham group) and, similarly, left to recover for 3 (n=3), 7 (n=5) or 28 (n=3) days. Brainstem sections from control (naïve) animals (n=2) were also analysed. The analysis of microglial response following LNI combined qualitative and quantitative approaches. Qualitative analysis was conducted based on criteria specified

previously by Colburn et al. (1997) and described on table 4.1; the quantitative analysis was obtained by measuring the positive area of microglial marker Iba1 staining (PAS%) in the Vc (please see section 2.5.1 in chapter 2 for more details).

Table 4.1. Criteria for qualitative microglia characterisation.

Microglial response	Score	Description
Baseline staining	.	Resting microglia showing ramified morphology with thin and long cytoplasmic extensions
Mild response	+	Still ramified but Iba1 immunoreactivity brighter and less space between cells
Moderate response	++	High Iba1 immunoreactivity, increased microglial density and less ramifications
Intense response	+++	High density of microglial cells and extensive overlapping with short thick ramifications and amoeboid form

Based on work from Colburn et al. (1997).

4.3. Results

4.3.1. Morphological changes and qualitative analysis

Microglia proliferated and presented different morphology following LNI. Control (naïve) animals did not have activated microglia as Iba1 had little immunoreactivity. In addition, microglial cells were spaced throughout the tissue (in the area analysed). However, LNI seemed to have triggered a microglial response as immunoreactivity to Iba1 was highly increased in particular at day 3 post-injury in the ipsilateral side. Microglial response occurred mainly in the superficial laminae (laminae I and II) and in figure 4.2 it is possible to observe Iba1 labelling in a representative brainstem section.

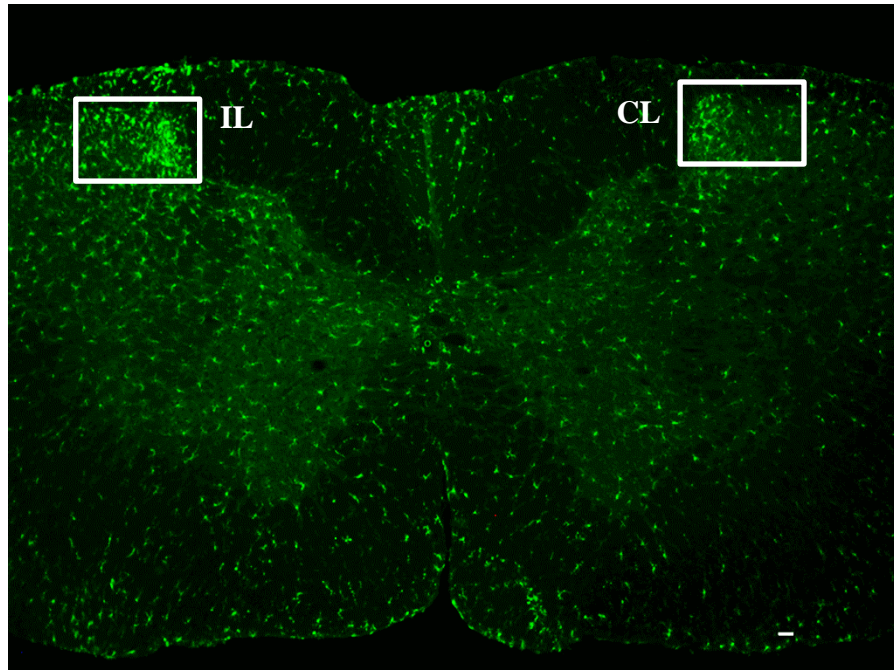


Figure 4.2. Microglia response in the trigeminal nucleus. Low magnification image taken at 960 μm . Scale bar 50 μm . White boxes represent area analysed. IL-ipsilateral, CL-contralateral.

Microglial cells adopted, in some cases, the characteristic amoeboid shape (figure 4.3).

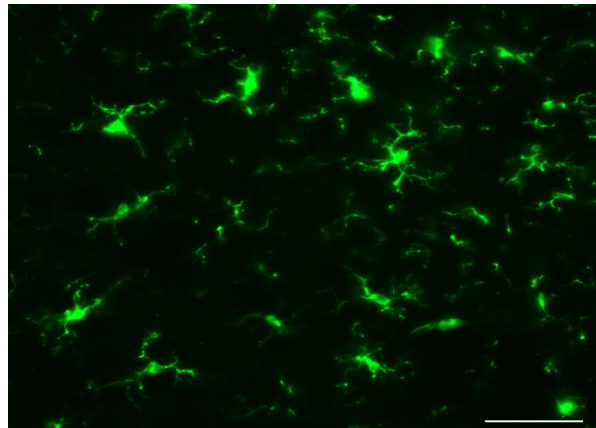


Figure 4.3. Activated microglial cells on day 3. High power image showing characteristic morphology of activated microglia, with amoeboid shape and shorter cytoplasmic ramifications, in the ipsilateral side of the Vc at day 3 after LNI. Scale bars: 50 μm .

On day 3 following LNI there was a high density of microglial cells present in the superficial lamina of the ipsilateral side throughout the area of the trigeminal nucleus analysed (figures 4.4-4.7). In particular, between 480 and 1680 μm caudal to obex there was extensive overlapping of microglial cells and the immunoreactivity to Iba1 antibody presented very bright staining (table 4.2). The contralateral side showed an increase in the brightness but the cells were spaced out through the tissue with no apparent overlapping. In the sham group there was very mild microglial response.

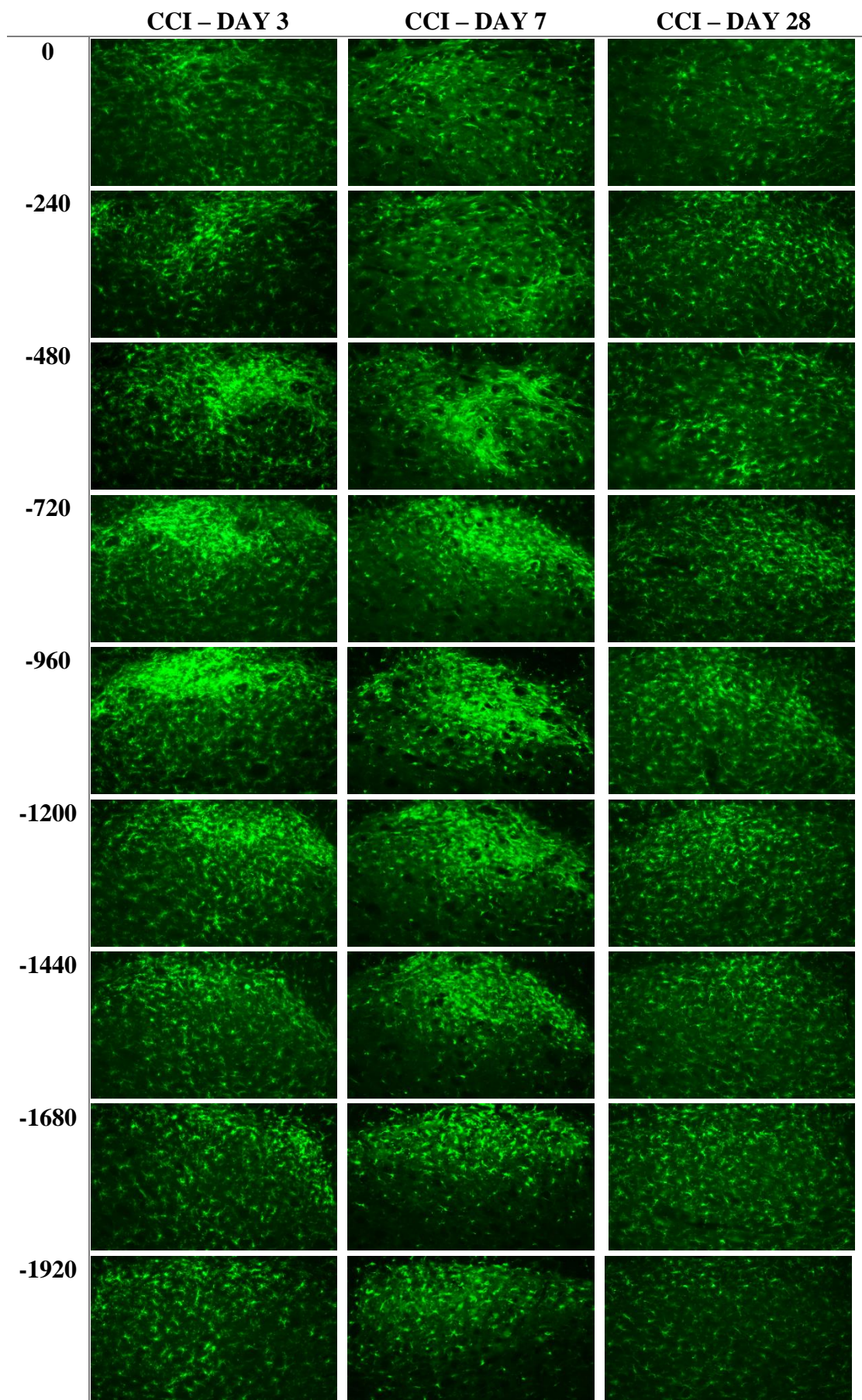
On day 7 post-injury, microglial cells were still activated. There was less microglial proliferation but cells presented an amoeboid shape and Iba1 staining was still bright in particular between 480 and 1440 μm caudal to obex. The sham group also presented activation of microglia, especially between 720 and 1200 μm caudal to obex (figures 4.4-4.7).

On day 28, microglia were mildly to moderately activated in the injured (CCI) group (figures 4.4 to 4.7) . However, cells were more ramified and only occasionally overlapping. The sham group presented very little response from microglia.

Table 4.2. Qualitative analysis of microglial response.

		Control (naïve) - IL	Sham - IL			CCI - IL		
			Day 3	Day 7	Day 28	Day 3	Day 7	Day 28
Microglial response (Iba1) in the ipsilateral Vc	0	.	.	.	+	+	+	+
	-240	.	+	+	+	+	+	+
	-480	.	+	++	+	+++	++	+
	-720	.	+	+++	+	+++	+++	++
	-960	.	+	+++	+	+++	+++	++
	-1200	.	+	+++	+	+++	+++	++
	-1440	.	+	++	.	+++	+++	+
	-1680	.	+	++	.	+++	++	+
	-1920	.	+	+	.	++	++	+
	-2160	.	+	+	.	++	++	+
	-2400	.	+	+	.	++	++	+
	-2640	.	+	.	.	++	++	+
	-2880	.	+	.	.	++	+	+
	-3120	.	+	.	.	++	.	.
	-3360	+	.	.

Scores were based on the analysis of ipsilateral sections from each group at each rostral-caudal level (obex to 3360 μ m caudal to obex). CCI day 3 (n=5), day 7 (n=3) and day 28 (n=5). Sham day 3 (n=3), day 7 (n=5) and day 28 (n=5). Control naïve (n=2). IL: ipsilateral. Distances in μ m.



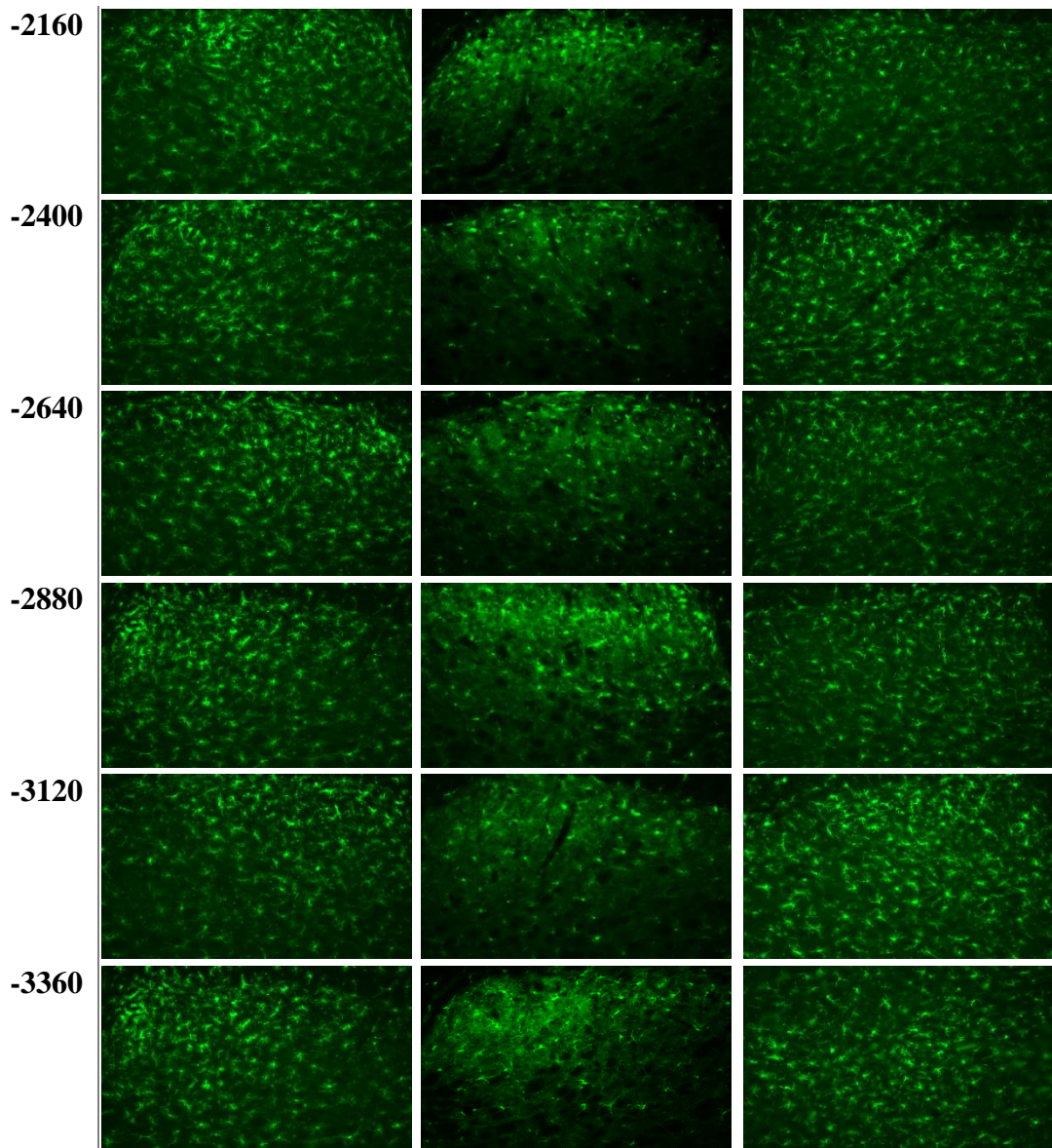
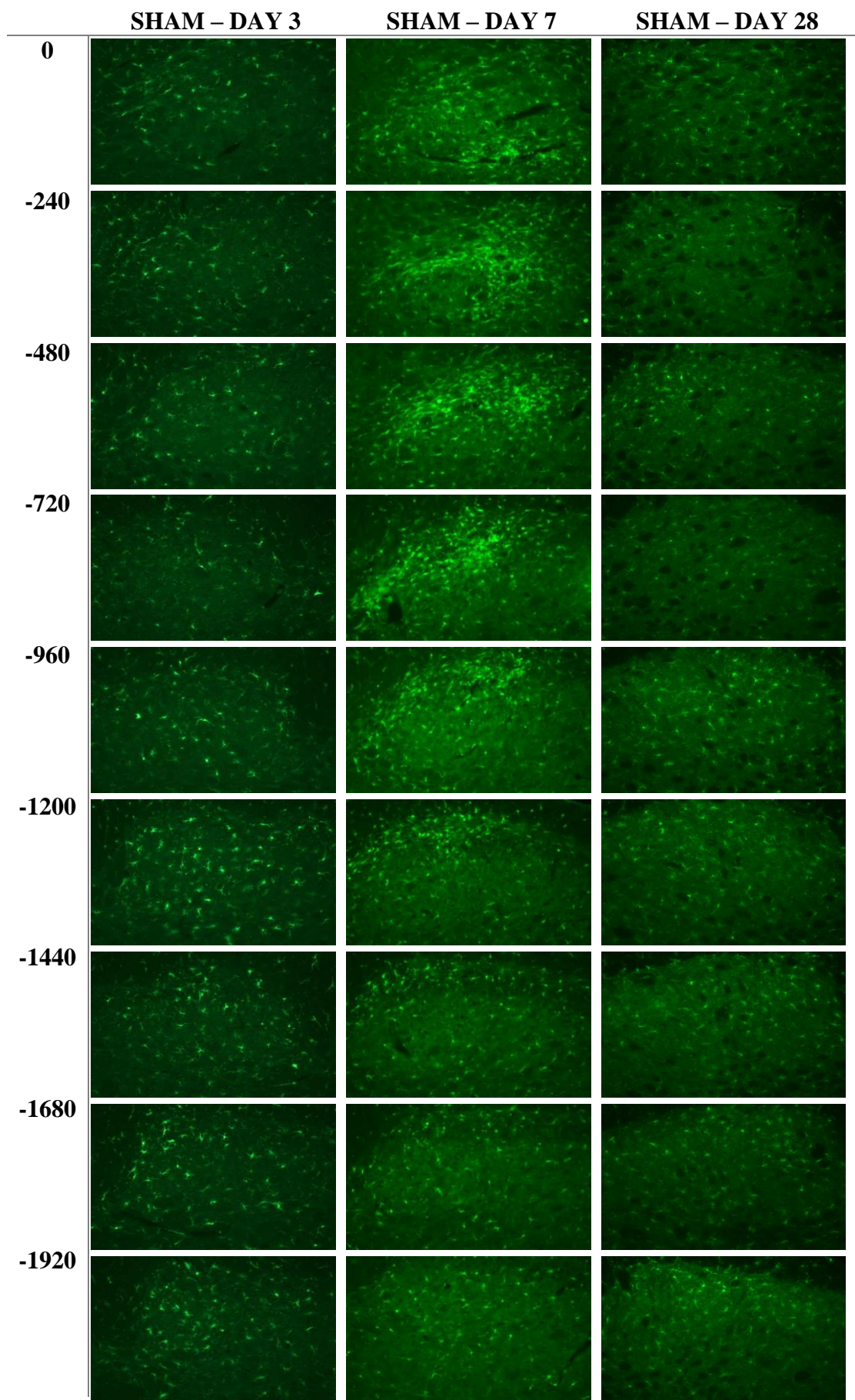


Figure 4.4. Microglia response in the Vc at 3, 7 and 28 days following LNI (CCI group). Showing representative images of Iba1 expression from obex (0 μm) to 1920 μm caudal to obex (previous page) and from 2160 to 3360 μm caudal to obex (current page). Distances from obex in μm .



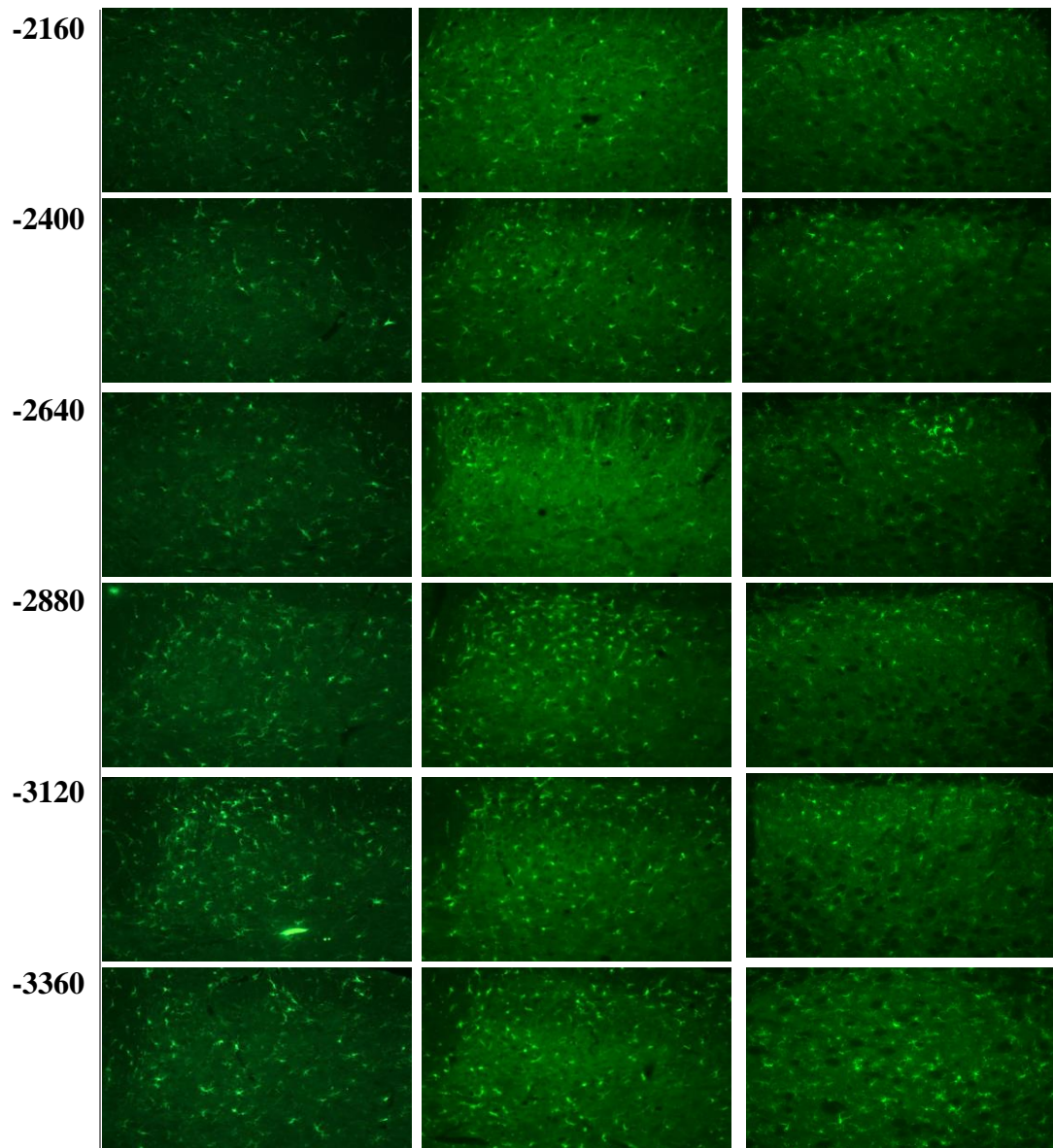


Figure 4.5. Microglia response in the Vc at 3, 7 and 28 days following sham operation of the lingual nerve (Sham group). Showing representative images of Iba1 expression from obex (0 μm) to 1920 μm caudal to obex (previous page) and from 2160 to 3360 μm caudal to obex (current page). Distances from obex in μm .

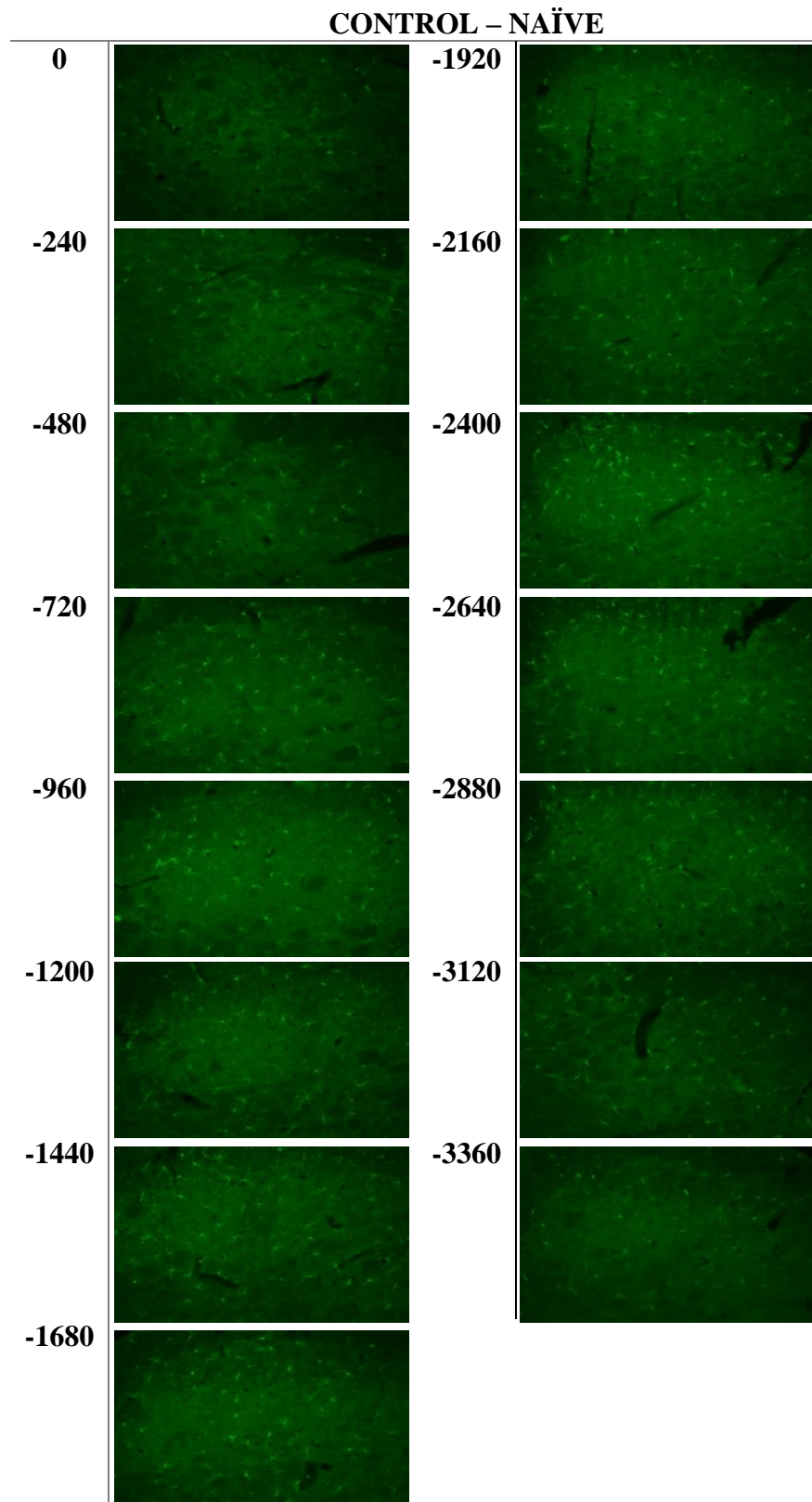


Figure 4.6. Microglia in the control naïve group. Showing representative Iba1 expression from obex (0 μm) to 1680 μm caudal to obex (on the left) and from 1920 to 3360 μm caudal to obex (on the right). Distances from obex in μm .

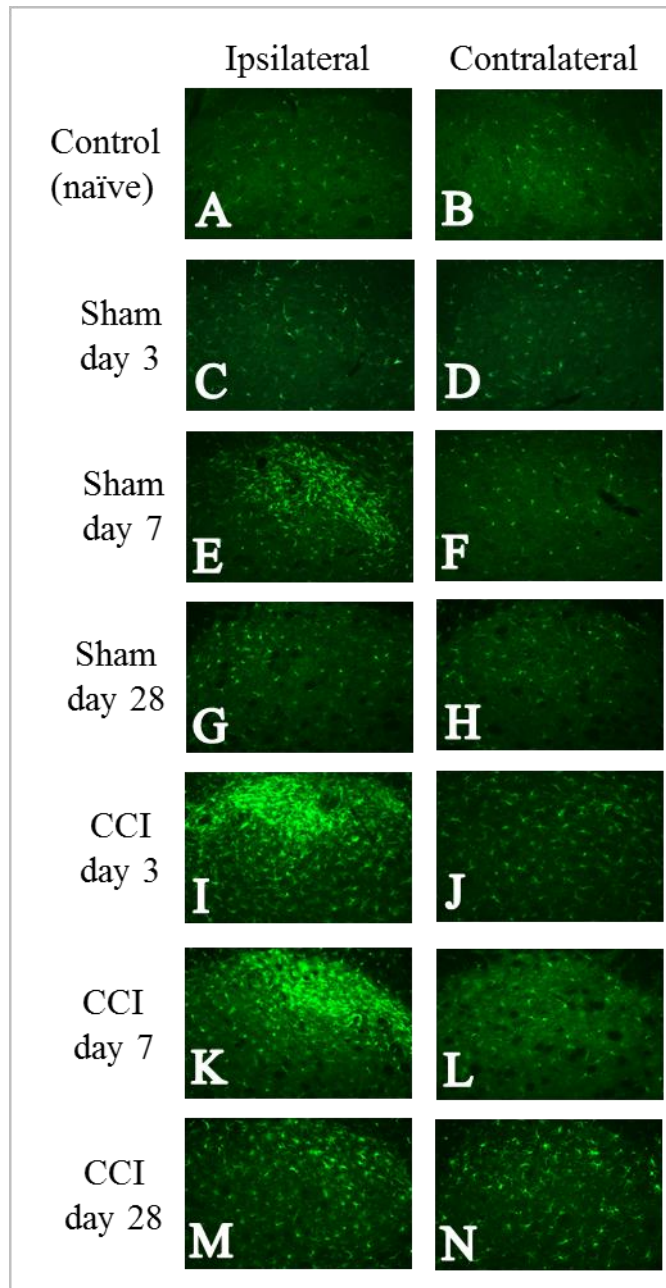


Figure 4.7. Representative images of microglia response (Iba1 expression) to lingual nerve injury at 720 μ m caudal to obex. A) Ipsilateral and B) contralateral of control (naïve) group. C-H) Microglia response in the Sham groups. C) Ipsilateral and D) contralateral of Sham group on day 3. E) Ipsilateral and F) contralateral of Sham group on day 7. G) Ipsilateral and H) contralateral of Sham group on day 28. I-N) Microglia response in the CCI group. I) Ipsilateral and J) contralateral of CCI group on day 3. K) Ipsilateral and L) contralateral of CCI group on day 7. M) Ipsilateral and N) contralateral of CCI group on day 28.

4.3.2. Microglia response on day 3 following lingual nerve injury

Quantitative analysis of the microglial response was conducted on day 3. The positive area of Iba1 staining (%) was measured in Vc both ipsilateral and contralateral to CCI and sham injury (figure 4.8-A, B). In order to control for individual variability of the animals and minimise the differences in staining between experiments, the ratio of the percentage area of Iba1 labelling in the ipsilateral over the contralateral side was calculated. This ratio was calculated for each level of the Vc (figure 4.8-C).

Microglia were differentially activated between the CCI, Sham groups and control groups ($F(2, 7)=36.75$, $p=0.0002$; two-way ANOVA repeated measures). Pairwise comparisons between the groups revealed that the microglial response was significantly higher in the CCI group when compared to the Sham group between 240 and 2640 μm caudal to obex (values caudal to obex: 240 to 1200 μm $p<0.0001$; 1440 and 1920 μm $p=0.0003$; 1680 μm $p=0.0001$; 2160 μm $p=0.0002$; 2400 μm $p=0.003$; 2640 μm $p=0.04$; Tukey's *post hoc* test). Similarly microglia were also significantly more activated in the CCI group compared to the control between 240 and 2400 μm caudal to obex (values caudal to obex: 240 μm $p=0.0002$; 480 to 1200 μm $p<0.0001$; 1440 μm $p=0.0003$; 1680 μm $p=0.0005$; 1920 μm $p=0.002$; 2160 μm $p=0.001$; 2400 μm $p=0.005$; Tukey's *post hoc* test). No statistical significant differences were found between Sham and Control groups.

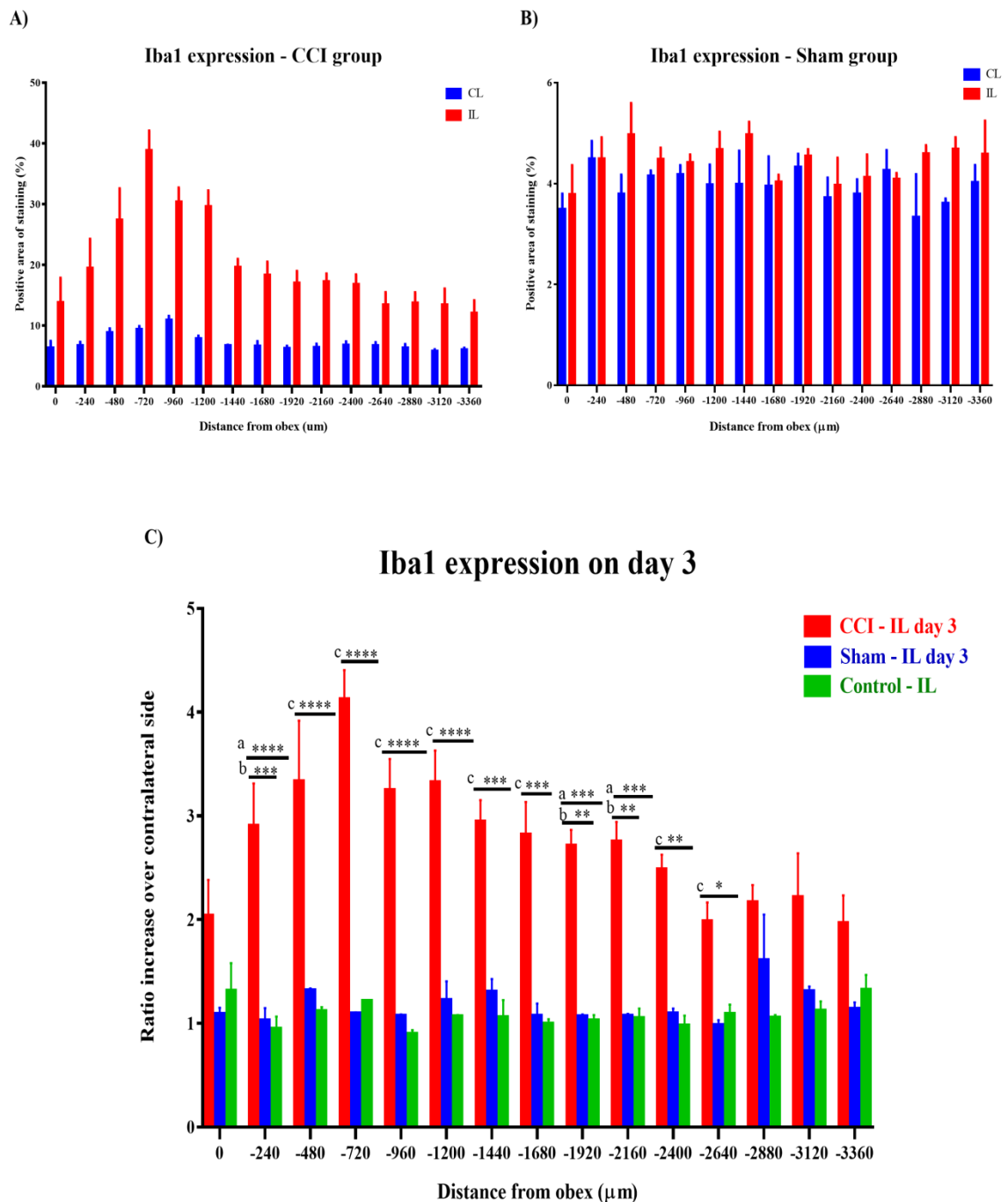


Figure 4.8. Analysis of microglial response on day 3 by quantification of positive area of Iba1 staining. A) Positive area of Iba1 staining in the CCI group (n=5). B) Positive area of Iba1 staining in the Sham group (n=3). C) Ipsilateral ratio increase over contralateral side: Iba1 expression was statistically significantly different between groups between 240 and 2640 μm caudal to obex. Asterisks represent statistical significance. * $p < 0.05$, ** $p < 0.01$, *** $p < 0.001$, **** $p < 0.0001$. a-CCI vs control, b-CCI vs Sham, c-CCI vs Sham and CCI vs Control. Two-way ANOVA repeated measures followed by Tukey's *post hoc* test.

4.3.3. Microglia response on day 7 following lingual nerve injury

Similarly to day 3, quantitative analysis of microglia response was also conducted 7 days following LNI. The positive area of Iba1 staining was measured both ipsilateral and contralateral sides of sham and CCI groups (figure 4.9-A, -B). For further analysis, the ratio increase in the ipsilateral over the contralateral site for each level of the Vc was calculated (figure 4.9-C). Microglia were differentially activated between the CCI and control groups and between Sham and control groups ($F(2, 7)=36.23, p=0.0002$; two-way ANOVA repeated measures).

Microglial response was not significantly higher in the CCI group when comparing to the Sham group. When comparing CCI with the Control group, Iba1 was significantly higher in the CCI group between 480 and 1680 μm caudal to obex (480 to 1440 μm $p<0.0001$; 1680 μm $p=0.0006$; Tukey's *post hoc* test). Statistically significant differences were present between Sham and Control group at 480 to 1440 μm caudal to obex (480 μm $p=0.0001$; 720 to 1200 μm $p<0.0001$; 1440 μm $p=0.004$; Tukey's *post hoc* test).

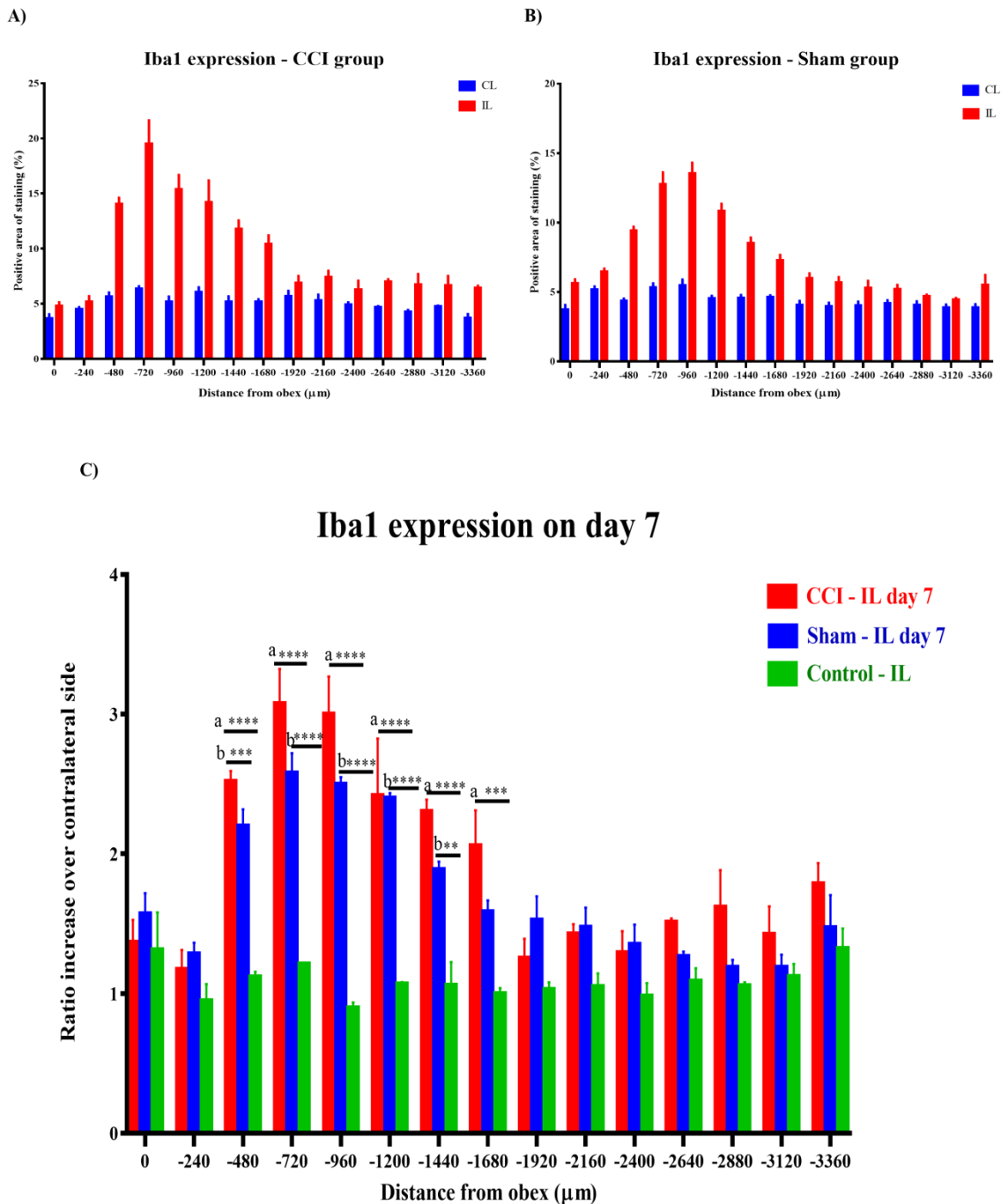


Figure 4.9. Analysis of microglial response on day 7 by quantification of Iba1 staining. A) Positive area of Iba1 staining (%) in the CCI group (n=3). B) Positive area of Iba1 staining (%) in the Sham group (n=5). C) Ipsilateral ratio increase over contralateral side: Iba1 expression was statistically significantly different between CCI and control groups from 480 to 1680 μm caudal to obex. Statistical differences were also found between Sham and Control groups from 480 to 1440 μm. Asterisks represent statistical significance. * $p < 0.05$, ** $p < 0.01$, **** $p < 0.0001$. a-CCI vs control, b-Sham vs Control. Two-way ANOVA repeated measures followed by Tukey's *post hoc* test.

4.3.4. Microglia response on day 28 following lingual nerve injury

Microglia response on day 28 post-injury was also quantified. The positive area of Iba1 staining was measured in both the ipsilateral and contralateral side of sham and CCI groups (figure 4.10-A, -B). Similarly to the analysis for the two other time-points, the ratio increase in the ipsilateral over the contralateral site for each level of the trigeminal nucleus was calculated and used for statistical analysis between groups (figure 4.10-C). On day 28, there was a statistically significant difference in Iba1 expression between the three groups ($F(2, 7)=8.959, p=0.01$; Two-way ANOVA repeated measures). Microglial response was significantly higher in the CCI group when comparing to the Sham and control groups from 720 to 1200 μm caudal to obex of the Vc (CCI vs Sham at 720 μm caudal to obex $p=0.005$, at 960 and 1200 μm $p=0.001$; CCI vs Control at 720 μm $p=0.03$, at 960 μm $p=0.0004$, and at 1200 μm $p=0.003$; Tukey's *post hoc* test). No statistical significant differences were found between Sham and Control groups.

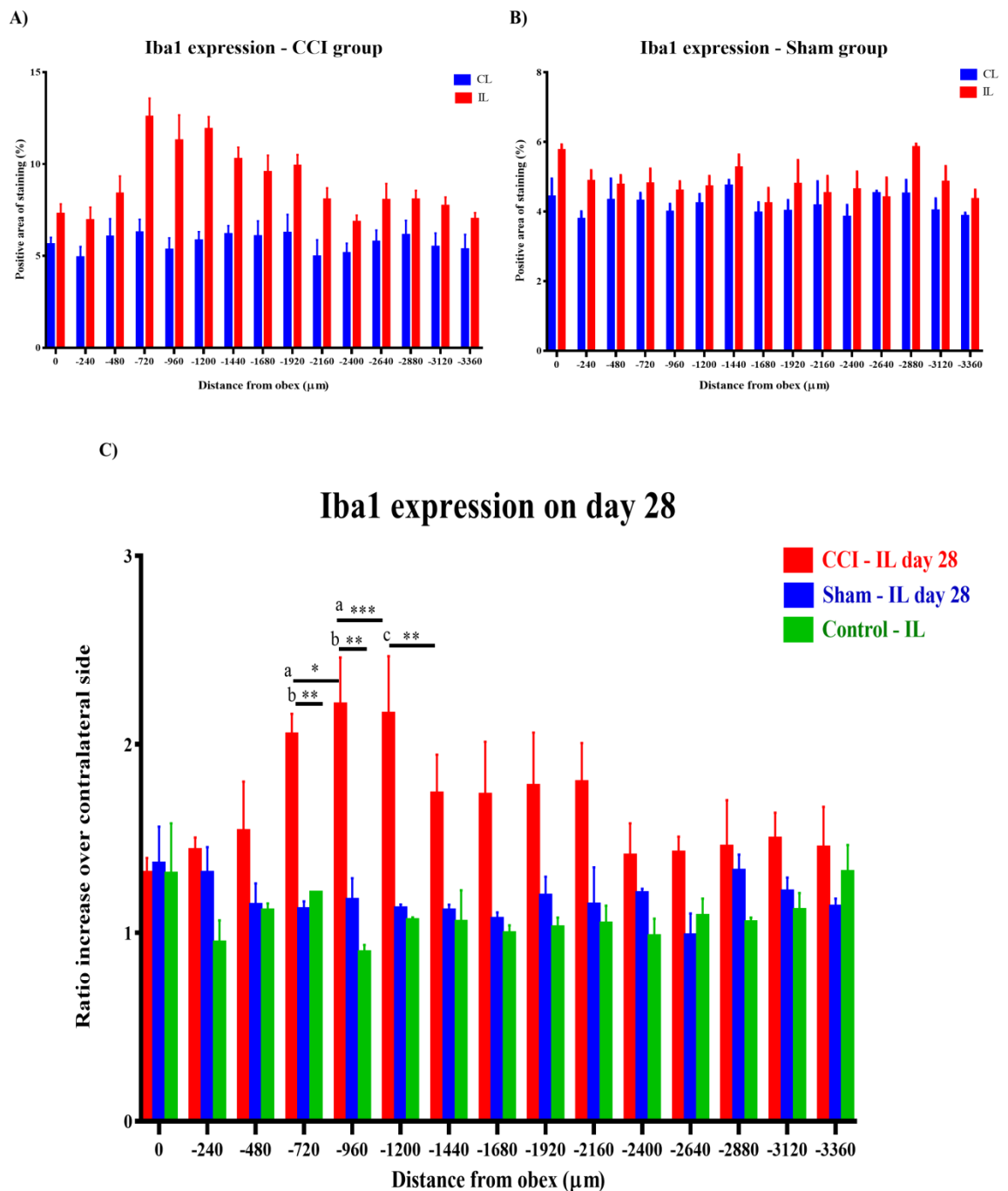


Figure 4.10. Analysis of microglial response on day 28 by quantification of Iba1 staining. A) Positive area of Iba1 staining (%) in the CCI group (n=5). B) Positive area of Iba1 staining (%) in the Sham group (n=3). C) Ipsilateral ratio increase over contralateral side: Iba1 expression was statistically significantly different between groups from 720 to 1200 μm caudal to obex. Asterisks represent statistical significance. * $p < 0.05$, ** $p < 0.01$, *** $p < 0.001$. a-CCI vs control, b-Sham vs Control. Two-way ANOVA repeated measures followed by Tukey's *post hoc* test.

4.3.5. Comparison of microglia response over time

When comparing microglia response in the ipsilateral side of the CCI (injured) group across time-points it was possible to observe statistical significant differences ($F(3, 11)=20.36, p<0.0001$; Two-way ANOVA repeated measures). The specific statistically different levels of the Vc are described in table 4.3.

As it is possible to observe in the graph of figure 4.8, microglial response on day 3 was the highest compared to any other day and control. The highest activation seems to occur at 720 μm caudal to obex three days following LNI.

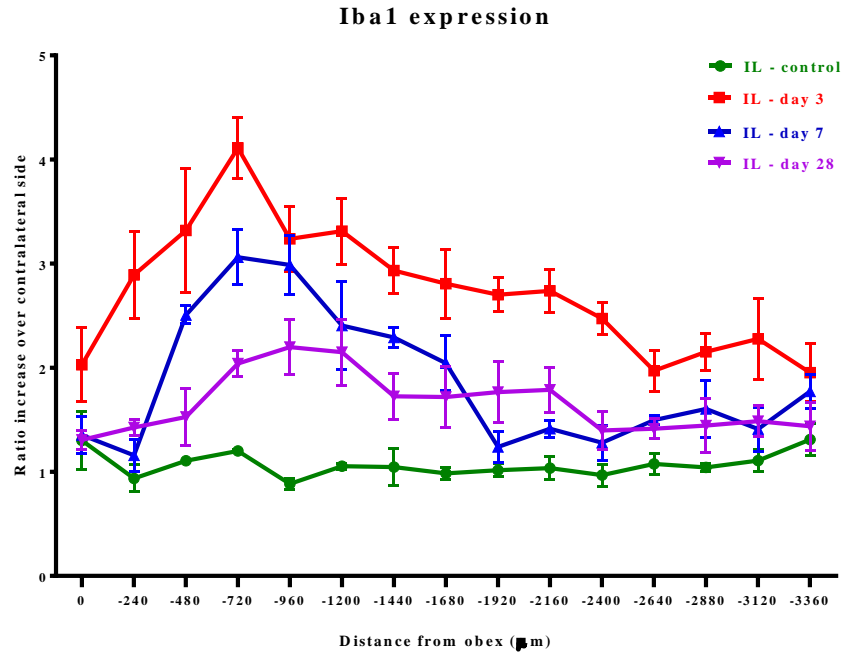


Figure 4.11. Comparative analysis of microglia response between time points. Statistical differences are described in table 4.3.

Table 4.3. Statistical differences between time points.

Distance from obex in the Vc	Groups	Adjusted <i>p</i> -value*
240 µm	IL - control vs. IL - day 3	<i>p</i> =0.0002
	IL - day 3 vs. IL - day 7	<i>p</i> =0.0001
	IL - day 3 vs. IL - day 28	<i>p</i> =0.0002
480 µm	IL - control vs. IL - day 3	<i>p</i> <0.0001
	IL - control vs. IL - day 7	<i>p</i> =0.0277
	IL - day 3 vs. IL - day 28	<i>p</i> <0.0001
720 µm	IL - control vs. IL - day 3	<i>p</i> <0.0001
	IL - control vs. IL - day 7	<i>p</i> =0.0014
	IL - day 3 vs. IL - day 7	<i>p</i> =0.0448
960 µm	IL - control vs. IL - day 3	<i>p</i> <0.0001
	IL - control vs. IL - day 7	<i>p</i> =0.0002
	IL - control vs. IL - day 28	<i>p</i> =0.0230
	IL - day 3 vs. IL - day 28	<i>p</i> =0.0155
1200 µm	IL - control vs. IL - day 3	<i>p</i> <0.0001
	IL - control vs. IL - day 7	<i>p</i> =0.0365
	IL - control vs. IL - day 28	<i>p</i> =0.0051
1440 µm	IL - control vs. IL - day 3	<i>p</i> =0.0003
	IL - control vs. IL - day 28	<i>p</i> =0.0033
1680 µm	IL - control vs. IL - day 3	<i>p</i> =0.0006
	IL - control vs. IL - day 28	<i>p</i> =0.0101
1920 µm	IL - control vs. IL - day 3	<i>p</i> =0.0017
	IL - day 3 vs. IL - day 7	<i>p</i> =0.0018
	IL - control vs. IL - day 28	<i>p</i> =0.0368
2160 µm	IL - control vs. IL - day 3	<i>p</i> =0.0015
	IL - day 3 vs. IL - day 7	<i>p</i> =0.0059
	IL - day 3 vs. IL - day 28	<i>p</i> =0.0324
2400 µm	IL - control vs. IL - day 3	<i>p</i> =0.0064
	IL - day 3 vs. IL - day 7	<i>p</i> =0.0163
	IL - day 3 vs. IL - day 28	<i>p</i> =0.0113

*Two-way ANOVA repeated measures with Tukey's *post hoc* corrections.

4.4. Discussion

Microglia response following Lingual nerve injury

Several pro-inflammatory mediators can trigger microglia activation, for instance lipopolysaccharide (LPS) released by bacteria, beta-amyloid peptide (Alzheimer's disease), and nerve injury (Graeber et al., 1988, Raghavendra et al., 2003, Tsuda et al., 2003, Piao et al., 2006, Zhang et al., 2007). Microglia, in response, can also release multiple mediators such as nitric oxide (NO), TNF- α , IL- β 1 and prostaglandins (Bianco et al., 2005, Berta, 2014) that will, in turn, activate astrocytes or neurones. The exact role of microglia following PNI has been the subject of much research over the past decade. However, microglial activation has not been widely studied in the Vc, and no previous studies have investigated microglial activation following rat LNI.

Previous tracing studies using horseradish peroxidase (HRP) have investigated trigeminal nerve somatotopic projections in the brainstem and have found that lingual nerve fibres, in specific, were present across the trigeminal-brainstem complex, mainly in the principal nucleus and trigeminal nucleus oralis and caudalis (Jacquin et al., 1983, Takemura et al., 1987). As mentioned previously (section 1.1 in chapter 1), it is considered that lingual nerve fibres transmitting nociceptive information terminate mainly in the Vc. Within the Vc, Takemura et al. (1987) has found the rat lingual nerve projecting mainly to the medial one-fourth, being particularly concentrated from obex to 1.2 mm caudal to obex. In that study lingual nerve fibres were present up to the most rostral part of the spinal cord dorsal horn. Within the brainstem section, those studies found that lingual nerve labelling was highly concentrated in laminae I and II, with very little labelling in laminae III and IV (Jacquin et al., 1983, Takemura et al., 1987). In the study described in this chapter, obex (the junction between the caudal end of the fourth ventricle and the rostral end of the central canal) was also used as a reference point for relative rostral-caudal location of microglial activation. Microglia activation was seen mainly in laminae I and II. In order to have a representation of the rostro-caudal extent of Vc, multiple sections at 240 μ m intervals were analysed and microglial activation following LNI was observed at all rostral-caudal levels analysed, even though at different intensities, on day 3 (time point with the greatest microglial response). The highest microglial activation in all CCI groups was detected in the most rostral parts to obex. Based on the tracing studies mentioned that showed lingual nerve projections in the Vc

mainly in the medial part, it is likely that microglia activation observed in the ipsilateral side of the CCI group was due to LNI.

On day 3, microglial cells had proliferated and presented an amoeboid morphology with short cytoplasmic extensions. This response was still present on day 7 but it was restricted to a smaller area of the Vc; however, microglial cells still presented an amoeboid shape. By day 28, microglial activation was significantly reduced when compared to day 3, with only sporadic activation in some areas of Vc. In terms of morphology, microglia showed longer ramifications. These results are in line with other studies that suggest that microglia are the first responders to a threat to the nervous system (Colburn et al., 1997, Raghavendra et al., 2003, Piao et al., 2006, Crown, 2012). For instance, Piao et al. (2006) have investigated microglial activation in the Vc of the rat after inferior alveolar nerve and mental nerve (nerves located in the mandibular division of the trigeminal nerve) transection at 2h, 1, 3, 7, 14 and 60 days using immunoreactivity of OX-42 (another microglial marker). They observed that microglial activation was present in the superficial laminae of the Vc: it started at day 1, was highest at day 3 and continued until day 7. By day 14 and 28 was already decreasing and on day 60 was at the same level as the contralateral side. The microglial activation was analysed at 1.2 mm intervals (obex was used as a reference point) and the highest activation was observed between obex and 6 mm caudal to obex. These results are in line with the temporal changes of the microglial study reported in this thesis. Even though microglia was activated, particularly on day 3 post-injury, at all rostral-caudal levels analysed in this thesis (obex to 3360 μm caudal to obex), the highest activation was detected between 480 and 1680 μm caudal to obex. In the other study mentioned, it was reported a broader microglia activation in the rostral-caudal levels than in the study reported in this thesis and that may be explained by the different nerves (inferior alveolar and mental nerve), the different type of injury (transection) and the fact that both nerves were co-injured. When they administrated minocycline, an inhibitor of microglia, p38 MAPK activation in microglial cells was blocked and the development of pain hypersensitivity was attenuated. Partial ligation of infraorbital nerve also leads to microglial activation within the Vc of the brainstem (Xu et al., 2008). In Xu's study, microglia were activated on day 1 post-injury and decreased by day 8; the greatest microglial activation was seen in the superficial laminae; no information on the rostral-caudal distribution of microglia response was provided. The infraorbital nerve is branch of the trigeminal nerve (as is the

lingual nerve) but is associated to the maxillary division. The microglial activation data in this thesis is in line with this study on the infraorbital nerve as microglia was activated at early time-points (even though different time-points were analysed).

Some of the most detailed reports of microglial responses following different nerve injury models have been conducted by Colburn et al. In a model of severe peripheral nerve freeze injury, it was found that microglia were activated in the spinal cord dorsal horn but no association with pain behaviours was found (Colburn et al., 1997). To evaluate microglial response to different types of injury Colburn et al. (1999) used multiple models of neuropathic pain such as spinal nerve ligation, dorsal root ligation and dorsal root transection. It was found that spinal nerve models produced microglial activation by day 7. Interestingly, it was found that microglia were strongly activated by nerve injury peripheral to the dorsal root ganglion, but not when injury was central. That study has also noted that sham-operated animals had some microglia response to injury, particularly at day 1 and 3. No clear justification was found but it was suggested that potential stress or accidental nerve injury during the surgery could have caused it. In the results described in this chapter, microglial activation in the sham group only occurred on day 7. Even though, microglia activation could have occurred from the inflammatory reaction to surgery in general, it was unexpected that it appeared only on day 7 and no significant microglia activation was detected on day 3 or 28 post sham operation. To confirm and dismiss the potential accidental injury to the nerve during the sham operation, the experiment was repeated on a separate occasion and extreme care was taken in order not to damage the lingual nerve during the exposure of the nerve; these animals were observed daily and it was possible to note local swelling (characteristic post-surgical effect) at the site of injury during the first 3 days post-surgery; however by day 7 there was no apparent swelling. Nevertheless, the same results were obtained and microglia were activated at specific levels of the Vc (the results reported include all animals analysed at day 7 post sham-operation). It is possible that a delayed microglia activation occurred in response to the initial post-surgical inflammation or that animals were under stress (even though there were no visible signs of that). By day 28, microglia activity was back to almost baseline levels.

As previously discussed in chapter 3, other studies in the lingual nerve have reported the development of spontaneous activity and mechanical sensitivity 3 days

following injury (Yates et al., 2000, Bird et al., 2003). These and further details on the relation of microglial response to the behavioural study reported in chapter 3, will be discussed in the General Discussion in chapter 7.

Methodological approach and statistical tests

In this study a rabbit polyclonal anti-Iba1 (ionized calcium-binding adaptor molecule 1) antibody was used, it was raised against a synthetic peptide corresponding to the C-terminus of Iba1. Iba1 protein has been used as a specific microglial marker because it was demonstrated that Iba1, within the nervous system, is expressed exclusively in microglial cells and not in neurones, astrocytes or oligodendrocytes (Imai et al., 1996, Ito et al., 1998). Iba1 protein seems to contribute to the motile characteristic of microglia as it interacted with Rac, which is a crucial mediator of membrane ruffling (Kanazawa et al., 2002). The ability to migrate is important for the phagocytosis role of microglia under disruption of homeostasis. In this line, it is logical that Iba1 expression is increased following LNI as this injury may have caused the synthesis and transport of several mediators to central terminals.

All tissues were processed according to the same immunohistochemical protocol and all images were taken and analysed with the same pre-determined parameters in order to minimise technical variations. In addition, for statistical analysis, the ratio increase in the ipsilateral over the contralateral site was used; this way animal individual variations and any differences in background staining were taken into account for each measurement. A two-ANOVA repeated measures was selected for statistical analysis as Iba1 was being quantified within the same tissue at different rostral-caudal levels. Tukey's *post hoc* corrections were applied, when ANOVA found to be statistically significant ($p \leq 0.05$), because there were 15 levels per animal analysed and, at least, three groups being compared; in this situation Tukey's test was found to be more appropriate as, for instance, Bonferroni corrections have less power.

Study limitations

Evidence from recent studies has suggested that female mice do not use a mechanism dependent on microglia to produce mechanical hyperalgesia and allodynia. Sorge et al. (2011) have found that Toll-like receptor 4 (known to be expressed in microglia) only mediate pain in male mice. Similarly P2X4R-induced release of BDNF

by microglia was only evident in male mice (Sorge et al., 2015). Recent studies suggest that female mice use a mechanism primarily dependent on T cells, and only when female mice were T cell deficient or treated with testosterone, they used the microglial-dependent pathway. However, in a model of bone cancer pain, p38 mitogen-activated protein kinase (MAPK) was shown to be activated in microglial cells when using female rats (Yang et al., 2015); in that study, minocycline (a known microglia inhibitor) reduced the late phase of cancer pain. This suggests that microglia may still have a role in chronic pain in females in certain conditions. In the study reported in this chapter, it was not possible to verify these reports because only male mice were used. Therefore, when interpreting the results that needs to be taking into consideration. In order to apply more generically, female mice need to be included in a future study.

Conclusions and future work

Microglial cells were activated in the early days post-injury in this model of LNI in male rats. It is known that microglia respond to several mediators and in turn release other potential pro-inflammatory mediators. The elevated response of microglia on day 3 may be responsible for the induction of neuronal hyper-excitability (central sensitisation) and contribute to the development of persistent pain in male rats.

In a future study it would be important to characterise the mediators being expressed and released by the microglial cells in order to confirm the actual contribution to central sensitisation. That may also help in the clarification of microglial activation on day 7 in the sham group. Microglia have also been shown to release anti-inflammatory mediators, so it has been suggested that microglia neurotoxicity may be due to loss of beneficial mechanisms or a shift to a pro-inflammatory mechanism (Lull and Block, 2010). Therefore, a characterisation of the type of mediators that are being expressed and whether different mediators are released between CCI and Sham groups may help clarify whether microglia activation in the sham group has a different biological role.

CHAPTER 5
RESOLVIN RECEPTORS EXPRESSION

5.1. Introduction

Resolvins are endogenous lipid mediators that have been shown to act in inflammation- and pain-associated conditions; they are known to bind to specific G protein-coupled receptors (GPCR): GPR32, BLT1, FPR2/ALX and ChemR23. Excluding GPR32 (which was an orphan receptor), the other three receptors, ChemR23, FPR2/ALX and BLT1, are well-known receptors involved in inflammatory responses, and their expression has been well characterised, particularly in immune cells (Bannenberg et al., 2007), further details are described in literature review (please see section 1.2.2 in chapter 1).

Accumulating evidence on the role of resolvins in reducing pain symptoms in pre-clinical pain models such as the spinal nerve ligation (SNL) and sciatic nerve chronic constriction injury (CCI) (Xu et al., 2013, Xu et al., 2010), suggests that their receptors may play a role in modulating pain processing in nervous system tissues. However, there is very little evidence of resolvins receptors expression in neurones and/or glial cells and, thus, a better characterisation of their expression is necessary.

It was hypothesised that resolvins receptors are expressed in the nervous system and that their expression may change following peripheral nerve injury. The overall aim was to identify the specific cells expressing resolvins receptors within the nervous system and characterise their expression following lingual nerve injury (LNI). The specific objectives were:

1. Investigate the expression of resolvins receptors GPR32, BLT1, FPR2/ALX and ChemR23 within pain processing regions of the nervous system (human lingual nerve neuroma and rat spinal cord and brainstem) using immunohistochemistry;
2. Identify the specific cells expressing these receptors;
3. Characterise the expression of ChemR23 in the trigeminal nucleus caudalis (Vc) following LNI at days 3, 7 and 28.

5.2. Methodological approach

Preliminary studies were conducted to determine whether immunohistochemical techniques could be applied to the study of resolvins receptors expression. Antibodies for each receptor were optimised using spare tissue available in the laboratory. Antibodies that produced clear immunohistochemical labelling, which appeared to be specific, were used for dual labelled with markers for specific cell types in order to further characterise

the expression of selected receptors. In addition changes in expression of selected receptors was investigated following nerve injury.

This chapter initially describes immunoreactivity for the receptors GPR32 and BLT1 (and neuronal and Schwann cell markers) in human lingual nerve neuromas and for the receptors FPR2/ALX and ChemR23 (and neuronal and glial cell markers) in the rat spinal cord and brainstem. Commercially available antibodies against GPR32 are only reactive to the human antigen. The antibody used for BLT1 immunostaining was only reactive with the human antigen in this study. The antibodies used for FPR2/ALX and ChemR23 immunostaining were successfully optimised in the rat tissues, but no successful optimisation (high background and lack of specificity) was obtained in the human tissues during the preliminary studies.

Further studies were conducted using a rat model of neuropathic pain (see Chapter 2, section 2.2) to characterise and quantify the expression of the resolvin receptor ChemR23 in the Vc following LNI. This study included brainstem sections collected from the experimental groups (CCI) at days 3 (n=5), 7 (n=3) and 28 (n=5) and from the sham-operated groups (sham) at days 3 (n=3), 7 (n=3) and 28 (n=3). Brainstem sections from a control (naïve) group (n=2) were also analysed.

As described in detail in chapter 2 section 2.4.1, in order to have an overall representation of the rostral-caudal levels of the Vc, 15 brainstem sections per animal were analysed starting at the level of the obex (considered 0 μm) and then every 240 μm until 3360 μm caudal to obex. The analysis of ChemR23 expression was obtained by quantifying the positive area of ChemR23 antibody staining in the brainstem (as described in section 2.5.1 in chapter 2).

5.3. Results

5.3.1. Expression of resolvins receptors

5.3.1.1. Human tissue

Immunohistochemistry for GPR32 and BLT1 produced clear positive staining in human lingual nerve neuromas (figures 5.1–5.4). Overall this appeared to be present in specific structures and levels of background staining were low. Control experiments consisted of omitting the primary antibody and incubating with respective secondary antibody alone. Pre-absorption controls were not carried out as respective blocking peptides were not commercially available.

The morphology of the labelled structures suggested that the majority of the positive labelling was present in either axons or Schwann cells, therefore dual labelling with specific markers for these cell types was undertaken. Details of the specific labelling patterns for GPR32 and BLT1 are given below.

GPR32

GPR32 was found to be expressed in human lingual nerve neuromas. Co-localisation with Schwann cell marker S-100 show labelling of GPR32 in Schwann cells (figure 5.1). Co-localisation with nerve fibre marker PGP9.5 show labelling in axons (figure 5.2).

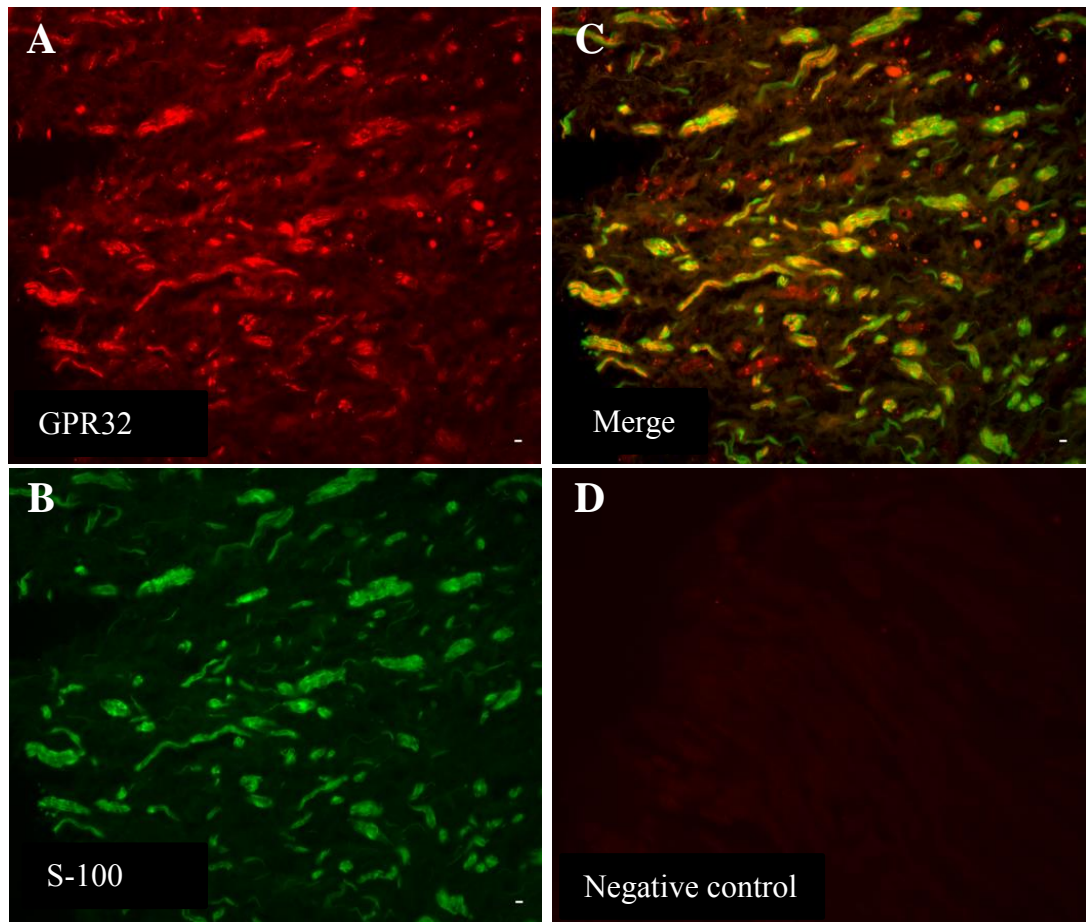


Figure 5.1. GPR32 is co-localised with S-100. A) Positive staining with antibody against GPR32. B) Positive staining with antibody against Schwann cell marker S-100 C) Double staining in yellow with GPR32 (red) and S-100 (green). D) Negative control by omission of primary antibody GPR32. Scale bar: 10 μm .

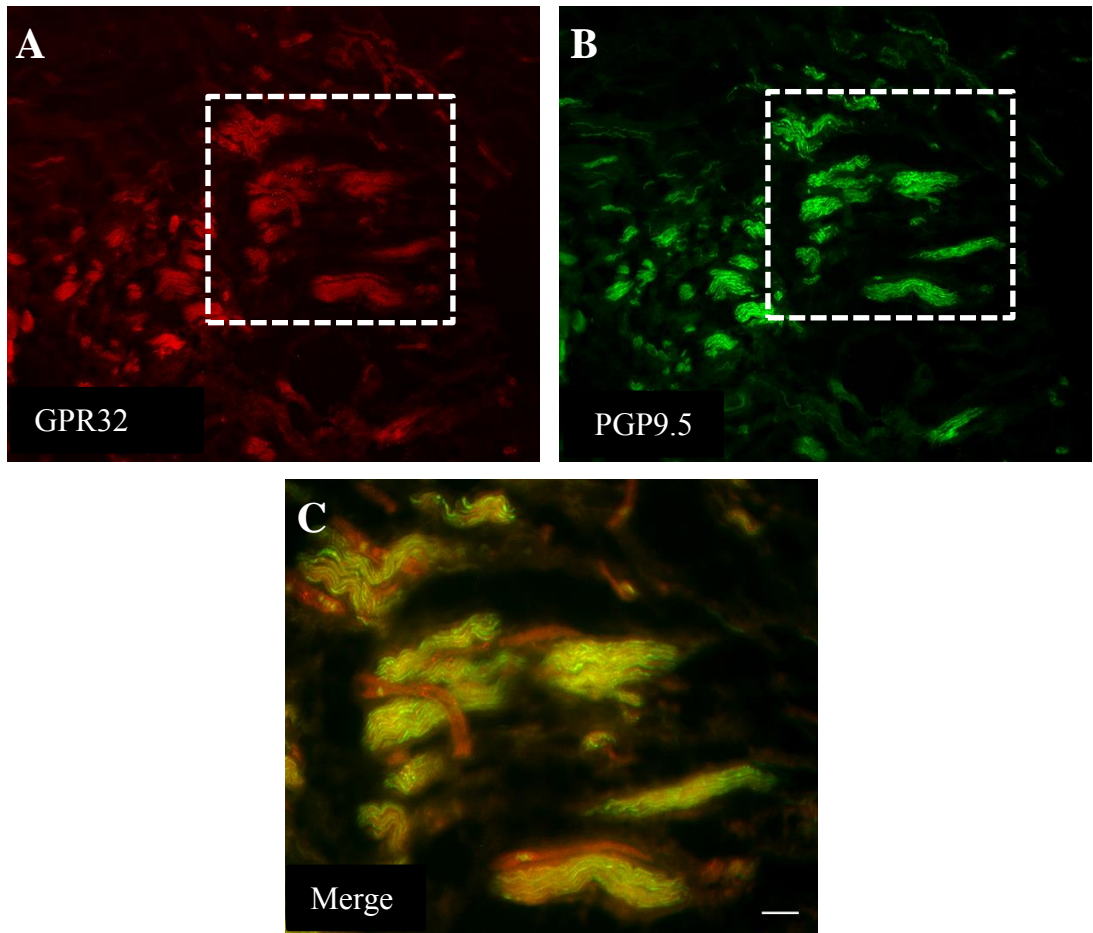


Figure 5.2. GPR32 and PGP9.5 dual labelling in human lingual nerve neuroma. A) Positive staining with antibody against GPR32. B) Positive staining with nerve fibre marker antibody, PGP9.5. C) Double staining in yellow with GPR32 (red) and S-100 (green). Scale bar: 50 μm .

BLT1

An antibody against BLT1 produced positive staining in human lingual nerve neuroma (figure 5.3 and 5.4). BLT1 staining appears to overlap with both the nerve fibre marker PGP9.5 (figure 5.3-C, -D) and the Schwann cell marker S-100 (figure 5.4-D, -E).

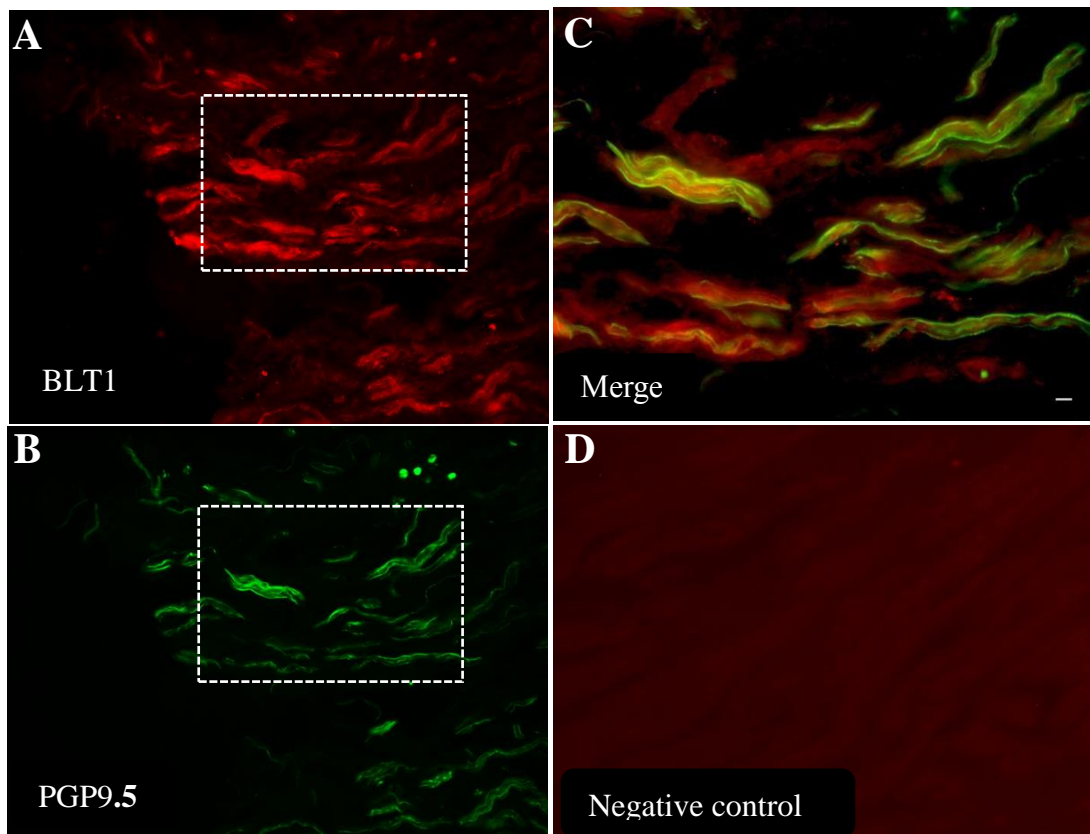


Figure 5.3. BLT1 and PGP9.5 dual labelling. BLT1 and PGP9.5 dual labelling. A) Positive staining with antibody against BLT1. B) Positive staining with antibody against nerve fibre PGP9.5. C) and D) Double staining with BLT1 (red) and PGP9.5 (green). D) Negative control by omission of BLT1 antibody. Scale bar: 10 μ m.

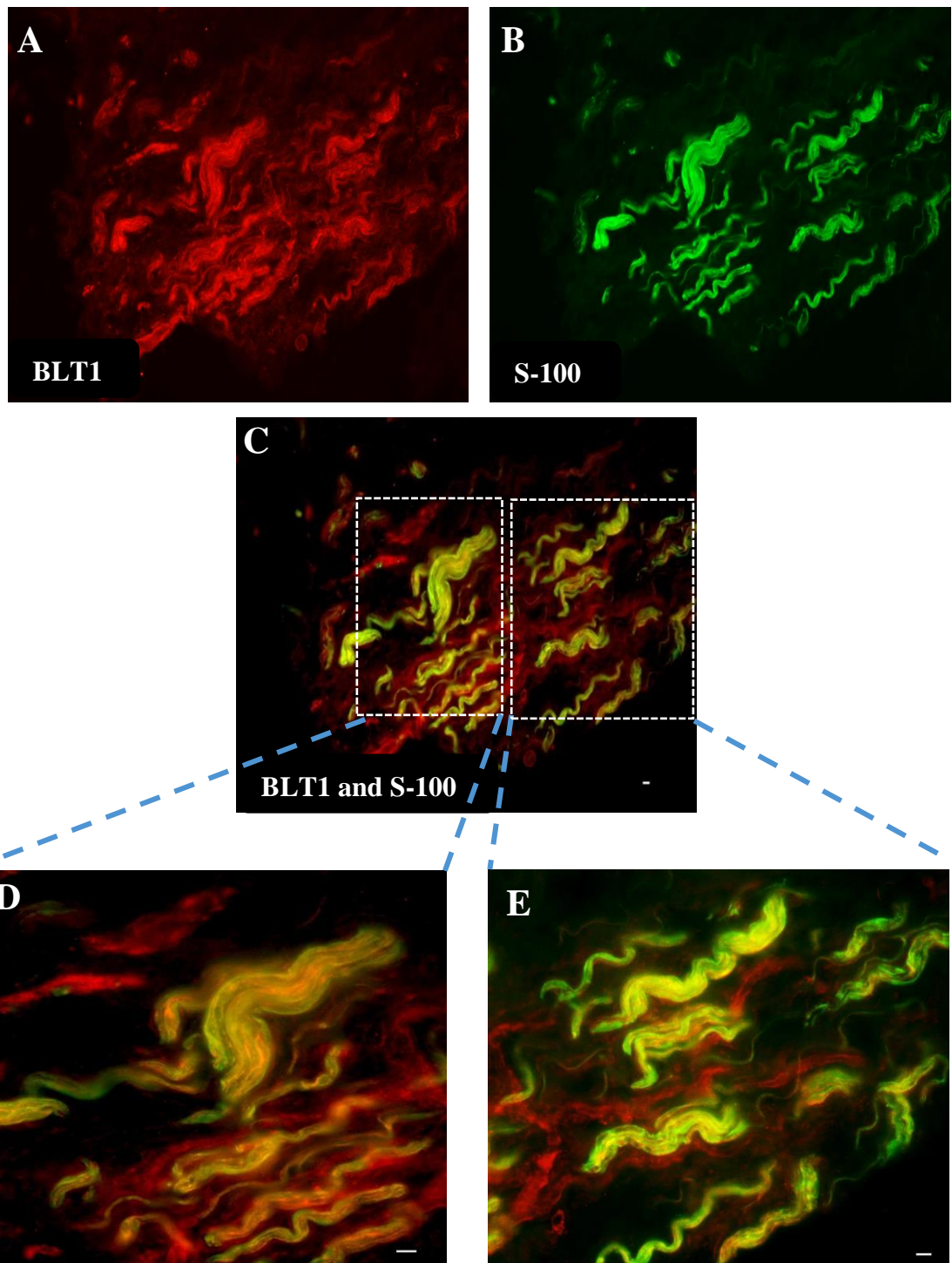


Figure 5.4. BLT1 seems to be expressed in Schwann cells. A) Positive staining with antibody against BLT1 in human lingual nerve neuroma. B) Positive staining with antibody against Schwann cell marker S-100. C) Double staining with BLT1 (red) and S-100 (green). D) and E) High magnification of the area indicated by the box shows co-localisation between BLT1 and S-100 (arrows). Scale bars: 10 μm .

5.3.1.1. Rat tissue

Immunohistochemistry for FPR2/ALX and ChemR23 produced positive staining in the rat spinal cord and brainstem (figures 5.5–5.11). For both antibodies, preabsorption controls was carried out with respective blocking peptides.

Dual labelling with specific markers for neurones, astrocytes and microglia was conducted and details of the specific labelling patterns for FPR2/ALX and ChemR23 are given below.

FPR2/ALX

FPR2/ALX antibody produced positive staining in the spinal cord and brainstem (figures 5.5 -5.7). The majority of positive staining was present in the grey matter and appeared to be present in neuronal cells (figures 5.4 and 5.7). To test the specificity a preabsorption control was performed. FPR2/ALX was pre-incubated with a blocking peptide (that was used to produce the antibody) for 24 h. Following pre-absorption, the antibody did not produce positive staining (5.7-D).

In order to investigate exactly which cell types were expressing FPR2/ALX, co-localisation studies were performed with markers of specific cell types. Positive dual labelling was obtained when FPR2/ALX was incubated with the neuronal marker NeuN, suggesting that FPR2/ALX is expressed in neurones in dorsal horn (figure 5.5) and trigeminal nucleus (figure 5.7).

Dual labelling for FPR2/ALX and the astrocyte marker GFAP, provided little indication of colocalisation of these two markers, suggesting that FPR2/ALX is not expressed in astrocytes (figure 5.6).

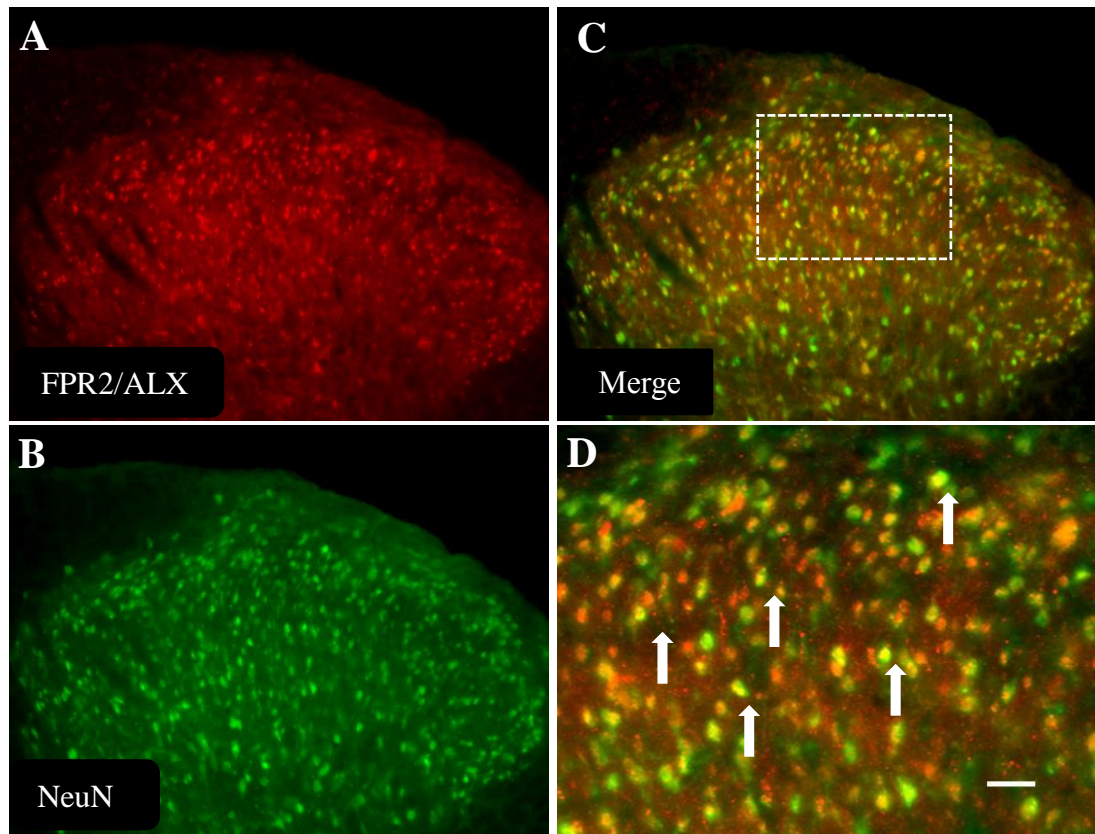


Figure 5.5. FPR2/ALX is expressed in spinal cord dorsal horn neurones. A) Positive staining with antibody against FPR2/ALX in rat spinal cord. B) Positive staining with antibody against neuronal marker NeuN in rat spinal cord. C) and D) Double staining with FPR2/ALX (red) and NeuN (green). D) High magnification of the area indicated by the box shows co-localisation between FPR2/ALX and NeuN (arrows). Scale bar: 50 μ m.

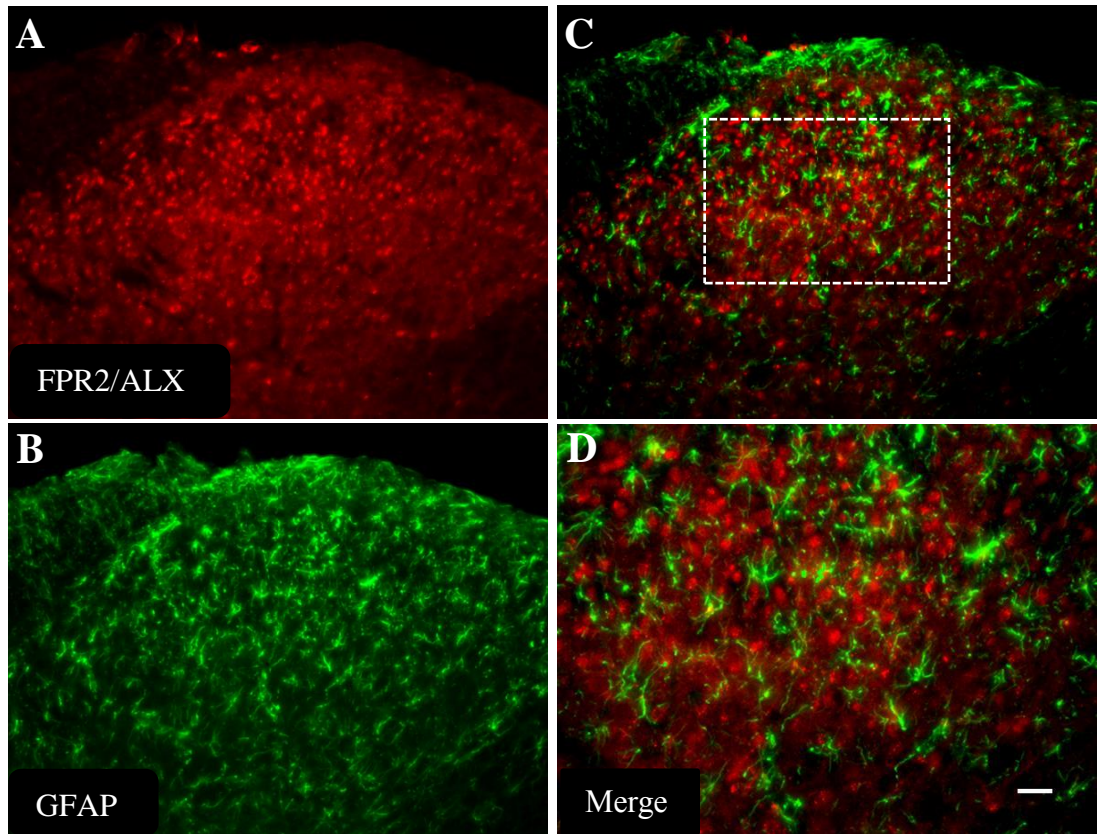


Figure 5.6. FPR2/ALX is not expressed in spinal cord astrocytes. A) Positive staining with antibody against FPR2/ALX in rat spinal cord. B) Positive staining with antibody against astrocyte marker GFAP in rat spinal cord. C) and D) Double staining with FPR2/ALX (red) and GFAP (green). D) High magnification of the area indicated by the box shows no co-localisation between FPR2/ALX and GFAP. Scale bar: 50 μ m.

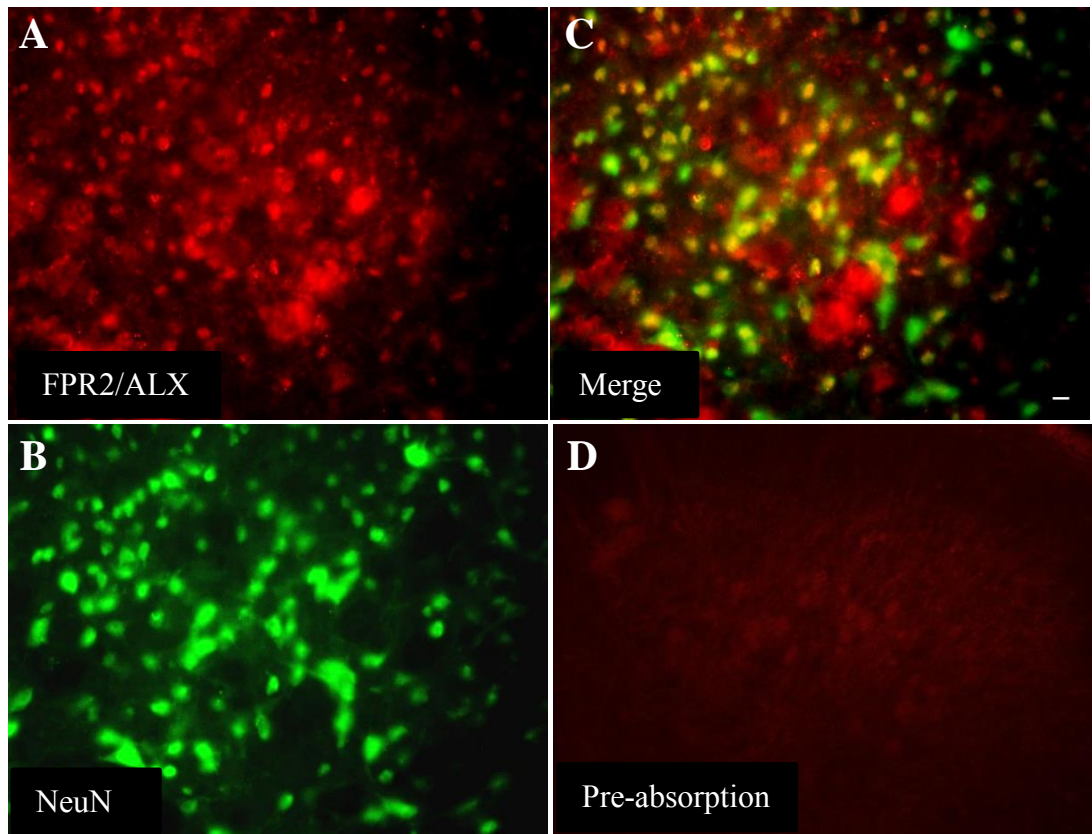


Figure 5.7. FPR2/ALX is expressed neurones within brainstem trigeminal nucleus. A) Positive staining with antibody against FPR2/ALX. B) Positive staining with antibody against neuronal marker NeuN. C) Double staining in yellow with FPR2/ALX (red) and NeuN (green). D) Pre-absorption with respective blocking peptide). Scale bar: 10 μ m.

ChemR23

Immunoreactivity for the ChemR23 antibody was observed in the spinal cord dorsal horn (figure 5.8 -5.10) and in the brainstem (figure 5.12). Positive staining was obtained in the grey matter and the morphology suggested this was present in neuronal cells. To test the specificity, ChemR23 was pre-incubated with a blocking peptide and, in that condition, the antibody did not produce positive staining (5.8-C and 5.12-D).

Next, co-localisation studies were performed in order to investigate which cell types expressed ChemR23. Positive dual labelling was obtained when incubating ChemR23 with the neuronal marker NeuN, suggesting that ChemR23 is expressed in neurones (figures 5.9, 5.10 and 5.12).

When incubated with the astrocyte marker GFAP, ChemR23 failed to produce positive staining. This result suggested that ChemR23 is not expressed in astrocytes (figure 5.11). Similarly, dual labelling with the microglial marker, Iba1, did not show co-localisation (figure 5.13).

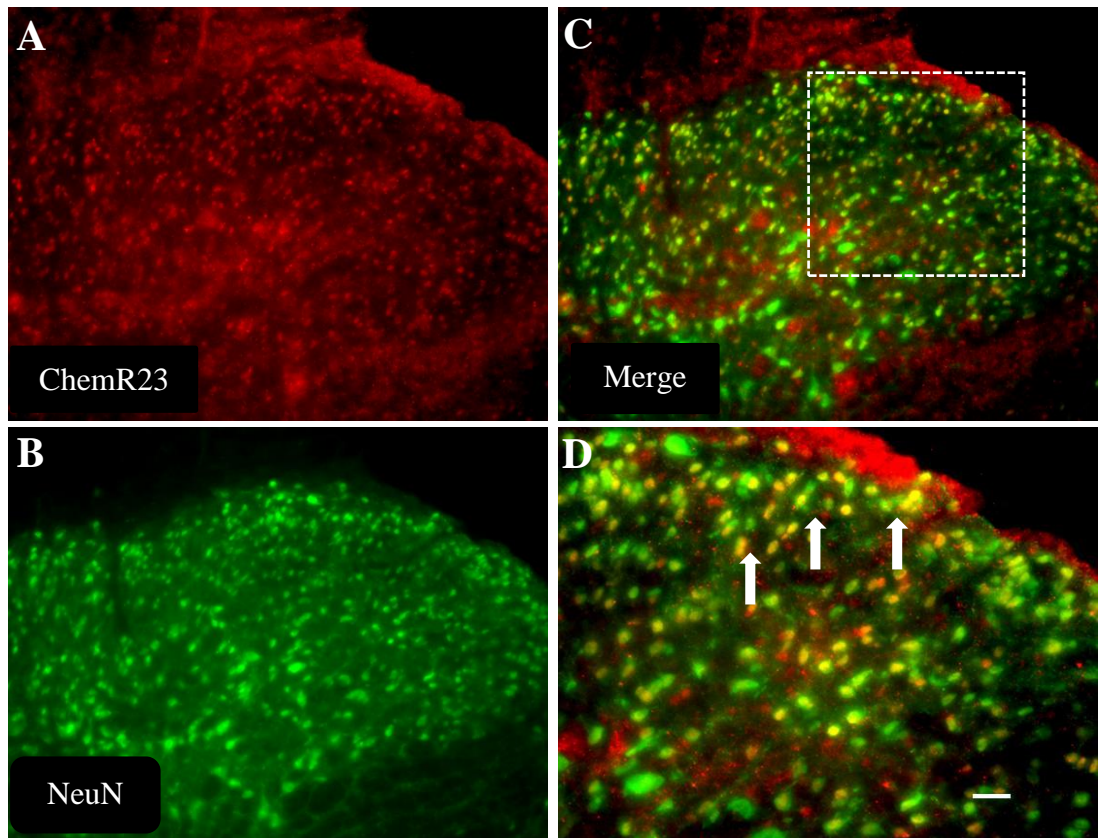


Figure 5.8. ChemR23 is expressed in spinal cord dorsal horn neurones. A) Positive staining with antibody against ChemR23 in rat spinal cord. B) Positive staining with antibody against neuronal marker NeuN in rat spinal cord. C) and D) Double staining with ChemR23 (red) and NeuN (green). D) High magnification of the area indicated by the box shows co-localisation between ChemR23 and NeuN (yellow, arrows). Scale bar: 50 μ m.

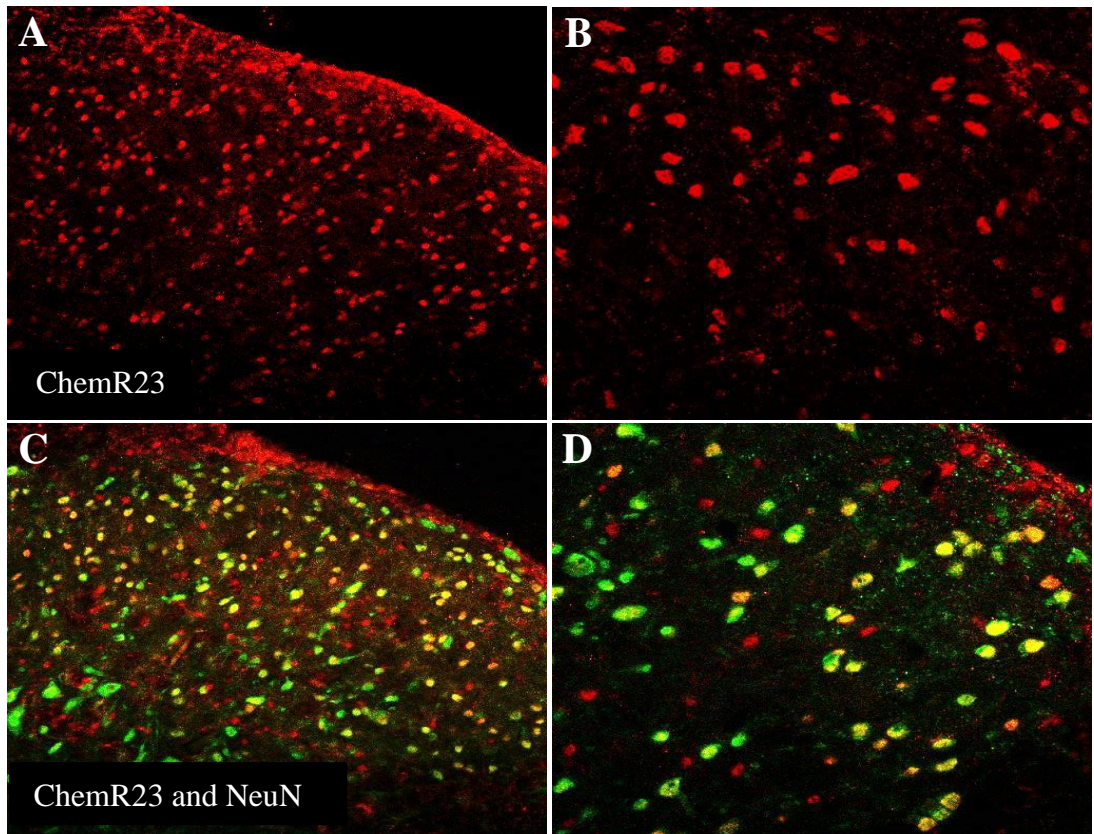


Figure 5.9. Confocal microscopy shows co-localisation of ChemR23 and NeuN. A) and B) show the expression of ChemR23 (red) in the dorsal horn. C) and D) show co-localisation (in yellow) of ChemR23 with the neuronal marker NeuN.

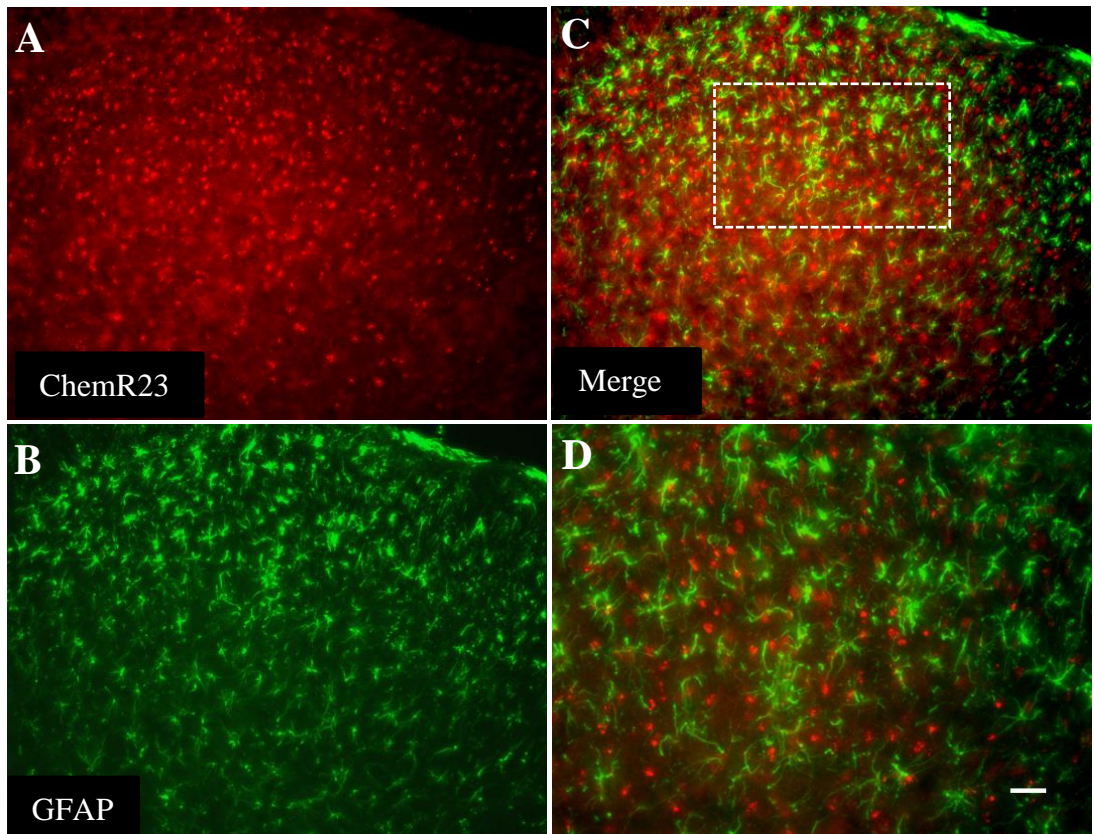


Figure 5.10. ChemR23 is not expressed in spinal cord astrocytes. A) Positive staining with antibody against ChemR23 in rat spinal cord. B) Positive staining with antibody against astrocyte marker GFAP in rat spinal cord. C) and D) Double staining with ChemR23 (red) and GFAP (green). D) High magnification of the area indicated by the box shows no co-localisation between ChemR23 and GFAP. Scale bar: 10 μ m.

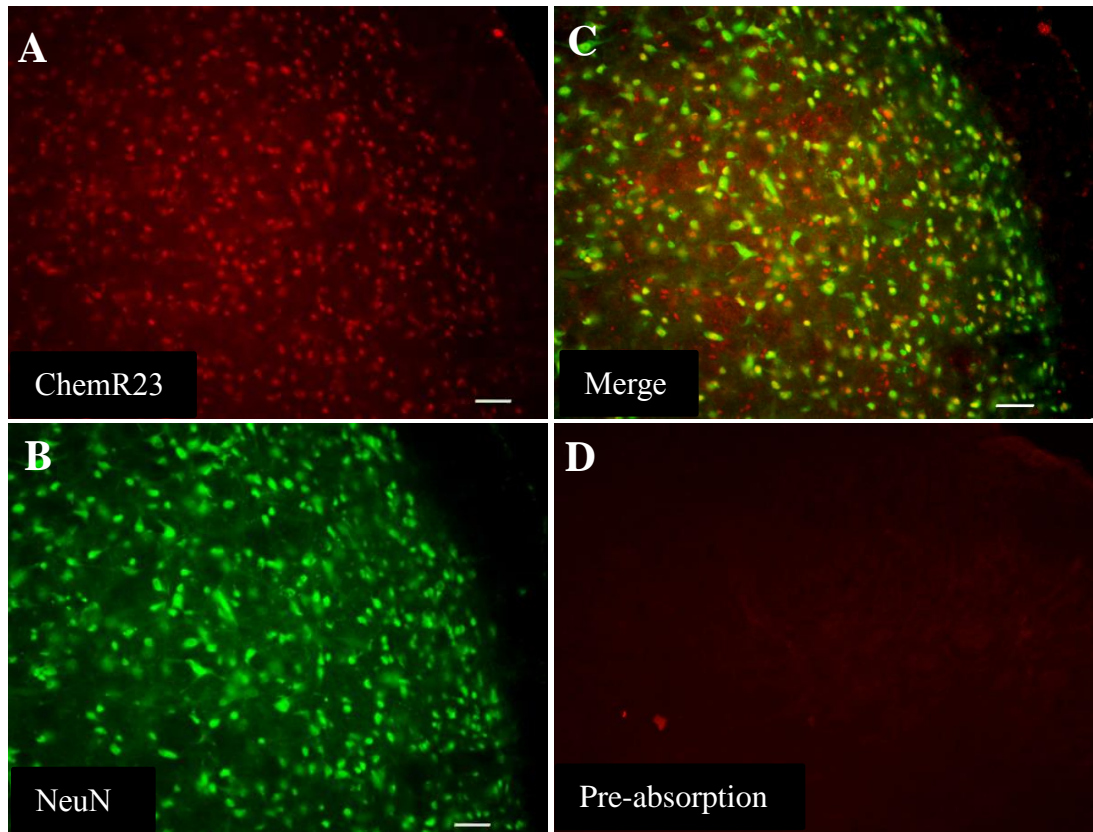


Figure 5.11. ChemR23 is expressed in neurones within the brainstem trigeminal nucleus. A) Positive staining with antibody against ChemR23. B) Positive staining with antibody against neuronal marker NeuN. C) Double staining in yellow with ChemR23 (red) and GFAP (green). D) Pre-absorption with respective blocking peptide. Scale bar: 50 μ m.

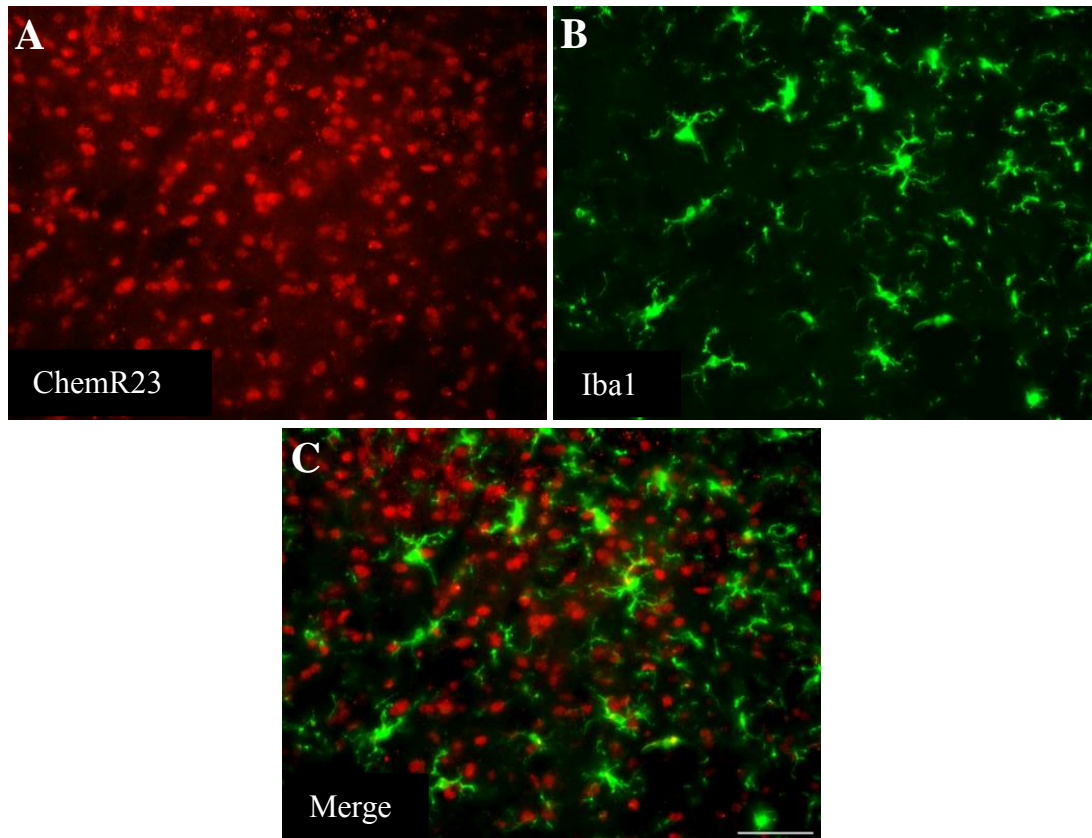


Figure 5.12. ChemR23 is not expressed in microglial cells within the brainstem trigeminal nucleus. A) Positive staining with antibody against ChemR23. B) Positive staining with antibody against microglial marker Iba1. C) Double staining in yellow with ChemR23 (red) and Iba1 (green). Scale bar: 50 μ m.

5.3.2. ChemR23 expression following lingual nerve injury

The expression of ChemR23 in the trigeminal nucleus (Vc) following LNI was investigated at day 3, 7 and 28 post-injury. ChemR23 was expressed in Vc and an increase in labelling was observed on the side ipsilateral to nerve injury (compared to the contralateral), in the region where microglial activation was observed within the brainstem section, in the laminar dorsal horn of the Vc (figure 5.13 and 5.15). Even though, ChemR23 was not found to be expressed in microglial cells in this study, activated microglial cells were observed surrounding ChemR23 expressing cells (figure 5.14-C).

ChemR23 was also detected in Vc tissue from control (naïve) animals but with weaker staining in general. Image analysis of ChemR23 expression was conducted by measurement of positive area of staining (%) in both ipsilateral and contralateral sides and statistical analysis between groups and at each time-point was conducted on the ratio increase over the contralateral side.

The level of ChemR23 labelling appeared greatest on day 3 post-injury and, in general, the biggest differences were found between injured and control naïve, rather than injured versus sham. Within the Vc, ChemR23 was expressed throughout the area analysed (obex to 3360 μm caudal to obex) but the most noticeable difference between groups was detected at 960 μm caudal to obex (figures 5.15 to 5.18).

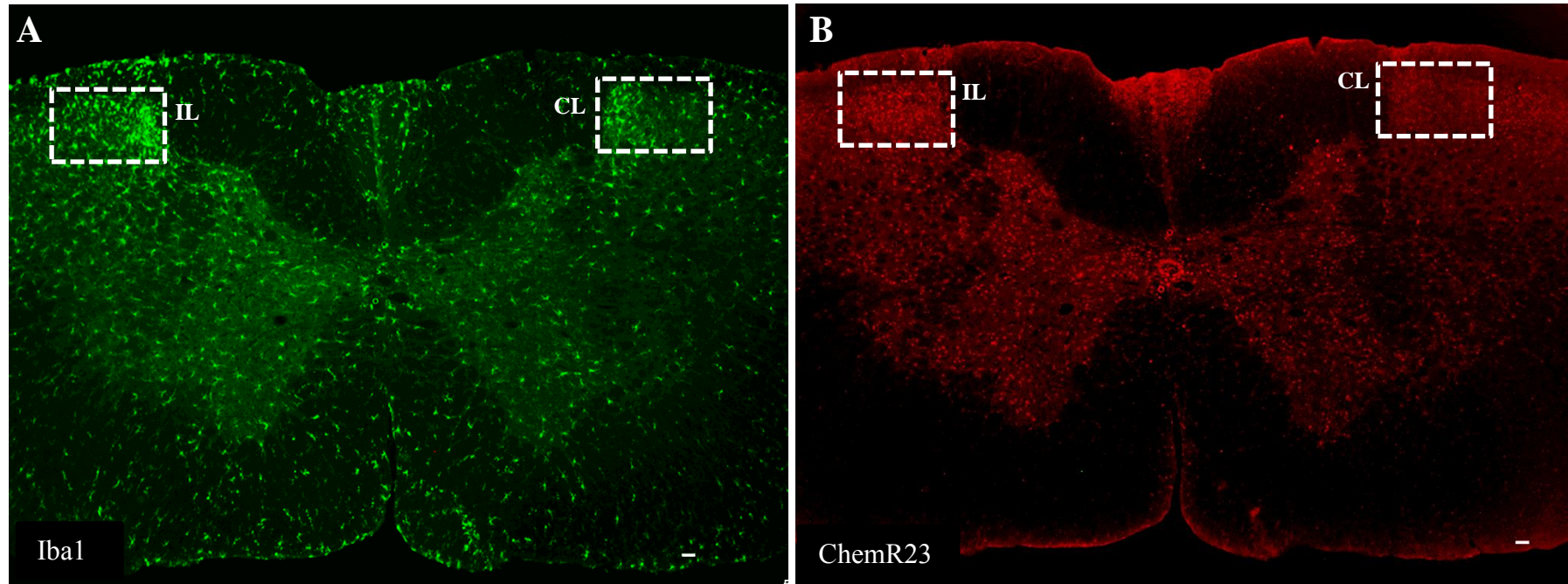


Figure 5.13. ChemR23 expression in the trigeminal nucleus in relation to microglial activation. A) Microglial activation. B) ChemR23 expression. Low magnification image taken at 960 μm caudal to obex. White boxes represent area analysed. Scale bar: 50 μm . CL: contralateral; IL: ipsilateral.

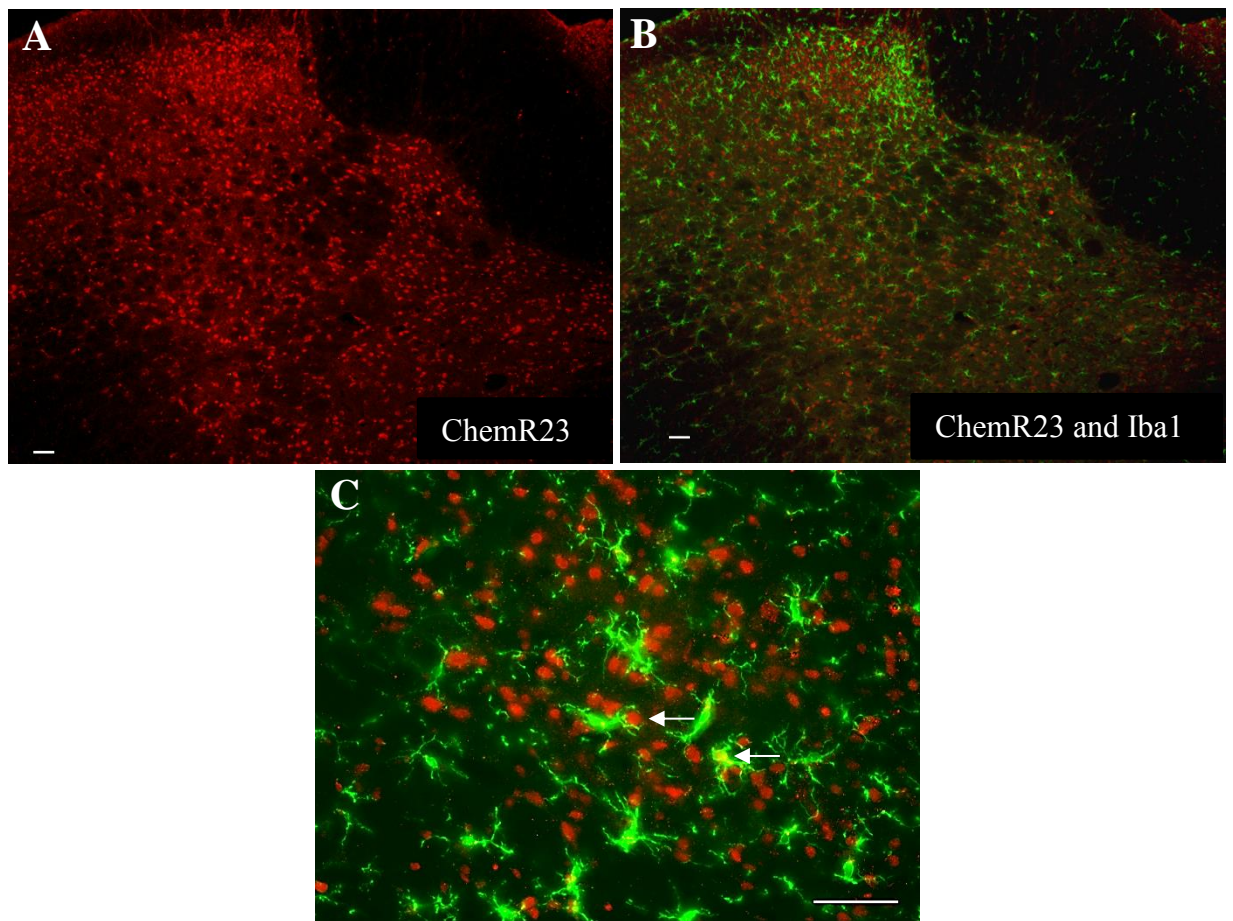


Figure 5.14. ChemR23 and microglia following lingual nerve injury. A) ChemR23 expression in the ipsilateral site of the Vc. B) ChemR23 and microglial activation. C) Microglial cell ramifications surrounding ChemR23 expressing cells (white arrows). Images correspond to higher power magnification of ipsilateral side of the Vc represented in figure 5.13 (previous page). Scale bar: 50 μm .

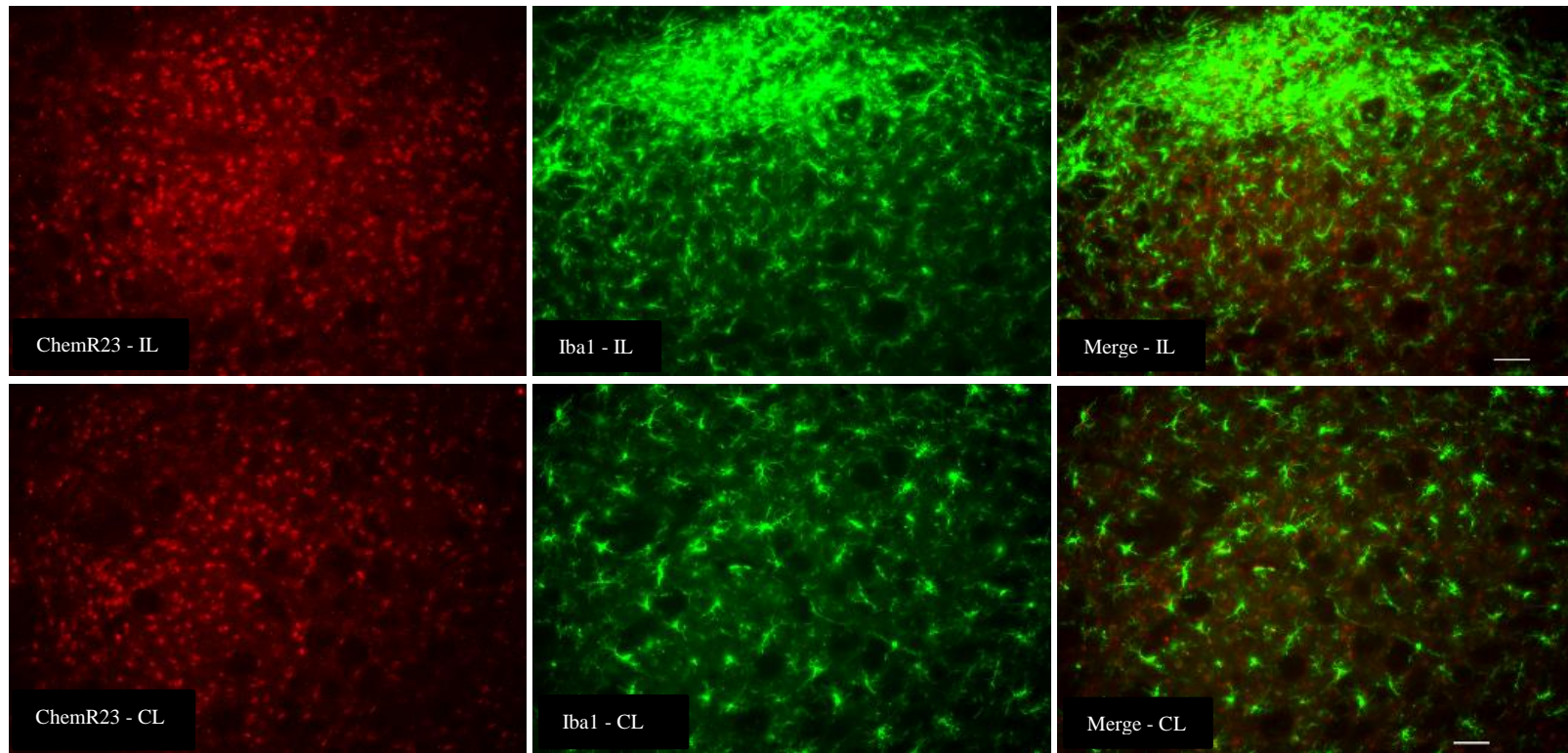
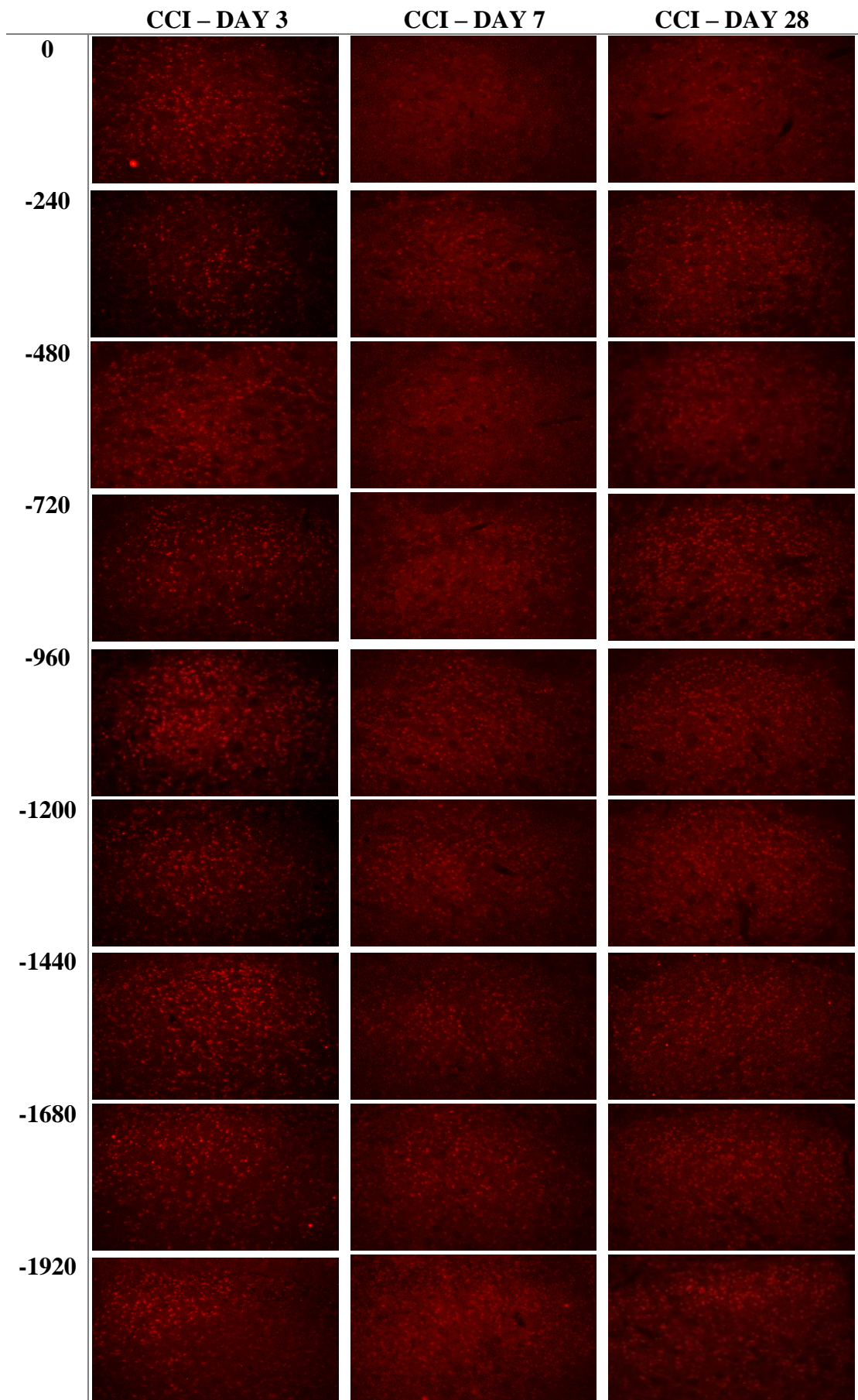


Figure 5.15. ChemR23 and microglia expression three days following lingual nerve injury in the Vc at 960 um caudal to obex. Scale bar 50 μ m.



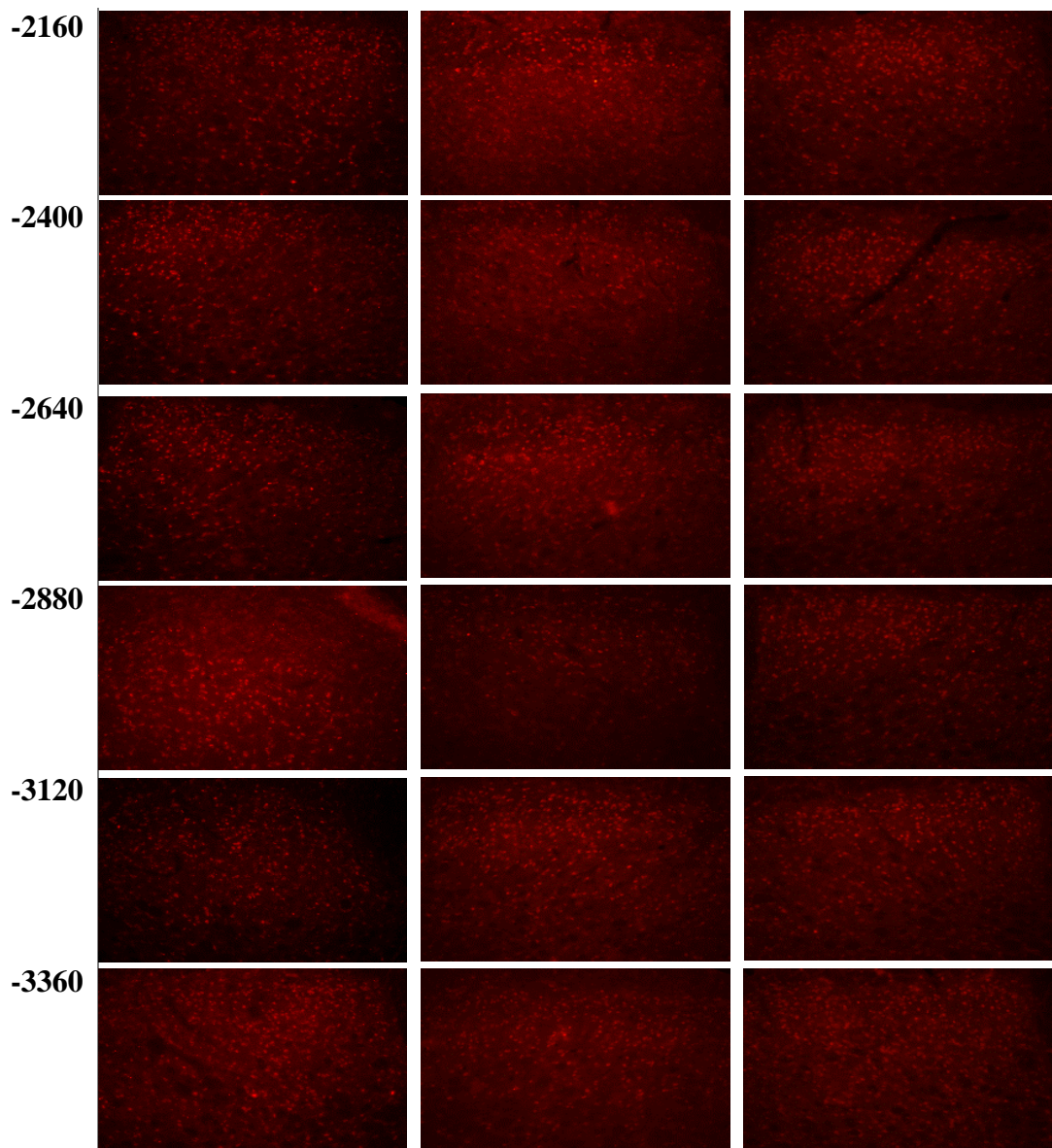
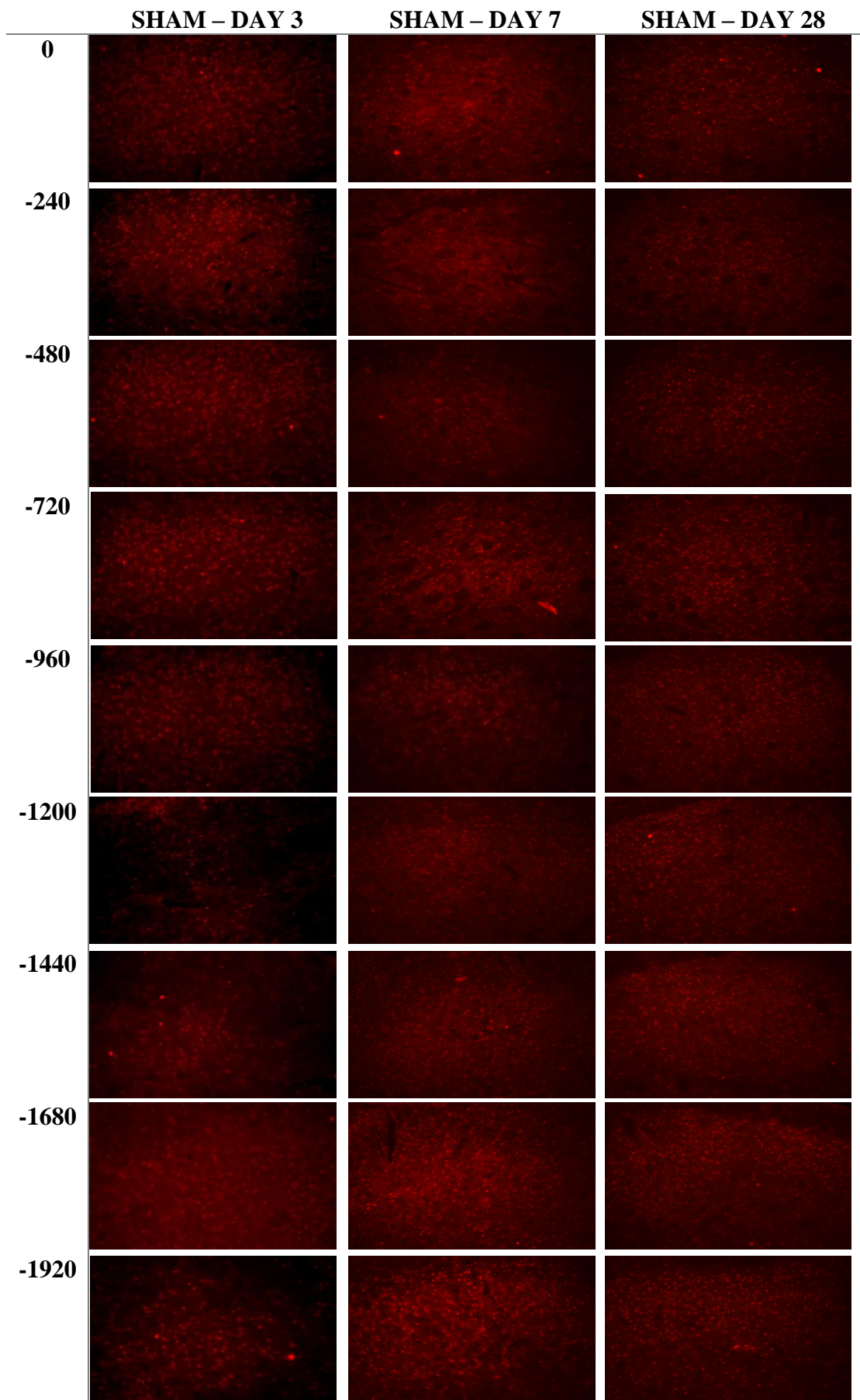


Figure 5.16. ChemR23 in CCI group. Showing representative images from obex (0 μm) to 1920 μm caudal to obex (previous page) and from 2160 to 3360 μm caudal to obex (current page). Distances from obex in μm .



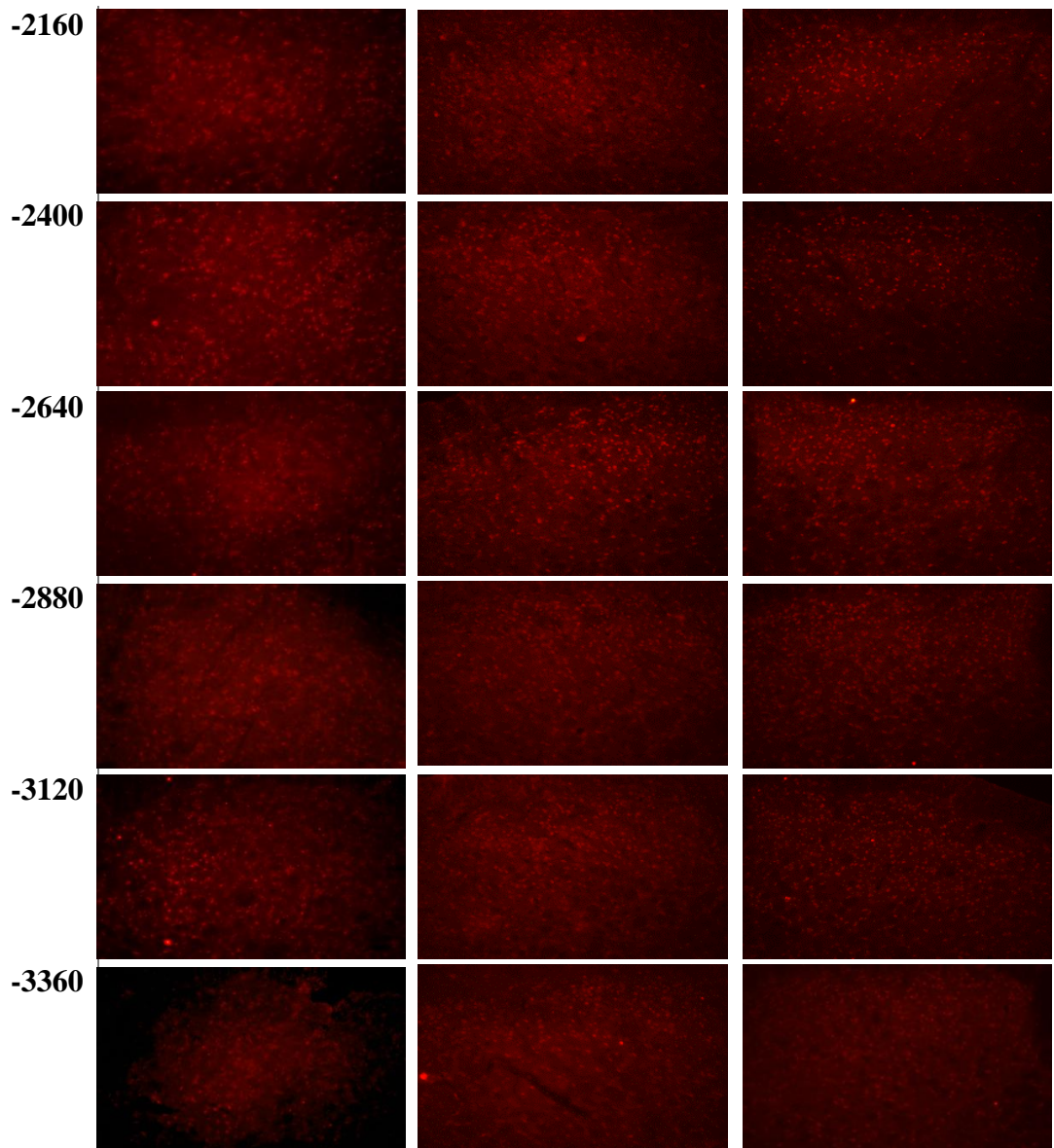


Figure 5.17. ChemR23 in Sham group. Showing representative images from obex ($0\ \mu\text{m}$) to $1920\ \mu\text{m}$ caudal to obex (previous page) and from 2160 to $3360\ \mu\text{m}$ caudal to obex (current page). Distances from obex in μm .

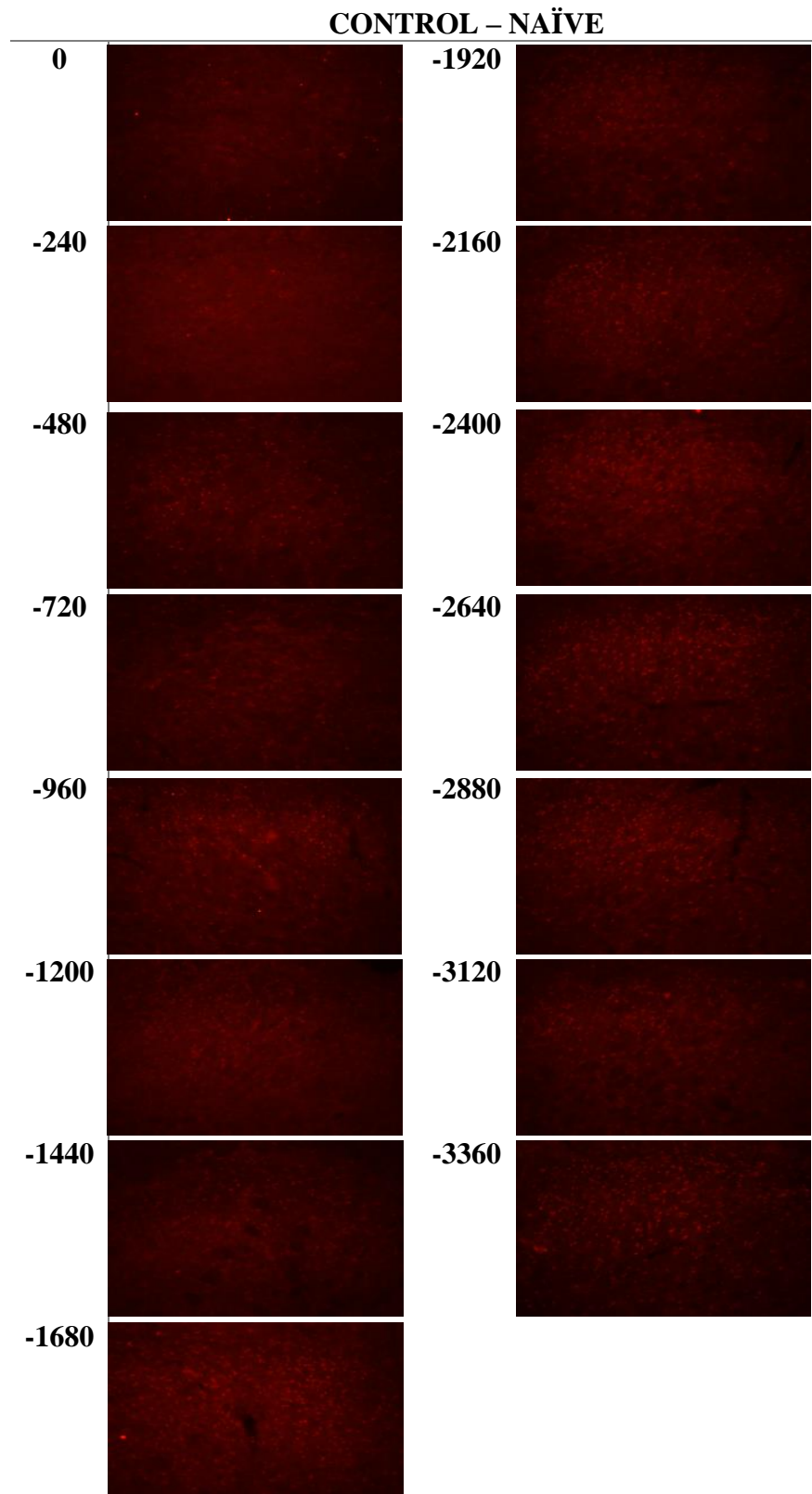


Figure 5.18. ChemR23 in the control naïve group. Showing representative ChemR23 expression from obex ($0 \mu\text{m}$) to $1680 \mu\text{m}$ caudal to obex (on the left) and from 1920 to $3360 \mu\text{m}$ caudal to obex (on the right). Distances from obex in μm .

5.3.2.1. ChemR23 expression in the trigeminal nucleus caudalis on day 3 following lingual nerve injury

ChemR23 expression in the Vc was analysed on day 3 post-injury. The positive area of ChemR23 staining was quantified in the Vc between obex (0 μm) and 3360 μm caudal to obex in both ipsilateral and contralateral sides in the CCI group (figure 5.19-A) and in the Sham group (figure 5.19-B). Similar to the analysis conducted to quantify Iba1 expression in Chapter 4, the ratio increase in the ipsilateral over the contralateral side was calculated for each level of the Vc (figure 5.19-C). There was a statistically significant difference in ChemR23 expression between groups ($F(2, 7)=46.46, p<0.0001$; Two-way ANOVA repeated measures). The ratio of ChemR23 staining over contralateral side was statistically significantly different in the CCI group when compared to the control (naïve) group between 240 to 960 μm and 1440 μm caudal to obex (240 μm : $p=0.006$; 480: $p=0.04$; 720 μm $p=0.02$; 960 μm $p<0.0001$; 1440 μm $p<0.0001$, Tukey's *post hoc* test). When comparing the CCI group with the Sham group statistical differences were found at 960 and 1440 μm caudal to obex (960 μm $p=0.05$; 1440 μm $p<0.0001$; Tukey's *post hoc* test).

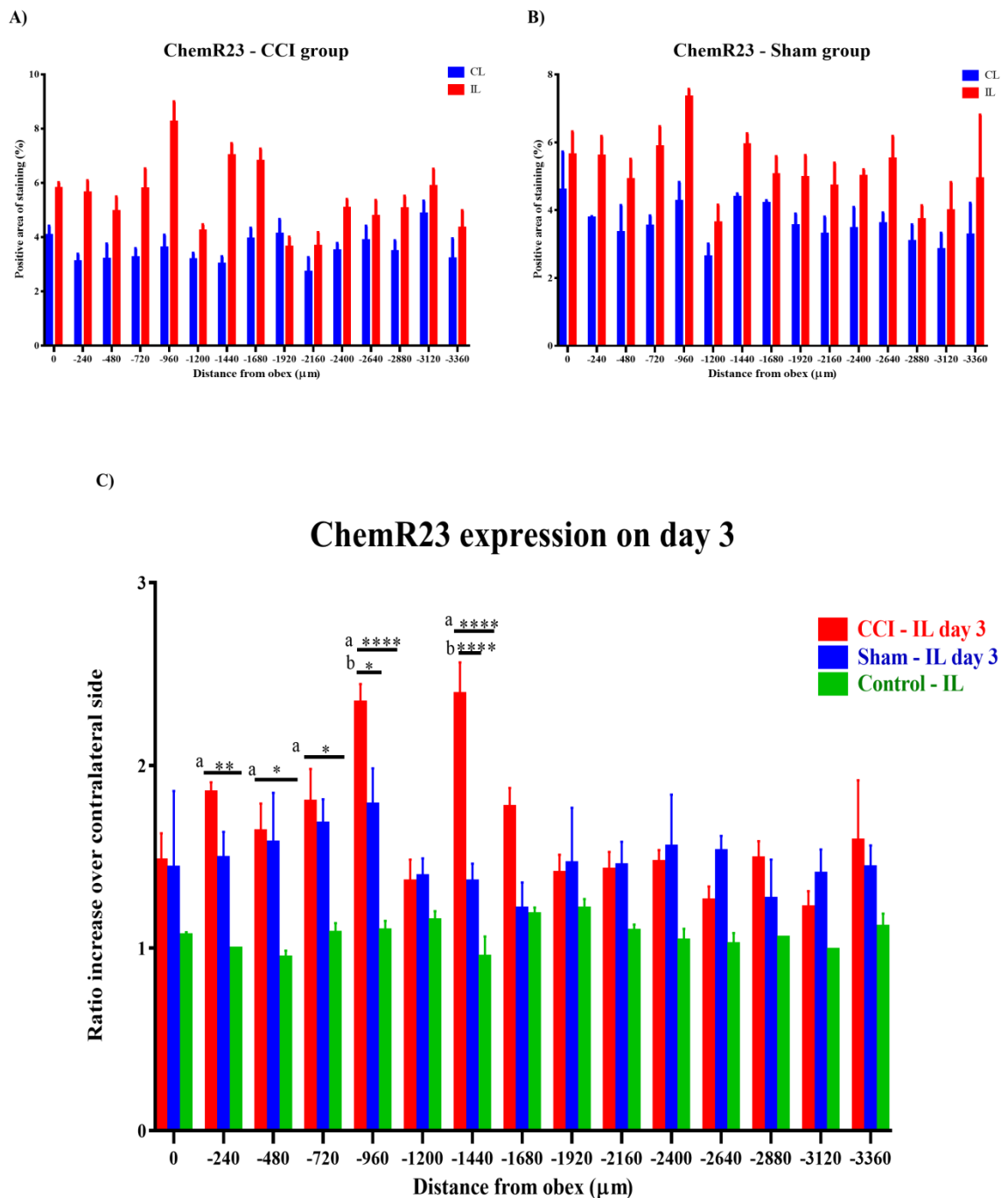


Figure 5.19. ChemR23 expression on day 3 following lingual nerve injury. A) Percentage of positive area of ChemR23 staining in the CCI group (n=5). B) Percentage of positive area of ChemR23 staining in the Sham group (n=3). C) Ipsilateral ratio increase over contralateral side: ChemR23 expression was higher in the CCI group between 240 to 720 μm caudal to obex (CCI vs Control) and 960 μm and 1440 μm caudal to obex (CCI vs Sham vs Control). Asterisks represent statistical significance. * $p < 0.05$, ** $p < 0.01$, **** $p < 0.0001$. a-CCI vs control, b-CCI vs Sham. Two-way ANOVA repeated measures followed by Tukey's *post hoc* test.

5.3.2.2. ChemR23 expression in the trigeminal nucleus caudalis on day 7 following lingual nerve injury

ChemR23 immunoreactivity was also quantified (PAS %) on day 7 in both the ipsilateral and contralateral side of CCI (figure 5.20-A) and Sham (figure 5.20-B) groups. Statistical analysis was performed using the ratio increase in the ipsilateral side over the contralateral at each level of the trigeminal nucleus (figure 5.20-C).

ChemR23 was differentially expressed between CCI and Sham groups and between CCI and Control groups ($F(2, 5)=7.065$, $p=0.04$, Two-way repeated measures ANOVA). Specific differences were found at 720 μm (CCI vs Control $p=0.008$, Tukey's *post hoc* test) and 960 μm (CCI vs Sham $p=0.0007$ and CCI vs Control $p<0.0001$; Tukey's *post hoc* test) caudal to obex.

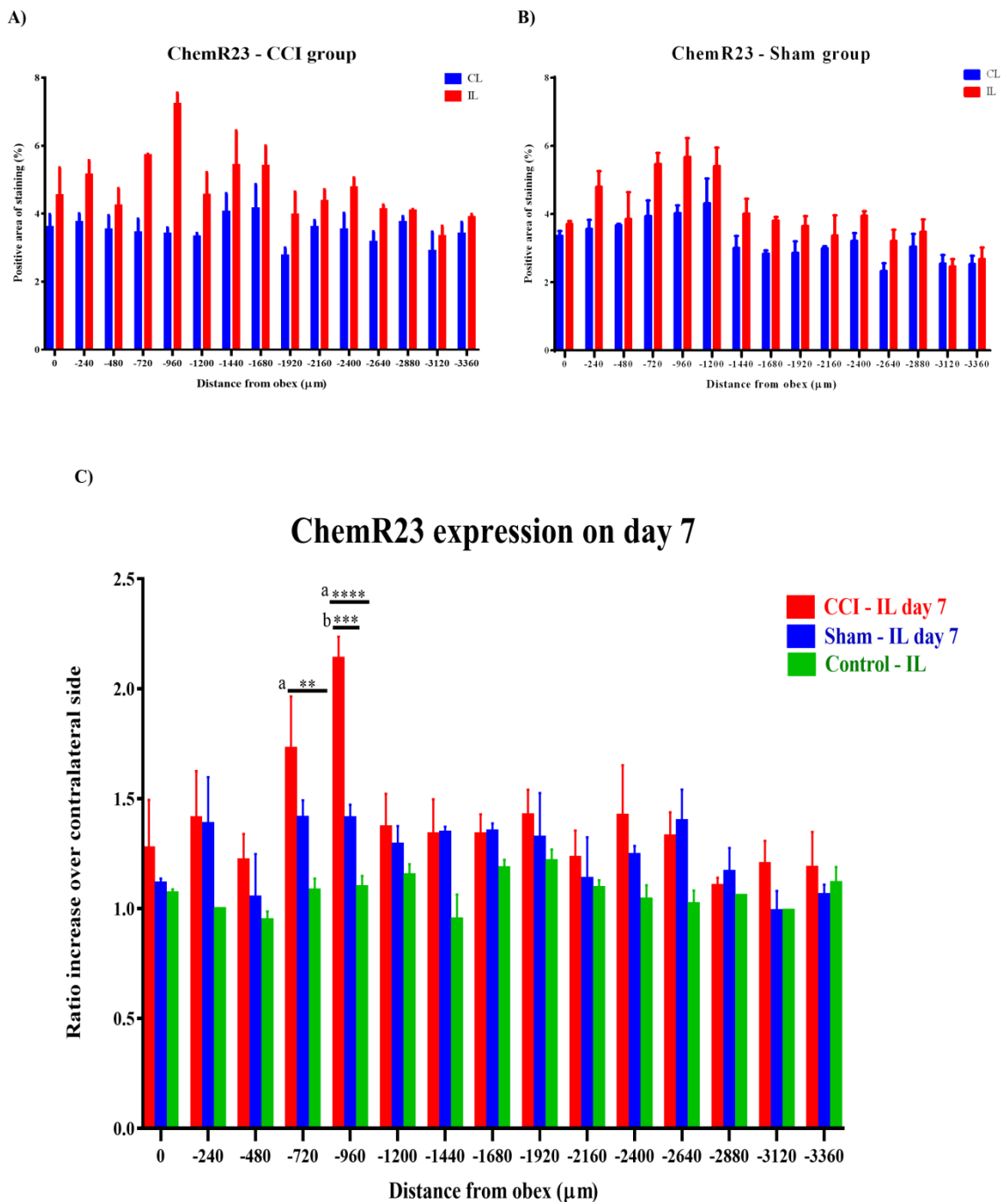


Figure 5.20. ChemR23 expression on day 7 following lingual nerve injury. A) Graph represents the percentage of positive area of ChemR23 labelling in the CCI group (n=3). B) Graph represents the percentage of positive area of ChemR23 labelling in the Sham group (n=3). D) Graphical representation of ipsilateral ratio increase over contralateral side: ChemR23 expression was higher in the CCI group between at 960 μm caudal to obex (CCI vs Sham vs Control). Asterisks represent statistical significance. *** $p < 0.001$, **** $p < 0.0001$. Two-way ANOVA repeated measures followed by Tukey's *post hoc* test.

5.3.2.3. ChemR23 expression in the trigeminal nucleus caudalis on day 28 following lingual nerve injury

ChemR23 labelling on day 28 post-injury was also measured. The positive area of ChemR23 labelling was measured in both ipsilateral and contralateral side of sham and CCI groups (figure 5.21-A, B). The ratio increase in the ipsilateral over the contralateral side for each level of the trigeminal nucleus was calculated and used for statistical analysis between groups (figure 5.21-C).

On day 28, there was a statistically significant difference in ChemR23 expression in the ipsilateral side between the three groups ($F(2, 7)=23.43, p=0.0008$; Two-way ANOVA repeated measures). Differences in ChemR23 expression between groups were found at 480 and 720 μm caudal to obex (CCI vs Control, 480 μm $p=0.008$, 720 μm $p=0.02$, Tukey's *post hoc* test) and at 960 μm caudal to obex (CCI vs Sham $p=0.002$ CCI vs Control $p=0.001$; Tukey's *post hoc* test).

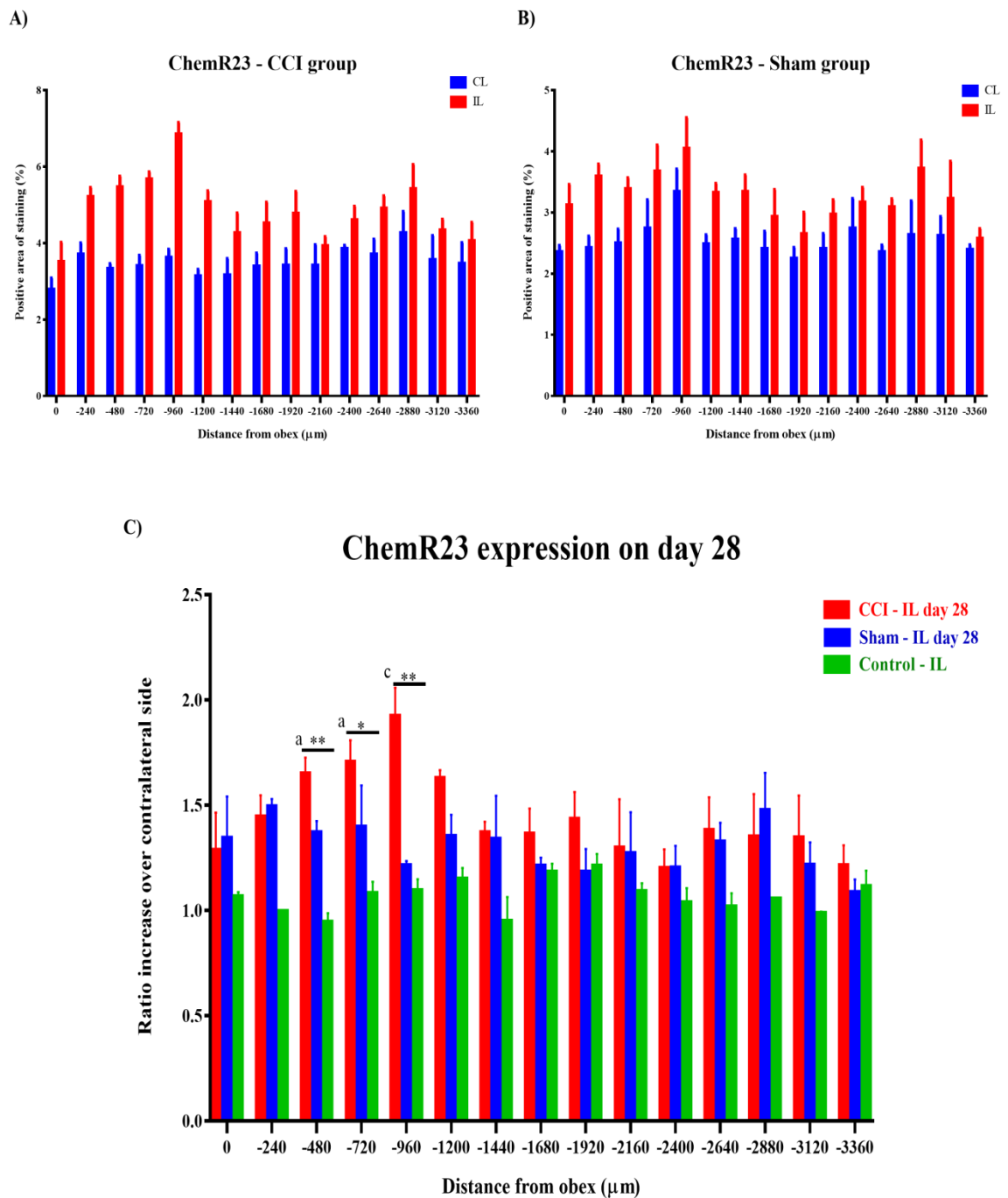


Figure 5.21. ChemR23 expression on day 28 following lingual nerve injury. A) Percentage of positive area of ChemR23 staining in the CCI group (n=5) in contralateral and ipsilateral side. B) Percentage of positive area of ChemR23 staining in the Sham group (n=3). D) Ipsilateral ratio increase over contralateral side: ChemR23 expression was higher in the CCI group between 480 and 720 μm caudal to obex (CCI vs Control) and at 960 μm caudal to obex (CCI vs Sham vs Control). Asterisks represent statistical significance. * $p < 0.05$, ** $p < 0.01$. Two-way ANOVA repeated measures followed by Tukey's *post hoc* test.

5.3.2.4. Comparison of ChemR23 expression over time

When comparing ChemR23 expression in the ipsilateral side of the CCI (injured) group between the time-points analysed it was possible to observe statistical significant differences ($F(3, 11)=23.33, p<0.0001$; Two-way ANOVA repeated measures). Specific rostral-caudal levels of the Vc where statistically significant differences were found between groups are reported on table 5.1. ChemR23 expression in the ipsilateral side of Vc at 960 μm caudal to obex was increased on day 3 and maintained up to day 28. No statistical differences were found between days 3, 7 and 28; however, ChemR23 expression was statistically significantly different when comparing days 3, 7 and 28 to the control group at this rostral-caudal level (figure 5.22). At 1440 μm caudal to obex, ChemR23 expression in the ipsilateral side of the CCI group on day 3 post-injury was statistically different from days 7, 28 and control (naïve) animals.

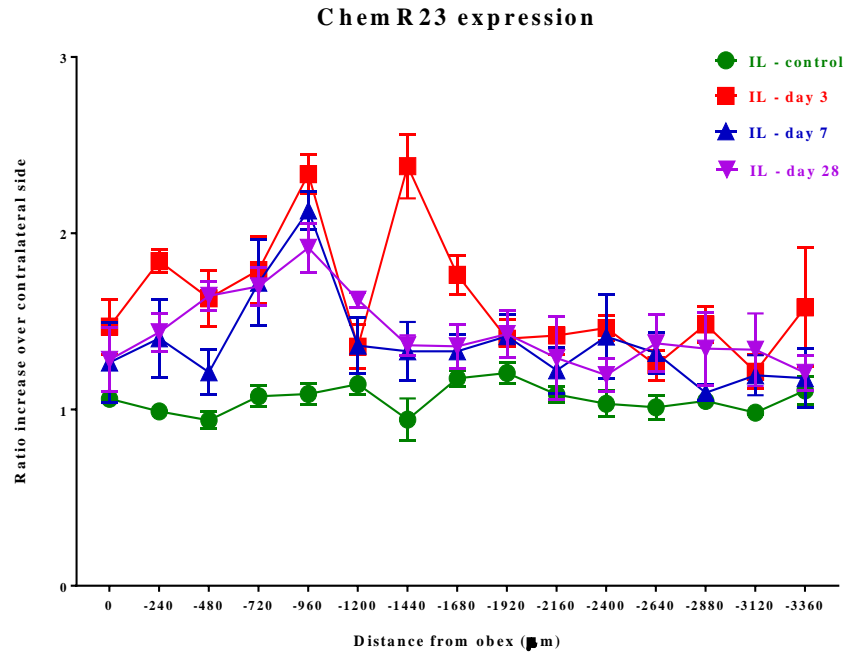


Figure 5.22. Comparison of ChemR23 expression at different time points. Statistical differences are described in table 5.1.

Table 5.1. Statistical differences between time-points.

Distance from obex in the Vc	Groups	Adjusted <i>p</i> -value*
240 µm	IL - control vs. IL - day 3	<i>p</i> =0.006
480 µm	IL - control vs. IL - day 3	<i>p</i> =0.04
	IL - control vs. IL - day 28	<i>p</i> =0.03
720 µm	IL - control vs. IL - day 3	<i>p</i> =0.03
960 µm	IL - control vs. IL - day 3	<i>p</i> <0.0001
	IL - control vs. IL - day 7	<i>p</i> =0.001
	IL - control vs. IL - day 28	<i>p</i> =0.008
1440 µm	IL - control vs. IL - day 3	<i>p</i> <0.0001
	IL - day 3 vs. IL - day 7	<i>p</i> <0.0001
	IL - day 3 vs. IL - day 28	<i>p</i> <0.0001

*Two-way ANOVA repeated measures with Tukey's *post hoc* corrections.

5.4. Discussion

Expression of resolvin receptors

Data from this study indicate that GPR32 and BLT1 are expressed in nerve fibres and Schwann cells in human lingual nerve neuroma, and that FPR2/ALX and ChemR23 are expressed in rat brainstem and spinal cord dorsal horn neurones.

GPR32

GPR32, previously an orphan receptor, is known to mediate RvD1 actions on human macrophages (Krishnamoorthy et al., 2010). The majority of studies on this receptor have been conducted in inflammatory conditions and, thus, immune cells such as macrophages are known to express GPR32 (Schmid et al., 2016, Krishnamoorthy et al., 2010). Using an antibody against human GPR32, it was detected the expression of GPR32 in a human lingual nerve neuroma, in nerve fibres and in Schwann cells. This result needs to be further investigated, in terms of the functional relevance of GPR32; based on studies that suggest that RvD1 (Krishnamoorthy et al., 2010) and RvD3 (Dalli et al., 2013) act through GPR32 to induce an anti-inflammatory environment, the expression of GPR32 specifically in Schwann cells may contribute to nerve regeneration. Because the orthologue in rodents to the human GPR32 has not been identified, studies with GPR32 knock-out mice have not been conducted and the functional role in an *in vivo* model has not been characterised.

BLT1

This receptor is known to be expressed in leukocytes, endothelial cells and vascular smooth muscle (Bäck et al., 2014, Qiu et al., 2006). Within the nervous system, BLT1 has been found to be expressed in rat and mouse DRG: one study has found BLT1 expressed in TRPV1 positive DRG neurones in mice (Andoh and Kuraishi, 2005) and, another study, in non-neuronal cells (not specified) in the rat DRG (Okubo et al., 2010). In the present study, BLT1 was found to be expressed in nerve fibres and in Schwann cells in human lingual nerve neuroma. The change in expression of receptors and neuropeptide release in nerve fibres after injury has been reported and further studies are required to investigate whether BLT1 is differentially expressed between painful and non-painful human neuromas and to characterise its functional role. Schwann cells are actively involved in the regeneration of injured nerve fibres, as previously mentioned. Even

though they are mainly known for over-expressing neurotrophic factors after nerve injury (Steed, 2011), it could be possible that they express BLT1 in response to nerve regeneration.

BLT1 is activated by leukotriene B4 (LTB4) and functions as chemoattractant for neutrophils during an inflammatory response (Arita et al., 2007). BLT1 knockout mice had reduced pain behaviours to formalin injection, suggesting that BLT1 can contribute to both peripheral inflammation and neuronal excitability in the spinal cord (Asahara et al., 2015). However, when RvE1 binds to BLT1, it inhibits LTB4 binding and also prevents LTB4 actions (Arita et al., 2007). BLT1 expression in human lingual nerve neuroma needs, as mentioned above, further studies in order to identify its functional role following peripheral nerve injury. Based on the evidence of RvE1 (partial agonist of BLT1) actions of anti-inflammatory and analgesic (Arita et al., 2007, Asahara et al., 2015), BLT1 may be a potential candidate as target for the treatment of nerve injury and neuropathic pain.

FPR2/ALX

FPR2/ALX is known to be expressed in neutrophils, monocytes, macrophages, immature dendritic cells and T cells (Maddox et al., 1997). Only recently, the expression profile of this receptor started to be reported in the nervous system. This receptor was observed in astrocytes in the spinal cord (Abdelmoaty et al., 2013) and in satellite glial cells and neurones in the DRG (Pei et al., 2011). The study in this chapter has detected FPR2/ALX expression in neurones within the dorsal horn in the spinal cord and in the trigeminal nucleus in the brainstem. Divergent results from the literature were obtained regarding the co-localisation of FPR2/ALX with the astrocyte marker GFAP. Even though, the same experimental conditions were used, the results from Abdelmoaty et al. (2013) were not reproduced. In order to test for antibody specificity, the antibody against FPR2/ALX was pre-absorbed with the respective blocking peptide and no positive staining was observed suggesting that the antibody was specific. More recently, a study in brain tissues derived from patients with Alzheimer's disease has shown that FPR2/ALX is expressed in neurones, microglia and astrocytes in hippocampus (Wang et al., 2015). This receptor and GPCR in general are known for the capacity to form heterodimers with other members of the GPCR family (Krishnamoorthy et al., 2010). In fact, Cooray et al. (2013) demonstrated that FPR2/ALX dimers with the FPR1 (formyl

peptide receptor 1) in order to activate specific intracellular signalling. In future studies it will be required to investigate whether this capacity to form heterodimers is present and if it can affect antibody specificity (that could eventually clarify the divergent results). FPR2/ALX mediates the actions of RvD1 and similarly to the other resolvin receptors can have a potential role in pain-associated diseases. In a model of osteoarthritis pain it was found that FPR2/ALX expression was not altered in a monosodium iodoacetate-induced osteoarthritis pain model when compared to saline-treated rats (Huang et al., 2017); however, it was found, at each point analysed (days 14 and 35), a positive correlation between the expression of FPR2/ALX and IL-1 β , TNF and COX-2 in the synovium, which are markers of inflammation. The administration of resolvin precursor of the D series resolvins reversed the pain behaviour in this model of osteoarthritis (Huang et al., 2017). However, it was not confirmed whether the effects were conducted specifically through FPR2/ALX modulation. As mentioned in the literature review (section 1.2.2 in Chapter 1), it seems that FPR2/ALX responds only to high concentrations of its agonist (Norling et al., 2012) and in Huang's study it was not reported whether the administration of the D series precursor led to increase in the expression of FPR2/ALX (even though they report the increase of RvD2 plasma levels following administration of the precursor). Therefore, the expression pattern of FPR2/ALX and potential functional role needs to be further studied in other models of chronic pain, for instance neuropathic pain, and its response to injury and/or agonist administration needs to be reported in order to clarify what may cause any differences observed.

ChemR23

Similarly to the other resolvin receptors, ChemR23 has also been better characterised in inflammatory conditions (Arita et al., 2007). To date, few studies have shown the expression of ChemR23 in the nervous system using immunohistochemistry. Xu et al. (2010) have demonstrated the expression of ChemR23 in DRG and spinal cord dorsal horn neurones. In the present study, the expression of ChemR23 was detected in spinal cord dorsal horn and in brainstem neurones, which is line with the study mentioned above (Xu et al., 2013).

ChemR23 is also known to be expressed in leukocytes cells such as macrophages (Zabel et al., 2006, Arita et al., 2005a), natural killer (NK) cells (Parolini et al., 2007) and

dendritic cells (Vermi et al., 2005). Connor et al. (2007) have demonstrated the expression of ChemR23 in a subset of microglia (colony-1-receptor-positive) that is close to retinal blood vessels. In addition, it was shown that RvE1 (ChemR23 ligand) attenuates neuropathic pain via microglia inhibition (Xu et al., 2013). However, in the pain model used in this study it was not possible to detect co-localisation of ChemR23 with the microglial marker, Iba1. It was, however, possible to observe that activated microglial cells surrounded ChemR23 expressing cells (figure 5.15).

As described in the literature review (section 1.1 in chapter 1), primary afferents carrying pain information from the body terminate in the spinal cord and from the orofacial area in the trigeminal nucleus (Vc) of the brainstem, where they synapse with second-order neurones and further transmit pain sensations to the brain. Therefore, these specific areas of the spinal cord and brainstem play an important role in pain processing and undergo changes after nerve injury and inflammation that may contribute to the exaggerated pain sensation (Todd, 2010). Thus, the expression of ChemR23 herein reported together with the analgesic actions of RvE1 (ChemR23 ligand) reported by Xu et al. (2010) may show an opportunity to novel targets for chronic pain. In fact, it was observed an apparent difference in immunoreactivity against ChemR23 antibody in the Vc of the brainstem between injured and non-injured animals. Therefore, quantification of ChemR23 expression in the Vc was conducted in a model of LNI at day 3, 7 and 28 post-injury. ChemR23 staining was higher at day 3 post-injury in specific parts of the Vc, especially when compared to the control (naïve) group. This is not surprising given the known role of ChemR23 in inflammatory conditions and the sham-operation can induce some inflammatory response. ChemR23 immunoreactivity was found to be increased in the CCI group up to day 28 compared to control. Even though, ChemR23 did not seem to be expressed in microglial cells, the highest immunoreactivity was found in the area surrounding microglia activation and, consequently, that area was chosen for data analysis. ChemR23 gene has been found to be differentially expressed in spinal cord dorsal horn between rat carrageen model of osteoarthritis and control (Meesawatsom et al., 2016). Additionally, Parkitna et al. (2006) detected the expression of ChemR23 gene in a microarray screening assay of the rat spinal cord dorsal horn and found that ChemR23 gene was up-regulated in the injured group (chronic constriction injury of the sciatic nerve) at days 3 and 14 when compared to the control groups. In that study, ChemR23 gene was not detected in DRG samples (Parkitna et al., 2006). ChemR23 was also found to be

highly expressed in tissues from patients with periodontitis, compared to healthy tissues, in particular in inflammatory cells (Özcan et al., 2017). The authors have suggested that this may be due to the chemoattractant effect of one of ChemR23 agonists chemerin, which was also increased in tissues from patients with periodontitis and may have recruited more immune cells that express ChemR23. It has also been suggested that increased levels of ChemR23 can be due to low levels of resolvins (compensatory effect) (Wang et al., 2015) which potentiates the binding of pro-inflammatory molecules. However, this still remains to be demonstrated.

ChemR23 has two known ligands: chemerin and RvE1. While chemerin is a chemoattractant, RvE1, in turn, induces resolution of inflammation by inducing the phagocytosis of apoptotic neutrophils by macrophages (Herová et al., 2015, Arita et al., 2007). While chemerin binding seems to have a pro-inflammatory effect (for instance, ChemR23 knock-out mice have less inflammatory cells at the site of inflammation and less inflammation (Demoor et al., 2011)), the binding of RvE1 activates human macrophages towards an anti-inflammatory pathway (Herová et al., 2015). In pain models, RvE1 has been suggested to inhibit the activation of TRPV1 by targeting substance P (SP) in peripheral sensory neurones (Jo et al., 2016) and in the DRG (Xu et al., 2010). RvE1 prevented TNF- α induced microglial activation in a model of neuropathic pain (Xu et al., 2013). Therefore, ChemR23 expression following LNI may provide a relevant target for neuropathic pain based on RvE1 actions.

Methodological approach

The use of immunohistochemistry in this study allowed the identification of resolvin receptors in the nervous system, and the use of blocking peptides (or incubation with the secondary antibody alone) permitted to test the specificity of the antibodies used. In addition, it was possible to identify the specific cells expressing the receptors of interest.

Quantification studies conducted for ChemR23 expression followed a very similar approach to that described regarding Iba1 expression in chapter 4. In fact, all images were taken and analysed choosing the same area of interest as that chosen for Iba1 quantification and care was taken to minimise technical variations. Statistical analysis was also conducted using the ratio increase in the ipsilateral over the contralateral side to account for animal individual variations differences in background staining. ChemR23 was analysed over multiple rostral-caudal levels of the Vc and, thus, a two-ANOVA

repeated measures was selected followed by Tukey's *post hoc* corrections (when ANOVA found to be statistically significant, $p \leq 0.05$).

Limitations of study

The immunohistochemical studies were limited to the tissues available in the lab and to the specificity of the antibodies used; therefore extended studies are required in order to characterise in other nervous system tissues.

The pilot studies presented in this chapter indicate for the first time the expression of resolvin receptors GPR32 and BLT1 in human lingual nerve neuromas but further work needs to be done to determine whether there is any correlation with the presence of clinical pain. Additionally, the antibodies against GPR32 and BLT1 do not have a blocking peptide available.

Conclusion and future work

In summary, by using immunohistochemistry it was possible to identify ChemR23 in spinal cord and brainstem neurones and, for the first time, ChemR23 expression was quantified in the Vc following LNI. In this study, FPR2/ALX was found to be expressed in neurones but not in astrocytes in the dorsal horn and Vc, and both GPR32 and BLT1 were expressed in nerve fibres and Schwann cells in human lingual nerve neuroma. These receptors are known to be activated by resolvins, which has been shown to attenuate pain symptoms in different models of pain (Ji et al., 2011). The results herein reported provide an insight into the expression of these receptors in the nervous system and create opportunity for further studies into the functional relevance of resolvins and its analogues in the reduction of pain symptoms. Resolvins are endogenous lipid mediators with anti-inflammatory and analgesic properties but degrade rapidly; a better understanding of the expression profile of their receptors and in which specific cells are expressed can contribute to improved drug design and therapeutics. However, it is also required to better characterise their mechanisms of action. In a future study it would be necessary to investigate the functional role of these receptors, in particular ChemR23, when administering resolvin molecules or analogues. In addition, it would be of interest to quantify the levels of endogenous resolvins following injury and to verify whether there is any correlation with expression of the receptors.

CHAPTER 6
MICRORNA EXPRESSION FOLLOWING
LINGUAL NERVE INJURY

6.1. Introduction

MicroRNAs (miRNAs) are capable of regulating cellular processes such as immune and inflammatory responses (Sayed and Abdellatif, 2011, Lim et al., 2005). They are small noncoding RNAs that suppress the expression of multiple genes, by interacting with the 3' untranslated region (UTR) of the messenger RNAs (mRNAs) (Lee et al., 1993). Pain, and specifically chronic pain, are characterised by the alteration in the expression and function of receptors and mediators (Sakai and Suzuki, 2014, Kusuda et al., 2011). These changes can lead to the hyper-excitability of nociceptors that generate action potentials to sub-threshold stimuli or in the absence of any detectable stimulus and contribute to the transmission of a continuous signal that can be further intensified in central terminals. This is a highly complex and regulated process and given the evidence that miRNAs can regulate gene expression, it was hypothesised that miRNAs can target relevant genes in the subsequent events post-nerve injury and, therefore, contribute to the changes in gene expression that occur in the peripheral nervous system following injury that lead to neuropathic pain.

The overall aim of this study was to investigate the expression of miRNAs following lingual nerve injury (LNI) and identify potential targets and pathways relevant in the context of nerve injury and chronic neuropathic pain. The specific objectives were:

1. Identify specific miRNAs differentially expressed in rat tissue and human lingual nerve tissue following LNI;
2. Identify target genes under the control of the specific miRNAs identified, using predictive algorithms such as TargetScan;
3. Identify pathways co-regulated by the identified targets and that may contribute to the development and maintenance of chronic pain, using MetaCore.
4. Examine whether any correlation exist between the expression of miRNAs and the feeding behaviour in the rat or the presence of clinical pain symptoms in human lingual nerve neuromas.

6.2. Methodological approach

Full details of the methods used are described in sections 2.6 to 2.8 in chapter 2. Briefly, human lingual nerve neuromas (n=12) and a pre-clinical rat model (n=6) were used (figure 6.1). The human tissues were obtained from an archive of lingual nerve neuromas collected from patients with LNI at Charles Clifford Dental Hospital in

Sheffield UK and were divided into painful (n=6) and non-painful (n=6) based on the pain VAS (visual analogue scale) score conducted by the clinician prior to nerve repair surgery. Rat lingual nerve and trigeminal ganglion tissues were collected three days after chronic constriction injury of the lingual nerve (CCI group) or sham-operation (Sham group). Following RNA extraction, all samples were examined with TaqMan® low density array (TLDA) cards and the results were, first normalised to the endogenous control (snrnaU6), and then analysed with statistical measures (for full details see section 2.8.4 in chapter 2). Specific miRNAs were validated with RT-qPCR using respective Taqman® probes and any correlation with behavioural data (rat samples) or clinical (human samples) was examined. Of note, for validation the same rat lingual nerve samples were used (so it could be correlated with behavioural data); in the human miRNA, validation was conducted with 11 samples used in miRNA TLDA screening with additional 5 other samples (please see table 6.2 in section 6.1.2.1)

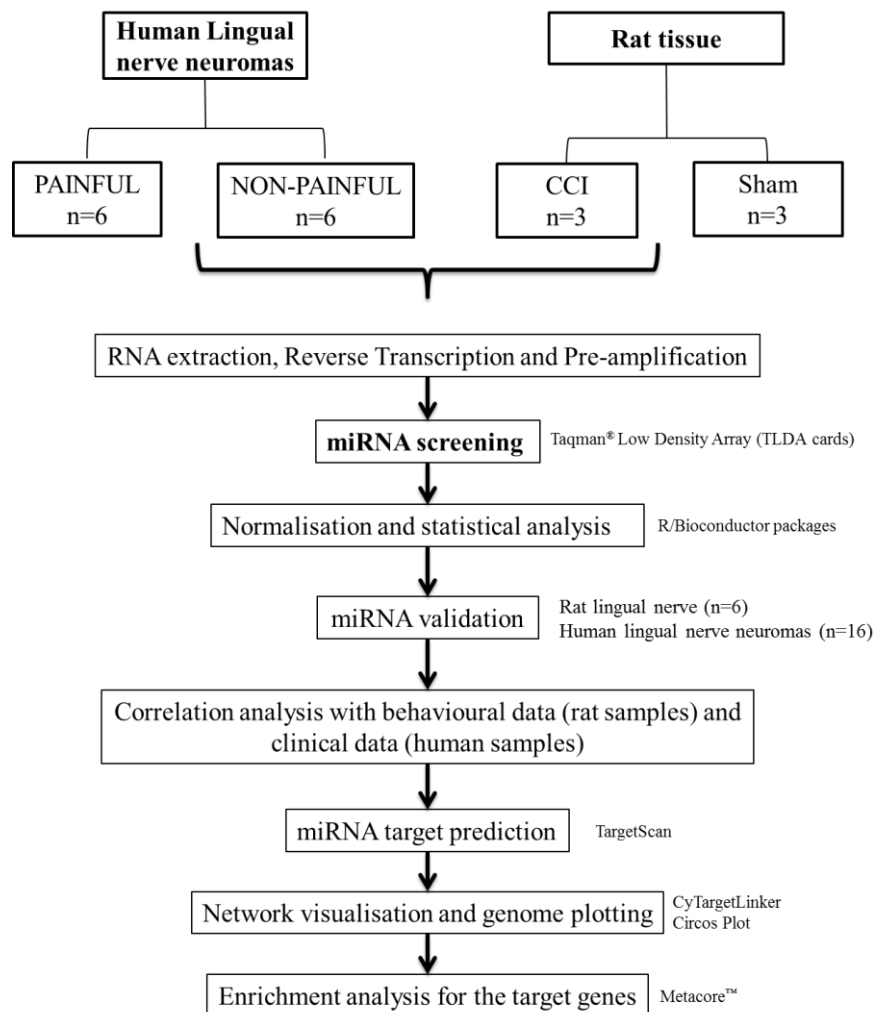


Figure 6.1. Diagram of the methodological approach.

Next, an *in silico* approach was adopted using bioinformatics tools: target genes were predicted using publicly available algorithms and networks and genome plots were created to visualise the interaction between miRNA and target genes. Lastly, gene enrichment analysis was conducted to identify relevant pathways potentially co-regulated by the predicted target genes under the control of the miRNAs of interest previously identified.

6.3. Results

6.3.1. miRNAs in rat tissues

The expression of miRNA was investigated in the lingual nerve (ipsilateral to injury or sham-operation) and respective ipsilateral trigeminal ganglion. Using the TLDA cards multiple miRNAs were screened and, within trigeminal ganglion samples, no statistically significant miRNAs were found between groups. In the rat lingual nerve, ten miRNAs were found to be significantly differentially expressed on day 3 post-injury, compared to the sham group (table 6.1) in the TLDA screening study.

Table 6.1. MiRNAs differentially expressed in the rat lingual nerve.

miRNA	$\Delta\Delta C_t$	Product Sum	Rank	Corrected <i>p</i> -value	Nominal <i>p</i> -value
mmu-miR-1951	12.22	1.1665		<i>p</i> <0.001	<i>p</i> <0.001
mmu-miR-1904	8.5	2.6207		<i>p</i> <0.001	<i>p</i> <0.001
mmu-miR-1982.2	8.99	4.5062		<i>p</i> <0.001	<i>p</i> <0.001
mmu-miR-694	5.08	8.6177		0.0200	<i>p</i> <0.001
mmu-miR-880	4.57	10.2436		0.0420	<i>p</i> <0.001
mmu-miR-1969	4.45	10.9349		0.0400	<i>p</i> <0.001
mmu-miR-763	4.17	12.1225		0.0457	<i>p</i> <0.001
mmu-miR-1957	-10.04	4.8553		0.03	<i>p</i> <0.001
rno-miR-138	-9.12	6.9537		0.02	<i>p</i> <0.001
rno-miR-667	8.55	3.452		<i>p</i> <0.001	<i>p</i> <0.001

Two of those miRNAs were selected for further analysis: rno-miR-138 (up-regulated) and rno-miR-667 (down-regulated). The TLDA card for rodent sample analysis, included miRNAs for both rat and mouse and these two miRNAs were selected because they were reported in miRBase database as being present in the rat genome (please see section 6.3.1.2. for further details).

The same samples were used for miRNA validation. In the validation study, only miR-138 was found to be differentially expressed (figure 6.2). However, it was found a correlation between the normalised deltaCt and the time drinking reward in the behavioural testing (based on the study reported in chapter 3) conducted at day 3 post-injury or sham-operation. The sample size needs to be taken into account when analysing this data.

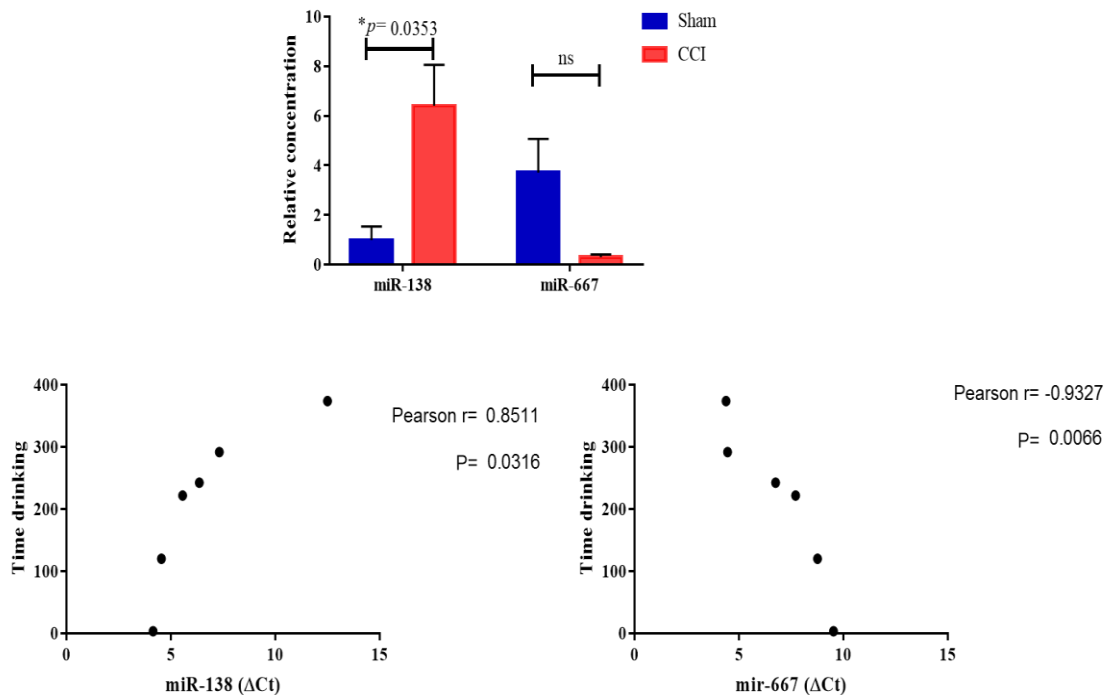


Figure 6.2. miRNA validation and correlation scatter plots. miR-138 was confirmed to be statistically significantly differentially expressed between sham and CCI group. MiR-667 was not statistically differentially expressed in the miRNA validation study (unpaired t-test). Pearson correlations showed a correlation between the expression of miR-138 and miR-667 with the time drinking on day 3 after CCI or sham-operation. miRNAs values represent normalised delta Ct values (ΔCt , the higher the Ct value, lower the expression of the miRNA). ns: not significant.

6.3.1.1. miRNA target prediction and gene enrichment analysis

Publicly available databases were used to look for predicted target genes of the identified miRNAs. Targetscan, MicroCosm and miRTarBase included in the CyTargetLinker app of Cytoscape were used to build a miRNA-target gene network (figure 6.2). Both miRNAs had common target genes and for the purpose of visualisation a search in gene database (<https://www.ncbi.nlm.nih.gov/gene>) was conducted for the term ‘pain gene’ and those (for instance, *trpv1*) are highlighted in red. The total of the

genes found with CytargerLinker were cross-referenced with only TargetScan targets when a cut-off of -0.4 was applied in the cumulative weighted context++ scores. (Nam et al., 2014, Agarwal et al., 2015). For rno-miR-138, a total of 119 target genes and for rno-miR-667 a total of 91 target genes passed this TargetScan cut-off selected, and were used for further analysis. The graphical display shows the interaction of miRNAs and target genes and demonstrates common predicted targets (figure 6.3 to 6.5).

Of note, it was decided to include mirR-667 in the target prediction and bioinformatics analysis based on the correlation with behavioural data and this will be further discussed in the disucssion in section 6.4.

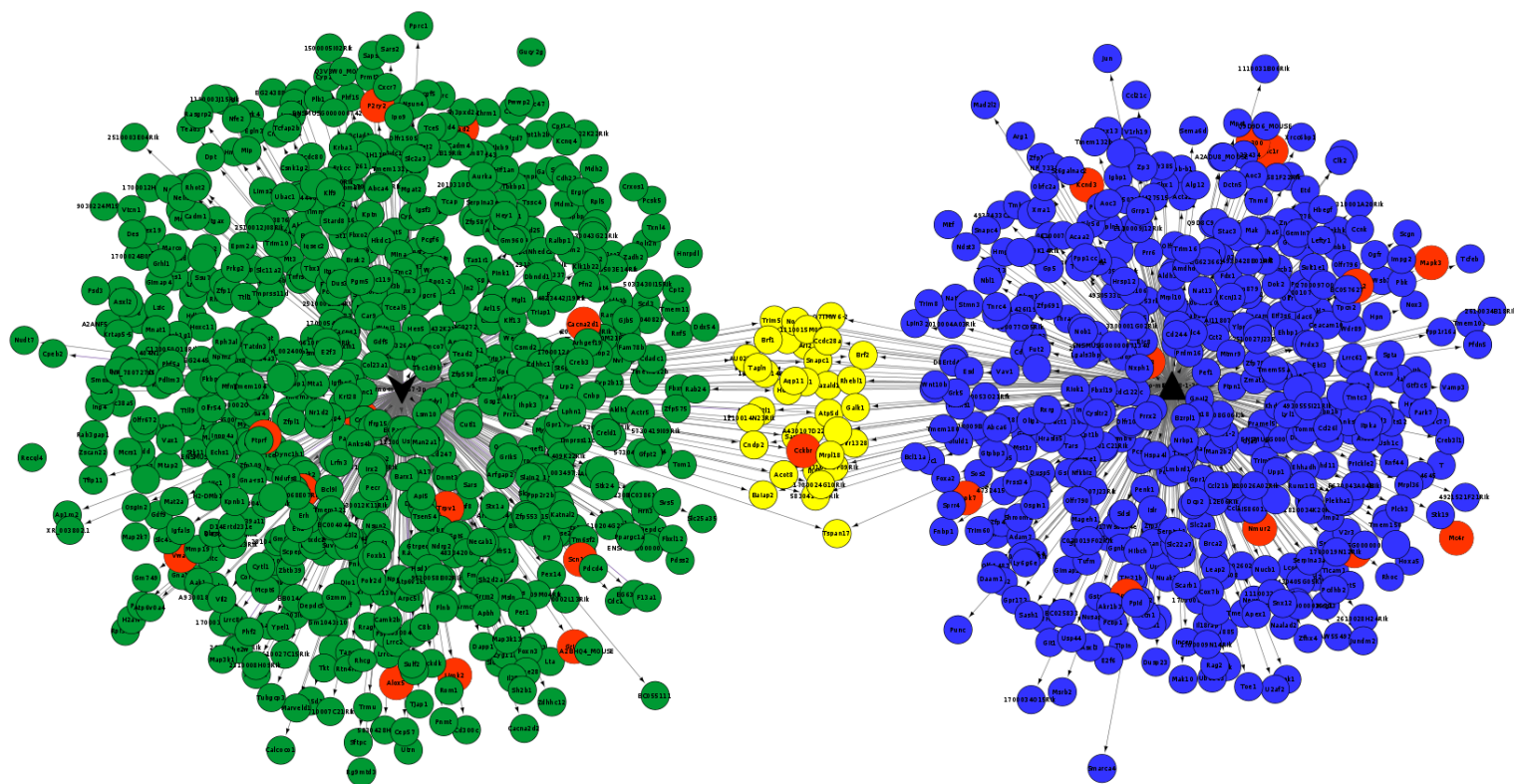


Figure 6.3. CyTargetLinker analysis and network visualisation of differentially expressed rat miRNAs and their predicted target genes. Nodes coloured in green are targets of rno-miR-667 and nodes coloured in blue are targets of rno-miR-138. The nodes coloured in yellow are targets of both rno-miR-138 and rno-miR-667, while nodes in red are examples of genes known to have a role in pain. This network was constructed and visualised using CyTargetLinker v3.0.1 and Cytoscape v3.4.0. There is no relation between the position of the nodes and the score of the target prediction.

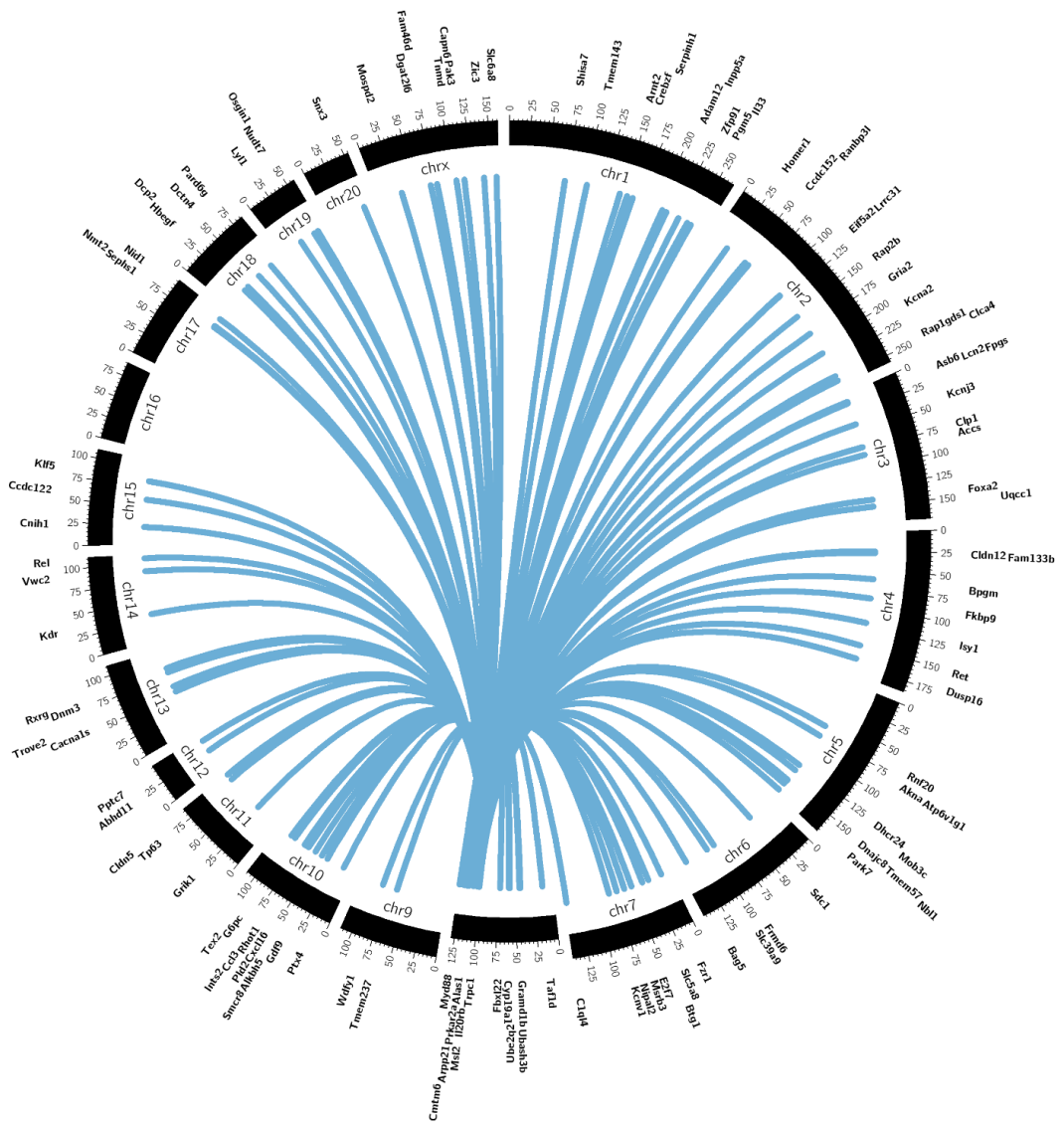


Figure 6.4. Circos v0.67 plot of rno-miR-138-1 and its target genes. The middle track represents the rat genome with each ideogram segment representing one chromosome. The outermost and inner tracks display the gene name and spatial location of each gene targeted by the miRNA. The gene for miR-138-1 is located in chromosome 8.

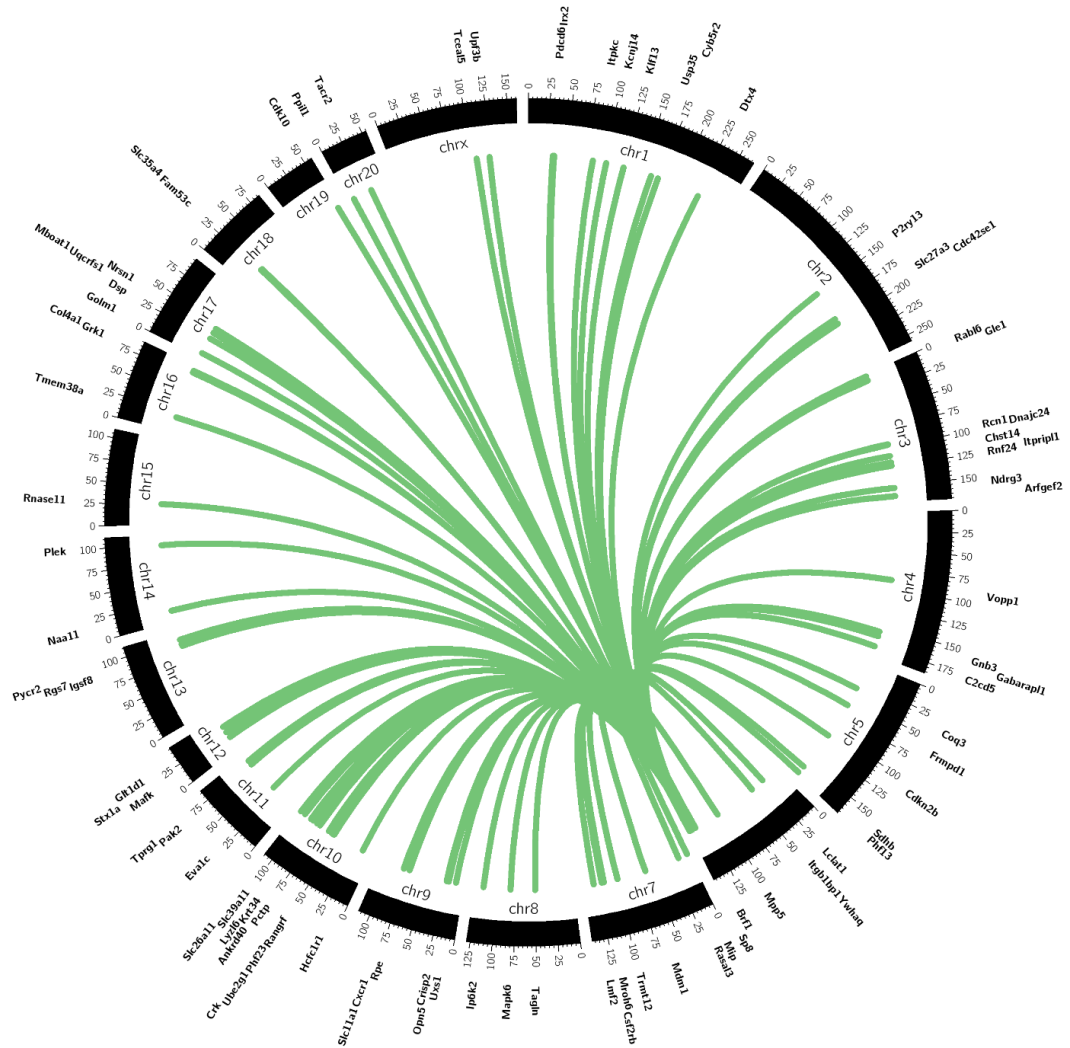


Figure 6.5. Circos v0.67 plot of rno-miR-667 and its target genes. The middle track represents the rat genome with each ideogram segment representing one chromosome. The outermost and inner tracks display the gene name and spatial location of each gene targeted by miR-667. The gene for miR-667 is located in chromosome 6.

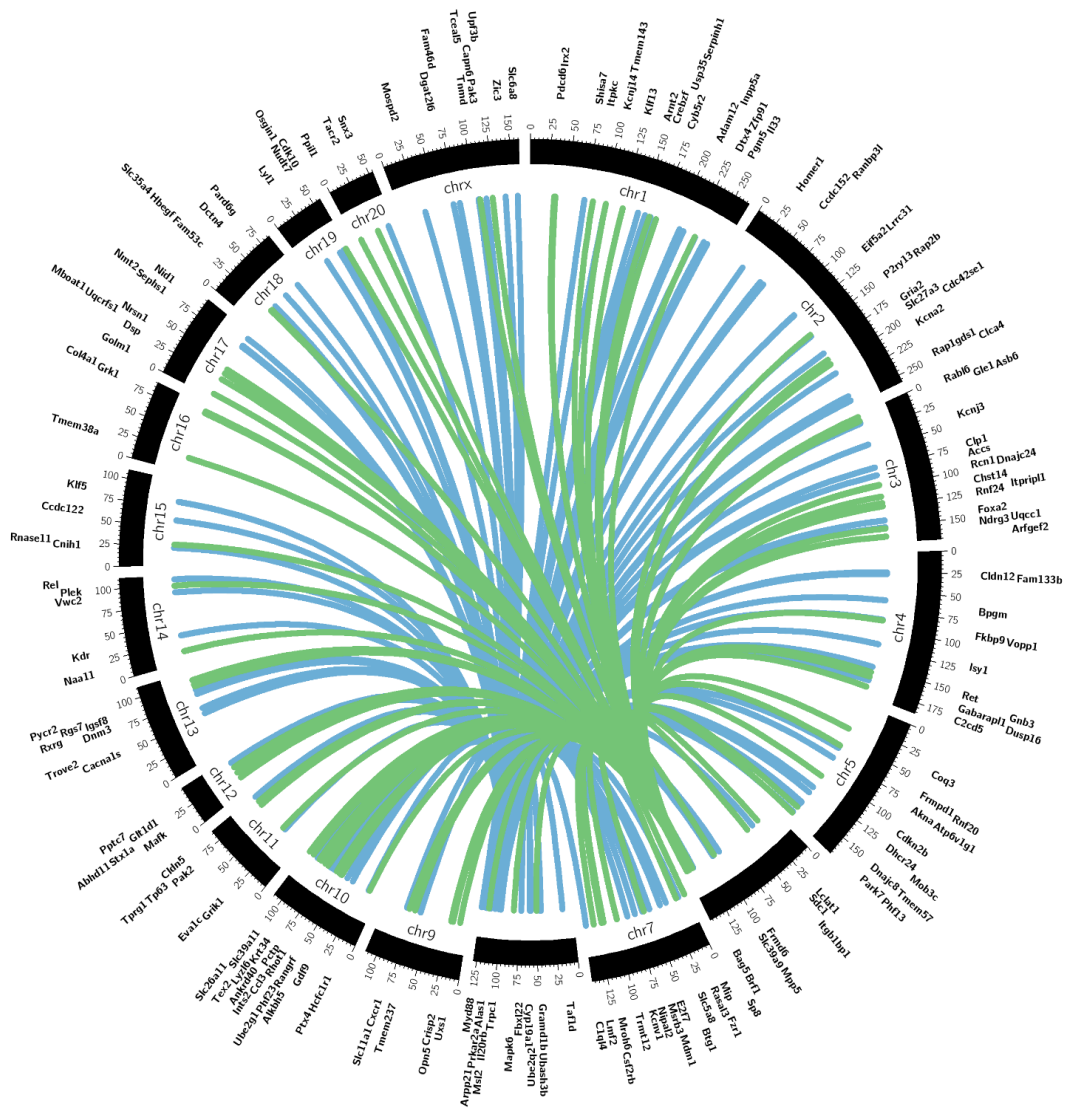


Figure 6.6. Circos v0.67 plot of rno-miR-138 (blue) and rno-miR-667 (green) and regulatory target genes. The middle track represents the rat genome with each ideogram segment representing one chromosome. The outermost and inner tracks display the gene name and spatial location of each gene targeted by the miRNAs.

Gene enrichment and pathway analysis were carried out using Metacore™ (see table A1 in Appendix). Process networks and pathway maps (MetaCore manually curated databases) and GO molecular functions and GO biological processes were analysed. The

results described below have been selected taking into account their relevance in pain, nerve injury and inflammation and selective examples are represented in figure 6.6. MetaCore process networks identified seven main networks. This included the neurophysiological process transmission of nerve impulse ($p=3.590E-03$) and wnt signal transduction ($p=4.972E-03$), cell adhesion ($p=1.056E-02$), chemotaxis ($p=2.336E-02$), calcium transport ($p=7.829E-02$), inflammation and neutrophil activation ($p=1.128E-01$) and neuropeptide signalling pathways ($p=1.129E-01$). The MetaCore™ pathway maps identified one main pathway: cell adhesion and chemokines ($p=5.598E-03$). MetaCore™ also incorporates external databases such as GO biological process and GO molecular function. The enrichment analysis for GO biological process included regulation of transmembrane transport ($p=2.038E-07$), regulation of ion transport ($p=1.512E-06$), interleukin-8-mediated signalling pathway ($p=2.832E-06$) and T-cell chemotaxis ($p=4.231E-06$). The GO molecular function identified ion transmembrane transporter activity ($p=4.347E-04$), voltage-gated cation channel activity ($p=1.983E-03$), potassium channel activity ($p=5.423E-03$), ion channel binding ($p=6.178E-03$).

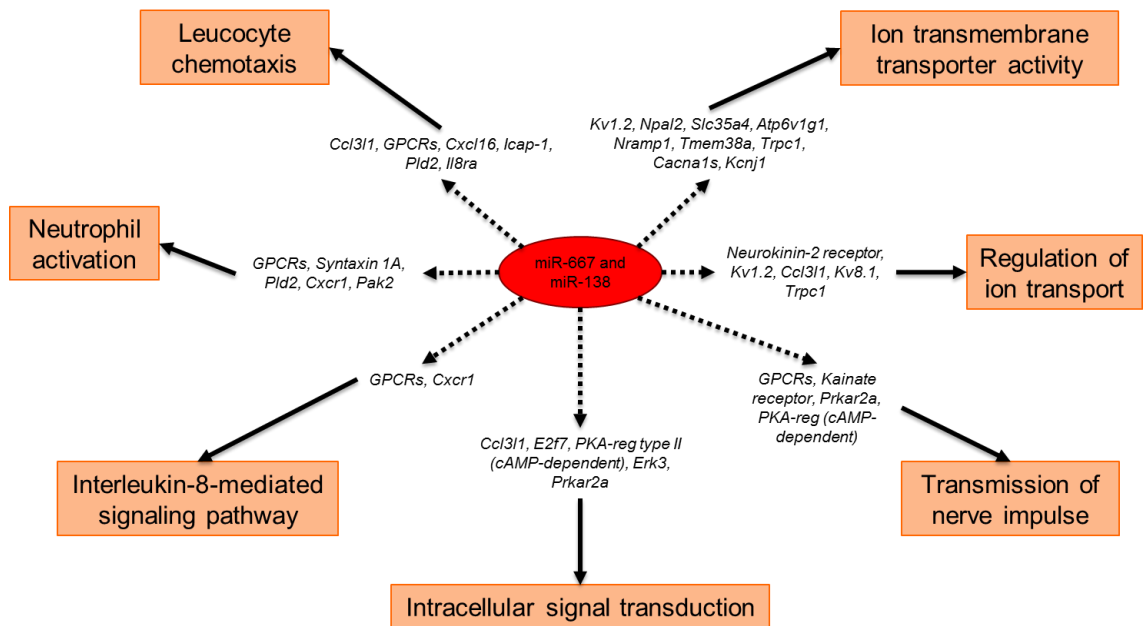


Figure 6.7. Example of genes and pathways targeted by miR-667 and miR-138. More details can be found in table A1 in Appendix.

6.3.1.2. Novel rat miRNAs

The rodent TLDA cards contain preloaded mouse and/or rat miRNA probes. In the rat lingual nerve samples analysed, the presence of miRNAs sequences that have only been reported in the mouse was detected. Performing a sequence blast against the rat genome detected a high similarity and presence of the precursor miRNAs for miR-1904 and miR-763 (figure 6.7). The stem loop sequence of miR-1904 is located on chromosome 13 of the mouse genome and it was identified a high similarity sequence for the rat genome on chromosome 2 with only two mismatches ($p=1E-27$, ident:97%). The mature sequence (22 nucleotides) corresponds to nucleotide 11 to 32 of the stem-loop and presents a mismatch outside the seed region on the position 12 ($p=0.18$, ident:95%).

Mir-763 stem-loop sequence is located on chromosome 10 of the mouse genome. A high similarity on chromosome 7 on the rat genome with 3 mismatches ($p=5E-48$, ident: 97%) was found. The mature miRNA sequence comprises nucleotides 38 to 59 and has an exact match in the rat genome ($p=8E-04$, ident:100%).

6.3.2. miRNAs in human lingual nerve neuroma

6.3.2.1. Clinical data analysis

The groups, painful and non-painful were established based on the pain VAS scores (table 6.2). In the non-painful group all patients reported an average pain VAS score of 2.89, which is largely considered as no pain (Jensen et al., 2003). Patients in the painful group had VAS scores ranging between 30 and 95, with an average of 55.13. Overall there was a significant difference between the two groups ($t=6.29$ $df=15$, $p<0.0001$). Pain VAS score were found to be mildly correlated with VAS scores on discomfort $r=0.5$, $p=0.05$ (Figure 6.9). No relationship was found neither between tingling and pain nor between tingling and discomfort.

Table 6.2. Clinical information of the patients included in this study

Non-painful						
Neuroma sample	Type	Age (years)	Gender	Pain VAS	Tingling VAS	Discomfort VAS
1#	NIC	42	F	0	33	10
2	NIC	36	F	0	25	79
3	NIC	27	F	1	1	81
4	NIC	38	F	3	10	38
5	NIC	60	M	4	7	6
6	NIC	59	F	5	38	58
7*	NEN	31	F	0	8	95
8*	NIC	47	F	5	94	89
9*	NIC	44	F	8	6	83
Painful						
Neuroma sample	Type	Age (years)	Gender	Pain VAS	Tingling VAS	Discomfort VAS
10	NIC	35	F	30	6	60
11	NEN	38	M	30	97	83
12	NIC	30	F	35	11	98
13	NIC	54	F	60	100	77
14	NIC	44	F	82	3	97
15	NIC	44	F	95	75	64
16*	NIC	29	F	42	0	70
17*	NIC	47	F	67	85	100

F, female; M, male; NIC: neuroma-in-continuity; NEN: nerve-end-neuroma; VAS, Visual Analogue Scale; time between injury and surgical repair ranged between 6 to 38 months.
#sample used only in miRNA screening; *samples used only in miRNA validation

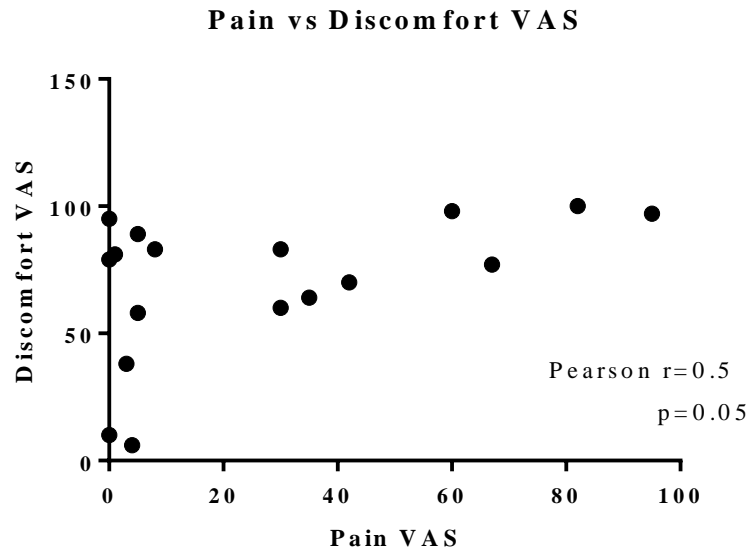


Figure 6.9. Pearson correlation scatter plot. Scatter plot showing the relationship between pain VAS and discomfort VAS scores.

6.3.2.2. miRNA expression analysis

Two miRNAs were found to be differentially expressed in human lingual nerve neuromas (table 6.3) in the TLDA card analysis.

Table 6.3. miRNA differentially expressed in human lingual nerve neuromas

miRNA	$\Delta\Delta C_t$	Fold change	p -value
hsa-miR-500a	5.704	0.019	0.021
hsa-miR-29a	6.222	0.013	0.001

Next, miRNA validation was conducted for the two miRNAs; miR-29a was found to be differentially expressed between groups ($t=2.769$ $df=14$, $p=0.02$) while miR-500a was not statistically significant (even though it was still down-regulated in the painful group). However, both miR-29a and miR-500a delta Ct (ΔC_t) were found to be inversely proportional to the pain VAS score (figure 6.9). No correlation between tingling or discomfort and miRNA expression were observed.

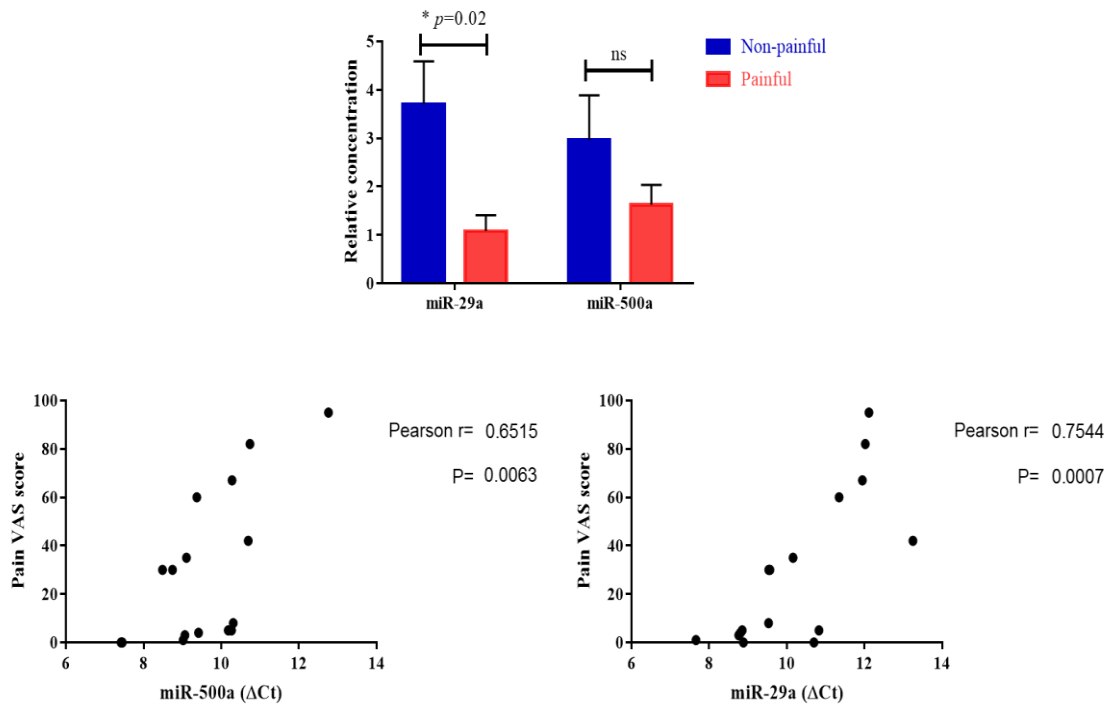


Figure 6.10. miRNA validation and correlation scatter plots. miR-29a was confirmed to be statistically significantly differentially expressed between painful and non-painful group. miR-500a was relatively down-regulated in the painful group but no statistical differences were found. Pearson correlations showed a moderate inverse correlation between the expression of miR-29a and miR-500a and the pain VAS scores. miRNAs values represent normalised delta Ct values (Δ Ct, the higher the Ct value, lower the expression of the miRNA). ns-not significant.

6.3.2.3. miRNA target prediction and gene enrichment analysis

Similarly to the process performed for the rat miRNAs, the same publicly available databases were used to look for predicted target genes of the identified human miRNAs. For visualisation purposes the miRNAs-target genes networks were again created with the CyTargetLinker app from Cytoscape, as represented in figure 6.10. The gene targets chosen for further analysis were ranked by the cumulative weighted context++ scores of TargetScan (cut-off -0.4) and cross-referenced resulting in 67 predicted targets for hsa-miR-29a and 115 for hsa-miR-500a. Genome wide insight into the interaction between both miRNAs and their target genes is represented in figures 6.11 to 6.13.

Similar to the approach taken for the rat miRNAs, it was also decided to include mirR-667 in the target prediction and bioinformatics analysis based on:the correlation with clinical data and this will also be further discussed in the disucssion in section 6.4.

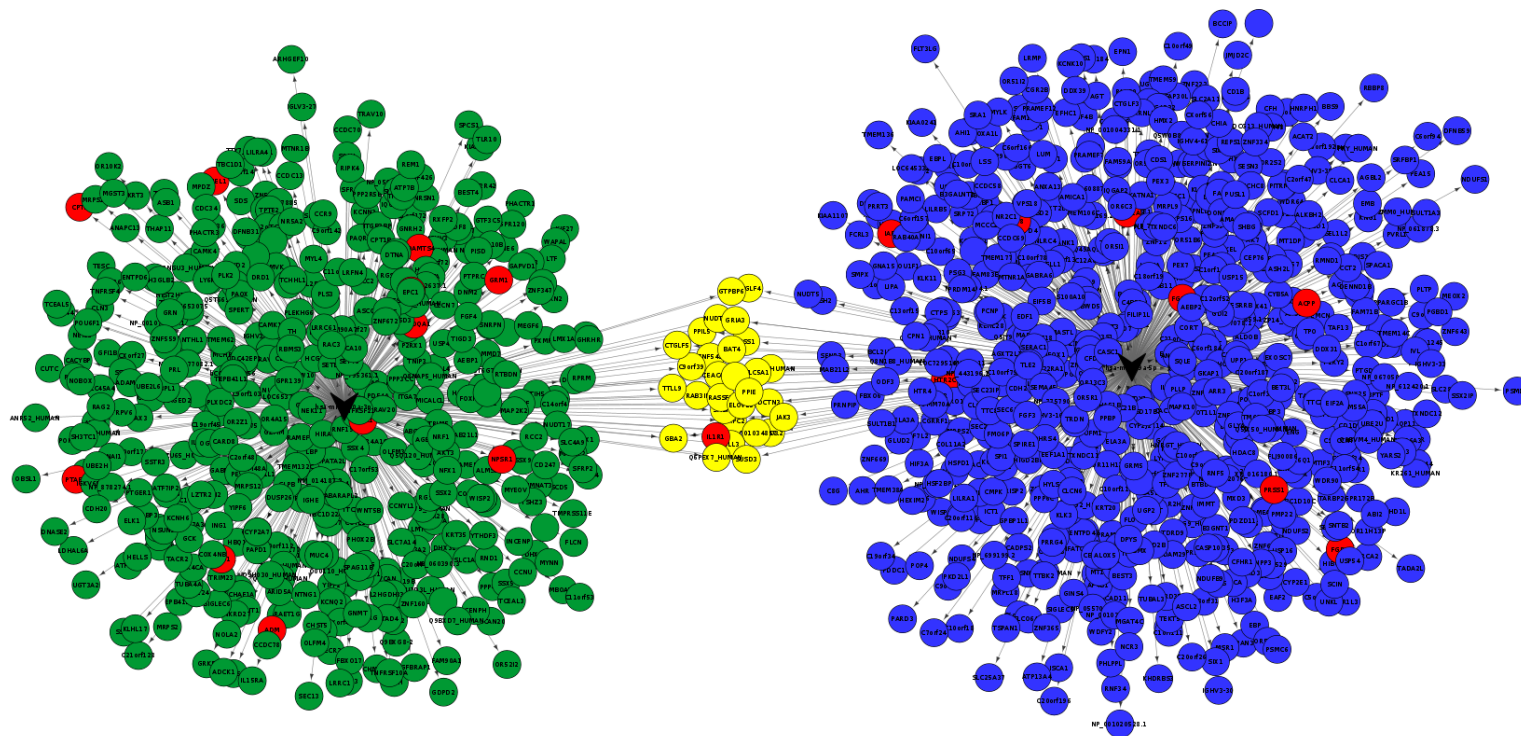


Figure 6.11. CyTargetLinker analysis and network visualisation of differentially expressed human neuromas miRNAs and their predicted target genes. Network enrichment genes for hsa-miR-29a and hsa-miR-500a were identified using microCosm, TargetScan and miRTarBase. Nodes coloured in blue are targets of hsa-miR-29a and nodes coloured in green are targets of hsa-miR-500a. The nodes coloured in yellow are targets of both hsa-miR-29a and hsa-miR-500a, while nodes in red are genes known to have a role in pain. This network was constructed and visualised using CyTargetLinker v3.0.1 and Cytoscape v3.4.0. There is no relation between the position of the nodes and the score of the target prediction.

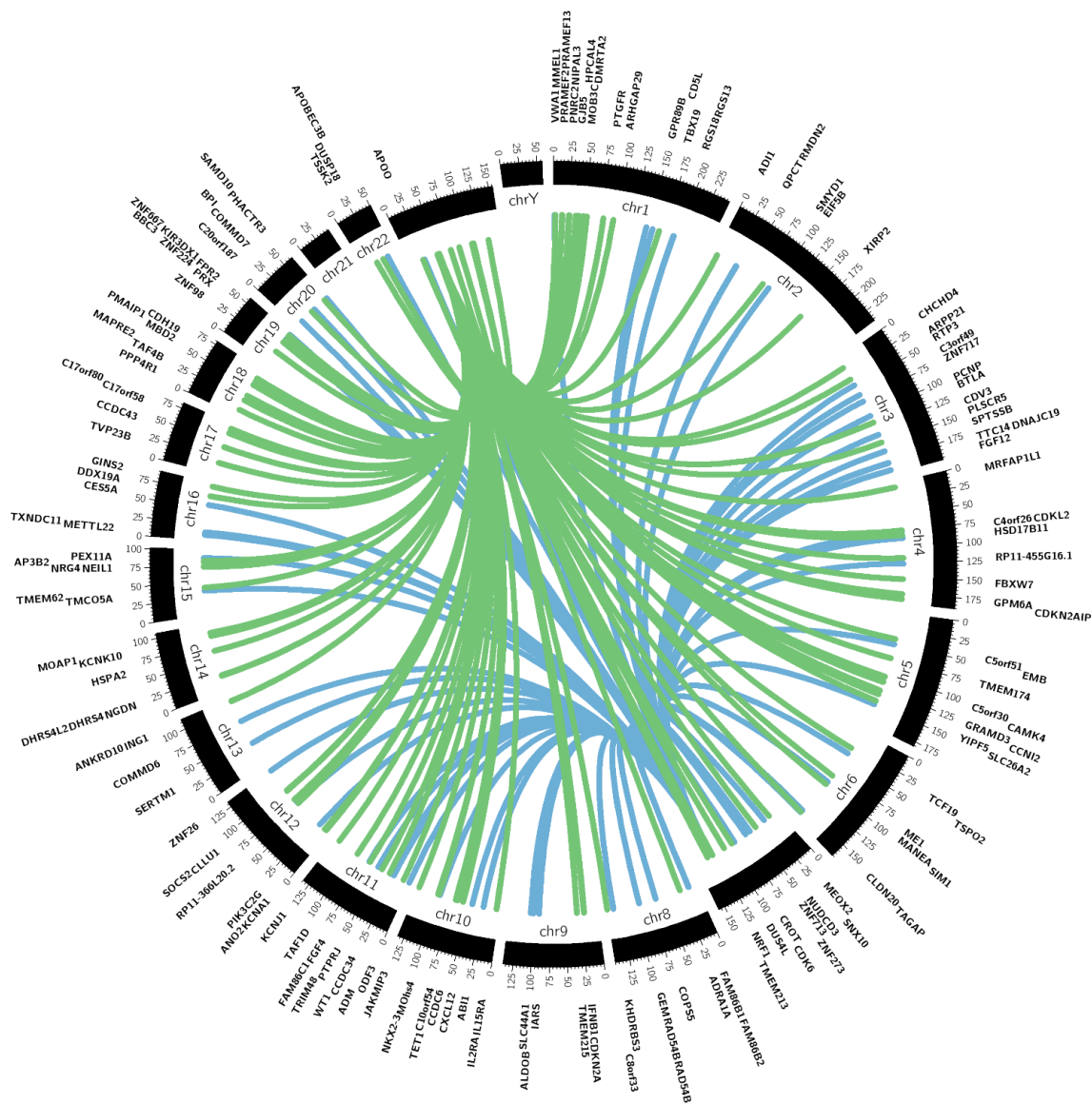


Figure 6.14. Circos v0.67 plot of hsa-miR-29a (blue) and hsa-miR-500a (green) and regulatory target genes. The middle track represents the human genome with each ideogram segment representing one chromosome. The outermost and inner tracks display the gene name and spatial location of each gene targeted by the miRNAs.

Enrichment and pathway analysis were carried out using MetaCore™ process networks, pathway maps, GO molecular functions and GO biological processes for the human miRNA target genes identified (see table A2 in Appendix). Here, it is reported the selected most relevant pathways in the context of pain, nerve injury and inflammation (see figure 6.14). MetaCore™ process networks identified three main pathways: inflammation and Jak-STAT Pathway ($p=8.124E-02$), potassium transport ($p=9.149E-02$) and chemotaxis ($p=1.201E-01$). MetaCore™ pathway maps included IL-16 signalling pathway ($p=1.750E-03$), IL-15 signalling via JAK-STAT cascade ($p=4.081E-03$) and impaired Lipoxin A4 signalling ($p=1.572E-02$). The enrichment by GO biological process retrieved the following: regulation of ion transmembrane transport ($p=3.212E-05$), negative regulation of leukocyte cell-cell adhesion ($p=3.865E-05$), negative regulation of cell activation ($p=4.233E-05$), regulation of transmembrane transport ($p=4.471E-05$), regulation of G-protein activated inward rectifier potassium channel activity ($p=4.851E-05$), transmembrane transport ($p=5.695E-05$), negative regulation of leukocyte activation ($p=6.445E-05$), negative regulation of cell growth ($p=6.648E-05$), negative regulation of cell-cell adhesion ($p=6.648E-05$), negative regulation of cell proliferation ($p=8.755E-05$), regulation of macrophage apoptotic process ($p=1.432E-04$). Additionally, GO molecular function identified several clusters associated with inflammation and ion and membrane transport: interleukin-2 receptor activity and interleukin-2 binding ($p=3.457E-04$), cytokine receptor activity ($p=7.337E-03$), ion channel activity ($p=2.972E-03$), substrate-specific channel activity ($p=3.728E-03$), gated channel activity ($p=5.361E-03$), voltage-gated channel activity ($p=5.516E-03$), voltage-gated ion channel activity ($p=5.516E-03$), channel activity ($p=6.416E-03$), transmembrane transporter activity ($p=6.419E-03$), substrate-specific transporter activity ($p=6.498E-03$) and passive transmembrane transporter activity ($p=6.500E-03$).

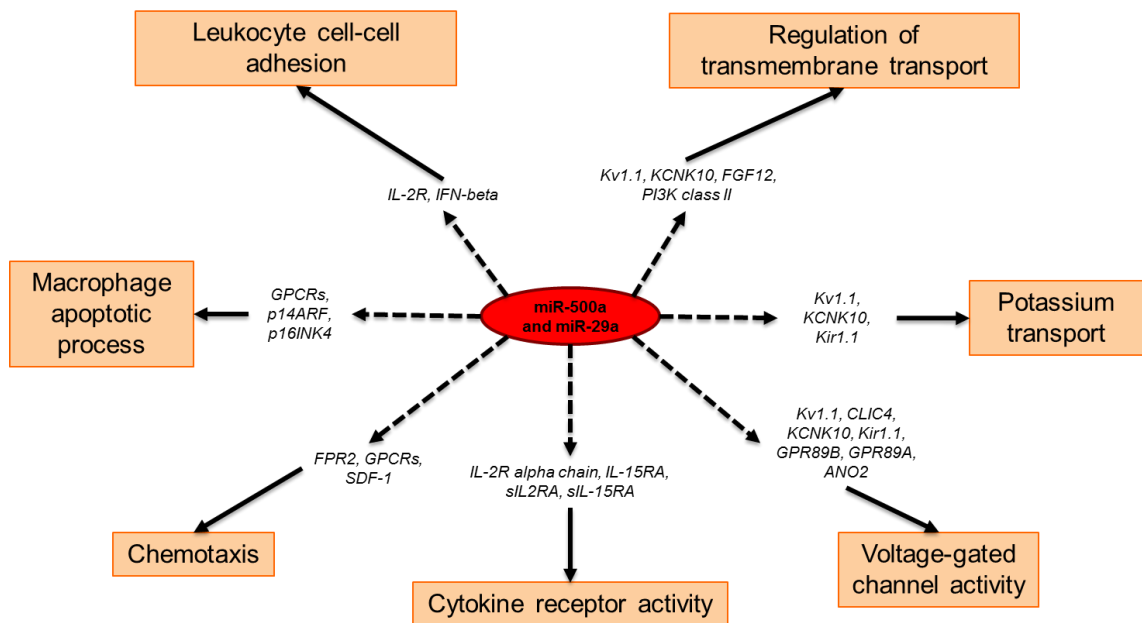


Figure 6.15. Example of genes and pathways targeted by miR-500a and miR-29a. More details can be found in table A2 in Appendix.

6.4. Discussion

The main findings of this study were: 1) rno-miR-667 was differentially expressed in the lingual nerve of injured rats (CCI group) compared to sham control rats. 2) the normalised delta Ct values of rno-miR-138 and rno-miR-667 were found to be correlated with the time drinking reward at day 3 post-injury. 3) Hsa-miR-29a was differentially expressed in lingual nerve neuromas of patients with higher pain VAS scores (painful group), compared to patients with lower pain VAS scores (non-painful group). 4) A statistically significant negative correlation was observed between the expression of both hsa-miR-29a and hsa-miR-500a with the pain VAS score; 4) target and gene enrichment analysis predicted that these miRNAs may target genes involved in inflammatory and pain related pathways.

miR-138-1

The gene that encodes for miR-138-1 is located in the long arm of chromosome 8 in position 8q32 and it is not inserted within a miRNA cluster. The origin transcript has 99 nucleotides (nucleotides 131,731,726-131,731,824 of the forward strand) and the maturation process leads to the formation of a 22 nucleotide sequence that corresponded to positions 61-82: miR-138-1-3p CGGCUACUUCACAACACCAGGG.

miR-138 has been found to be downregulated in the rodent DRG 7 days following sciatic nerve transection (Strickland et al., 2011). miR-138 is highly present in the brain synapses and a previous study has shown that miR-138 targets the depalmitoylation enzyme Acyl protein thioesterase 1 (APT1), which has been linked to the regulation of dendritic spine size in neurones of the rat hippocampus (Siegel et al., 2009).

miR-667

miR-667 gene is located in the long arm of chromosome 6 in position 6q32 of the rat genome. The origin transcript has 92 nucleotides (nucleotides 133,869,570 - 133,869,661 of the positive strand) and after processing results in a 22 nucleotide sequence, which corresponds to position 56-77 of the transcript: miR-667-3p UGACACCUGCCACCCAGCCCAA. The miR-667 gene in chromosome 6 is clustered with other miRNAs: rno-mir-3579, rno-mir-380, rno-mir-323, rno-mir-758. rno-mir-329, rno-mir-494, rno-mir-679, rno-mir-1193, rno-mir-666, rno-mir-543, rno-mir-495, rno-mir-667, rno-mir-376c, rno-mir-376b, rno-mir-3595, rno-mir-376, rno-mir-300, rno-mir-381, rno-mir-487b, rno-mir-3576, rno-mir-539, rno-mir-6331, rno-mir-544.

In vivo studies demonstrated that miR-667 is correlated with lower levels of catechol-O-methyltransferase (*Comt*) mRNA in the brain and the administration of lentiviral injections of this miRNA increase hypersensitivity in the mouse formalin model (Segall et al., 2015). COMT is an enzyme that degrades catecholamines such as dopamine and epinephrine and lower levels have been associated with hyperalgesia states in previous studies (K Segall et al., 2012).

miR-29a

miR-29 gene is located in the long arm of chromosome 7 in position 7q32.3. The precursor transcript has 64 nucleotides (130,876,747-130,876,810 from the terminus of the long arm, qter) and the maturation process leads to a 22 nucleotide sequence obtained from nucleotides 4-25 in the transcript: hsa-miR-29a-5p ACUGAUUUCUUUGGUGUUCAG. miR-29a is clustered in chromosome 7 with hsa-mir-29b-1 and hsa-mir-29a.

miR-29 has been found in blood microvesicles, small bowel, and colon tissues of irritable bowel syndrome (IBS) patients. Its presence has been associated with increased intestinal permeability and chronic visceral pain as inhibiting the expression of miR-29a

in vitro restored intestinal permeability (Zhou et al., 2009). Genda et al. (2013) found that miR-29 was decreased in spinal cord dorsal horn 7 days after CCI of rat sciatic nerve. miR-29 was also found to be downregulated in the ipsilateral trigeminal ganglion 4 h after administration of complete Freund's adjuvant (CFA) in a model of inflammatory muscle pain (Bai et al., 2007).

miR-500a

miR-500a gene is located in the short arm of chromosome X in position Xp11.23. The precursor has 84 nucleotides (50,008,431-50,008,514 from the terminus of the short arm, pter) and after processing the mature miRNA sequence contains 22 nucleotides, spanning from 52-73 nucleotides in the transcript: hsa-mir-500a-3p, AUGCACCUGGGCAAGGAUUCUG. The miR-500 gene in the chromosome X is clustered with other miRNAs: hsa-mir-532, hsa-mir-188, hsa-mir-500a, hsa-mir-362, hsa-mir-501, hsa-mir-500b, hsa-mir-660, hsa-mir-502 (Kozomara and Griffiths-Jones, 2014).

miR-500 has been found to be expressed in the central nervous system and it is thought to have a major role in its development (Wheeler G., et al 2006). miR-500 is downregulated in rat DRG after sciatic nerve resection at 4, 7, and 14 days (Yu et al., 2011) and in the spinal cord dorsal horn neurones 7 days after CCI of sciatic nerve (Genda et al., 2013). In addition, miR-500 significantly downregulates neurokinin-1 (NK1) receptors in patients with bladder pain syndrome (Freire et al., 2010). NK1 receptor is known to be triggered by the binding of SP and it produces mechanical hyperalgesia and allodynia (Carlton et al., 1996). In another study, miR-500 increased after administration of paclitaxel or L5 ventral root transection and modulated the downregulation of Glutamic Acid Decarboxylase 67 (GAD67) (Huang et al., 2016). GAD67 is an enzyme that regulates the function of GABAergic synapses in spinal cord dorsal horn neurones. In the same study, miR-500 knockout or the use of an antagomir led to GABAergic synapses function repair and alleviated the pain behaviour in rats, suggesting that miR-500 negatively contributes to GABAergic synapses function through the regulation of GAD67. In a study conducted in human whole blood samples collected from patients with complex regional pain syndrome (CRPS), Orlova et al. (2011) found that, even though miR-500 was not significantly altered between CRPS patients and controls, the levels of this miRNA were negatively correlated with the symptoms of hypoesthesia. miR-500 gene is located in chromosome X. It is important to note that the majority of patients in this study

were female (table 6.2). Recent evidence by Linnstaedt et al. (2015) have found miRNAs enriched for the chromosome X in patients with persistent musculoskeletal pain, suggesting that miRNAs can play a role in sex-specific pain differences. There have also been some studies associating miRNAs in the X chromosome to potential sex-specific immune responses (Pinheiro et al., 2011). In fact, it has been shown that the Y chromosome in several mammalian species has no miRNA genes. However, further studies, on the potential role of miRNAs in general and miR-500a in particular, in sex-specific pain differences are required.

Of note, the trigeminal ganglia (cell bodies) of the lingual nerve were examined and no miRNAs were found to be differentially expressed when applying the same analysis parameters as for the lingual nerve samples. A possible explanation is that the relative percentage of cell bodies from the lingual nerve in the trigeminal ganglia is low and by analysing the whole ganglion the differentially expressed miRNAs were not sufficient to be detected. That was, in fact, the reason that at this point, it was decided not to analyse miRNA expression in the trigeminal nucleus of the brainstem as it is important to restrict the tissue analysis to the projections of the lingual nerve (so the effect is not diluted/lost by analysing the whole tissue). Future studies are required to verify the origin of the miRNAs here identified. In the case of the rat lingual nerve tissues, even though the miRNAs identified were not found in the trigeminal ganglia tissues it does not mean necessarily that they are not neuron-specific miRNAs. There have been reports of axonal transport of miRNAs and, for instance, Natera-Naranjo et al. (2010) have found that specific miRNAs are located in the distal part of sympathetic axons in higher quantity than that in the cell bodies.

The potential novel rat miRNAs described in Section 6.3.1.2 had a high similarity when searching with BLAST (Basic Local Alignment Search Tool) against the rat genome. Because they have high number (miRNAs are usually numbered sequentially) it may be possible that they are recently discovered miRNAs in the mouse and have not been validated in the rat. Therefore, further validation is required to verify whether miR-763 and miR-1904 are in fact present in the rat and whether they are functional miRNAs.

Gene enrichment and pathway analysis

The bioinformatics approach carried out showed that predicted target genes were statistically enriched for inflammation, chemotaxis, signal transduction and ion transmembrane transport for both rat and human miRNAs. The gene enrichment analysis with the rat miRNAs identified target genes involved in the Wnt signalling pathway. Wnts are known to participate in the regulation of neuron repulsion during axonal guidance (Onishi et al., 2014). Inflammation is an important event that can sensitise the nociceptors and enhance a continuous pain signal. When tissue or nerve injury occurs several pro-inflammatory mediators are released and can directly activate and/or sensitise nociceptors facilitating the transmission of the nociceptive signal (Basbaum et al., 2009). For instance, c-c motif chemokine ligand 3 (*Ccl3*, targeted by rno-miR-138 with a 8mer canonical binding) and c-x-c motif chemokine receptor 1 (*Cxcr1*, also known as il8ra, targeted by rno-miR-667 with two possible canonical bindings: 7mer-A1 and 8mer) were enriched for chemotaxis that contributes to the inflammatory event. *Ccl3* is one cytokine gene located on chromosome 10 of the rat genome and encodes a protein that binds to several chemokine receptors, including chemokine binding protein 2 and chemokine (C-C motif) receptor 5 (CCR5). CXCR1 is a receptor for interleukin-8. Transient receptor potential cation channel, subfamily C, member 1 (*Trpc1*) is a gene targeted by rno-miR-138 (8mer canonical binding) and it is located on chromosome 8 in the rat genome. It is a nonspecific cation channel that contributes to nociceptor sensitisation (Alessandri-Haber et al., 2009).

Target gene enrichment analysis of differentially expressed human miRNAs showed that potassium voltage gated channels are potentially targeted. For instance, *Kcna1* is a gene located on chromosome 12 in the human genome and encodes for the potassium voltage gated channel subfamily A member 1. This gene is predicted to be targeted by hsa-miR-500a (in addition to 8mer and 7mer-m8, a poorly conserved 6mer binding site is also predicted). Another example is *Kcnj1*, a potassium inwardly-rectifying channel subfamily J member 1, which is also predicted to be targeted by hsa-miR-500a (7mer-m8 canonical binding), is a gene located in human genome chromosome 11. Many studies have demonstrated the role of potassium channels in diseases including pain, in particular the potassium voltage-gated channel subfamily Q (Wang and Li, 2016, Abd-Elseyed et al., 2015) and these findings suggest that hsa-miR-500a can contribute to the regulation of several potassium channels. As miR-500a is located in chromosome X, further studies are required to investigate the significance of these findings.

Hsa-miR-29a was found to target genes that regulate inflammatory and immune mechanisms, mainly genes that encode GPCRs and interleukin receptors. For instance, the gene *FPR2* is a target for this miRNA (an 8mer canonical binding) and this gene is located on chromosome 19; FPR2/ALX is the protein, a GPCR, as described in section 1.2.2 in chapter 1. Previous studies showed that activation of FPR2/ALX stopped the recruitment of neutrophils, facilitated resolution of inflammation and inhibited the release of cytokines and chemokines (Krishnamoorthy et al., 2012, Devchand et al., 2003). More recently, work by Martini et al. (2016), Pei et al. (2011) and Meesawatson et al. (2016) have also reported its role in inhibiting pain processing in animal models. This receptor is classified as a multi-recognition receptor as it binds to multiple molecules including lipoxin A4, resolvin D1, peptides and proteins (annexin and serum amyloid A), showing a ligand specific effect (Cooray et al., 2013, Chiang et al., 2006). FPR2/ALX has been reported to be regulated by, at least, one other miRNA, the miR-181b, in human macrophages (Pierdomenico et al., 2015). In this thesis, FPR2/ALX was found to be expressed in neurones within the spinal cord dorsal horn and brainstem (please see section 5.3.1.2 in chapter 5); further studies are required to confirm whether FPR2/ALX is expressed in peripheral nerves, namely in human lingual nerve neuromas. In the long term, the interaction between miR-29a and *FPR2* needs to be confirmed and functional studies into whether miR-29a suppresses *FPR2* translation are required.

Methodological approach and limitations of the study

In this study, the expression of miRNAs in rat and human lingual nerve tissues was analysed. Taqman[®] low density array (TLDA) cards were used to screen and profile the miRNA expression; this array is aligned with the miRBase database (release 20) and uses microfluidic cards that contain preloaded miRNA probes. The advantage of the TLDA cards was the simultaneous and quick analysis of up to 758 miRNAs and controls in combination with the polymerase chain reaction (PCR) standard protocol. In addition to rat tissues, human lingual nerve neuromas were also examined in this study in order to establish, when possible, any correlations with clinical pain symptoms.

The miRNAs found to be differentially expressed in the miRNA screening were further analysed using public available databases for targets based on the TargetScan algorithm. As mentioned in the respective sections, it was decided to use for further analysis the four miRNAs identified in the miRNA screening with the TLDA cards (even

though only two – one in the rat lingual nerve and the other in the human samples – were statistically significant in the miRNA validation) because 1) those miRNAs showed correlation with behavioural or clinical data and 2) it has been suggested that it is more biologically meaningful to investigate multiple miRNAs that can potentially target the same genes (Fan et al., 2016); for instance, in *C. elegans*, it has been shown that the knockdown of a specific miRNA has very little effect on the phenotype (Miska et al., 2007) and evidence indicates that miRNAs may target genes cooperatively (Schmiedel et al., 2015, Krek et al., 2005), thus conducting a bioinformatics analysis on multiple miRNAs may result in more meaningful targets for future biological validation. Additionally, one limitation of this study was the sample size and results need to be interpreted taking that into account. The small number of samples included may explain the variation in the validation studies compared with the initial TLDA screening as, for instance, the miR-500a showed a moderate correlation with pain VAS score in the human samples. In terms of the animal study, it respected the 3Rs and minimised the number of animals used for an initial screening of miRNA study in this model (Kilkenny et al., 2012). However, these results will need to be validated in a future study with a bigger sample size. The absence of healthy human lingual nerve samples to be used as controls limited the conclusions; however, a statistically significant correlation between the expression of the miRNAs and the pain VAS scores was observed. Regarding the human tissues it is worth pointing that they were fixed and had been stored for periods of several months before extraction and analysis, which could explain the RNA degradation observed in these samples. However, several studies have demonstrated that miRNA is usually more stable than mRNA in fixed samples (Doleshal et al., 2008, Xi et al., 2007, Siebolts et al., 2009, Jung et al., 2010). In addition the bioinformatics analysis was based on predicted targets rather than experimentally validated assays. However, the TargetScan algorithm used in this study to predict targets has been shown to have high concordance with experimental validation (Lewis et al., 2003) and has the advantage of giving genome-wide insight.

Human neuroma samples represent a rare archive of well-characterised human tissues with a specific injury. In addition to nerve and Schwann cells, these neuromas contain scar and connective tissue. In fact, Vora et al. (2007) demonstrated that leukocytes and macrophages cells are also present in human lingual nerve neuromas, in particular in regions associated with viable nerve tissue. Therefore, in a future study it will be

necessary to characterise the respective neuroma associated with miRNA expression in order to investigate the percentage of different type of cells present and, it will also be important, to identify which cells are expressing the potential miRNAs identified.

Different miRNAs were identified in the rat and in the human lingual nerve samples used; however, the miRNAs identified have predicted target genes involved in similar pathways. One possible explanation is the fact that rat lingual nerve tissues were collected and analysed in a specific time point (3 days following injury) and human lingual neuroma tissues had variable time points between injury and tissue analysis (ranging from 7 to 36 months). In addition, miRNA expression is a dynamic process and there is evidence that miRNAs can change in expression over time in the same tissue and pain condition (Sakai and Suzuki, 2014). Furthermore, literature has suggested that the development and the maintenance of chronic pain is controlled by differing molecular mechanisms (Ji et al., 2003, Crown, 2012), denoting that different miRNAs may be in control at different stages.

Conclusions and future studies

In summary, this study has demonstrated that specific miRNAs are differentially expressed following LNI. Predictive analyses suggested, that these miRNAs may interact with target genes that participate in inflammatory and signal transduction pathways, thus can contribute to the molecular changes that occur after a peripheral nerve injury. Further studies are required to evaluate possible physiological effects of these and other miRNAs in pain mechanisms.

The rat pre-clinical model of neuropathic pain can be further studied, particularly, future studies identifying and profiling miRNA expression at different time points and in different tissues (trigeminal ganglion and brainstem) are of interest. It would also be required to verify the correlation found between normalised expression of miRNAs and the time drinking and investigate its functional importance. In order to investigate miRNA targets of specific miRNAs, functional studies *in vitro* may be conducted. The transfection of miRNA mimics (chemically synthesized, double-stranded RNAs which mimic mature endogenous miRNAs) or miRNA inhibitors (single-stranded modified RNAs that specifically inhibit miRNA function) into cultured neurones, followed by downstream gene expression analysis or phenotypic analysis, may be useful in validating the miRNAs targets identified and in assessing its functional role.

CHAPTER 7
GENERAL DISCUSSION

7.1. Summary of findings

The work reported in this thesis enabled the characterisation of lingual nerve injury (LNI) in the rat, in terms of behavioural and microglial response. Furthermore, resolvin receptors and miRNA expression were also described following LNI.

1. LNI in the rat decreased the time accessing a reward and the volume of reward consumed at specific time points after injury. A novel behavioural testing method was developed and this may be useful to assess feeding behaviour following LNI.

2. LNI produced microglia activation. Microglial activation was significantly increased on day 3 following LNI at specific rostral-caudal levels. By day 28 post-injury microglia were only mildly activated and in a more restricted part of the rostral-caudal levels analysed.

3. Resolvin receptors were found to be expressed in specific cells within the nervous system tissues. ChemR23, in particular, was found to be up-regulated at specific rostral-caudal levels of the Vc following LNI.

4. Specific miRNAs were identified following LNI. miR-138 was found to be differentially expressed in the rat lingual nerve between CCI and Sham groups. miR-138 and miR-667 were associated with the time drinking reward. miR-29a was differentially expressed between painful and non-painful human lingual nerve neuromas and miR-500a and miR29a showed a moderate inverse correlation with the painVAS score.

Resolvins have been suggested to have a role in treating pain-associated diseases, similar to miRNAs that recently have shown a key role in regulating gene expression. Acknowledging the need for functional studies for both resolvin receptors and miRNA, the findings described in this thesis may facilitate identification of potential targets for the treatment of neuropathic pain.

7.2. Animal model of neuropathic pain: effect of LNI in feeding behaviour and microglia response

The use of animals for the study of chronic pain is very important. Even though from time to time the validity of animal models in pain studies is questioned, their contribution is undeniable. There are cases of successful translation of novel analgesics to the clinic in which pre-clinical studies demonstrated a reversion in thermal and mechanical sensitivity (Kontinen and Meert, 2003); in addition, the use of animals gives the advantage of accessing tissues within the central nervous system that otherwise would not be accessible. Certainly today there is brain imaging but to access the cellular and molecular level, tissues collected from the highly complex pain transmission system, are undoubtedly a great resource.

LNI as a model of neuropathic pain has not been widely studied in terms of characterisation of behaviour and glial responses. In this thesis, behavioural and microglial responses were characterised up to 28 days following LNI.

Time drinking (total and maximum uninterrupted during the testing period), volume ingested and number of attempts were clearly decreased on day 3 following LNI (number of attempts in the CCI group, however, were not statistically different from the sham group). When looking at the specific time points when microglia and ChemR23 were analysed (figure 7.1) it is possible to detect an inverse tendency with the behavioural data, in particular at day 3. All three parameters of the feeding behaviour were decreased while both microglia and ChemR23 were increased (sum of ratio increase over contralateral side in the Vc) in the CCI group. These results require further investigation in particular whether microglia inhibition and or ChemR23 action (by administration of an agonist) would have any effect on the feeding behaviour.

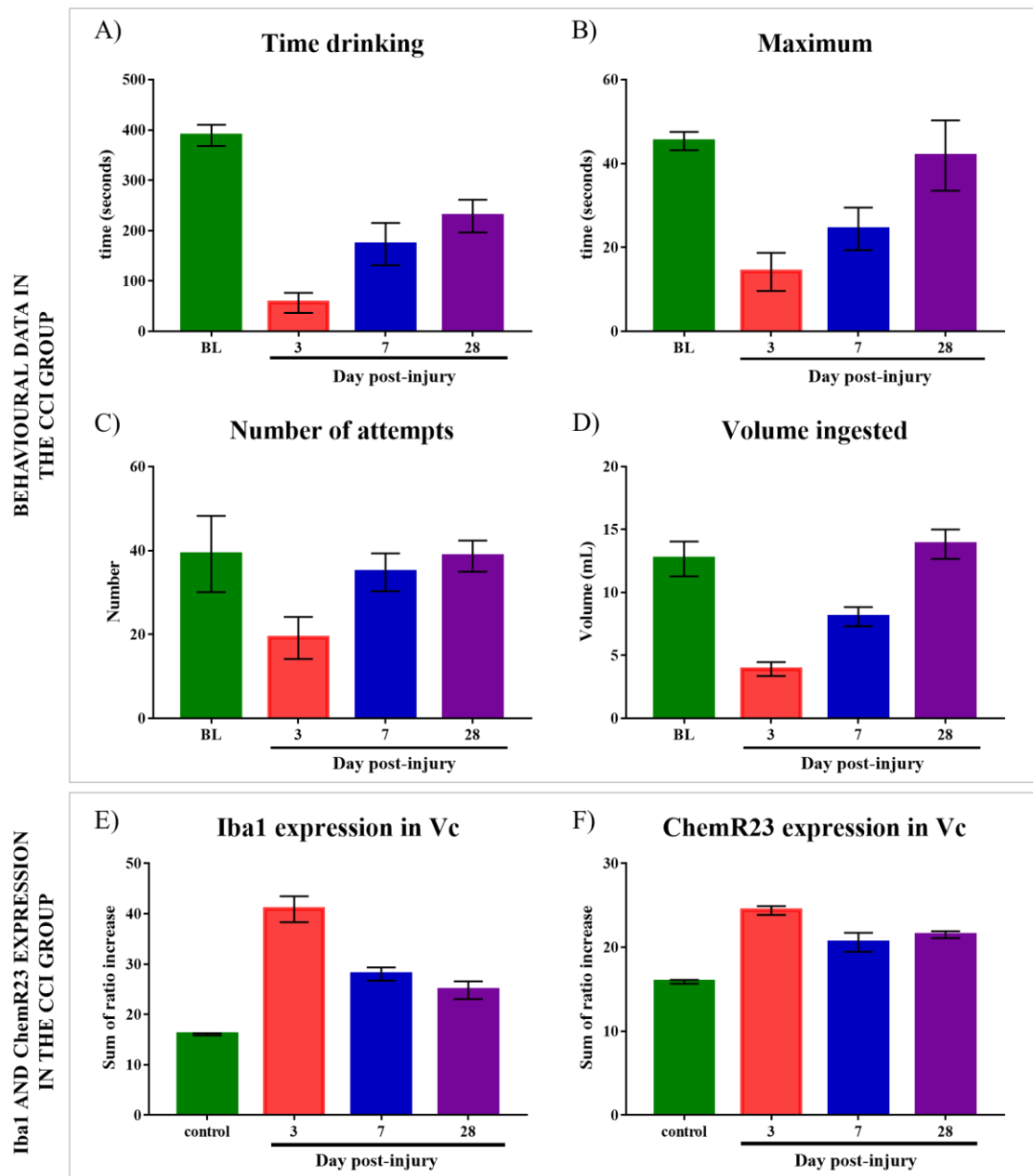


Figure 7.1. Feeding behaviour and Iba1 and ChemR23 expression following lingual nerve injury. A-D) Average of each feeding behaviour parameter in the CCI group at days 3, 7 and 28 post-injury. E-F) Sum of ratio over contralateral side in the Vc of Iba1 and ChemR23, respectively, at days 3, 7 and 28 in the CCI groups. Please note that graphs have different scales.

Previous studies using the LNI have found the accumulation of several neuropeptides (such as SP and CGRP) at the site of injury at day 3 (Bird et al., 2003) and the development of spontaneous activity and mechanical sensitivity, also, at day 3 post-injury (Yates et al., 2000). These studies suggest that the increase in levels of neuropeptides could lead to spontaneous activity (or increased spontaneous activity could also result in increased release of neuropeptides, creating a positive feedback loop). In fact, it is known that SP and CGRP, for instance, can further sensitise the nociceptors and contribute to increased hyperexcitability (Loescher et al., 2001, Smith et al., 2005). In other studies conducted in the trigeminal system, namely in inferior alveolar nerve, identical results were observed at day 3, for spontaneous activity and neuropeptide expression. In addition, the sodium channels Nav1.8 and 1.9 were increased following injury to inferior alveolar nerve (like the lingual nerve, it is also part of the mandibular division of the trigeminal nerve) at day 3, which correlated with spontaneous activity recorded at the same time post-injury (Bongenhielm and Robinson, 1996, Bongenhielm and Robinson, 1998). The sodium channel Nav1.8 in particular has been found to accumulate after injury in human lingual nerve neuroma tissues (Bird et al., 2013). As mentioned in chapter 1, depolarisation of sodium channels can create action potentials that may increase the conduction of the noxious stimulus, and these previous studies indicate that, some specific sodium channels at least in the trigeminal system, in addition to neuropeptide expression, could also be related to increased spontaneous activity. Therefore, the spontaneous activity recorded at day 3 post-injury in the previous studies mentioned, could similarly contribute to increased release of neurotransmitters and other mediators in central terminals that, in turn, could activate microglia. In addition to microglia being known as a first responder to injury, the previous studies mentioned above have found the highest changes in expression of neuropeptides and in spontaneous activity by day 3. In the feeding behaviour described in chapter 3, the highest changes were also observed in early time points when compared to baseline (in the CCI group). Taken together, this suggests that is at early period after injury that most changes occur and indicates that these early stages post-injury may be important for the development of neuropathic pain. However, further studies are required, for instance, to better characterise the potential link between the results in this thesis and the previous findings. Additionally, investigation of potential spontaneous activity and microglia response specifically at day 14 is of interest, based on

the significant decrease in time drinking detected during the feeding behaviour studies (chapter 3).

7.3. Resolvin receptors and miRNA expression

7.3.1. Resolvin receptors expression

The findings reported in these studies, in chapter 5, indicate a potential role for resolvin receptors as drug targets for neuropathic pain. As described in the literature review in section 1.2 in chapter 1, resolvins have been shown to act in pain associated diseases. Prior to this work, very little was known about the expression of resolvin receptors within the nervous system and across pain transmitting tissues. In this thesis, it was found that resolvin receptors are expressed in specific cells. In addition, it was observed that ChemR23 was up-regulated in the Vc following LNI, demonstrating its potential role as a drug target for neuropathic pain. Previous studies conducted by Xu et al. (2010) have shown that RvE1 through ChemR23 can reduce inflammatory and neuropathic pain symptoms.

The same area of interest for ChemR23 expression within each brainstem section was selected as for Iba1 quantification (as by observation it was where the differences between ipsilateral and contralateral were identified) and, thus, the same rostral-caudal levels of the Vc were analysed. When analysing within each rostral-caudal level of the Vc, ChemR23 expression was highest at 960 μm caudal to obex (from day 3 and up to day 28) and at 1440 μm caudal to obex (on day 3) while microglial activation was detected in general across all rostral-caudal levels of the Vc (in particular at day 3) with a peak at 720 μm caudal to obex (see figure 5.22 in chapter 5 and figure 4.11 in chapter 4).

The sum of the ratio increase in the ipsilateral side over the contralateral side in all of the rostral-caudal levels of the Vc analysed was used to verify any correlation between microglia and ChemR23. As seen in figure 7.1-E, -F) (please see page 201), both Iba1 and ChemR23 expression were the highest at day 3 post-injury (in the CCI group) in the overall rostral-caudal levels of the Vc analysed (even though, as mentioned above, ChemR23 was only increased at specific rostral-caudal levels). By day 7 and 28, microglia activation had decreased; ChemR23 expression reduced at day 7 but showed a little increase in the overall Vc by day 28.

Iba1 and ChemR23 expression in the CCI group showed a strong Pearson correlation (figure 7.2); however, only on day 28 the linear association was found to be

statistically significant. This suggests that there is a tendency between Iba1 and ChemR23 expression and further studies (possibly with a bigger sample size) may help verify these results.

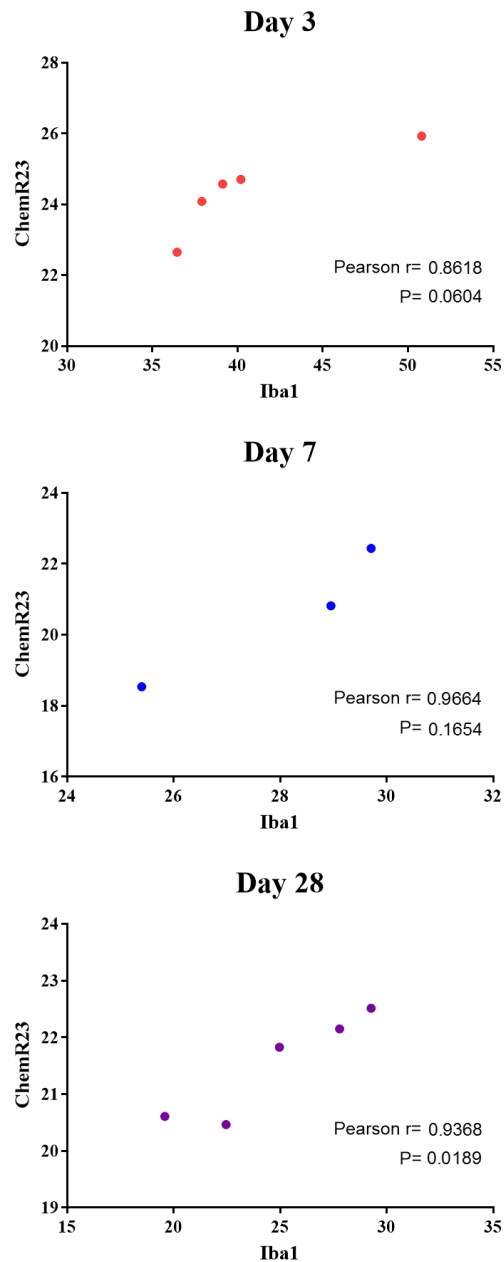


Figure 7.2. Analysis of Iba1 (microglial marker) and ChemR23 expression correlation following lingual nerve injury. A statistically significant positive correlation was found on day 28.

7.3.2. miRNA expression

MicroRNAs (miRNAs) are small non-coding RNAs capable of regulating the expression of several genes. As described in the literature review in section 1.3 in chapter 1, recently miRNAs have been studied with more detail in pain associated diseases. The miRNA study conducted in this thesis identified specific miRNAs of potential interest.

It had been suggested in previous studies published by the Serhan group (first to identify resolvins) that miRNAs and resolvins may be inter-regulated. Interestingly, miRNA target prediction conducted in this thesis for miR-29a identified a resolvin receptor, the FPR2/ALX, as a potential target in the human lingual nerve neuromas. This finding opens the possibility to study two highly promising targets (resolvin receptors and miRNAs) potentially involved in the same pathway in a clinically relevant tissue for nerve injury and pain treatments.

7.4. General approach and study limitations

Work conducted in this thesis took a broad approach to characterise behavioural and microglial response to LNI and to study the expression of potential targets following such injury. An overall approach, with analysis of peripheral and central tissues allied with human samples is a great advantage in basic science research. In fact, recent studies have been focusing in the use of human tissues or combination of human and animal tissues and/or *in vitro* studies; because that will allow the identification of biomarkers and targets potentially more translational (Gruber et al., 2008, Nissenbaum, 2012, Anand et al., 2015, Borsook et al., 2014, Buckley et al., 2017).

The sample sizes were defined based on previous studies conducted in Professor Boissonade's laboratory or based in the literature (as mentioned in chapter 2). In terms of human samples, these were limited to availability and costs of TLDA cards (for the miRNA study). Unless otherwise stated, all work described in this thesis was conducted by the same investigator in order to reduce investigator variability and reproducibility tests were performed where applicable.

The use of a behavioural method to assess feeding behavior following LNI that was in general independent of the investigator, was a great advantage and allowed the study without the normally investigator bias associated with traditional behavioural testing. Resolvin receptors and Iba1 expression studies were based in the use of immunohistochemical techniques. Indirect immunofluorescence is an established method

in Professor Boissonade's laboratory with some studies published in both human lingual nerve neuromas and animal tissues (Biggs et al., 2007a, Bird et al., 2013, Bird et al., 2007, Evans et al., 2012, Evans et al., 2014, Morgan et al., 2009, Vora et al., 2007). An advantage of this technique is that allows not only the determination of the presence of a receptor or protein but also its localisation within the tissue. In addition, the dual labelling with specific cell markers allows the identification of the cells expressing the receptor. Therefore, in the context of the work conducted in this thesis, this technique is useful and particularly suitable to determine and visualise the exact rostral-caudal and anatomical part of the brainstem section of microglial activation and ChemR23 expression following LNI. In addition, correlation studies were conducted between initial and repeated measures and demonstrated the reproducibility of the image analysis and quantification method used (please see section 2.10 in chapter 2). Image analysis methods were quantitative, but qualitative assessment of labelling was also undertaken and described for Iba1 and ChemR23 expression in the respective chapter, in order to give a more complete characterisation of the microglial response and ChemR23 expression.

As mentioned in the literature review in section 1.2.1 in chapter 1, resolvins are derived from *omega-3* fatty acids and, thus, it is considered that the content of *omega-3* in the diet can influence the expression of resolvins. However, based on literature search it is not clear whether diet can influence the expression of resolvin receptors. The animals used in this thesis were subject to the same diet (see table 7.1 and figure A1 in Appendix for details), thus comparable within this study, but no conclusions can be made regarding the effect of the diet on receptor ChemR23 and FPR2/ALX expression and in the behavioural study. Nevertheless, it has been suggested that the diet of the animals used in pain studies can influence behavioural results. As mentioned in section 2.2.2 in chapter 2 animals were not fasting prior to the behavioural testing and all animals were again subject to the same diet so comparable within this study. The role of *omega-3* is widely considered to be beneficial to maintenance of a healthy lifestyle (further details were described section 1.2.1 in chapter 1); in addition, *omega-3* is an important component of synaptic membranes lipids in the mammalian brain and evidence has shown an important role in the development of the nervous system (Innis, 2008). Some studies have found that a higher intake of *omega-3* fatty acids has beneficial effects after PNI. For instance, a clinical study in patients with diabetic neuropathy found that α -lipoic acid administration reduced dysaesthesia symptoms when compared to placebo (Foster, 2007,

Ziegler et al., 2006). A case report of 5 patients with neuropathic pain that were supplemented with *omega-3* showed an improvement in the symptoms and suggests that *omega-3* supplements together with other medical treatments can help in the management of neuropathic pain (Ko et al., 2010). Studies conducted in fat-1 mice (unlike other mammals, they can synthesise *omega-3* from *omega-6*) found that the presence of high levels of *omega-3* led to reduction of pain sensitivity in a model of inflammatory pain (Zhang et al., 2017). However, there is a clear need to identify the actual role of *omega-3* (Galán-Arriero et al., 2017). Pérez et al. (2005) found a direct correlation between the percentage of *omega-3* fatty acids and neuropathic pain behaviours in a rat model. Animals that took a diet with higher percentage of *omega-3* demonstrated increased heat hyperalgesia but the mechanisms underlying this findings were reported. This was associated with the potential role of *omega-3* in the early development of the nervous tissue.

Table 7.1. Fatty acid composition in the rat diet used.

Fatty acids	% (pellet)
C16:0 Palmitic	0.7
C18:0 Stearic	0.2
C18:1 ω 9 Oleic	1.2
C18:2 ω 6 Linoleic (18:2n-6)	3.1
C18:3 ω 3 Linolenic (18:3n-3)	0.3
Total Polyunsaturated	3.4
Total monounsaturated	1.3
Total Saturated	0.9

7.5. Future studies

Future studies derived from work conducted in this thesis may include functional study of resolvin and miRNA mimics/inhibitors administration following LNI. It would be interesting to test whether RvE1 (that binds ChemR23) would reverse or attenuate the effect of LNI on feeding behaviour. Further studies are also required to validate some of the targets identified for each miRNA and test its functional role.

In order to complement the behavioural and microglial study described in this thesis, it would also be required to characterise the response of astrocytes following LNI. In addition, it would be of interest to study whether administration of a microglial inhibitor

such as minocycline would prevent microglial activation and would have any effect in the behavioural response.

In future studies would also be important to include female and male rats, to produce more clinically relevant results.

7.6. Conclusion

In conclusion, this thesis has identified a novel behavioural model for investigating the potential mechanisms behind the development of chronic pain after LNI. As described in section 1.4 in chapter 1, LNI in human patients can have an impact in eating and, in the pre-clinical model used in this thesis, the injury had an effect in the feeding behaviour. In addition, it has been suggested that persistent sensory alteration in patients after LNI may be caused by central changes and this thesis has found microglial activation at early stages post-injury, which may be associated with the development of chronic neuropathic pain, at least in male subjects.

The up-regulation of ChemR23 in the ipsilateral side of the Vc after LNI and the dysregulation of specific miRNAs in the peripheral nerves suggest that they may be potential targets for improved therapeutics for neuropathic pain, in particular that arising from LNI.

APPENDIX

Appendix 1: Target genes and pathways predicted to be under control of the miRNAs identified.

Table A1. Target genes for miR-667 and miR-138

GO molecular function	Examples of target genes	p-value
cation transmembrane transporter activity	Creatine transporter 1 (SLC6A8), Kv1.2, NPAL2, SLC35A4, ATP6V1G1, UQCRFS1, NRAMP1, TMEM38A, SLC39A11, GluR5, Kv8.1, Kir3.1, SLC39A9, TRPC1, CACNA1S, KCNJ14	3.84E-04
substrate-specific transmembrane transporter activity	Creatine transporter 1 (SLC6A8), Kv1.2, NPAL2, SLC35A4, ATP6V1G1, UQCRFS1, NRAMP1, TMEM38A, SLC39A11, SLC5A8, MIP26, GluR5, Kv8.1, GluR2, Kir3.1, SLC39A9, TRPC1, CACNA1S, SLC26A11, KCNJ14, CLCA4	4.103E-04
ion transmembrane transporter activity	Creatine transporter 1 (SLC6A8), Kv1.2, NPAL2, SLC35A4, ATP6V1G1, UQCRFS1, NRAMP1, TMEM38A, SLC39A11, GluR5, Kv8.1, GluR2, Kir3.1, SLC39A9, TRPC1, CACNA1S, SLC26A11, KCNJ14, CLCA4	4.347E-04
inorganic cation transmembrane transporter activity	Creatine transporter 1 (SLC6A8), Kv1.2, NPAL2, ATP6V1G1, UQCRFS1, NRAMP1, TMEM38A, SLC39A11, Kv8.1, Kir3.1, SLC39A9, TRPC1, CACNA1S, KCNJ14	5.547E-04
substrate-specific transporter activity	Creatine transporter 1 (SLC6A8), Kv1.2, NPAL2, SLC35A4, ATP6V1G1, UQCRFS1, NRAMP1, TMEM38A, SLC39A11, SLC5A8, ICAP-1, MIP26, MOG1, GluR5, Kv8.1, GluR2, Kir3.1, SLC39A9, TRPC1, CACNA1S, SLC26A11, KCNJ14, CLCA4	6.416E-04

transporter activity	Creatine transporter 1 (SLC6A8), Kv1.2, NPAL2, SLC35A4, ATP6V1G1, UQCRFS1, RENT3B, NRAMP1, TMEM38A, SLC39A11, SLC5A8, PC-TP, ICAP-1, MIP26, MOG1, GluR5, Kv8.1, NGAL, GluR2, Kir3.1, SLC39A9, TRPC1, CACNA1S, SLC26A11, KCNJ14, CLCA4	6.728E-04
voltage-gated cation channel activity	Kv1.2, GluR5, Kv8.1, Kir3.1, CACNA1S, KCNJ14	1.983E-03
potassium channel activity	Kv1.2, TMEM38A, Kv8.1, Kir3.1, KCNJ14	5.423E-03
ion channel binding	Syntaxin 1A, 14-3-3 theta, MOG1, Homer 1, TRPC1	6.18E-03
GO biological process	Examples of target genes	p-value
ion transport	Creatine transporter 1 (SLC6A8), Kv1.2, NPAL2, K(+) channel, subfamily J, SLC35A4, CCL3L1, ATP6V1G1, UQCRFS1, Galpha(i)-specific peptide GPCRs, NRAMP1, Syntaxin 1A, TMEM38A, SLC39A11, ATP6V1G, SLC5A8, Ionotropic glutamate receptor, MIP26, GluR5, CYB5R2, Kv8.1, NGAL, Galpha(q)-specific peptide GPCRs, RXR, SLC27A3, GluR2, Kir3.1, SLC39A9, TRPC1, Kainate receptor, IHPK2, CACNA1S, Galpha(q)-specific Class A Orphan/other GPCRs, SLC26A11, KCNJ14, 14-3-3, CLCA4, Dynamin	4.97E-08

regulation of transmembrane transport	Kv1.2, K(+) channel, subfamily J, Sts-1, Galpha(i)-specific peptide GPCRs, 14-3-3 theta, G-protein beta, Ionotropic glutamate receptor, MOG1, GluR5, Kv8.1, Galpha(q)-specific peptide GPCRs, Homer 1, DJ-1, Kir3.1, TRPC1, Kainate receptor, CACNA1S, KCNJ14, 14-3-3, Dynamin	2.038E-07
regulation of ion transmembrane transport	Kv1.2, K(+) channel, subfamily J, Sts-1, Galpha(i)-specific peptide GPCRs, 14-3-3 theta, G-protein beta, Ionotropic glutamate receptor, MOG1, GluR5, Kv8.1, Galpha(q)-specific peptide GPCRs, Homer 1, Kir3.1, TRPC1, Kainate receptor, CACNA1S, KCNJ14, 14-3-3, Dynamin	5.704E-07
regulation of ion transport	Neurokinin-2 receptor, Kv1.2, K(+) channel, subfamily J, CCL3L1, Sts-1, Galpha(i)-specific peptide GPCRs, 14-3-3 theta, G-protein beta, Ionotropic glutamate receptor, MOG1, GluR5, Kv8.1, Galpha(q)-specific peptide GPCRs, Homer 1, DJ-1, Kir3.1, TRPC1, Kainate receptor, CACNA1S, Galpha(q)-specific Class A Orphan/other GPCRs, KCNJ14, 14-3-3, Dynamin	1.512E-06
cellular response to interleukin-8, interleukin-8-mediated signaling pathway	Galpha(i)-specific peptide GPCRs, Galpha(q)-specific peptide GPCRs, IL8RA	2.83E-06
intracellular signal transduction	PAK3, RGS7, CRK, CCL3L1, Galpha(i)-specific peptide GPCRs, NRAMP1, RASAL3, VEGFR-2, HB-EGF, 14-3-3 theta, InPP5A, G-protein beta, CNIL, c-Rel (NF-kB subunit), MyD88, ICAP-1, p63, Miro-1, Rap1GDS1, RAP-2B, PLD2, SPEC1,	3.93E-06

	CSF2RB, ZFP91, RET, Galpha(q)-specific peptide GPCRs, E2F7, PKA-reg type II (cAMP-dependent), DHC24, DJ-1, C9orf86, BIG2, Pleckstrin, Galpha(q)-specific Class A Orphan/other GPCRs, ASB6, PP2C, ERK3, PRKAR2A, 14-3-3, PKA-reg (cAMP-dependent)	
T cell chemotaxis	CCL3L1, Galpha(i)-specific peptide GPCRs, CXCL16, Galpha(q)-specific peptide GPCRs	4.23E-06
MetaCore pathways		
Cell adhesion_Chemokines and adhesion	CRK, VEGFR-2, IL8RA, Collagen IV	5.60E-03
MetaCore networks	Examples of target genes	p-value
Neurophysiological process_Transmission of nerve impulse	Galpha(i)-specific peptide GPCRs, Ionotropic glutamate receptor, GluR5, GluR2, Kainate receptor, PRKAR2A, PKA-reg (cAMP-dependent), GABARAPL1	3.59E-03
Signal transduction_WNT signaling	HB-EGF, HNF3-beta, p63, PKA-reg type II (cAMP-dependent), ERK3, PRKAR2A, PKA-reg (cAMP-dependent)	4.97E-03
Cell adhesion_Leucocyte chemotaxis	CCL3L1, Galpha(i)-specific peptide GPCRs, CXCL16, ICAP-1, PLD2, Galpha(q)-specific peptide GPCRs, IL8RA	1.06E-02
Chemotaxis	CCL3L1, Galpha(i)-specific peptide GPCRs, CXCL16, Galpha(q)-specific peptide GPCRs, IL8RA	2.34E-02

Transport_Calcium transport	Reticulocalbin 1, Ionotropic glutamate receptor, Homer 1, TRPC1, CACNA1S	7.829E-02
Inflammation_Neutrophil activation	Galpha(i)-specific peptide GPCRs, Syntaxin 1A, PLD2, IL8RA, PAK2	1.13E-01
Signal transduction_Neuropeptide signaling pathways	Neurokinin-2 receptor, Galpha(i)-specific peptide GPCRs, Galpha(q)-specific peptide GPCRs, PKA-reg (cAMP-dependent)	1.13E-01
MetaCore diseases biomarkers	Examples of target genes	p-value
Mouth Diseases	Neurokinin-2 receptor, Ro60, DTX4, FAM53C, K(+) channel, subfamily J, Syndecan-1, HSP47, FAM133B, NRAMP1, N-myristoyltransferase, CXCL16, KIAA1754L, PARD6G, VEGFR-2, G-protein beta, c-Rel (NF-kB subunit), COL4A1, GLE1, MyD88, ARPP- 21, ATP6V1G, NMT2, Ionotropic glutamate receptor, DAN, p63, PPTC7, Miro-1, CDH1, IL20RB, CSF2RB, ZFP91, Kv8.1, TRMT12, E2F7, PKA-reg type II (cAMP-dependent), RXR, GDF9, CYP19, PARD6, LRRC31, OKL38, IL8RA, TEX2, Galpha(t)-specific GPCRs, FRMPD1, CACNA1S, GPCRs, RXRG, PP2C, Collagen IV, PRKAR2A, 14-3-3, FAM46D, INTS2, CLCA4, PKA-reg (cAMP-dependent), ARNT2, Desmoplakin, DPH4, Dynamin	1.51E-05
Epilepsy, Generalized	K(+) channel, subfamily J, Galpha(i)-specific peptide GPCRs, Ionotropic glutamate receptor, GluR5, Kir3.1, Kainate receptor	2.24E-04

Table A2. Target genes for miR-500a and miR29a.

GO molecular function	Examples of target genes	p-value
interleukin-2 receptor activity and interleukin-2 binding	IL-2R alpha chain, sIL2RA	3.46E-04
cytokine receptor activity	IL-2R alpha chain, IL-15RA, sIL2RA, sIL-15RA	7.34E-03
ion channel activity	SLC26A2, ANO2, Kv1.1, CLIC4, KCNK10, GPM6A, SAP102, Kir1.1, GPR89B, GPR89A	2.97E-03
substrate-specific transmembrane transporter activity	SLC26A2, SLC44A1, SLC35E3, ANO2, Kv1.1, GLUT3, CLIC4, Embigin, KCNK10, GPM6A, SLC2A14, SAP102, C3orf55, Kir1.1, GPR89B, GPR89A, NPAL3	2.695E-03
gated channel activity	ANO2, Kv1.1, CLIC4, KCNK10, SAP102, Kir1.1, GPR89B, GPR89A	5.36E-03
voltage-gated channel activity	Kv1.1, CLIC4, KCNK10, Kir1.1, GPR89B, GPR89A	5.52E-03
voltage-gated ion channel activity	Kv1.1, CLIC4, KCNK10, Kir1.1, GPR89B, GPR89A	5.52E-03
channel activity	SLC26A2, ANO2, Kv1.1, CLIC4, KCNK10, GPM6A, SAP102, Kir1.1, GPR89B, GPR89A	6.42E-03
transmembrane transporter activity	SLC26A2, SLC44A1, SLC35E3, ANO2, Kv1.1, GLUT3, CLIC4, Embigin, KCNK10, GPM6A, SLC2A14, SAP102, C3orf55, Kir1.1, GPR89B, GPR89A, NPAL3	6.42E-03
substrate-specific transporter activity	SLC26A2, SLC44A1, SLC35E3, ANO2, Kv1.1, GLUT3, CLIC4, Embigin, PLSCR5, KCNK10, GPM6A, SLC2A14, SAP102,	6.50E-03

	C3orf55, Kir1.1, GPR89B, GPR89A, NPAL3	
passive transmembrane transporter activity	SLC26A2, ANO2, Kv1.1, CLIC4, KCNK10, GPM6A, SAP102, Kir1.1, GPR89B, GPR89A	6.50E-03
GO biological process	Examples of target genes	p-value
regulation of ion transmembrane transport	K(+) channel, subfamily J, Kv1.1, CLIC4, KCNK10, FGF12, PI3K class II, Galpha(q)-specific prostanoid GPCRs, HSP70, Galpha(q)-specific peptide GPCRs, HSPA2, PDE, Kir1.1, GPR89B, GPR89A	3.212E-05
negative regulation of leukocyte cell-cell adhesion	IL-2R alpha chain, IFN-beta, BTLA, SDF-1, PDE, PP2135, p14ARF, p16INK4	3.865E-05
negative regulation of cell activation	IL-2R alpha chain, IFN-beta, BTLA, Galpha(q)-specific prostanoid GPCRs, Galpha(q)-specific peptide GPCRs, PDE, BPI, PP2135, p14ARF, p16INK4	4.23E-05
regulation of transmembrane transport	K(+) channel, subfamily J, Kv1.1, CLIC4, KCNK10, FGF12, PI3K class II, Galpha(q)-specific prostanoid GPCRs, HSP70, Galpha(q)-specific peptide GPCRs, HSPA2, PDE, Kir1.1, GPR89B, GPR89A	4.471E-05
regulation of G-protein activated inward rectifier potassium channel activity	K(+) channel, subfamily J, Kir1.1	4.851E-05
transmembrane transport	K(+) channel, subfamily J, SLC26A2, SLC44A1, SLC35E3, TAFs, ANO2, Kv1.1, SLC25A31, CHCHD4,	5.70E-05

	GLUT3, CLIC4, Embigin, KCNK10, GPM6A, SLC2A14, HSP70, Galpha(q)-specific peptide GPCRs, PUMA, SAP102, C3orf55, PDE, Kir1.1, GPR89B, NPAL3	
negative regulation of leukocyte activation	IL-2R alpha chain, IFN-beta, BTLA, Galpha(q)-specific peptide GPCRs, PDE, BPI, PP2135, p14ARF, p16INK4	6.45E-05
negative regulation of cell growth	ING1, DEP-1, HSP70, Galpha(q)-specific peptide GPCRs, PUMA, CARF, WT1, p14ARF, p16INK4	6.648E-05
negative regulation of cell-cell adhesion	IL-2R alpha chain, IFN-beta, BTLA, Galpha(q)-specific prostanoid GPCRs, SDF-1, PDE, PP2135, p14ARF, p16INK4	6.65E-05
negative regulation of cell proliferation	IL-2R alpha chain, NOXA, TAFs, E3b1(ABI-1), FBXW7, ING1, DEP-1, Adrenomedullin, BTLA, HSP70, Galpha(q)-specific peptide GPCRs, Skp2/TrCP/FBXW, SAP102, PDE, PP2135, WT1, p14ARF, CDK6, p16INK4	8.76E-05
regulation of macrophage apoptotic process	Galpha(q)-specific peptide GPCRs, p14ARF, p16INK4	1.432E-04
MetaCore pathways	Examples of target genes	p-value
Immune response_T cell subsets: cell surface markers	IL-2R alpha chain, IL-15RA, BTLA	1.49E-03
Immune response_IL-16 signaling pathway	IL-2R alpha chain, Skp2/TrCP/FBXW, SDF-1	1.75E-03

Immune response_IL-15 signaling via JAK-STAT cascade	IL-15RA, sIL-15RA	4.08E-03
Impaired Lipoxin A4 signaling in CF	SOCS2, FPRL1	1.572E-02
Development_Lipoxin inhibitory action on PDGF, EGF and LTD4 signaling	SOCS2, FPRL1	1.071E-02
MetaCore networks	Examples of target genes	p-value
Inflammation_Jak-STAT Pathway	IL-15RA, SOCS2, IFN-beta, SDF-1	8.12E-02
Transport_Potassium transport	K(+) channel, subfamily J, Kv1.1, KCNK10, Kir1.1	9.15E-02
Chemotaxis	FPRL1, Galpha(q)-specific peptide GPCRs, SDF-1	1.20E-01

Appendix 2: Details of the rat diet used in this thesis.

Harlan Laboratories

2018

Teklad Global 18% Protein Rodent Diet

Product Description- 2018 is a fixed formula, non-autoclavable diet manufactured with high quality ingredients and designed to support gestation, lactation, and growth of rodents. 2018 does not contain alfalfa, thus lowering the occurrence of natural phytoestrogens. Typical isoflavone concentrations (daidzein + genistein aglycone equivalents) range from 150 to 250 mg/kg. Exclusion of alfalfa reduces chlorophyll, improving optical imaging clarity. Absence of animal protein and fish meal minimizes the presence of nitrosamines. Also available certified (2018C) and irradiated (2918). For autoclavable diet, refer to 2018S (Sterilizable) or 2018SX (Extruded & Sterilizable).

Ingredients (in descending order of inclusion)- Ground wheat, ground corn, wheat middlings, dehulled soybean meal, corn gluten meal, soybean oil, calcium carbonate, dicalcium phosphate, brewers dried yeast, iodized salt, L-lysine, DL-methionine, choline chloride, kaolin, magnesium oxide, vitamin E acetate, menadione sodium bisulfite complex (source of vitamin K activity), manganese oxide, ferrous sulfate, zinc oxide, niacin, calcium pantothenate, copper sulfate, pyridoxine hydrochloride, riboflavin, thiamin mononitrate, vitamin A acetate, calcium iodate, vitamin B₁₂ supplement, folic acid, biotin, vitamin D₃ supplement, cobalt carbonate.

Macronutrients		
Crude Protein	%	18.6
Fat (ether extract) ^a	%	6.2
Carbohydrate (available) ^b	%	44.2
Crude Fiber	%	3.5
Neutral Detergent Fiber ^c	%	14.7
Ash	%	5.3
Energy Density ^d	kcal/g (kJ/g)	3.1 (13.0)
Calories from Protein	%	24
Calories from Fat	%	18
Calories from Carbohydrate	%	58
Minerals		
Calcium	%	1.0
Phosphorus	%	0.7
Non-Phytate Phosphorus	%	0.4
Sodium	%	0.2
Potassium	%	0.6
Chloride	%	0.4
Magnesium	%	0.2
Zinc	mg/kg	70
Manganese	mg/kg	100
Copper	mg/kg	15
Iodine	mg/kg	6
Iron	mg/kg	200
Selenium	mg/kg	0.23
Amino Acids		
Aspartic Acid	%	1.4
Glutamic Acid	%	3.4
Alanine	%	1.1
Glycine	%	0.8
Threonine	%	0.7
Proline	%	1.6
Serine	%	1.1
Leucine	%	1.8
Isoleucine	%	0.8
Valine	%	0.9
Phenylalanine	%	1.0
Tyrosine	%	0.6
Methionine	%	0.4
Cystine	%	0.3
Lysine	%	0.9
Histidine	%	0.4
Arginine	%	1.0
Tryptophan	%	0.2

Standard Product Form: Pellet

Vitamins		
Vitamin A ^{e,f}	IU/g	15.0
Vitamin D ₃ ^{g,h}	IU/g	1.5
Vitamin E	IU/kg	110
Vitamin K ₃ (menadione)	mg/kg	50
Vitamin B ₁ (thiamin)	mg/kg	17
Vitamin B ₂ (riboflavin)	mg/kg	15
Niacin (nicotinic acid)	mg/kg	70
Vitamin B ₆ (pyridoxine)	mg/kg	18
Pantothenic Acid	mg/kg	33
Vitamin B ₁₂ (cyanocobalamin)	mg/kg	0.08
Biotin	mg/kg	0.40
Folate	mg/kg	4
Choline	mg/kg	1200
Fatty Acids		
C16:0 Palmitic	%	0.7
C18:0 Stearic	%	0.2
C18:1ω9 Oleic	%	1.2
C18:2ω6 Linoleic	%	3.1
C18:3ω3 Linolenic	%	0.3
Total Saturated	%	0.9
Total Monounsaturated	%	1.3
Total Polyunsaturated	%	3.4
Other		
Cholesterol	mg/kg	--

^a Ether extract is used to measure fat in pelleted diets, while an acid hydrolysis method is required to recover fat in extruded diets. Compared to ether extract, the fat value for acid hydrolysis will be approximately 1% point higher.

^b Carbohydrate (available) is calculated by subtracting neutral detergent fiber from total carbohydrates.

^c Neutral detergent fiber is an estimate of insoluble fiber, including cellulose, hemicellulose, and lignin. Crude fiber methodology underestimates total fiber.

^d Energy density is a calculated estimate of metabolizable energy based on the Atwater factors assigning 4 kcal/g to protein, 9 kcal/g to fat, and 4 kcal/g to available carbohydrate.

^e Indicates added amount but does not account for contribution from other ingredients.

^f 1 IU vitamin A = 0.3 µg retinol

^g 1 IU vitamin D = 25 ng cholecalciferol

For nutrients not listed, insufficient data is available to quantify.

Nutrient data represent the best information available, calculated from published values and direct analytical testing of raw materials and finished product. Nutrient values may vary due to the natural variations in the ingredients, analysis, and effects of processing.

Teklad Diets are designed and manufactured for research purposes only.

Harlan, Harlan Laboratories, Helping you do research better, and the Harlan logo are trademarks and trade names of Harlan Laboratories, Inc. © 2008 Harlan Laboratories, Inc.

harlanTM
Helping you do research better



Teklad Diets, Madison WI | www.harlan.com | tekkladinfo@harlan.com | (800) 483-5523

RMS-0906-US-EN-02-DS-2018

Figure A1. Details of the rat diet.

REFERENCES

- ABD-ELSAIED, A. A., IKEDA, R., JIA, Z., LING, J., ZUO, X., LI, M. & GU, J. G. 2015. KCNQ channels in nociceptive cold-sensing trigeminal ganglion neurons as therapeutic targets for treating orofacial cold hyperalgesia. *Molecular pain*, 11, 45.
- ABDELMOATY, S., WIGERBLAD, G., BAS, D. B., CODELUPPI, S., FERNANDEZ-ZAFRA, T., EL-AWADY, E.-S., MOUSTAFA, Y., ABDELHAMID, A. L.-D., BRODIN, E. & SVENSSON, C. I. 2013. Spinal actions of lipoxin A4 and 17(R)-resolvin D1 attenuate inflammation-induced mechanical hypersensitivity and spinal TNF release. *PLoS One*, 8, e75543.
- AGARWAL, V., BELL, G. W., NAM, J.-W. & BARTEL, D. P. 2015. Predicting effective microRNA target sites in mammalian mRNAs. *Elife*, 4, e05005.
- AHMADI, S., LIPPROSS, S., NEUHUBER, W. L. & ZEILHOFER, H. U. 2002. PGE2 selectively blocks inhibitory glycinergic neurotransmission onto rat superficial dorsal horn neurons. *Nature Neuroscience*, 5, 34-40.
- ALESSANDRI-HABER, N., DINA, O. A., CHEN, X. & LEVINE, J. D. 2009. TRPC1 and TRPC6 channels cooperate with TRPV4 to mediate mechanical hyperalgesia and nociceptor sensitization. *Journal of Neuroscience*, 29, 6217-6228.
- ALESSANDRI-HABER, N., DINA, O. A., JOSEPH, E. K., REICHLING, D. & LEVINE, J. D. 2006. A Transient Receptor Potential Vanilloid 4-Dependent Mechanism of Hyperalgesia Is Engaged by Concerted Action of Inflammatory Mediators. *The Journal of Neuroscience*, 26, 3864-3874.
- ANDOH, T. & KURASHI, Y. 2005. Expression of BLT1 leukotriene B 4 receptor on the dorsal root ganglion neurons in mice. *Molecular brain research*, 137, 263-266.
- ARITA, M., BIANCHINI, F., ALIBERTI, J., SHER, A., CHIANG, N., HONG, S., YANG, R., PETASIS, N. A. & SERHAN, C. N. 2005a. Stereochemical assignment, antiinflammatory properties, and receptor for the omega-3 lipid mediator resolvin E1. *J Exp Med*, 201, 713-22.
- ARITA, M., CLISH, C. B. & SERHAN, C. N. 2005b. The contributions of aspirin and microbial oxygenase to the biosynthesis of anti-inflammatory resolvins: novel oxygenase products from omega-3 polyunsaturated fatty acids. *Biochem Biophys Res Commun*, 338, 149-57.
- ARITA, M., OH, S. F., CHONAN, T., HONG, S., ELANGO VAN, S., SUN, Y.-P., UDDIN, J., PETASIS, N. A. & SERHAN, C. N. 2006. Metabolic Inactivation of Resolvin E1 and Stabilization of Its Anti-inflammatory Actions. *Journal of Biological Chemistry*, 281, 22847-22854.
- ARITA, M., OHIRA, T., SUN, Y. P., ELANGO VAN, S., CHIANG, N. & SERHAN, C. N. 2007. Resolvin E1 Selectively Interacts with Leukotriene B4 Receptor BLT1 and ChemR23 to Regulate Inflammation. *The Journal of Immunology*, 178, 3912-3917.
- ASAHARA, M., ITO, N., YOKOMIZO, T., NAKAMURA, M., SHIMIZU, T. & YAMADA, Y. 2015. The absence of the leukotriene B 4 receptor BLT1 attenuates peripheral inflammation and spinal nociceptive processing following intraplantar formalin injury. *Molecular pain*, 11, 11.
- ATKINS, S. 03/05/2017 2017. RE: Incidence of lingual nerve injury, personal communication.

- BÄCK, M., POWELL, W. S., DAHLÉN, S.-E., DRAZEN, J. M., EVANS, J. F., SERHAN, C. N., SHIMIZU, T., YOKOMIZO, T. & ROVATI, G. E. 2014. Update on leukotriene, lipoxin and oxoeicosanoid receptors: IUPHAR Review 7. *British Journal of Pharmacology*, 171, 3551-3574.
- BAI, G., AMBALAVANAR, R., WEI, D. & DESSEM, D. 2007. Downregulation of selective microRNAs in trigeminal ganglion neurons following inflammatory muscle pain. *Molecular Pain*, 3, 15.
- BANDELL, M., STORY, G. M., HWANG, S. W., VISWANATH, V., EID, S. R., PETRUS, M. J., EARLEY, T. J. & PATAPOUTIAN, A. 2004. Noxious Cold Ion Channel TRPA1 Is Activated by Pungent Compounds and Bradykinin. *Neuron*, 41, 849-857.
- BANNENBERG, G., ARITA, M. & SERHAN, C. N. 2007. Endogenous receptor agonists: resolving inflammation. *ScientificWorldJournal*, 7, 1440-62.
- BANNENBERG, G. & SERHAN, C. N. 2010. Specialized pro-resolving lipid mediators in the inflammatory response: An update. *Biochim Biophys Acta*, 1801, 1260-73.
- BANNENBERG, G. L., CHIANG, N., ARIEL, A., ARITA, M., TJONAHEN, E., GOTLINGER, K. H., HONG, S. & SERHAN, C. N. 2005. Molecular Circuits of Resolution: Formation and Actions of Resolvins and Protectins. *The Journal of Immunology*, 174, 4345-4355.
- BARCLAY, J., PATEL, S., DORN, G., WOTHERSPOON, G., MOFFATT, S., EUNSON, L., ABDEL'AL, S., NATT, F., HALL, J., WINTER, J., BEVAN, S., WISHART, W., FOX, A. & GANJU, P. 2002. Functional Downregulation of P2X3 Receptor Subunit in Rat Sensory Neurons Reveals a Significant Role in Chronic Neuropathic and Inflammatory Pain. *The Journal of Neuroscience*, 22, 8139-8147.
- BARTEL, D. P. 2004. MicroRNAs: genomics, biogenesis, mechanism, and function. *cell*, 116, 281-297.
- BARTEL, D. P. 2009. MicroRNAs: target recognition and regulatory functions. *cell*, 136, 215-233.
- BARTOSHUK, L. M., SNYDER, D. J., GRUSHKA, M., BERGER, A. M., DUFFY, V. B. & KVETON, J. F. 2005. Taste damage: previously unsuspected consequences. *Chemical senses*, 30, i218-i219.
- BASBAUM, A. I., BAUTISTA, D. M., SCHERRER, G. & JULIUS, D. 2009. Cellular and molecular mechanisms of pain. *Cell*, 139, 267-284.
- BASBAUM, A. I. & WOOLF, C. J. 1999. Pain. *Current Biology*, 9, R429-R431.
- BENNETT, G. J. & XIE, Y.-K. 1988. A peripheral mononeuropathy in rat that produces disorders of pain sensation like those seen in man. *Pain*, 33, 87-107.
- BENNETT, M. I. & SIMPSON, K. H. 2004. Gabapentin in the treatment of neuropathic pain. *Palliative Medicine*, 18, 5-11.
- BERTA, T. 2014. Extracellular caspase-6 drives murine inflammatory pain via microglial TNF-alpha secretion. *J Clin Invest*, 124.
- BHALALA, O. G., PAN, L., SAHNI, V., MCGUIRE, T. L., GRUNER, K., TOURTELLOTTE, W. G. & KESSLER, J. A. 2012. microRNA-21 Regulates Astrocytic Response Following Spinal Cord Injury. *The Journal of Neuroscience*, 32, 17935-17947.
- BHAVE, G. & GEREAU, R. W. T. 2004. Posttranslational mechanisms of peripheral sensitization. *J Neurobiol*, 61, 88-106.
- BIANCO, F., PRAVETTONI, E., COLOMBO, A., SCHENK, U., MÖLLER, T., MATTEOLI, M. & VERDERIO, C. 2005. Astrocyte-derived ATP induces vesicle

- shedding and IL-1 β release from microglia. *The Journal of Immunology*, 174, 7268-7277.
- BIGGS, J. E., YATES, J. M., LOESCHER, A. R., CLAYTON, N. M., BOISSONADE, F. M. & ROBINSON, P. P. 2007a. Changes in vanilloid receptor 1 (TRPV1) expression following lingual nerve injury. *European Journal of Pain*, 11, 192-201.
- BIGGS, J. E., YATES, J. M., LOESCHER, A. R., CLAYTON, N. M., BOISSONADE, F. M. & ROBINSON, P. P. 2007b. Vanilloid receptor 1 (TRPV1) expression in lingual nerve neuromas from patients with or without symptoms of burning pain. *Brain Research*, 1127, 59-65.
- BIRD, E., BOISSONADE, F. & ROBINSON, P. 2003. Neuropeptide expression following ligation of the ferret lingual nerve. *Archives of oral biology*, 48, 541-546.
- BIRD, E., CHRISTMAS, C., LOESCHER, A., SMITH, K., ROBINSON, P., BLACK, J., WAXMAN, S. & BOISSONADE, F. 2013. Correlation of Nav1.8 and Nav1.9 sodium channel expression with neuropathic pain in human subjects with lingual nerve neuromas. *Molecular Pain*, 9, 52.
- BIRD, E. V. 2004. *Immunocytochemical studies on neuromas of branches of the trigeminal nerve*. PhD, University of Sheffield.
- BIRD, E. V., LONG, A., BOISSONADE, F. M., FRIED, K. & ROBINSON, P. P. 2002. Neuropeptide expression following constriction or section of the inferior alveolar nerve in the ferret. *Journal of the Peripheral Nervous System*, 7, 168-180.
- BIRD, E. V., ROBINSON, P. P. & BOISSONADE, F. M. 2007. Nav1.7 sodium channel expression in human lingual nerve neuromas. *Archives of Oral Biology*, 52, 494-502.
- BLACK, J. A., CUMMINS, T. R., PLUMPTON, C., CHEN, Y. H., HORMUZDIAR, W., CLARE, J. J. & WAXMAN, S. G. 1999. Upregulation of a silent sodium channel after peripheral, but not central, nerve injury in DRG neurons. *Journal of Neurophysiology*, 82, 2776-2785.
- BLEEHEN, T. & KEELE, C. A. 1977. Observations on the algogenic actions of adenosine compounds on the human blister base preparation. *Pain*, 3, 367-377.
- BOHR, S., PATEL, S. J., SARIN, D., IRIMIA, D., YARMUSH, M. L. & BERTHIAUME, F. 2013. Resolvin D2 prevents secondary thrombosis and necrosis in a mouse burn wound model. *Wound Repair Regen*, 21, 35-43.
- BONDUE, B., WITTAMER, V. & PARMENTIER, M. 2011. Chemerin and its receptors in leukocyte trafficking, inflammation and metabolism. *Cytokine & Growth Factor Reviews*, 22, 331-338.
- BONGENHIELM, U. & ROBINSON, P. 1996. Spontaneous and mechanically evoked afferent activity originating from myelinated fibres in ferret inferior alveolar nerve neuromas. *Pain*, 67, 399-406.
- BONGENHIELM, U. & ROBINSON, P. 1998. Afferent activity from myelinated inferior alveolar nerve fibres in ferrets after constriction or section and regeneration. *Pain*, 74, 123-132.
- BOUCHER, Y., CARSTENS, M. I., SAWYER, C. M., ZANOTTO, K. L., MERRILL, A. W. & CARSTENS, E. 2013. Capsaicin avoidance as a measure of chemical hyperalgesia in orofacial nerve injury models. *Neuroscience letters*, 543, 37-41.
- BOUCHER, Y., SIMONS, C. T., CARSTENS, M. I. & CARSTENS, E. 2014. Effects of gustatory nerve transection and/or ovariectomy on oral capsaicin avoidance in rats. *PAIN®*, 155, 814-820.

- BOWLER, K. E., WORSLEY, M. A., BROAD, L., SHER, E., BENSCHOP, R., JOHNSON, K., BOISSONADE, F. M., ROBINSON, P. P. & YATES, J. M. 2011. The effect of a monoclonal antibody to calcitonin-gene related peptide (CGRP) on injury-induced ectopic discharge following lingual nerve injury. *Neuroscience letters*, 505, 146-149.
- BURNSTOCK, G. & WOOD, J. N. 1996. Purinergic receptors: their role in nociception and primary afferent neurotransmission. *Current Opinion in Neurobiology*, 6, 526-532.
- BURR, G. O. B. A. M. M. 1929. A new deficiency disease produced by the rigid exclusion of fat from the diet. *The Journal of Biological Chemistry*, LXXXII, No. 2, 82:345-367.
- BUSSEROLLES, J., TSANTOULAS, C., ESCHALIER, A. & GARCÍA, J. A. L. 2016. Potassium channels in neuropathic pain: advances, challenges, and emerging ideas. *Pain*, 157, S7-S14.
- CAHILL, C. M., XUE, L., GRENIER, P., MAGNUSSEN, C., LECOUR, S. & OLMSTEAD, M. C. 2013. Changes in morphine reward in a model of neuropathic pain. *Behavioural pharmacology*, 24, 207-213.
- CARLTON, S. M., ZHOU, S. & COGGESHALL, R. E. 1996. Localization and activation of substance P receptors in unmyelinated axons of rat glabrous skin. *Brain research*, 734, 103-108.
- CASH, J. L., HART, R., RUSS, A., DIXON, J. P. C., COLLEDGE, W. H., DORAN, J., HENDRICK, A. G., CARLTON, M. B. L. & GREAVES, D. R. 2008. Synthetic chemerin-derived peptides suppress inflammation through ChemR23. *The Journal of Experimental Medicine*, 205, 767-775.
- CATERINA, M. J., LEFFLER, A., MALMBERG, A. B., MARTIN, W. J., TRAFTON, J., PETERSEN-ZEITZ, K. R., KOLTZENBURG, M., BASBAUM, A. I. & JULIUS, D. 2000. Impaired Nociception and Pain Sensation in Mice Lacking the Capsaicin Receptor. *Science*, 288, 306-313.
- CHA, M., KOHAN, K. J., ZUO, X., LING, J. X. & GU, J. G. 2012. Assessment of chronic trigeminal neuropathic pain by the orofacial operant test in rats. *Behavioural brain research*, 234, 82-90.
- CHEN, H.-P., ZHOU, W., KANG, L.-M., YAN, H., ZHANG, L., XU, B.-H. & CAI, W.-H. 2014. Intrathecal miR-96 Inhibits Nav1.3 Expression and Alleviates Neuropathic Pain in Rat Following Chronic Construction Injury. *Neurochemical Research*, 39, 76-83.
- CHENG, J. K. & JI, R. R. 2008. Intracellular signaling in primary sensory neurons and persistent pain. *Neurochem Res*, 33, 1970-8.
- CHESLER, E. J., WILSON, S. G., LARIVIERE, W. R., RODRIGUEZ-ZAS, S. L. & MOGIL, J. S. 2002. Identification and ranking of genetic and laboratory environment factors influencing a behavioral trait, thermal nociception, via computational analysis of a large data archive. *Neuroscience & Biobehavioral Reviews*, 26, 907-923.
- CHEUNG, L. K., LEUNG, Y., CHOW, L., WONG, M., CHAN, E. & FOK, Y. 2010. Incidence of neurosensory deficits and recovery after lower third molar surgery: a prospective clinical study of 4338 cases. *International journal of oral and maxillofacial surgery*, 39, 320-326.
- CHIANG, H. R., SCHOENFELD, L. W., RUBY, J. G., AUYEUNG, V. C., SPIES, N., BAEK, D., JOHNSTON, W. K., RUSS, C., LUO, S. & BABIARZ, J. E. 2010. Mammalian microRNAs: experimental evaluation of novel and previously annotated genes. *Genes & development*, 24, 992-1009.

- CHIANG, N., FREDMAN, G., BACKHED, F., OH, S. F., VICKERY, T., SCHMIDT, B. A. & SERHAN, C. N. 2012. Infection regulates pro-resolving mediators that lower antibiotic requirements. *Nature*, 484, 524-528.
- CHIANG, N., SERHAN, C. N., DAHLÉN, S.-E., DRAZEN, J. M., HAY, D. W., ROVATI, G. E., SHIMIZU, T., YOKOMIZO, T. & BRINK, C. 2006. The lipoxin receptor ALX: potent ligand-specific and stereoselective actions in vivo. *Pharmacological reviews*, 58, 463-487.
- CHIANG, N., TAKANO, T., ARITA, M., WATANABE, S. & SERHAN, C. N. 2003. A novel rat lipoxin A4 receptor that is conserved in structure and function. *British Journal of Pharmacology*, 139, 89-98.
- CHOI, Y.-J., KIM, J. Y., JIN, W.-P., KIM, Y.-T., JAHNG, J. W. & LEE, J.-H. 2013. Disruption of oral sensory relay to brain increased anxiety-and depression-like behaviours in rats. *Archives of oral biology*, 58, 1652-1658.
- CHRISTODOULOU, F., RAIBLE, F., TOMER, R., SIMAKOV, O., TRACHANA, K., KLAUS, S., SNYMAN, H., HANNON, G. J., BORK, P. & ARENDT, D. 2010. Ancient animal microRNAs and the evolution of tissue identity. *Nature*, 463, 1084-1088.
- COLAS, R. A., SHINOHARA, M., DALLI, J., CHIANG, N. & SERHAN, C. N. 2014. Identification and signature profiles for pro-resolving and inflammatory lipid mediators in human tissue. *Am J Physiol Cell Physiol*.
- COLBURN, R., DELEO, J., RICKMAN, A., YEAGER, M., KWON, P. & HICKEY, W. 1997. Dissociation of microglial activation and neuropathic pain behaviors following peripheral nerve injury in the rat. *Journal of neuroimmunology*, 79, 163-175.
- COLBURN, R., RICKMAN, A. & DELEO, J. 1999. The effect of site and type of nerve injury on spinal glial activation and neuropathic pain behavior. *Experimental neurology*, 157, 289-304.
- COLLOCA, L., LUDMAN, T., BOUHASSIRA, D., BARON, R., DICKENSON, A. H., YARNITSKY, D., FREEMAN, R., TRUINI, A., ATTAL, N., FINNERUP, N. B., ECCLESTON, C., KALSO, E., BENNETT, D. L., DWORKIN, R. H. & RAJA, S. N. 2017. Neuropathic pain. *Nature reviews. Disease primers*, 3, 17002-17002.
- CONNOR, W. E. 2000. Importance of n-3 fatty acids in health and disease. *The American Journal of Clinical Nutrition*, 71, 171S-175S.
- COORAY, S. N., GOBBETTI, T., MONTERO-MELENDEZ, T., MCARTHUR, S., THOMPSON, D., CLARK, A. J., FLOWER, R. J. & PERRETTI, M. 2013. Ligand-specific conformational change of the G-protein-coupled receptor ALX/FPR2 determines proresolving functional responses. *Proceedings of the National Academy of Sciences*, 110, 18232-18237.
- COSTIGAN, M., SCHOLZ, J. & WOOLF, C. J. 2009. Neuropathic pain: a maladaptive response of the nervous system to damage. *Annu Rev Neurosci*, 32, 1-32.
- COULL, J. A. M., BEGGS, S., BOUDREAU, D., BOIVIN, D., TSUDA, M., INOUE, K., GRAVEL, C., SALTER, M. W. & DE KONINCK, Y. 2005. BDNF from microglia causes the shift in neuronal anion gradient underlying neuropathic pain. *Nature*, 438, 1017-1021.
- COWARD, K., PLUMPTON, C., FACER, P., BIRCH, R., CARLSTEDT, T., TATE, S., BOUNTRA, C. & ANAND, P. 2000. Immunolocalization of SNS/PN3 and NaN/SNS2 sodium channels in human pain states. *Pain*, 85, 41-50.
- CROWN, E. D. 2012. The role of mitogen activated protein kinase signaling in microglia and neurons in the initiation and maintenance of chronic pain. *Experimental neurology*, 234, 330-339.

- DALLI, J., WINKLER, J. W., COLAS, R. A., ARNARDOTTIR, H., CHENG, C.-Y. C., CHIANG, N., PETASIS, N. A. & SERHAN, C. N. 2013. Resolvin D3 and aspirin-triggered resolvin D3 are potent immunoresolvents. *Chemistry & biology*, 20, 188-201.
- DAVENPORT, A. P., ALEXANDER, S. P. H., SHARMAN, J. L., PAWSON, A. J., BENSON, H. E., MONAGHAN, A. E., LIEW, W. C., MPAMHANGA, C. P., BONNER, T. I., NEUBIG, R. R., PIN, J. P., SPEDDING, M. & HARMAR, A. J. 2013. International Union of Basic and Clinical Pharmacology. LXXXVIII. G Protein-Coupled Receptor List: Recommendations for New Pairings with Cognate Ligands. *Pharmacological Reviews*, 65, 967-986.
- DAVIES, S. L., LOESCHER, A. R., CLAYTON, N. M., BOUNTRA, C., ROBINSON, P. P. & BOISSONADE, F. M. 2006. Changes in sodium channel expression following trigeminal nerve injury. *Experimental Neurology*, 202, 207-216.
- DE POORTER, C., BAERTSOEN, K., LANNOY, V., PARMENTIER, M. & SPRINGAEL, J.-Y. 2013. Consequences of ChemR23 Heteromerization with the Chemokine Receptors CXCR4 and CCR7. *PLoS ONE*, 8, e58075.
- DEMOOR, T., BRACKE, K. R., DUPONT, L. L., PLANTINGA, M., BONDUE, B., ROY, M.-O., LANNOY, V., LAMBRECHT, B. N., BRUSSELLE, G. G. & JOOS, G. F. 2011. The role of ChemR23 in the induction and resolution of cigarette smoke-induced inflammation. *The Journal of immunology*, 186, 5457-5467.
- DEVCHAND, P. R., ARITA, M., HONG, S., BANNENBERG, G., MOUSSIGNAC, R.-L., GRONERT, K. & SERHAN, C. N. 2003. Human ALX receptor regulates neutrophil recruitment in transgenic mice: roles in inflammation and host defense. *The FASEB Journal*, 17, 652-659.
- DEVOR, M., GOVRIN-LIPPMANN, R. & ANGELIDES, K. 1993. Na⁺ channel immunolocalization in peripheral mammalian axons and changes following nerve injury and neuroma formation. *Journal of Neuroscience*, 13, 1976-1992.
- DEVOR, M., KELLER, C. H., DEERINCK, T. J., LEVINSON, S. R. & ELLISMAN, M. H. 1989. Na⁺ channel accumulation on axolemma of afferent endings in nerve end neuromas in *Apteronotus*. *Neuroscience Letters*, 102, 149-154.
- DIB-HAJJ, S. D., FJELL, J., CUMMINS, T. R., ZHENG, Z., FRIED, K., LAMOTTE, R., BLACK, J. A. & WAXMAN, S. G. 1999. Plasticity of sodium channel expression in DRG neurons in the chronic constriction injury model of neuropathic pain. *Pain*, 83, 591-600.
- DING, H.-K., SHUM, F. W., KO, S. W. & ZHUO, M. 2005. A new assay of thermal-based avoidance test in freely moving mice. *The Journal of Pain*, 6, 411-416.
- DOLAN, J. C., LAM, D. K., ACHDJIAN, S. H. & SCHMIDT, B. L. 2010. The dolognawmeter: a novel instrument and assay to quantify nociception in rodent models of orofacial pain. *Journal of neuroscience methods*, 187, 207-215.
- DOLESHAL, M., MAGOTRA, A. A., CHOUDHURY, B., CANNON, B. D., LABOURIER, E. & SZAFRANSKA, A. E. 2008. Evaluation and validation of total RNA extraction methods for microRNA expression analyses in formalin-fixed, paraffin-embedded tissues. *The Journal of Molecular Diagnostics*, 10, 203-211.
- DUFTON, N. & PERRETTI, M. 2010. Therapeutic anti-inflammatory potential of formyl-peptide receptor agonists. *Pharmacology & Therapeutics*, 127, 175-188.
- DUNN, P. M., ZHONG, Y. & BURNSTOCK, G. 2001. P2X receptors in peripheral neurons. *Progress in Neurobiology*, 65, 107-134.

- DWORKIN, R. H., BACKONJA, M., ROWBOTHAM, M. C., ALLEN, R. R., ARGOFF, C. R., BENNETT, G. J., BUSHNELL, M. C., FARRAR, J. T., GALER, B. S., HAYTHORNTHWAITE, J. A., HEWITT, D. J., LOESER, J. D., MAX, M. B., SALTARELLI, M., SCHMADER, K. E., STEIN, C., THOMPSON, D., TURK, D. C., WALLACE, M. S., WATKINS, L. R. & WEINSTEIN, S. M. 2003. Advances in Neuropathic Pain: Diagnosis, Mechanisms, and Treatment Recommendations. *Archives of Neurology*, 60, 1524-1534.
- EVANS, L. J., LOESCHER, A. R., BOISSONADE, F. M., WHAWELL, S. A., ROBINSON, P. P. & ANDREW, D. 2014. Temporal mismatch between pain behaviour, skin Nerve Growth Factor and intra-epidermal nerve fibre density in trigeminal neuropathic pain. *BMC neuroscience*, 15, 1.
- FABBRETTI, E. 2013. ATP P2X3 receptors and neuronal sensitization. *Frontiers in Cellular Neuroscience*, 7.
- FAVEREAUX, A., THOUMINE, O., BOUALI-BENAZZOZ, R., ROQUES, V., PAPON, M. A., SALAM, S. A., DRUTEL, G., LÉGER, C., CALAS, A., NAGY, F. & LANDRY, M. 2011. Bidirectional integrative regulation of Cav1.2 calcium channel by microRNA miR-103: Role in pain. *EMBO Journal*, 30, 3830-3841.
- FIGLIORE, S., MADDOX, J. F., PEREZ, H. D. & SERHAN, C. N. 1994. Identification of a human cDNA encoding a functional high affinity lipoxin A4 receptor. *The Journal of Experimental Medicine*, 180, 253-260.
- FOSSAT, P., DOBREMEZ, E., BOUALI-BENAZZOZ, R., FAVÉREAU, A., BERTRAND, S. S., KILK, K., LÉGER, C., CAZALETS, J. R., LANGEL, Ü., LANDRY, M. & NAGY, F. 2010. Knockdown of L calcium channel subtypes: Differential effects in neuropathic pain. *Journal of Neuroscience*, 30, 1073-1085.
- FOSTER, T. S. 2007. Efficacy and safety of α -lipoic acid supplementation in the treatment of symptomatic diabetic neuropathy. *The Diabetes Educator*, 33, 111-117.
- FRADE, J. M. & BARDE, Y.-A. 1998. Nerve growth factor: two receptors, multiple functions. *BioEssays*, 20, 137-145.
- FREDERICK, J., BUCK, M. E., MATSON, D. J. & CORTRIGHT, D. N. 2007. Increased TRPA1, TRPM8, and TRPV2 expression in dorsal root ganglia by nerve injury. *Biochemical and Biophysical Research Communications*, 358, 1058-1064.
- FREDMAN, G., LI, Y., DALLI, J., CHIANG, N. & SERHAN, C. N. 2012. Self-limited versus delayed resolution of acute inflammation: temporal regulation of pro-resolving mediators and microRNA. *Sci Rep*, 2, 639.
- FREDMAN, G., OZCAN, L., SPOLITU, S., HELLMANN, J., SPITE, M., BACKS, J. & TABAS, I. 2014. Resolvin D1 limits 5-lipoxygenase nuclear localization and leukotriene B4 synthesis by inhibiting a calcium-activated kinase pathway. *Proceedings of the National Academy of Sciences*, 111, 14530-14535.
- FREIRE, M. O. & VAN DYKE, T. E. 2013. Natural resolution of inflammation. *Periodontol 2000*, 63, 149-64.
- FREIRE, V. S., BURKHARD, F. C., KESSLER, T. M., KUHN, A., DRAEGER, A. & MONASTYRSKAYA, K. 2010. MicroRNAs may mediate the down-regulation of neurokinin-1 receptor in chronic bladder pain syndrome. *The American journal of pathology*, 176, 288-303.
- FRIEDMAN, R. C., FARH, K. K.-H., BURGE, C. B. & BARTEL, D. P. 2009. Most mammalian mRNAs are conserved targets of microRNAs. *Genome research*, 19, 92-105.
- GALÁN-ARRIERO, I., SERRANO-MUÑOZ, D., GÓMEZ-SORIANO, J., GOICOECHEA, C., TAYLOR, J., VELASCO, A. & ÁVILA-MARTÍN, G. 2017.

- The role of Omega-3 and Omega-9 fatty acids for the treatment of neuropathic pain after neurotrauma. Elsevier.
- GAUDET, A. D., POPOVICH, P. G. & RAMER, M. S. 2011. Wallerian degeneration: gaining perspective on inflammatory events after peripheral nerve injury. *Journal of neuroinflammation*, 8, 110.
- GAVVA, N. R., TREANOR, J. J., GARAMI, A., FANG, L., SURAPANENI, S., AKRAMI, A., ALVAREZ, F., BAK, A., DARLING, M. & GORE, A. 2008. Pharmacological blockade of the vanilloid receptor TRPV1 elicits marked hyperthermia in humans. *Pain*, 136, 202-210.
- GENDA, Y., ARAI, M., ISHIKAWA, M., TANAKA, S., OKABE, T. & SAKAMOTO, A. 2013. microRNA changes in the dorsal horn of the spinal cord of rats with chronic constriction injury: A TaqMan® Low Density Array study. *International journal of molecular medicine*, 31, 129-137.
- GISSI 1999. Dietary supplementation with n-3 polyunsaturated fatty acids and vitamin E after myocardial infarction: results of the GISSI-Prevenzione trial. *The Lancet*, 354, 447-455.
- GOLD, M. S. & GEBHART, G. F. 2010. Nociceptor sensitization in pain pathogenesis. *Nat Med*, 16, 1248-57.
- GOLDMAN, D. W. & GOETZL, E. J. 1984. Heterogeneity of human polymorphonuclear leukocyte receptors for leukotriene B₄. Identification of a subset of high affinity receptors that transduce the chemotactic response. *The Journal of Experimental Medicine*, 159, 1027-1041.
- GRACE, P. M., HUTCHINSON, M. R., MAIER, S. F. & WATKINS, L. R. 2014. Pathological pain and the neuroimmune interface. *Nat Rev Immunol*, 14, 217-31.
- GRAEBER, M. B., STREIT, W. J. & KREUTZBERG, G. W. 1988. The microglial cytoskeleton: vimentin is localized within activated cells in situ. *Journal of neurocytology*, 17, 573-580.
- GREGORY, R., CHENDRIMADA, T. & SHIEKHATTAR, R. 2006. MicroRNA Biogenesis: Isolation and Characterization of the Microprocessor Complex. In: YING, S.-Y. (ed.) *MicroRNA Protocols*. Humana Press.
- GRIMSON, A., FARH, K. K.-H., JOHNSTON, W. K., GARRETT-ENGELE, P., LIM, L. P. & BARTEL, D. P. 2007. MicroRNA targeting specificity in mammals: determinants beyond seed pairing. *Molecular cell*, 27, 91-105.
- GUILLOT, X., SEMERANO, L., DECKER, P., FALGARONE, G. & BOISSIER, M. C. 2012. Pain and immunity. *Joint Bone Spine*, 79, 228-36.
- HA, M. & KIM, V. N. 2014. Regulation of microRNA biogenesis. *Nature reviews Molecular cell biology*, 15, 509-524.
- HAAS-STAPLETON, E. J., LU, Y., HONG, S., ARITA, M., FAVORETO, S., NIGAM, S., SERHAN, C. N. & AGABIAN, N. 2007. *Candida albicans* Modulates Host Defense by Biosynthesizing the Pro-Resolving Mediator Resolvin E1. *PLoS ONE*, 2, e1316.
- HAN, J., PEDERSEN, J. S., KWON, S. C., BELAIR, C. D., KIM, Y.-K., YEOM, K.-H., YANG, W.-Y., HAUSSLER, D., BLELLOCH, R. & KIM, V. N. 2009. Posttranscriptional crossregulation between Drosha and DGCR8. *Cell*, 136, 75-84.
- HASHIZUME, H., DELEO, J. A., COLBURN, R. W. & WEINSTEIN, J. N. 2000. Spinal Glial Activation and Cytokine Expression After Lumbar Root Injury in the Rat. *Spine*, 25, 1206-1217.

- HAUSSER, J. & ZAVOLAN, M. 2014. Identification and consequences of miRNA-target interactions [mdash] beyond repression of gene expression. *Nature Reviews Genetics*, 15, 599-612.
- HELLMANN, J., TANG, Y., KOSURI, M., BHATNAGAR, A. & SPITE, M. 2011. Resolvin D1 decreases adipose tissue macrophage accumulation and improves insulin sensitivity in obese-diabetic mice. *The FASEB Journal*, 25, 2399-2407.
- HEO, I., JOO, C., CHO, J., HA, M., HAN, J. & KIM, V. N. 2008. Lin28 mediates the terminal uridylation of let-7 precursor MicroRNA. *Molecular cell*, 32, 276-284.
- HEROVÁ, M., SCHMID, M., GEMPERLE, C. & HERSBERGER, M. 2015. ChemR23, the receptor for chemerin and resolvin E1, is expressed and functional on M1 but not on M2 macrophages. *The Journal of Immunology*, 194, 2330-2337.
- HONG, S., GRONERT, K., DEVCHAND, P. R., MOUSSIGNAC, R. L. & SERHAN, C. N. 2003. Novel docosatrienes and 17S-resolvins generated from docosahexaenoic acid in murine brain, human blood, and glial cells. Autacoids in anti-inflammation. *J Biol Chem*, 278, 14677-87.
- HONG, S., PORTER, T. F., LU, Y., OH, S. F., PILLAI, P. S. & SERHAN, C. N. 2008. Resolvin E1 Metabolome in Local Inactivation during Inflammation-Resolution. *The Journal of Immunology*, 180, 3512-3519.
- HONG, S., TJONAHEN, E., MORGAN, E. L., LU, Y., SERHAN, C. N. & ROWLEY, A. F. 2005. Rainbow trout (*Oncorhynchus mykiss*) brain cells biosynthesize novel docosahexaenoic acid-derived resolvins and protectins—Mediator lipidomic analysis. *Prostaglandins & Other Lipid Mediators*, 78, 107-116.
- HUANG, J., BURSTON, J. J., LI, L., ASHRAF, S., MAPP, P. I., BENNETT, A. J., RAVIPATI, S., POUSINIS, P., BARRETT, D. A., SCAMMELL, B. E. & CHAPMAN, V. 2017. Targeting the D Series Resolvin Receptor System for the Treatment of Osteoarthritis Pain. *Arthritis & Rheumatology*, 69, 996-1008.
- HUANG, Z.-Z., WEI, J.-Y., OU-YANG, H.-D., LI, D., XU, T., WU, S.-L., ZHANG, X.-L., LIU, C.-C., MA, C. & XIN, W.-J. 2016. mir-500-Mediated GAD67 Downregulation Contributes to Neuropathic Pain. *Journal of Neuroscience*, 36, 6321-6331.
- HUDSON, L. J., BEVAN, S., WOTHERSPOON, G., GENTRY, C., FOX, A. & WINTER, J. 2001. VR1 protein expression increases in undamaged DRG neurons after partial nerve injury. *European Journal of Neuroscience*, 13, 2105-2114.
- IASP. 2014. *IASP Taxonomy* [Online]. Available: <http://www.iasp-pain.org/Education/Content.aspx?ItemNumber=1698> [Accessed 30/07 2014].
- IM, D. S. 2012. Omega-3 fatty acids in anti-inflammation (pro-resolution) and GPCRs. *Prog Lipid Res*, 51, 232-7.
- IMAI, Y., IBATA, I., ITO, D., OHSAWA, K. & KOHSAKA, S. 1996. A novel gene in the major histocompatibility complex class III region encoding an EF hand protein expressed in a monocytic lineage. *Biochemical and biophysical research communications*, 224, 855-862.
- INNIS, S. M. 2008. Dietary omega 3 fatty acids and the developing brain. *Brain research*, 1237, 35-43.
- ISOBE, Y., ARITA, M., MATSUEDA, S., IWAMOTO, R., FUJIHARA, T., NAKANISHI, H., TAGUCHI, R., MASUDA, K., SASAKI, K., URABE, D., INOUE, M. & ARAI, H. 2012. Identification and structure determination of novel anti-inflammatory mediator resolvin E3, 17,18-dihydroxyeicosapentaenoic acid. *J Biol Chem*, 287, 10525-34.

- ITO, D., IMAI, Y., OHSAWA, K., NAKAJIMA, K., FUKUUCHI, Y. & KOHSAKA, S. 1998. Microglia-specific localisation of a novel calcium binding protein, Iba1. *Molecular brain research*, 57, 1-9.
- JACQUIN, M. F., SEMBA, K., EGGER, M. D. & RHOADES, R. W. 1983. Organization of HRP - labeled trigeminal mandibular, primary afferent neurons in the rat. *Journal of Comparative Neurology*, 215, 397-420.
- JENSEN, M. P., CHEN, C. & BRUGGER, A. M. 2003. Interpretation of visual analog scale ratings and change scores: a reanalysis of two clinical trials of postoperative pain. *The Journal of pain*, 4, 407-414.
- JI, R.-R., BERTA, T. & NEDERGAARD, M. 2013. Glia and pain: Is chronic pain a gliopathy? *PAIN®*, 154, Supplement 1, S10-S28.
- JI, R.-R., KOHNO, T., MOORE, K. A. & WOOLF, C. J. 2003. Central sensitization and LTP: do pain and memory share similar mechanisms? *Trends in neurosciences*, 26, 696-705.
- JI, R.-R., XU, Z.-Z., STRICHARTZ, G. & SERHAN, C. N. 2011. Emerging roles of resolvins in the resolution of inflammation and pain. *Trends in neurosciences*, 34, 599-609.
- JO, Y. Y., LEE, J. Y. & PARK, C.-K. 2016. Resolvin E1 inhibits substance P-induced potentiation of TRPV1 in primary sensory neurons. *Mediators of inflammation*, 2016.
- JORDT, S.-E., BAUTISTA, D. M., CHUANG, H.-H., MCKEMY, D. D., ZYGMUNT, P. M., HOGESTATT, E. D., MENG, I. D. & JULIUS, D. 2004. Mustard oils and cannabinoids excite sensory nerve fibres through the TRP channel ANKTM1. *Nature*, 427, 260-265.
- JULIUS, D. 2013. TRP channels and pain. *Annu Rev Cell Dev Biol*, 29, 355-84.
- JUNG, M., SCHAEFER, A., STEINER, I., KEMPKENSTEFFEN, C., STEPHAN, C., ERBERSDOBLER, A. & JUNG, K. 2010. Robust microRNA stability in degraded RNA preparations from human tissue and cell samples. *Clinical chemistry*, 56, 998-1006.
- K SEGALL, S., MAIXNER, W., BELFER, I., WILTSHIRE, T., SELTZER, Z. & DIATCHENKO, L. 2012. Janus molecule I: dichotomous effects of COMT in neuropathic vs nociceptive pain modalities. *CNS & Neurological Disorders-Drug Targets (Formerly Current Drug Targets-CNS & Neurological Disorders)*, 11, 222-235.
- KANAZAWA, H., OHSAWA, K., SASAKI, Y., KOHSAKA, S. & IMAI, Y. 2002. Macrophage/microglia-specific protein Iba1 enhances membrane ruffling and Rac activation via phospholipase C- γ -dependent pathway. *Journal of Biological Chemistry*, 277, 20026-20032.
- KERNISANT, M., GEAR, R. W., JASMIN, L., VIT, J.-P. & OHARA, P. T. 2008. Chronic constriction injury of the infraorbital nerve in the rat using modified syringe needle. *Journal of neuroscience methods*, 172, 43-47.
- KILKENNY, C., BROWNE, W. J., CUTHILL, I. C., EMERSON, M. & ALTMAN, D. G. 2012. Improving bioscience research reporting: the ARRIVE guidelines for reporting animal research. *Osteoarthritis and cartilage*, 20, 256-260.
- KIM, Y.-K., WEE, G., PARK, J., KIM, J., BAEK, D., KIM, J.-S. & KIM, V. N. 2013. TALEN-based knockout library for human microRNAs. *Nature structural & molecular biology*, 20, 1458.
- KING, T. & PORRECA, F. 2014. Preclinical assessment of pain: improving models in discovery research. *Behavioral Neurobiology of Chronic Pain*. Springer.

- KO, G. D., NOWACKI, N. B., ARSENEAU, L., EITEL, M. & HUM, A. 2010. Omega-3 fatty acids for neuropathic pain: case series. *The Clinical journal of pain*, 26, 168-172.
- KOBILKA, B. K. 2007. G protein coupled receptor structure and activation. *Biochimica et Biophysica Acta (BBA) - Biomembranes*, 1768, 794-807.
- KOCERHA, J., FAGHIHI, M. A., LOPEZ-TOLEDANO, M. A., HUANG, J., RAMSEY, A. J., CARON, M. G., SALES, N., WILLOUGHBY, D., ELMEN, J., HANSEN, H. F., ORUM, H., KAUPPINEN, S., KENNY, P. J. & WAHLESTEDT, C. 2009. MicroRNA-219 modulates NMDA receptor-mediated neurobehavioral dysfunction. *Proceedings of the National Academy of Sciences*, 106, 3507-3512.
- KONTINEN, V. & MEERT, T. 2003. Predictive validity of neuropathic pain models in pharmacological studies with a behavioral outcome in the rat: a systematic review. *PROGRESS IN PAIN RESEARCH AND MANAGEMENT*, 24, 489-498.
- KOZOMARA, A. & GRIFFITHS-JONES, S. 2014. miRBase: annotating high confidence microRNAs using deep sequencing data. *Nucleic acids research*, 42, D68-D73.
- KRETSCHMER, T., HAPPEL, L. T., ENGLAND, J. D., NGUYEN, D. H., TIEL, R. L., BEUERMAN, R. W. & KLINE, D. G. 2002. Clinical Article Accumulation of PN1 and PN3 Sodium Channels in Painful Human Neuroma-Evidence from Immunocytochemistry. *Acta Neurochirurgica*, 144, 803-810.
- KRISHNAMOORTHY, S., RECCHIUTI, A., CHIANG, N., FREDMAN, G. & SERHAN, C. N. 2012. Resolvin D1 receptor stereoselectivity and regulation of inflammation and proresolving microRNAs. *The American journal of pathology*, 180, 2018-2027.
- KRISHNAMOORTHY, S., RECCHIUTI, A., CHIANG, N., YACOUBIAN, S., LEE, C.-H., YANG, R., PETASIS, N. A. & SERHAN, C. N. 2010. Resolvin D1 binds human phagocytes with evidence for proresolving receptors. *Proceedings of the National Academy of Sciences*, 107, 1660-1665.
- KUNER, R. 2010. Central mechanisms of pathological pain. *Nat Med*, 16, 1258-66.
- KUSUDA, R., CADETTI, F., RAVANELLI, M. I., SOUSA, T. A., ZANON, S., DE LUCCA, F. L. & LUCAS, G. 2011. Differential expression of microRNAs in mouse pain models. *Molecular pain*, 7, 17.
- KYNAST, K. L., RUSSE, O. Q., MÖSER, C. V., GEISSLINGER, G. & NIEDERBERGER, E. 2013. Modulation of central nervous system-specific microRNA-124a alters the inflammatory response in the formalin test in mice. *Pain*, 154, 368-376.
- LAGOS-QUINTANA, M., RAUHUT, R., MEYER, J., BORKHARDT, A. & TUSCHL, T. 2003. New microRNAs from mouse and human. *Rna*, 9, 175-179.
- LAI, J., PORRECA, F., HUNTER, J. C. & GOLD, M. S. 2004. VOLTAGE-GATED SODIUM CHANNELS AND HYPERALGESIA. *Annual Review of Pharmacology and Toxicology*, 44, 371-397.
- LAU, B. K. & VAUGHAN, C. W. 2014. Descending modulation of pain: the GABA disinhibition hypothesis of analgesia. *Curr Opin Neurobiol*, 29C, 159-164.
- LAWSON, L., PERRY, V., DRI, P. & GORDON, S. 1990. Heterogeneity in the distribution and morphology of microglia in the normal adult mouse brain. *Neuroscience*, 39, 151-170.
- LEE, R. C., FEINBAUM, R. L. & AMBROS, V. 1993. The *C. elegans* heterochronic gene *lin-4* encodes small RNAs with antisense complementarity to *lin-14*. *Cell*, 75, 843-854.

- LEWIS, B. P., BURGE, C. B. & BARTEL, D. P. 2005. Conserved seed pairing, often flanked by adenosines, indicates that thousands of human genes are microRNA targets. *cell*, 120, 15-20.
- LEWIS, B. P., SHIH, I.-H., JONES-RHOADES, M. W., BARTEL, D. P. & BURGE, C. B. 2003. Prediction of mammalian microRNA targets. *Cell*, 115, 787-798.
- LI, Z. & RANA, T. M. 2014. Therapeutic targeting of microRNAs: current status and future challenges. *Nature reviews Drug discovery*, 13, 622-638.
- LIM, L. P., LAU, N. C., GARRETT-ENGELE, P., GRIMSON, A., SCHELTER, J. M., CASTLE, J., BARTEL, D. P., LINSLEY, P. S. & JOHNSON, J. M. 2005. Microarray analysis shows that some microRNAs downregulate large numbers of target mRNAs. *Nature*, 433, 769-773.
- LIMA-GARCIA, J. F., DUTRA, R. C., DA SILVA, K., MOTTA, E. M., CAMPOS, M. M. & CALIXTO, J. B. 2011. The precursor of resolvin D series and aspirin-triggered resolvin D1 display anti-hyperalgesic properties in adjuvant-induced arthritis in rats. *British Journal of Pharmacology*, 164, 278-293.
- LINLEY, J. E., ROSE, K., OOI, L. & GAMPER, N. 2010. Understanding inflammatory pain: ion channels contributing to acute and chronic nociception. *Pflugers Arch*, 459, 657-69.
- LINSTAEDT, S. D., WALKER, M. G., PARKER, J. S., YEH, E., ZIMNY, E., LEWANDOWSKI, C., HENDRY, P. L., DAMIRON, K., PEARSON, C. & VELILLA, M.-A. 2015. MicroRNA circulating in the early aftermath of motor vehicle collision predict persistent pain development and suggest a role for microRNA in sex-specific pain differences. *Molecular pain*, 11, 66.
- LOESCHER, A., BOISSONADE, F. & ROBINSON, P. 2001. Calcitonin gene-related peptide modifies the ectopic discharge from damaged nerve fibres in the ferret. *Neuroscience letters*, 300, 71-74.
- LOPEZ-SANTIAGO, L. F., PERTIN, M., MORISOD, X., CHEN, C., HONG, S., WILEY, J., DECOSTERD, I. & ISOM, L. L. 2006. Sodium Channel β 2 Subunits Regulate Tetrodotoxin-Sensitive Sodium Channels in Small Dorsal Root Ganglion Neurons and Modulate the Response to Pain. *The Journal of Neuroscience*, 26, 7984-7994.
- LULL, M. E. & BLOCK, M. L. 2010. Microglial activation and chronic neurodegeneration. *Neurotherapeutics*, 7, 354-365.
- LUNDEEN, K. A., SUN, B., KARLSSON, L. & FOURIE, A. M. 2006. Leukotriene B4 Receptors BLT1 and BLT2: Expression and Function in Human and Murine Mast Cells. *The Journal of Immunology*, 177, 3439-3447.
- MADDOX, J. F., HACHICHA, M., TAKANO, T., PETASIS, N. A., FOKIN, V. V. & SERHAN, C. N. 1997. Lipoxin A4 Stable Analogs Are Potent Mimetics That Stimulate Human Monocytes and THP-1 Cells via a G-protein-linked Lipoxin A4 Receptor. *Journal of Biological Chemistry*, 272, 6972-6978.
- MADERNA, P., COTTELL, D. C., TOIVONEN, T., DUFTON, N., DALLI, J., PERRETTI, M. & GODSON, C. 2010. FPR2/ALX receptor expression and internalization are critical for lipoxin A4 and annexin-derived peptide-stimulated phagocytosis. *The FASEB Journal*, 24, 4240-4249.
- MARCHESE, A., NGUYEN, T., MALIK, P., XU, S., CHENG, R., XIE, Z., HENG, H. H. Q., GEORGE, S. R., KOLAKOWSKI JR, L. F. & O'DOWD, B. F. 1998. Cloning Genes Encoding Receptors Related to Chemoattractant Receptors. *Genomics*, 50, 281-286.
- MÅRTENSSON, U. E. A., MARIA FENYÖ, E., OLDE, B. & OWMAN, C. 2006. Characterization of the human chemerin receptor – ChemR23/CMKLR1 – as co-

- receptor for human and simian immunodeficiency virus infection, and identification of virus-binding receptor domains. *Virology*, 355, 6-17.
- MARTIN, T. J., KIM, S. A. & EISENACH, J. C. 2006. Clonidine maintains intrathecal self-administration in rats following spinal nerve ligation. *Pain*, 125, 257-263.
- MARTINI, A. C., BERTA, T., FORNER, S., CHEN, G., BENTO, A. F., JI, R.-R. & RAE, G. A. 2016. Lipoxin A4 inhibits microglial activation and reduces neuroinflammation and neuropathic pain after spinal cord hemisection. *Journal of Neuroinflammation*, 13, 75.
- MAS, E., CROFT, K. D., ZAHRA, P., BARDEN, A. & MORI, T. A. 2012. Resolvins D1, D2, and Other Mediators of Self-Limited Resolution of Inflammation in Human Blood following n-3 Fatty Acid Supplementation. *Clinical Chemistry*, 58, 1476-1484.
- MAUDERLI, A. P., ACOSTA-RUA, A. & VIERCK, C. J. 2000. An operant assay of thermal pain in conscious, unrestrained rats. *Journal of neuroscience methods*, 97, 19-29.
- MEESAWATSOM, P., BURSTON, J., HATHWAY, G., BENNETT, A. & CHAPMAN, V. 2016. Inhibitory effects of aspirin-triggered resolvin D1 on spinal nociceptive processing in rat pain models. *Journal of neuroinflammation*, 13, 233.
- METHNER, A., HERMEY, G., SCHINKE, B. & HERMANS-BORGMEYER, I. 1997. A Novel G Protein-Coupled Receptor with Homology to Neuropeptide and Chemoattractant Receptors Expressed during Bone Development. *Biochemical and Biophysical Research Communications*, 233, 336-342.
- MEYER, R. B., SHAHROK 2013. Etiology and Prevention of Nerve Injuries. In: MILORO, M. (ed.) *Trigeminal Nerve Injuries*. Springer-Verlag Berlin Heidelberg.
- MILLIGAN, E. D. & WATKINS, L. R. 2009. Pathological and protective roles of glia in chronic pain. *Nat Rev Neurosci*, 10, 23-36.
- MITTAL, A., RANGANATH, V. & NICHANI, A. 2010. Omega fatty acids and resolution of inflammation: A new twist in an old tale. *J Indian Soc Periodontol*, 14, 3-7.
- MOGIL, J. S. 2009. Animal models of pain: progress and challenges. *Nature Reviews Neuroscience*, 10, 283-294.
- MOGIL, J. S. 2017. Laboratory environmental factors and pain behavior: the relevance of unknown unknowns to reproducibility and translation. *Lab animal*, 46, 136.
- MOGIL, J. S. & CRAGER, S. E. 2004. What should we be measuring in behavioral studies of chronic pain in animals? *Pain*, 112, 12-15.
- MORGAN, C. R., BIRD, E. V., ROBINSON, P. P. & BOISSONADE, F. M. 2009. TRPA1 expression in human lingual nerve neuromas in patients with and without symptoms of dysaesthesia. *Neuroscience Letters*, 465, 189-193.
- MOULIN, C. T. A. D. E. 2013. *Neuropathic Pain: Causes, Management and Understanding*, Cambridge University Press.
- MURPHY, N. P., MILLS, R. H., CAUDLE, R. M. & NEUBERT, J. K. 2014. Operant assays for assessing pain in preclinical rodent models: highlights from an orofacial assay. *Behavioral Neurobiology of Chronic Pain*. Springer.
- NAM, J.-W., RISSLAND, O. S., KOPPSTEIN, D., ABREU-GOODGER, C., JAN, C. H., AGARWAL, V., YILDIRIM, M. A., RODRIGUEZ, A. & BARTEL, D. P. 2014. Global analyses of the effect of different cellular contexts on microRNA targeting. *Molecular cell*, 53, 1031-1043.

- NASSAR, M. A., LEVATO, A., STIRLING, L. C. & WOOD, J. N. 2005. Neuropathic pain develops normally in mice lacking both Na v 1.7 and Na v 1.8. *Molecular pain*, 1, 24.
- NASSAR, M. A., STIRLING, L. C., FORLANI, G., BAKER, M. D., MATTHEWS, E. A., DICKENSON, A. H. & WOOD, J. N. 2004. Nociceptor-specific gene deletion reveals a major role for Nav1. 7 (PN1) in acute and inflammatory pain. *Proceedings of the national Academy of Sciences of the United States of America*, 101, 12706-12711.
- NATERA-NARANJO, O., ASCHRAFI, A., GIOIO, A. E. & KAPLAN, B. B. 2010. Identification and quantitative analyses of microRNAs located in the distal axons of sympathetic neurons. *Rna*.
- NAVRATILOVA, E., ATCHERLEY, C. W. & PORRECA, F. 2015. Brain circuits encoding reward from pain relief. *Trends in neurosciences*, 38, 741-750.
- NEUBERT, J. K., WIDMER, C. G., MALPHURS, W., ROSSI, H. L., VIERCK, C. J. & CAUDLE, R. M. 2005. Use of a novel thermal operant behavioral assay for characterization of orofacial pain sensitivity. *Pain*, 116, 386-395.
- NORLING, L. V., DALLI, J., FLOWER, R. J., SERHAN, C. N. & PERRETTI, M. 2012. Resolvin D1 limits polymorphonuclear leukocyte recruitment to inflammatory loci: receptor-dependent actions. *Arterioscler Thromb Vasc Biol*, 32, 1970-8.
- NORLING, L. V., SPITE, M., YANG, R., FLOWER, R. J., PERRETTI, M. & SERHAN, C. N. 2011. Cutting Edge: Humanized Nano-Proresolving Medicines Mimic Inflammation-Resolution and Enhance Wound Healing. *The Journal of Immunology*, 186, 5543-5547.
- NOVAKOVIC, S. D., TZOUMAKA, E., MCGIVERN, J. G., HARAGUCHI, M., SANGAMESWARAN, L., GOGAS, K. R., EGLIN, R. M. & HUNTER, J. C. 1998. Distribution of the tetrodotoxin-resistant sodium channel PN3 in rat sensory neurons in normal and neuropathic conditions. *Journal of Neuroscience*, 18, 2174-2187.
- OH, S. F., DONA, M., FREDMAN, G., KRISHNAMOORTHY, S., IRIMIA, D. & SERHAN, C. N. 2012. Resolvin E2 formation and impact in inflammation resolution. *The Journal of Immunology*, 188, 4527-4534.
- OKUBO, M., YAMANAKA, H., KOBAYASHI, K., FUKUOKA, T., DAI, Y. & NOGUCHI, K. 2010. Expression of leukotriene receptors in the rat dorsal root ganglion and the effects on pain behaviors. *Molecular pain*, 6, 57.
- ONISHI, K., HOLLIS, E. & ZOU, Y. 2014. Axon guidance and injury—lessons from Wnts and Wnt signaling. *Current opinion in neurobiology*, 27, 232-240.
- ORLOVA, I. A., ALEXANDER, G. M., QURESHI, R. A., SACAN, A., GRAZIANO, A., BARRETT, J. E., SCHWARTZMAN, R. J. & AJIT, S. K. 2011. MicroRNA modulation in complex regional pain syndrome. *Journal of translational medicine*, 9, 195.
- ÖZCAN, E., SAYGUN, N. I., ILİKÇİ, R., KARSLIÖĞLU, Y., MUŞABAK, U. & YEŞİLLİK, S. 2017. Evaluation of chemerin and its receptors, ChemR23 and CCRL2, in gingival tissues with healthy and periodontitis. *Odontology*, 1-8.
- PAN, Z., ZHU, L. J., LI, Y. Q., HAO, L. Y., YIN, C., YANG, J. X., GUO, Y., ZHANG, S., HUA, L., XUE, Z. Y., ZHANG, H. & CAO, J. L. 2014. Epigenetic modification of spinal miR-219 expression regulates chronic inflammation pain by targeting CaMKIIgamma. *J Neurosci*, 34, 9476-83.
- PARK, C. K., XU, Z. Z., LIU, T., LÜ, N., SERHAN, C. N. & JI, R. R. 2011. Resolvin D2 is a potent endogenous inhibitor for transient receptor potential subtype

- V1/A1, inflammatory pain, and spinal cord synaptic plasticity in mice: distinct roles of resolvin D1, D2, and E1. *J Neurosci*, 31, 18433-8.
- PARKITNA, J. R., KOROSTYNSKI, M., KAMINSKA-CHOWANIEC, D., OBARA, I., MIKA, J., PRZEWLOCKA, B. & PRZEWLOCKI, R. 2006. COMPARISON OF GENE EXPRESSION PROFILES. *Journal of Physiology and Pharmacology*, 57, 401-414.
- PAROLINI, S., SANTORO, A., MARCENARO, E., LUINI, W., MASSARDI, L., FACCHETTI, F., COMMUNI, D., PARMENTIER, M., MAJORANA, A. & SIRONI, M. 2007. The role of chemerin in the colocalization of NK and dendritic cell subsets into inflamed tissues. *Blood*, 109, 3625-3632.
- PAROO, Z., YE, X., CHEN, S. & LIU, Q. 2009. Phosphorylation of the human microRNA-generating complex mediates MAPK/Erk signaling. *Cell*, 139, 112-122.
- PASERO, C. 2004. Pathophysiology of neuropathic pain. *Pain Management Nursing*, 5, 3-8.
- PATAPOUTIAN, A., TATE, S. & WOOLF, C. J. 2009. Transient receptor potential channels: targeting pain at the source. *Nat Rev Drug Discov*, 8, 55-68.
- PEI, L., ZHANG, J., ZHAO, F., SU, T., WEI, H., TIAN, J., LI, M. & SHI, J. 2011. Annexin 1 exerts anti-nociceptive effects after peripheral inflammatory pain through formyl-peptide-receptor-like 1 in rat dorsal root ganglion. *British journal of anaesthesia*, 107, 948-958.
- PÉREZ, J., WARE, M. A., CHEVALIER, S., GOUGEON, R. & SHIR, Y. 2005. Dietary omega-3 fatty acids may be associated with increased neuropathic pain in nerve-injured rats. *Anesthesia & Analgesia*, 101, 444-448.
- PIAO, Z. G., CHO, I.-H., PARK, C. K., HONG, J. P., CHOI, S.-Y., LEE, S. J., LEE, S., PARK, K., KIM, J. S. & OH, S. B. 2006. Activation of glia and microglial p38 MAPK in medullary dorsal horn contributes to tactile hypersensitivity following trigeminal sensory nerve injury. *Pain*, 121, 219-231.
- PIEHL, F. & LIDMAN, O. 2001. Neuroinflammation in the rat – CNS cells and their role in the regulation of immune reactions. *Immunological Reviews*, 184, 212-225.
- PIERDOMENICO, A. M., RECCHIUTI, A., SIMIELE, F., CODAGNONE, M., MARI, V. C., DAVÌ, G. & ROMANO, M. 2015. MicroRNA-181b regulates ALX/FPR2 receptor expression and proresolution signaling in human macrophages. *Journal of Biological Chemistry*, 290, 3592-3600.
- PINHEIRO, I., DEJAGER, L. & LIBERT, C. 2011. X - chromosome - located microRNAs in immunity: Might they explain male/female differences? *Bioessays*, 33, 791-802.
- PIPPI, R., SPOTA, A. & SANTORO, M. 2017. Prevention of lingual nerve injury in third molar surgery: literature review. *Journal of Oral and Maxillofacial Surgery*.
- PRESCOTT, D. & MCKAY, D. M. 2011. *Aspirin-triggered lipoxin enhances macrophage phagocytosis of bacteria while inhibiting inflammatory cytokine production*.
- PRICE, D. D. 2000. Psychological and neural mechanisms of the affective dimension of pain. *Science*, 288, 1769-1772.
- PSYCHOGIOS, N., HAU, D. D., PENG, J., GUO, A. C., MANDAL, R., BOUATRA, S., SINELNIKOV, I., KRISHNAMURTHY, R., EISNER, R., GAUTAM, B., YOUNG, N., XIA, J., KNOX, C., DONG, E., HUANG, P., HOLLANDER, Z., PEDERSEN, T. L., SMITH, S. R., BAMFORTH, F., GREINER, R., MCMANUS, B., NEWMAN, J. W., GOODFRIEND, T. & WISHART, D. S. 2011. The Human Serum Metabolome. *PLoS ONE*, 6, e16957.

- QIU, H., JOHANSSON, A.-S., SJÖSTRÖM, M., WAN, M., SCHRÖDER, O., PALMBLAD, J. & HAEGGSTRÖM, J. Z. 2006. Differential induction of BLT receptor expression on human endothelial cells by lipopolysaccharide, cytokines, and leukotriene B4. *Proceedings of the National Academy of Sciences*, 103, 6913-6918.
- RAGHAVENDRA, V., TANGA, F. & DELEO, J. A. 2003. Inhibition of microglial activation attenuates the development but not existing hypersensitivity in a rat model of neuropathy. *Journal of Pharmacology and Experimental Therapeutics*, 306, 624-630.
- RECCHIUTI, A., KRISHNAMOORTHY, S., FREDMAN, G., CHIANG, N. & SERHAN, C. N. 2011. MicroRNAs in resolution of acute inflammation: identification of novel resolvin D1-miRNA circuits. *The FASEB Journal*, 25, 544-560.
- RENTON, T. 2013. Nonsurgical Management of Trigeminal Nerve Injuries. In: MILORO, M. (ed.) *Trigeminal Nerve Injuries*. Springer-Verlag Berlin Heidelberg.
- REXED, B. 1952. The cytoarchitectonic organization of the spinal cord in the cat. *Journal of Comparative Neurology*, 96, 415-495.
- ROBINSON, P., LOESCHER, A. & SMITH, K. 2000. A prospective, quantitative study on the clinical outcome of lingual nerve repair. *British Journal of Oral and Maxillofacial Surgery*, 38, 255-263.
- ROBINSON, P. & SMITH, K. 1996. A study on the efficacy of late lingual nerve repair. *British Journal of Oral and Maxillofacial Surgery*, 34, 96-103.
- ROBINSON, P. P., LOESCHER, A. R., YATES, J. M. & SMITH, K. G. 2004. Current management of damage to the inferior alveolar and lingual nerves as a result of removal of third molars. *British Journal of Oral and Maxillofacial Surgery*, 42, 285-292.
- ROBINSON, P. P. S., KEITH G; HILLERUP, SØREN 2013. Outcomes of Trigeminal Nerve Repair. In: MILORO, M. (ed.) *Trigeminal Nerve Injuries*. Springer-Verlag Berlin Heidelberg.
- ROSÉN, A., TARDAST, A. & SHI, T.-J. 2016. How Far Have We Come in the Field of Nerve Regeneration After Trigeminal Nerve Injury? *Current Oral Health Reports*, 3, 309-313.
- RUGGIERO, S. L. P., MICHAEL 2013. Guidelines for Diagnosis and Treatment of Trigeminal Nerve Injuries. In: MILORO, M. (ed.) *Trigeminal Nerve Injuries*. Springer-Verlag Berlin Heidelberg.
- SAKAI, A., SAITOW, F., MIYAKE, N., MIYAKE, K., SHIMADA, T. & SUZUKI, H. 2013. *miR-7a alleviates the maintenance of neuropathic pain through regulation of neuronal excitability*.
- SAKAI, A. & SUZUKI, H. 2013. Nerve injury-induced upregulation of miR-21 in the primary sensory neurons contributes to neuropathic pain in rats. *Biochemical and Biophysical Research Communications*, 435, 176-181.
- SAKAI, A. & SUZUKI, H. 2014. Emerging roles of microRNAs in chronic pain. *Neurochem Int*.
- SAMSON, M., EDINGER, A. L., STORDEUR, P., RUCKER, J., VERHASSELT, V., SHARRON, M., GOVAERTS, C., MOLLEREAU, C., VASSART, G., DOMS, R. W. & PARMENTIER, M. 1998. ChemR23, a putative chemoattractant receptor, is expressed in monocyte-derived dendritic cells and macrophages and is a coreceptor for SIV and some primary HIV-1 strains. *European Journal of Immunology*, 28, 1689-1700.

- SAYED, D. & ABDELLATIF, M. 2011. MicroRNAs in development and disease. *Physiological reviews*, 91, 827-887.
- SCHMID, M., GEMPERLE, C., RIMANN, N. & HERSBERGER, M. 2016. Resolvin D1 polarizes primary human macrophages toward a proresolution phenotype through GPR32. *The Journal of Immunology*, 196, 3429-3437.
- SEGALL, S. K., SHABALINA, S. A., MELOTO, C. B., WEN, X., CUNNINGHAM, D., TARANTINO, L. M., WILTSHIRE, T., GAUTHIER, J., TOHYAMA, S. & MARTIN, L. J. 2015. Molecular genetic mechanisms of allelic specific regulation of murine Comt expression. *Pain*, 156, 1965.
- SERHAN, C. N. 2010. Novel lipid mediators and resolution mechanisms in acute inflammation: to resolve or not? *Am J Pathol*, 177, 1576-91.
- SERHAN, C. N. & CHIANG, N. 2013. Resolution phase lipid mediators of inflammation: agonists of resolution. *Curr Opin Pharmacol*, 13, 632-40.
- SERHAN, C. N., CHIANG, N. & VAN DYKE, T. E. 2008. Resolving inflammation: dual anti-inflammatory and pro-resolution lipid mediators. *Nat Rev Immunol*, 8, 349-61.
- SERHAN, C. N., CLISH, C. B., BRANNON, J., COLGAN, S. P., CHIANG, N. & GRONERT, K. 2000. Novel Functional Sets of Lipid-Derived Mediators with Antiinflammatory Actions Generated from Omega-3 Fatty Acids via Cyclooxygenase 2–Nonsteroidal Antiinflammatory Drugs and Transcellular Processing. *The Journal of Experimental Medicine*, 192, 1197-1204.
- SERHAN, C. N., HONG, S., GRONERT, K., COLGAN, S. P., DEVCHAND, P. R., MIRICK, G. & MOUSSIGNAC, R. L. 2002. Resolvins: a family of bioactive products of omega-3 fatty acid transformation circuits initiated by aspirin treatment that counter proinflammation signals. *J Exp Med*, 196, 1025-37.
- SERHAN, C. N. & SAVILL, J. 2005. Resolution of inflammation: the beginning programs the end. *Nat Immunol*, 6, 1191-7.
- SERPELL, M. & GROUP, N. P. S. 2002. Gabapentin in neuropathic pain syndromes: a randomised, double-blind, placebo-controlled trial. *Pain*, 99, 557-566.
- SESSLE, B. 2005. Peripheral and central mechanisms of orofacial pain and their clinical correlates. *Minerva anesthesiologica*, 71, 117-136.
- SESSLE, B. J. 2000. Acute and Chronic Craniofacial Pain: Brainstem Mechanisms of Nociceptive Transmission and Neuroplasticity, and Their Clinical Correlates. *Critical Reviews in Oral Biology & Medicine*, 11, 57-91.
- SHIN, C., NAM, J.-W., FARH, K. K.-H., CHIANG, H. R., SHKUMATAVA, A. & BARTEL, D. P. 2010. Expanding the microRNA targeting code: functional sites with centered pairing. *Molecular cell*, 38, 789-802.
- SIEBOLTS, U., VARNHOLT, H., DREBBER, U., DIENES, H.-P., WICKENHAUSER, C. & ODENTHAL, M. 2009. Tissues from routine pathology archives are suitable for microRNA analyses by quantitative PCR. *Journal of clinical pathology*, 62, 84-88.
- SIEGEL, G., OBERNOSTERER, G., FIORE, R., OEHMEN, M., BICKER, S., CHRISTENSEN, M., KHUDAYBERDIEV, S., LEUSCHNER, P. F., BUSCH, C. J. & KANE, C. 2009. A functional screen implicates microRNA-138-dependent regulation of the depalmitoylation enzyme APT1 in dendritic spine morphogenesis. *Nature cell biology*, 11, 705-716.
- SMITH, G. D., GUNTHORPE, M. J., KELSELL, R. E., HAYES, P. D., REILLY, P., FACER, P., WRIGHT, J. E., JERMAN, J. C., WALHIN, J. P., OOI, L., EGERTON, J., CHARLES, K. J., SMART, D., RANDALL, A. D., ANAND, P.

- & DAVIS, J. B. 2002. TRPV3 is a temperature-sensitive vanilloid receptor-like protein. *Nature*, 418, 186-190.
- SMITH, P. L., LOESCHER, A. R., BOISSONADE, F. M. & ROBINSON, P. P. 2005. The effect of substance P on the spontaneous discharge from injured inferior alveolar nerve fibres in the ferret. *Experimental neurology*, 191, 285-291.
- SOMMER, C. & BIRKLEIN, F. 2011. Resolvins and inflammatory pain. *F1000 Med Rep*, 3, 19.
- SORGE, R. E., LACROIX-FRALISH, M. L., TUTTLE, A. H., SOTOCINAL, S. G., AUSTIN, J.-S., RITCHIE, J., CHANDA, M. L., GRAHAM, A. C., TOPHAM, L. & BEGGS, S. 2011. Spinal cord Toll-like receptor 4 mediates inflammatory and neuropathic hypersensitivity in male but not female mice. *Journal of Neuroscience*, 31, 15450-15454.
- SORGE, R. E., MAPPLEBECK, J. C., ROSEN, S., BEGGS, S., TAVES, S., ALEXANDER, J. K., MARTIN, L. J., AUSTIN, J. S., SOTOCINAL, S. G., CHEN, D., YANG, M., SHI, X. Q., HUANG, H., PILLON, N. J., BILAN, P. J., TU, Y., KLIP, A., JI, R. R., ZHANG, J., SALTER, M. W. & MOGIL, J. S. 2015. Different immune cells mediate mechanical pain hypersensitivity in male and female mice. *Nat Neurosci*, 18, 1081-3.
- SORGE, R. E., MARTIN, L. J., ISBESTER, K. A., SOTOCINAL, S. G., ROSEN, S., TUTTLE, A. H., WIESKOPF, J. S., ACLAND, E. L., DOKOVA, A. & KADOURA, B. 2014. Olfactory exposure to males, including men, causes stress and related analgesia in rodents. *Nature methods*, 11, 629-632.
- SORKIN, L. S., XIAO, W. H., WAGNER, R. & MYERS, R. R. 1997. Tumour necrosis factor- α induces ectopic activity in nociceptive primary afferent fibres. *Neuroscience*, 81, 255-262.
- SOTOCINAL, S. G., SORGE, R. E., ZALOUM, A., TUTTLE, A. H., MARTIN, L. J., WIESKOPF, J. S., MAPPLEBECK, J. C., WEI, P., ZHAN, S. & ZHANG, S. 2011. The Rat Grimace Scale: a partially automated method for quantifying pain in the laboratory rat via facial expressions. *Molecular pain*, 7, 55.
- SPITE, M., NORLING, L. V., SUMMERS, L., YANG, R., COOPER, D., PETASIS, N. A., FLOWER, R. J., PERRETTI, M. & SERHAN, C. N. 2009. Resolvin D2 is a potent regulator of leukocytes and controls microbial sepsis. *Nature*, 461, 1287-1291.
- SPURR, L., NADKARNI, S., PEDERZOLI-RIBEIL, M., GOULDING, N. J., PERRETTI, M. & D'ACQUISTO, F. 2011. Comparative analysis of Annexin A1-formyl peptide receptor 2/ALX expression in human leukocyte subsets. *International Immunopharmacology*, 11, 55-66.
- STEED, M. B. 2011. Peripheral nerve response to injury. *Atlas of the Oral and Maxillofacial Surgery Clinics*, 19, 1-13.
- STRICKLAND, I. T., RICHARDS, L., HOLMES, F. E., WYNICK, D., UNEY, J. B. & WONG, L.-F. 2011. Axotomy-Induced miR-21 Promotes Axon Growth in Adult Dorsal Root Ganglion Neurons. *PLoS ONE*, 6, e23423.
- SUN, Y. P., OH, S. F., UDDIN, J., YANG, R., GOTLINGER, K., CAMPBELL, E., COLGAN, S. P., PETASIS, N. A. & SERHAN, C. N. 2007. Resolvin D1 and its aspirin-triggered 17R epimer. Stereochemical assignments, anti-inflammatory properties, and enzymatic inactivation. *J Biol Chem*, 282, 9323-34.
- SUTHERLAND, S. P., BENSON, C. J., ADELMAN, J. P. & MCCLESKEY, E. W. 2001. Acid-sensing ion channel 3 matches the acid-gated current in cardiac ischemia-sensing neurons. *Proceedings of the National Academy of Sciences*, 98, 711-716.

- SUZUKI, H., BECKH, S., KUBO, H., YAHAGI, N., ISHIDA, H., KAYANO, T., NODA, M. & NUMA, S. 1988. Functional expression of cloned cDNA encoding sodium channel III. *FEBS Letters*, 228, 195-200.
- TABAS, I. 2010. Macrophage death and defective inflammation resolution in atherosclerosis. *Nat Rev Immunol*, 10, 36-46.
- TAKANO, T., FIORE, S., MADDUX, J. F., BRADY, H. R., PETASIS, N. A. & SERHAN, C. N. 1997. Aspirin-triggered 15-Epi-Lipoxin A4 (LXA4) and LXA4 Stable Analogues Are Potent Inhibitors of Acute Inflammation: Evidence for Anti-inflammatory Receptors. *The Journal of Experimental Medicine*, 185, 1693-1704.
- TAKEMURA, M., SUGIMOTO, T. & SAKAI, A. 1987. Topographic organization of central terminal region of different sensory branches of the rat mandibular nerve. *Experimental neurology*, 96, 540-557.
- TAM TAM, S., BASTIAN, I., ZHOU, X. F., VANDER HOEK, M., MICHAEL, M. Z., GIBBINS, I. L. & HABERBERGER, R. V. 2011. MicroRNA-143 expression in dorsal root ganglion neurons. *Cell and Tissue Research*, 346, 163-173.
- TANG, X., LI, M., TUCKER, L. & RAMRATNAM, B. 2011. Glycogen synthase kinase 3 beta (GSK3 β) phosphorylates the RNAase III enzyme Droscha at S300 and S302. *PloS one*, 6, e20391.
- TANGA, F. Y., NUTILE-MCMENEMY, N. & DELEO, J. A. 2005. The CNS role of Toll-like receptor 4 in innate neuroimmunity and painful neuropathy. *Proceedings of the National Academy of Sciences of the United States of America*, 102, 5856-5861.
- TSUDA, M., SHIGEMOTO-MOGAMI, Y., KOIZUMI, S. & MIZOKOSHI, A. 2003. P2X4 receptors induced in spinal microglia gate tactile allodynia after nerve injury. *Nature*, 424, 778.
- VASO, A., ADAHAN, H.-M., GJIKA, A., ZAHAJ, S., ZHURDA, T., VYSHKA, G. & DEVOR, M. 2014. Peripheral nervous system origin of phantom limb pain. *PAIN*, 155, 1384-1391.
- VERGE, G. M., MILLIGAN, E. D., MAIER, S. F., WATKINS, L. R., NAEVE, G. S. & FOSTER, A. C. 2004. Fractalkine (CX3CL1) and fractalkine receptor (CX3CR1) distribution in spinal cord and dorsal root ganglia under basal and neuropathic pain conditions. *European Journal of Neuroscience*, 20, 1150-1160.
- VERMI, W., RIBOLDI, E., WITTAMER, V., GENTILI, F., LUINI, W., MARRELLI, S., VECCHI, A., FRANSSSEN, J.-D., COMMUNI, D. & MASSARDI, L. 2005. Role of ChemR23 in directing the migration of myeloid and plasmacytoid dendritic cells to lymphoid organs and inflamed skin. *Journal of Experimental Medicine*, 201, 509-515.
- VIERCK, C., HANSSON, P. & YEZIERSKI, R. 2008. Clinical and pre - clinical pain assessment: Are we measuring the same thing? *Pain*, 135, 7-10.
- VOETS, T., DROOGMANS, G., WISSENBACH, U., JANSSENS, A., FLOCKERZI, V. & NILIUS, B. 2004. The principle of temperature-dependent gating in cold- and heat-sensitive TRP channels. *Nature*, 430, 748-754.
- VORA, A. R., BODELL, S. M., LOESCHER, A. R., SMITH, K. G., ROBINSON, P. P. & BOISSONADE, F. M. 2007. Inflammatory cell accumulation in traumatic neuromas of the human lingual nerve. *archives of oral biology*, 52, 74-82.
- VOS, B. P., STRASSMAN, A. M. & MACIEWICZ, R. J. 1994. Behavioral evidence of trigeminal neuropathic pain following chronic constriction injury to the rat's infraorbital nerve. *Journal of Neuroscience*, 14, 2708-2723.

- WAGNER, R. & MYERS, R. R. 1996. Endoneurial injection of TNF-[alpha] produces neuropathic pain behaviors. *NeuroReport*, 7, 2897-2902.
- WALKER, K. M., URBAN, L., MEDHURST, S. J., PATEL, S., PANESAR, M., FOX, A. J. & MCINTYRE, P. 2003. The VR1 antagonist capsazepine reverses mechanical hyperalgesia in models of inflammatory and neuropathic pain. *Journal of Pharmacology and Experimental Therapeutics*, 304, 56-62.
- WALL, P., DEVOR, M., INBAL, R., SCADDING, J., SCHONFELD, D., SELTZER, Z. & TOMKIEWICZ, M. 1979. Autotomy following peripheral nerve lesions: experimental anesthesia dolorosa. *Pain*, 7, 103-113.
- WANG, H. & WOOLF, C. J. 2005. Pain TRPs. *Neuron*, 46, 9-12.
- WANG, J.-J. & LI, Y. 2016. KCNQ potassium channels in sensory system and neural circuits. *Acta Pharmacologica Sinica*, 37, 25-33.
- WANG, X., ZHU, M., HJORTH, E., CORTÉS-TORO, V., EYJOLFSDOTTIR, H., GRAFF, C., NENNESMO, I., PALMBLAD, J., ERIKSDOTTER, M. & SAMBAMURTI, K. 2015. Resolution of inflammation is altered in Alzheimer's disease. *Alzheimer's & dementia*, 11, 40-50. e2.
- WANG, Z., FILGUEIRAS, L. R., WANG, S., SEREZANI, A. P. M., PETERS-GOLDEN, M., JANCAR, S. & SEREZANI, C. H. 2014. Leukotriene B4 Enhances the Generation of Proinflammatory MicroRNAs To Promote MyD88-Dependent Macrophage Activation. *The Journal of Immunology*, 192, 2349-2356.
- WAXMAN, S. G., CUMMINS, T. R., DIB-HAJJ, S., FJELL, J. & BLACK, J. A. 1999. Sodium channels, excitability of primary sensory neurons, and the molecular basis of pain. *Muscle and Nerve*, 22, 1177-1187.
- WAXMAN, S. G., KOCSIS, J. D. & BLACK, J. A. 1994. Type III sodium channel mRNA is expressed in embryonic but not adult spinal sensory neurons, and is reexpressed following axotomy. *Journal of Neurophysiology*, 72, 466-470.
- WEI, H., HÄMÄLÄINEN, M. M., SAARNILEHTO, M., KOIVISTO, A. & PERTOVAARA, A. 2009. Attenuation of Mechanical Hypersensitivity by an Antagonist of the TRPA1 Ion Channel in Diabetic Animals. *Anesthesiology*, 111, 147-154 10.1097/ALN.0b013e3181a1642b.
- WEIDNER, C., KLEDE, M., RUKWIED, R., LISCHETZKI, G., NEISIUS, U., SKOV, P. S., PETERSEN, L. J. & SCHMELZ, M. 2000. Acute Effects of Substance P and Calcitonin Gene-Related Peptide in Human Skin - A Microdialysis Study. *J Invest Dermatol*, 115, 1015-1020.
- WEISS, G. A., TROXLER, H., KLINKE, G., ROGLER, D., BRAEGGER, C. & HERSBERGER, M. 2013. High levels of anti-inflammatory and pro-resolving lipid mediators lipoxins and resolvins and declining docosahexaenoic acid levels in human milk during the first month of lactation. *Lipids in Health and Disease*, 12, 89.
- WHEELER, B. M., HEIMBERG, A. M., MOY, V. N., SPERLING, E. A., HOLSTEIN, T. W., HEBER, S. & PETERSON, K. J. 2009. The deep evolution of metazoan microRNAs. *Evolution & development*, 11, 50-68.
- WHEELER, G., NTOUNIA-FOUSARA, S., GRANDA, B., RATHJEN, T. & DALMAY, T. 2006. Identification of new central nervous system specific mouse microRNAs. *FEBS letters*, 580, 2195-2200.
- WINKELSTEIN, B. A., RUTKOWSKI, M. D., SWEITZER, S. M., PAHL, J. L. & DELEO, J. A. 2001. Nerve injury proximal or distal to the DRG induces similar spinal glial activation and selective cytokine expression but differential behavioral responses to pharmacologic treatment. *The Journal of Comparative Neurology*, 439, 127-139.

- WITTAMER, V., FRANSSSEN, J.-D., VULCANO, M., MIRJOLET, J.-F., LE POUL, E., MIGEOTTE, I., BRÉZILLON, S., TYLDESLEY, R., BLANPAIN, C., DETHEUX, M., MANTOVANI, A., SOZZANI, S., VASSART, G., PARMENTIER, M. & COMMUNI, D. 2003. Specific Recruitment of Antigen-presenting Cells by Chemerin, a Novel Processed Ligand from Human Inflammatory Fluids. *The Journal of Experimental Medicine*, 198, 977-985.
- WOOD, J. N., BOORMAN, J. P., OKUSE, K. & BAKER, M. D. 2004. Voltage-gated sodium channels and pain pathways. *J Neurobiol*, 61, 55-71.
- WOOLF, C. J. & MA, Q. 2007. Nociceptors--noxious stimulus detectors. *Neuron*, 55, 353-64.
- WOOLF, C. J. & MANNION, R. J. 1999. Neuropathic pain: aetiology, symptoms, mechanisms, and management. *The Lancet*, 353, 1959-1964.
- WOOLF, C. J. & SALTER, M. W. 2000. Neuronal Plasticity: Increasing the Gain in Pain. *Science*, 288, 1765-1768.
- XI, Y., NAKAJIMA, G., GAVIN, E., MORRIS, C. G., KUDO, K., HAYASHI, K. & JU, J. 2007. Systematic analysis of microRNA expression of RNA extracted from fresh frozen and formalin-fixed paraffin-embedded samples. *Rna*, 13, 1668-1674.
- XU, M., AITA, M. & CHAVKIN, C. 2008. Partial infraorbital nerve ligation as a model of trigeminal nerve injury in the mouse: behavioral, neural, and glial reactions. *The Journal of Pain*, 9, 1036-1048.
- XU, Q. & YAKSH, T. L. 2011. A brief comparison of the pathophysiology of inflammatory versus neuropathic pain. *Curr Opin Anaesthesiol*, 24, 400-7.
- XU, Z.-Z., ZHANG, L., LIU, T., PARK, J. Y., BERTA, T., YANG, R., SERHAN, C. N. & JI, R.-R. 2010. Resolvins RvE1 and RvD1 attenuate inflammatory pain via central and peripheral actions. *Nature medicine*, 16, 592-597.
- XU, Z. Z., BERTA, T. & JI, R. R. 2013. Resolvin E1 inhibits neuropathic pain and spinal cord microglial activation following peripheral nerve injury. *J Neuroimmune Pharmacol*, 8, 37-41.
- YAMAMOTO, T. 2008. Central mechanisms of roles of taste in reward and eating. *Acta Physiologica Hungarica*, 95, 165-186.
- YANG, Y., LI, H., LI, T.-T., LUO, H., GU, X.-Y., LÜ, N., JI, R.-R. & ZHANG, Y.-Q. 2015. Delayed activation of spinal microglia contributes to the maintenance of bone cancer pain in female Wistar rats via P2X7 receptor and IL-18. *Journal of Neuroscience*, 35, 7950-7963.
- YATES, J., SMITH, K. & ROBINSON, P. 2000. Ectopic neural activity from myelinated afferent fibres in the lingual nerve of the ferret following three types of injury. *Brain research*, 874, 37-47.
- YE, R. D., CAVANAGH, S. L., QUEHENBERGER, O., PROSSNITZ, E. R. & COCHRANE, C. G. 1992. Isolation of a cDNA that encodes a novel granulocyte N-formyl peptide receptor. *Biochemical and Biophysical Research Communications*, 184, 582-589.
- YOKOUCHI, K., FUKUSHIMA, N., KAKEGAWA, A., KAWAGISHI, K., FUKUYAMA, T. & MORIIZUMI, T. 2007. Functional role of lingual nerve in breastfeeding. *International journal of developmental neuroscience*, 25, 115-119.
- YU, B., ZHOU, S., QIAN, T., WANG, Y., DING, F. & GU, X. 2011. Altered microRNA expression following sciatic nerve resection in dorsal root ganglia of rats. *Acta Biochim Biophys Sin*, 43, 909-915.
- ZABEL, B. A., OHYAMA, T., ZUNIGA, L., KIM, J.-Y., JOHNSTON, B., ALLEN, S. J., GUIDO, D. G., HANDEL, T. M. & BUTCHER, E. C. 2006. Chemokine-like

- receptor 1 expression by macrophages in vivo: regulation by TGF- β and TLR ligands. *Experimental hematology*, 34, 1106-1114.
- ZENG, Y., SANKALA, H., ZHANG, X. & GRAVES, P. R. 2008. Phosphorylation of Argonaute 2 at serine-387 facilitates its localization to processing bodies. *Biochemical Journal*, 413, 429-436.
- ZHAI, B., YANG, H., MANCINI, A., HE, Q., ANTONIOU, J. & DI BATTISTA, J. A. 2010. Leukotriene B(4) BLT receptor signaling regulates the level and stability of cyclooxygenase-2 (COX-2) mRNA through restricted activation of Ras/Raf/ERK/p42 AUF1 pathway. *J Biol Chem*, 285, 23568-80.
- ZHANG, E., KIM, J.-J., SHIN, N., YIN, Y., NAN, Y., XU, Y., HONG, J., HSU, T. M., CHUNG, W. & KO, Y. 2017. High Omega-3 Polyunsaturated Fatty Acids in fat-1 Mice Reduce Inflammatory Pain. *Journal of Medicinal Food*.
- ZHANG, J., HOFFERT, C., VU, H. K., GROBLEWSKI, T., AHMAD, S. & O'DONNELL, D. 2003. Induction of CB2 receptor expression in the rat spinal cord of neuropathic but not inflammatory chronic pain models. *European Journal of Neuroscience*, 17, 2750-2754.
- ZHANG, J., SHI, X. Q., ECHEVERRY, S., MOGIL, J. S., DE KONINCK, Y. & RIVEST, S. 2007. Expression of CCR2 in both resident and bone marrow-derived microglia plays a critical role in neuropathic pain. *Journal of Neuroscience*, 27, 12396-12406.
- ZHAO, J., LEE, M.-C., MOMIN, A., CENDAN, C.-M., SHEPHERD, S. T., BAKER, M. D., ASANTE, C., BEE, L., BETHRY, A., PERKINS, J. R., NASSAR, M. A., ABRAHAMSEN, B., DICKENSON, A., COBB, B. S., MERKENSCHLAGER, M. & WOOD, J. N. 2010. Small RNAs Control Sodium Channel Expression, Nociceptor Excitability, and Pain Thresholds. *The Journal of Neuroscience*, 30, 10860-10871.
- ZHOU, Q., SOUBA, W. W., CROCE, C. M. & VERNE, G. N. 2009. MicroRNA-29a regulates intestinal membrane permeability in patients with irritable bowel syndrome. *Gut, gut*. 2009.181834.
- ZICCARDI, V. S., ROBIE 2013. Surgical Management of Lingual Nerve Injuries. In: MILORO, M. (ed.) *Trigeminal Nerve Injuries*. Springer-Verlag Berlin Heidelberg.
- ZIEGLER, D., AMETOV, A., BARINOV, A., DYCK, P. J., GURIEVA, I., LOW, P. A., MUNZEL, U., YAKHNO, N., RAZ, I. & NOVOSADOVA, M. 2006. Oral treatment with α -lipoic acid improves symptomatic diabetic polyneuropathy. *Diabetes care*, 29, 2365-2370.
- ZUO, X., LING, J. X., XU, G.-Y. & GU, J. G. 2013. Operant behavioral responses to orofacial cold stimuli in rats with chronic constrictive trigeminal nerve injury: effects of menthol and capsazepine. *Molecular pain*, 9, 28.
- ZYGMUNT, P. & HÖGESTÄTT, E. 2014. TRPA1. In: NILIUS, B. & FLOCKERZI, V. (eds.) *Mammalian Transient Receptor Potential (TRP) Cation Channels*. Springer Berlin Heidelberg.